FAT REPLACING STRATEGIES FOR FULL-FAT ICE CREAM XIANGYU LIU 2024

FAT REPLACING STRATEGIES FOR FULL-FAT ICE CREAM

ROLE OF FAT, POLYSACCHARIDE STRUCTURE AND PROTEIN DISPERSIBILITY

XIANGYU LIU

Propositions

1. To modify the melting, textural and sensory properties of ice cream, it is more important to control the fat destabilization than the fat content.

(this thesis)

2. The choice of fat replacers for ice cream depends on their impact on texture rather than their lubricating properties.

(this thesis)

3. The slow development of computer-aided food engineering limits the potential for efficient food design and production. (Datta, A., Nicolaï, B., Vitrac, O. et al. Computer-aided food engineering. Nat Food 3, 894–904, 2022).

4. Providing training on digital literacy for contributors to ChatGPT is necessary to improve the users' moral judgement. (Krügel, S., Ostermaier, A. & Uhl, M. ChatGPT's inconsistent moral advice influences users' judgment. Sci Rep 13, 4569, 2023).

5. Absorbing diverse academic perspectives and elaborating them with the individual's own interpretation is the most efficient way of expanding critical thinking skills.

6. Based on the benefits for emotional well-being, junk foods should be considered healthy.

Propositions belonging to the thesis, entitled

Fat replacing strategies for full-fat ice cream: Role of fat, polysaccharide structure and protein dispersibility

Xiangyu Liu

Wageningen, 16 January 2024

Fat replacing strategies for full-fat ice cream

Role of fat, polysaccharide structure and protein dispersibility

Xiangyu Liu

Thesis committee

Promotor

Dr E. Scholten
Associate professor, Physics and Physical Chemistry of Foods
Wageningen University & Research

Co-promotor

Dr G. Sala
Senior Scientist, Physics and Physical Chemistry of Foods
Wageningen University & Research

Other members

Prof. Dr K. Hettinga, Wageningen University & Research
Dr F. Boerboom, FrieslandCampina, Wageningen
Dr S. Martinez-Monteagudo, New Mexico State University, Las Cruses, USA
Dr M. Meinders, Wageningen University & Research

This research was conducted under the auspices of VLAG graduate school (Biobased, Biomolecular, Chemical, Food, and Nutrition sciences)

Fat replacing strategies for full-fat ice cream

Role of fat, polysaccharide structure and protein dispersibility

Xiangyu Liu

Thesis

submitted in fulfillment of the requirements for the degree of doctor
at Wageningen University
by the authority of the Rector Magnificus,
Prof. Dr A.P.J. Mol,
in the presence of the
Thesis Committee appointed by the Academic Board
to be defended in public
on Tuesday 16 January 2024
at 4 p.m. in the Omnia Auditorium.

Xiangyu Liu
Fat replacing strategies for full-fat ice cream: Role of fat, polysaccharide structure and protein dispersibility
223 pages

PhD thesis, Wageningen University, Wageningen, the Netherlands (2024)
With references, with summary in English

ISBN: 978-94-6447-983-6
DOI: https://doi.org/10.18174/642186

Contents

Chapter 1

General introduction

1.1 Ice cream microstructure

Ice cream is a frozen food product containing a minimum of 5% fat and 2.5% milk protein, which is obtained by heat-treating and freezing an emulsion of fat, milk solids and sugar (or sweetener), with or without other substances (Clarke, 2015). Ice cream includes all whipped dairy products that are manufactured by freezing and are consumed in the frozen state, also products containing either dairy or non-dairy fats, premium (higher-fat) versions, "light" (lower-fat) versions, ice milk, sherbet, water ice and fruit ice (Goff, 2006). The basic structure of an ice cream mix is that of a simple emulsion, with a discrete phase of partially crystalline fat globules surrounded by an interfacial layer composed of proteins and surfactants. The final ice cream is a complex food colloidal system, containing dispersed air cells and ice crystals in a continuous viscous serum phase. Fat plays an important role, as partially-destabilized fat globules can lead to the formation of a network, which surrounds the air bubbles and contributes to the solid-like structure of the final product (Fig. 1.1).

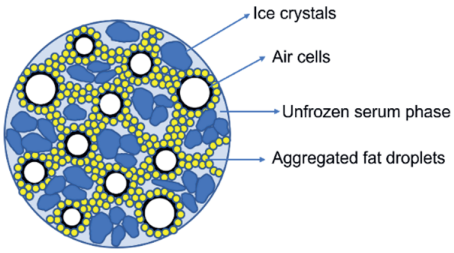

Fig. 1.1. Simplified structure of ice cream.

The high amounts of fat (10-16 %) in ice cream do not comply with a healthy lifestyle, and, therefore, there is a need for approaches to lower fat content in this food and increase the flexibility in the ingredient choice. Although low-fat ice creams are already available on the market, fat reduction while retaining the textural and sensory quality of full-fat products still remains a challenge. For example, it has been shown that as the fat content decreases, ice cream becomes less white, harder, melts more quickly and is perceived grittier and more watery (Cooper, 2017; Genovese, Balivo, Salvati, & Sacchi, 2022; Nagarawatta, 2000; Roland, Phillips, & Boor, 1999b; Skryplonek, et al., 2019). To face the mentioned challenge, many fat replacers are nowadays used in ice cream formulations (Brennan & Tudorica, 2008; Guven, Karaca, & Kacar, 2003; Mahdian & Karazhian, 2013; Mostafavi, Tehrani, & Mohebbi, 2017; Nagarawatta, 2000; Nishinari, Zhang, & Ikeda, 2000; Prindiville, Marshall, & Heymann, 2000; Roland, et al., 1999b; Salem, Hamad, & Ashoush, 2016; Sun, Chen, Liu, Li, & Yu, 2015; Surapat & Rugthavon, 2003; Yazici & Akgun, 2004; Yilsay,

Yilmaz, & Bayizit, 2006), so that the undesirable properties that might arise from fat reduction or removal can be mitigated. However, none of these fat replacers seem to provide good quality when used individually, and, therefore, they are often used in combination. Although some quality aspects can be improved, suitable melting behavior in low-fat ice cream is not easily provided by fat replacers, and conflicting results have been reported regarding the effect of different fat replacers on this functional property (Mahdian, et al., 2013; Roland, et al., 1999b; Soukoulis, Chandrinos, & Tzia, 2008). This indicates that there is still a knowledge gap on the relationship between ice cream texture and its composition, and systematic studies to relate these aspects are required. The main goal of this thesis was to gain an understanding of the role of fat in the development of ice cream texture, and, based on the knowledge gained, investigate the potential of different fat reduction strategies.

1.2 Role of fat in ice cream microstructure

The structure of ice cream is determined by the ice fraction, the size of ice crystals, the overrun, i.e., the amount of air present, and the specific viscoelastic properties of the unfrozen matrix, also referred to as serum phase. Fat plays a very important role in this structure, as solid fat globules have the ability to attach to the air bubbles, thereby affecting the overrun and the stability of the air cells. During the preparation of the ice cream, the fat globules in milk and cream are pushed together, inducing a process called partial coalescence, thereby forming a fat crystal network around the air bubbles (Goff, Verespej, & Smith, 1999). The process of fat destabilization during the ice cream making process is shown in Fig. 1.2 (Cheng, Dudu, Li, & Yan, 2020).

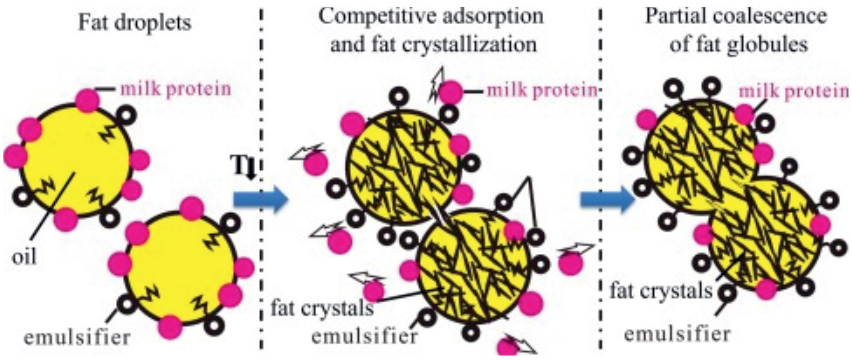

Fig. 1.2. Partial coalescence of fat during the ice cream making process (Cheng, et al., 2020).

Two phenomena occur during aging process: destabilization of fat globules upon

addition of surfactants, resulting from the competitive adsorption between surfactants and milk proteins, and partial coalescence of the globules during freezing. Due to partial coalescence, fat aggregates are formed in the mix, and then a three-dimensional fat network is obtained, which will affect the structure of the ice cream. It is known that partially coalesced fat is mainly responsible for stabilizing the air cells and for the formation of a fat network in the unfrozen serum phase separating the air cells (Chang & Hartel, 2002; Goff, 1997; Méndez-Velasco & Goff, 2012; VanWees & Hartel, 2018).

Although many studies have been published on the role of surfactant in partial coalescence, (Fredrick, Walstra, & Dewettinck, 2010; Jiang, Jing, Xiong, & Liu, 2019; McClements, 2012; Munk, Erichsen, & Andersen, 2014; Segall & Goff, 2002), there is still a lack of information relating the effect of the degree of fat destabilization and fat network formation to the structure and textural properties of ice cream. Research on ice cream is challenging, as often multiple structural features are varied at the same time, which makes it difficult to isolate the role of the fat itself. For example, a greater degree of fat destabilization has been shown to reduce the melting rate, but in these studies the overrun also changed. It is known that overrun is also affected by the degree of fat destabilization (Warren & Hartel, 2014, 2018; Wu, Freire, & Hartel, 2019). It is therefore difficult to isolate the effect of the individual structural features. In addition, contradicting results have also been seen for the effect of the degree of fat destabilization on textural properties, such as hardness. Destabilized fat was found to provide a network among the air cells, thereby increasing hardness (Muse & Hartel, 2004). However, another research showed that no significant correlation was found between destabilized fat and hardness (Amador, Hartel, & Rankin, 2017). This was attributed to differences in secondary effects, such as ice crystal size (Amador, et al., 2017). To clarify the effect of specific structural features of ice cream on the hardness, it would be required to vary only one element at a time while keeping other variables constant. Besides hardness, fat content and degree of fat destabilization also affect mix viscosity and/or serum phase viscosity, increasing their shear-thinning behavior, and the formation of a fat network can provide solid-like properties to the ice cream. This will eventually affect structural properties such as hardness and shape retention after melting. Many studies considered that the mix viscosity is the main factor affecting the ice cream microstructure and sensory properties (Amador, et al., 2017; Bahramparvar & Mazaheri Tehrani, 2011; Javidi, Razavi, Behrouzian, & Alghooneh, 2016; Mahdian, et al., 2013; Soukoulis, et al., 2008; Varela, Pintor, & Fiszman, 2014), However, for sensory perception, the viscosity of the serum phase resulting from freeze concentration of the liquid phase may become more relevant than mix viscosity,

as the mouthfeel of ice cream is more related to its frozen form (Amador, et al., 2017). Unfortunately, serum phase viscosity cannot be measured, and investigations on this parameter are usually based on extrapolations of mix viscosity. A sample with a higher mix viscosity is generally believed to have a higher serum phase viscosity, but this is not always true. So, new methods should be developed to determine the serum phase viscosity, and the importance of serum phase viscosity for the textural and sensory properties of ice cream should be further clarified. Additionally, the link between changes in viscoelastic properties and other ice cream characteristics is not known. Therefore, the analysis of the formation of the fat network itself can provide some useful information about the effect of fat on other structural elements, contributing to clarify the individual contribution of different fat network characteristics.

1.3 Ice cream sensory properties

Due to its large effect on structure, fat also has a positive effect on the sensory perception of ice cream. For example, it contributes to a smooth, creamy and thick consistency, and fat-containing ice cream often melts rather slowly, providing a long-lasting evolution of sensorial parameters (Amador, et al., 2017; Mahdian, et al., 2013; Nagarawatta, 2000; Prindiville, et al., 2000; Roland, Phillips, & Boor, 1999a; Yilsay, et al., 2006). When fat is removed from ice cream, negative sensory attributes, like hardness, grittiness, and wateriness, become more prevalent. The sensory attributes of ice cream have also been linked to other factors, such as overrun, ice crystal size and serum phase viscosity. For example, overrun has been linked to creamier products, together with a richer mouthfeel (Park, et al., 2015). Smoothness has been mainly linked to the size and morphology of the ice crystals. Small ice crystals lead to less icy and less sandy perception, and, therefore, a uniform distribution of small ice crystals is critical for obtaining high quality ice cream (Buyck, Baer, & Choi, 2011; Flores & Goff, 1999). Smoothness and a rich mouthfeel are also obtained by increasing the viscosity of the serum phase. In addition, a higher viscosity has also been shown to decrease perception of wateriness, iciness and coarseness (Soukoulis et al., (Soukoulis, et al., 2008). Overall, many thickeners have been shown to positively affect the sensory perception of ice cream, such as guar gum, gelatin, acacia gum, and sodium alginate (Minhas, Sidhu, Mudahar, & Singh, 2002). However, also here, there is a lack of research on the individual contribution of different structural elements on sensory perception, as most of these studies focused on ice cream with very diverse structures. In addition, some complex attributes, such as creaminess, fattiness and slipperiness, cannot be easily linked to a specific structural feature, and thus more information is still required to describe the relation between structure and

perception. For such complex attributes, also lubrication properties are important (Kokini, Kadane, & Cussler, 1977), but such aspects are currently not taken into account for ice cream. More insights into the relation among ice cream structure, lubrication properties and sensory perception are needed.

1.4 Ice cream tribological properties

Lubrication research, also known as tribology, is a field studying lubrication, friction, and wear between two surfaces in relative motion. The lubrication properties of food have aroused enormous interest among food scientists, as they provides relevant relations between the structure of food systems and surface-related sensorial attributes, such as creaminess and smoothness (Kokini, et al., 1977; Malone, Appelqvist, & Norton, 2003; Selway & Stokes, 2013). For example, creaminess is one of the pleasant sensorial attributes of food, and a linear inverse correlation between perceived creaminess and measured friction coefficients has been reported for milk (Chojnicka-Paszun, De Jongh, & De Kruif, 2012), model emulsions (Ji, Otter, Cornacchia, Sala, & Scholten, 2023)and emulsion-filled gels (de Wijk & Prinz, 2005; Dresselhuis, et al., 2007). There seems to be agreement that lubrication properties can reflect fat-related sensorial attributes, as the presence of fat can reduce friction in many food systems, resulting in a creamier and smoother sensation (Chojnicka-Paszun, et al., 2012; Upadhyay, Aktar, & Chen, 2020). However, lubrication properties have not been investigated for ice cream yet, as no appropriate methods have been established to measure its lubrication properties, especially in frozen state. As the structure of ice cream changes with temperature due to the disappearance of ice crystals, reduction in serum phase viscosity and changes in the fat network, the relation between structure, lubrication properties and sensory perception is even more difficult to understand. To better comprehend how sensory attributes can be linked to the structure and lubrication of ice cream, first such changes in structure and lubrication should be clarified.

1.5 Potential fat replacers for ice cream

As discussed above, fat is a critical ingredient in ice cream, having a significant impact on its physical, rheological and tribological properties, and, therefore, the reduction of fat in ice creams affects both the texture and sensory perception. The main effects of fat reduction are expected to be an increase in melting rate, a decrease in air bubbles stability, and, therefore, a lower feeling of creaminess and mouthcoating. Several fat replacers have been investigated in low-fat and fat-free ice creams. Based on their composition, fat replacers are mainly categorized into three groups: carbohydrate-,

protein-, and lipid-based (Akbari, Eskandari, & Davoudi, 2019). Carbohydrate-based fat replacers are the most common, and they can act as fat replacers by increasing viscosity (Brennan, et al., 2008; Lucca & Tepper, 1994). The most common carbohydrate-based fat replacers used in ice cream are maltodextrin (Mojtaba Azari-Anpar, Khomeiri, Ghafouri-Oskuei, & Aghajani, 2017; Güzeler, Kaçar, & Say, 2011), plant gums (Azari-Anpar, Soltani Tehrani, Aghajani, & Khomeiri, 2017; Aziz, Sofian-Seng, Yusop, Kasim, & Razali, 2018; Guven, et al., 2003; Javidi, et al., 2016), modified starch (Salem, et al., 2016; Subroto, Indiarto, Djali, & Rosyida, 2020; Surapat, et al., 2003; Surendra Babu, Parimalavalli, & Jagan Mohan, 2018) and dietary fibers (Crizel, Araujo, Rios, Rech, & Flôres, 2014; Guo, et al., 2018; Yu, Zeng, Wang, & Regenstein, 2021). In literature, the function of polysaccharides in low-fat or fat-free ice cream has been ascribed to viscosity enhancement. However, in some studies the effect of polysaccharides was investigated at a constant concentration, which resulted in different viscosity values in the samples. This made it difficult to distinguish the exact role of viscosity from that of the structure of the polysaccharides in the different structural and physical properties of ice cream. Besides viscosity, different polysaccharides also have different shear-thinning behavior and ability to incorporate air cells, and provide a network by gelation in the serum phase. However, how these specific properties affect the ice cream characteristics is not known. In addition, it has been shown that molecular characteristics, such as molecular weight and rigidity, influence the lubrication functionality in liquids (Ji, et al., 2022), but it is unclear how differences in lubrication behavior of carbohydrates may affect the perception of ice cream. Therefore, the exact role of carbohydrates in textural, rheological, lubrication and sensory properties of ice cream needs to be further clarified.

Apart from carbohydrates, proteins are also promising fat replacers due to their multiple functional properties. Although proteins are less efficient in affecting viscosity compared with carbohydrates, they can provide different functionalities in ice cream, such as foaming and gelation. As proteins have the ability to stabilize interfaces, they may contribute to incorporating air cells into ice cream (Zayas & Zayas, 1997). Additionally, proteins may also contribute to viscosity increase and structure formation in the serum phase among air cells (Nishinari, et al., 2000). Studies on protein-based fat replacers in ice cream have mainly focused on milk proteins (Mostafavi, et al., 2017; Prindiville, et al., 2000; Yilsay, et al., 2006). These studies showed that the presence of protein in low-fat ice cream slowed down the melting rate and improved sensory properties, lowering coldness and increasing smoothness. However, these low-fat ice creams did not match the satisfying sensory profile of a

full-fat ice cream. Instead of animal proteins, plant proteins may be an alternative to replace fat in ice cream, especially due to concerns related to environmental sustainability. It is not known whether plant proteins alone can be used as fat replacers, and which characteristics of the plant proteins are desired. Based on this, the individual effect of soy protein dispersibility on the structural and sensory properties of fat-free was investigated in this thesis.

1.6 Methodologies to study ice cream properties

1.6.1 Textural properties

Generally, hardness and scoopability are used to represent the textural properties of ice cream. Hardness is usually measured with a Texture Analyzer. It refers to the resistance of the ice cream to deformation (Muse, et al., 2004), and is defined as the maximum peak force during penetration (Fig. 1.3 top). Another aspect important for ice cream is scoopability. However, no method is currently available to measure this property. In this thesis, we employed a new method to measure the scoopability using Texture Analyzer as well (Fig. 1.3 bottom). A spoon probe in combination with an ice cream holder was used, where the scooping spoon was forced into the ice cream with a constant velocity over a certain distance, and the area under the curve (scooping energy) was used as a measure of scoopability. As hardness is also affecting the data obtained from a scoopability test, more specific information about ice cream structure is expected to be extracted by this new method.

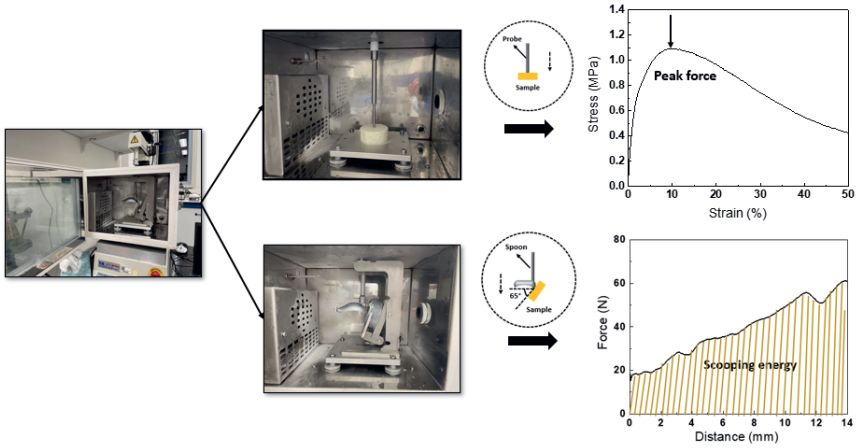

Fig. 1.3. Schematic representation of hardness (top) and scoopability (bottom) measurement setups and the typical curves.

1.6.2 Rheological properties

Oscillatory rheology is often used for the characterization of a variety of food systems, but has not been used often for ice cream. Only a limited number of studies can be found in the literature (Eisner, Wildmoser, & Windhab, 2005; Granger, Leger, Barey, Langendorff, & Cansell, 2005; Wildmoser, Scheiwiller, & Windhab, 2004). However, this technique can provide valuable information on the structure of ice cream, both in the frozen state and during melting, as the viscoelastic properties of the sample can be measured as a function of temperature. A typical setup and the obtained curve of both the storage and loss modulus versus temperature are shown in Fig. 1.4. Three zones can be identified in the curves: (1) zone I, from -20 to -3 °C: in this temperature range the solid behavior of the sample dominates the rheological properties, as the ice cream is still in its frozen state; (2) zone II, between -3 to 4 °C: in this region, the moduli show a steep decrease, which indicates fast-melting of the ice cream; (3) zone III, from 4 to 10 °C: within this zone, the rheological behavior is dominated by the microstructure of the molten ice cream. As limited research has been performed with oscillatory rheology, our understanding of how different structural features relate to the different moduli is still unsatisfactory. Overall, this is a promising method, which could provide more insights into the structural organization of the structure at different stages of consumption.

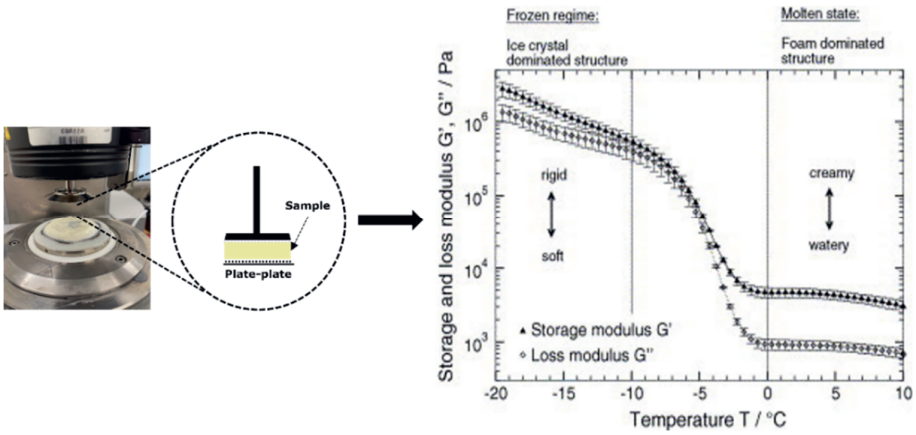

Fig. 1.4. Setup of temperature sweep measurements in ice cream and its typical curves. Three zones (I, II and III) relating to different states of ice cream are identified (Eisner, et al., 2005).

1.6.3 Lubrication properties

In recent research, many commercial tribometers have been used to characterize the tribological behavior of food (Fuhrmann, Aguayo-Mendoza, Jansen, Stieger, & Scholten, 2020; Rudge, Scholten, & Dijksman, 2019; Sarkar & Krop, 2019). Most measurements are currently performed with a rheometer equipped with a tribology accessory (Fig. 1.5a). This setup performs a rotary movement, and can only be used for liquid samples. Therefore, in ice cream research it can only be used to measure the lubrication properties of molten samples, but not of frozen ones. No method is currently available to measure the lubrication properties of frozen ice cream, although this may be more related to changes during oral processing and melting. Therefore, in this thesis we examined the suitability of a different tribometer (TriboLab, Fig. 1.5b), and a schematic representation of the set-up is shown in Fig. 1.5b. The mentioned tribometer uses an oscillation linear movement and contains a sample holder also suitable for solid foods. We developed a new methodology to determine the lubrication properties of ice cream during the melting process.

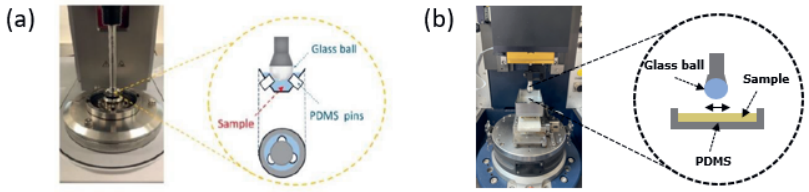

Fig. 1.5. Schematic representation of the tribological set-up used for the present thesis: a glass ball sliding over a PDMS surface with (a) a rotary movement (Anton Paar) or (b) an oscillating movement in a linear direction (Bruker TriboLab).

1.6.4 Melting properties

To obtain information on the melting properties of ice cream, currently a simple gravimetric melting test is performed, where the ice cream is placed on top of a mesh (Muse, et al., 2004; Roland, et al., 1999a; Sakurai, 1996; Warren, et al., 2018). A typical melting curve is obtained (Fig. 1.6a), from which three parameters are normally extracted to describe the melting behavior: (1) the lag time (min), which is the time at which the first droplet drops; (2) the melting rate (%/min), which corresponds to the slope of the curve weight versus time; and (3) the melted percentage (%), which is taken as the loss of the ice cream in percentage after complete melting. Alternatively, as shown in Fig. 1.6b, melting properties can also be extracted from the results of oscillatory measurements, where changes in the

viscoelastic properties during the temperature sweep (slope of zone II) can be related to the melting profile (Javidi, et al., 2016; Mahdian, et al., 2013; Mostafavi, et al., 2017; Sharma, Singh, & Yadav, 2017).

As both mentioned methods cannot really reflect the melting of the sample in the mouth, in this thesis a third methodology was developed to characterize the melting behavior using a tribometer. To be more specific, a certain force was applied and a linear movement was used during the tribological measurements, and the changes in penetration distance of the probe into the sample during melting were measured (Fig. 6c). The results from the different methods were compared, and the tribology test was expected to a more promising method to represent the melting of the sample during oral consumption.

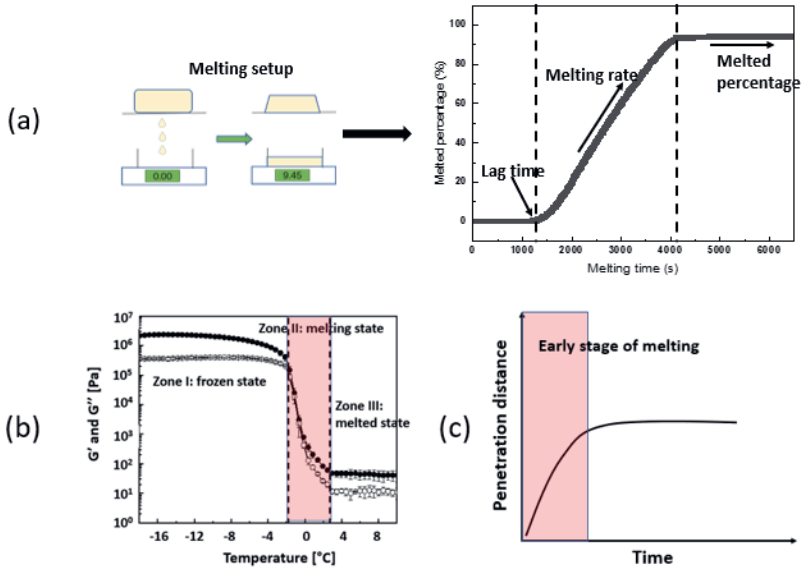

Fig. 1.6. (a): schematic representation of the melting setup for gravimetric tests and the typical melting curve. Three parameters (lag time, melting rate and melted percentage) are extracted from the curve. (b): changes of viscoelastic properties with temperature during rheological measurement. (c): changes of penetration distance of a probe into the sample with melting during tribological measurement.

1.6.5 Ice cream microstructure observation

Several methods have been used to observe different features of the ice cream microstructure. Cryo-SEM has been used to study ice crystals and air bubble size and

distribution (Flores, et al., 1999; Guo, et al., 2017; Masselot, Bosc, & Benkhelifa, 2021; Wildmoser, et al., 2004). Cryo-SEM allows for high-resolution imaging of the microstructure of ice cream at low temperatures, providing detailed information about the microstructure, such as ice crystals, air cells, fat globules, and serum phase, at a sub-micron scale (Goff, 2002). To visualize the air cells and the serum phase in 3D, X-ray microtomography techniques have been recently employed (Guo, et al., 2017). However, this method can only distinguish between the dispersed air phase and the non-air phase, as it relies on density differences between phases. The density of ice crystals, fat particles and unfrozen serum phase is around 1 g/cm^3. So, the density of these three phases does not differ enough to obtain proper images of ice cream by XRT. Nonetheless, the density of air cells is around 0.001 g/cm^3, which is significantly lower than that of the other phases. Therefore, air bubbles in a solid material can be well detected and analyzed. X-rays are transmitted through the sample, where density variation within the sample leads to amplitude variations in the radiation. The altered rays are captured by sensors on the other side of the sample. The sample is continually rotated slightly between scans, and as shown in Fig. 1.7, a section of two-dimensional projections is collected by the sensors, which are reconstructed into a three-dimensional volume of both the air phase and serum phase with proprietary image processing software. After that, the software generates data on the mean size of air cells, air volume and the mean distance between air cells (serum thickness). More information on the structural organization of ice cream can likely be obtained with this method.

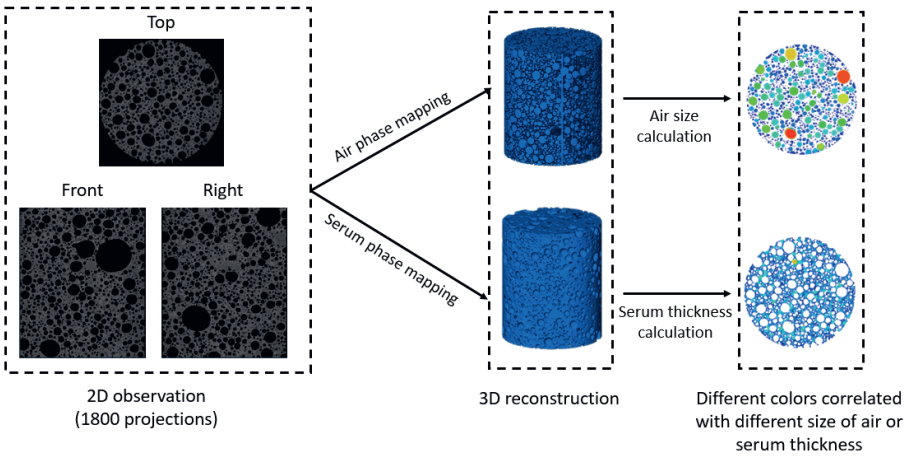

Fig. 1.7. Images of the 3D microstructure of ice cream and of air cell size and serum thickness.

1.7 Aim and outline of this thesis

A schematic representation of the whole thesis is shown in Fig. 1.8. In **Chapter 2**, we investigated the effect of fat aggregate size and percentage on fat network formation and, ultimately, on the melting properties of ice cream. To achieve the formulated aims, we prepared three different series of simplified ice cream models by changing fat content, emulsifier concentration or solid fat content to vary fat destabilization degree and network formation separately, while keeping the overrun similar. Furthermore, to understand the effect of other structural features, in **Chapter 3**, the individual roles of fat network, overrun and ice crystal size in the viscoelastic behavior, hardness and melting properties of ice cream were clarified by changing only one of these characteristics at a time, while keeping the others constant. Using the knowledge obtained from the first two **Chapters**, we developed two fat replacing strategies. In **Chapter 4**, flexible and rigid polysaccharides differing in rheological properties were selected as fat replacers to better understand how both mix and serum phase viscosity relate to different structural and sensory aspects of low-fat ice cream. We discussed what type of polysaccharides are more suitable as fat replacers and how this is related to the specific rheological properties imparted by the polysaccharides. In **Chapter 5**, to test the potential of plant proteins as a fat replacer in ice cream, we selected soy protein as a representative, and investigated how the specific features of particles made with it could be linked to different properties of the samples. We created three series of ice creams differing in particle size, dispersibility and/or viscosity to investigate the individual effect of these properties on the physical, rheological, tribological and sensory properties of fat-free ice cream. In both **Chapters 4 and 5**, we also measured the tribological properties of molten ice cream and linked them to the sensory perception of the samples. In **Chapter 6** we provide a proof-of-concept study to measure lubrication properties also during melting. For the study reported in this chapter, we developed a new method to measure lubrication behavior, and we linked this to different structural features of frozen ice cream. Finally, **Chapter 7** summarizes the findings presented in the different chapters and provides an integrated discussion regarding the complex relationship between ice cream texture, property and sensory. The significance of these results and their implications are also provided together with an outlook for further research.

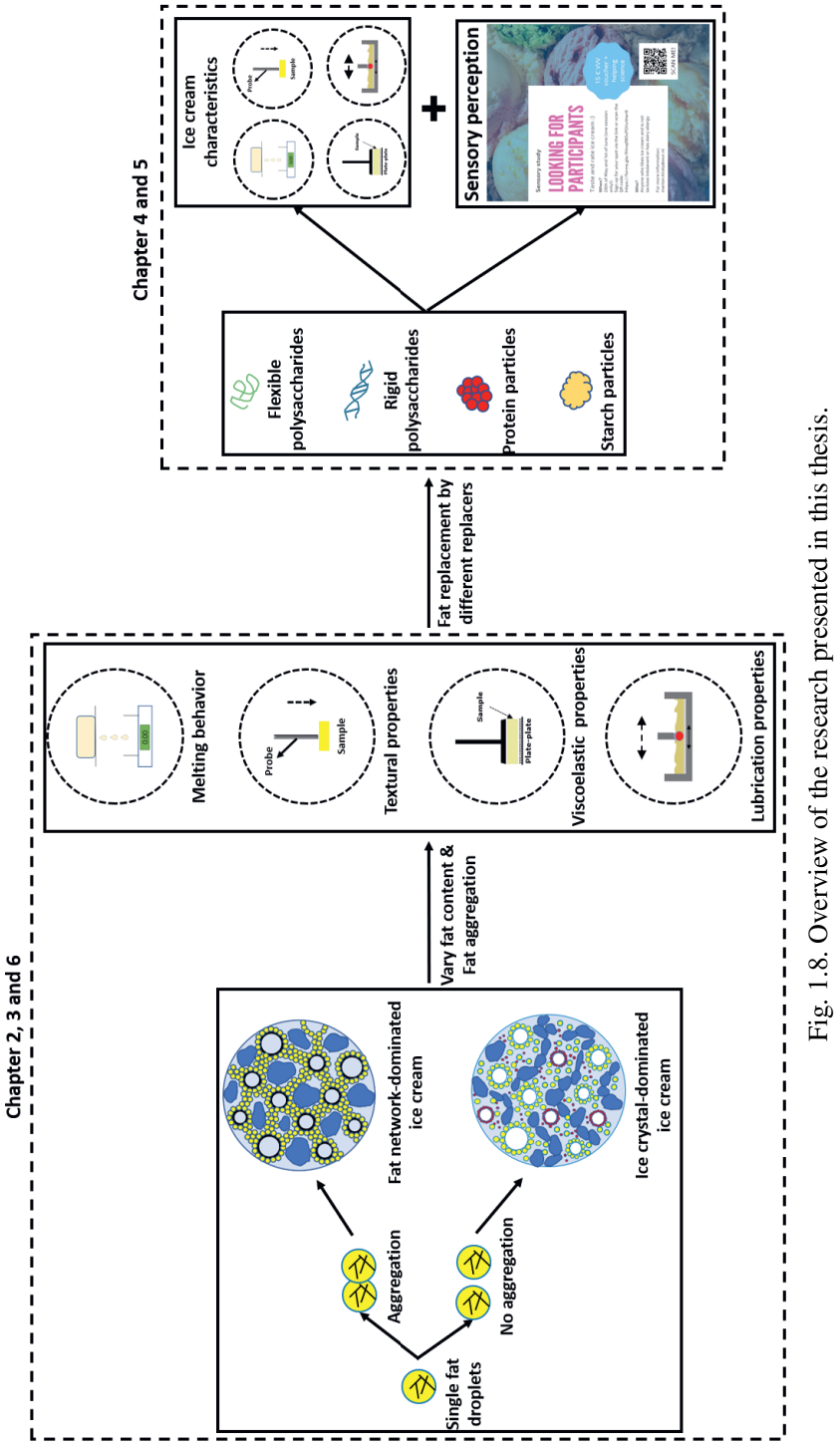

Fig. 1.8. Overview of the research presented in this thesis.

References

Akbari, M., Eskandari, M. H., & Davoudi, Z. (2019). Application and functions of fat replacers in low-fat ice cream: A review. *Trends in food science & technology, 86*, 34-40.

Amador, J., Hartel, R., & Rankin, S. (2017). The effects of fat structures and ice cream mix viscosity on physical and sensory properties of ice cream. *Journal of food science, 82*(8), 1851-1860.

Azari-Anpar, M., Khomeiri, M., Ghafouri-Oskuei, H., & Aghajani, N. (2017). Response surface optimization of low-fat ice cream production by using resistant starch and maltodextrin as a fat replacing agent. *Journal of food science and technology, 54*, 1175-1183.

Azari-Anpar, M., Soltani Tehrani, N., Aghajani, N., & Khomeiri, M. (2017). Optimization of the new formulation of ice cream with native Iranian seed gums (Lepidium perfoliatum and Lepidium sativum) using response surface methodology (RSM). *Journal of food science and technology, 54*, 196-208.

Aziz, N. S., Sofian-Seng, N.-S., Yusop, S. M., Kasim, K. F., & Razali, N. S. M. (2018). Functionality of okra gum as a novel carbohydrate-based fat replacer in ice cream. *Food Science and Technology Research, 24*(3), 519-530.

Bahramparvar, M., & Mazaheri Tehrani, M. (2011). Application and functions of stabilizers in ice cream. *Food Reviews International, 27*(4), 389-407.

Brennan, C. S., & Tudorica, C. M. (2008). Carbohydrate-based fat replacers in the modification of the rheological, textural and sensory quality of yoghurt: comparative study of the utilisation of barley beta-glucan, guar gum and inulin. *International journal of food science & technology, 43*(5), 824-833.

Buyck, J. R., Baer, R. J., & Choi, J. (2011). Effect of storage temperature on quality of light and full-fat ice cream. *Journal of dairy science, 94*(5), 2213-2219.

Chang, Y., & Hartel, R. W. (2002). Stability of air cells in ice cream during hardening and storage. *Journal of Food Engineering, 55*(1), 59-70.

Cheng, J., Dudu, O. E., Li, X., & Yan, T. (2020). Effect of emulsifier-fat interactions and interfacial competitive adsorption of emulsifiers with proteins on fat crystallization and stability of whipped-frozen emulsions. *Food hydrocolloids, 101*, 105491.

Chojnicka-Paszun, A., De Jongh, H. H. J., & De Kruif, C. G. (2012). Sensory perception and lubrication properties of milk: Influence of fat content. *International Dairy Journal, 26*(1), 15-22.

Clarke, C. (2015). *The science of ice cream*: Royal Society of Chemistry.

Cooper, H. R. (2017). Texture in dairy products and its sensory evaluation. In *Food texture* (pp. 217-250): Routledge.

Crizel, T. d. M., Araujo, R. R. d., Rios, A. d. O., Rech, R., & Flôres, S. H. (2014). Orange fiber as a novel fat replacer in lemon ice cream. *Food Science and Technology, 34*, 332-340.

de Wijk, R. A., & Prinz, J. F. (2005). The role of friction in perceived oral texture. *Food Quality and Preference, 16*(2), 121-129.

Dresselhuis, D. M., Klok, H. J., Stuart, M. A. C., de Vries, R. J., van Aken, G. A., & de Hoog, E. H. A. (2007). Tribology of o/w emulsions under mouth-like conditions: determinants of friction. *Food Biophysics, 2*, 158-171.

Eisner, M. D., Wildmoser, H., & Windhab, E. J. (2005). Air cell microstructuring in a high viscous ice cream matrix. *Colloids and Surfaces A: Physicochemical and Engineering Aspects, 263*(1-3), 390-399.

Flores, A. A., & Goff, H. D. (1999). Ice crystal size distributions in dynamically frozen model solutions and ice cream as affected by stabilizers. *Journal of dairy science, 82*(7), 1399-1407.

Fredrick, E., Walstra, P., & Dewettinck, K. (2010). Factors governing partial coalescence in oil-in-water emulsions. *Advances in colloid and interface science, 153*(1-2), 30-42.

Fuhrmann, P. L., Aguayo-Mendoza, M., Jansen, B., Stieger, M., & Scholten, E. (2020). Characterisation of friction behaviour of intact soft solid foods and food boli. *Food hydrocolloids, 100*, 105441.

Genovese, A., Balivo, A., Salvati, A., & Sacchi, R. (2022). Functional ice cream health benefits and sensory implications. *Food Research International*, 111858.

Goff, H. D. (1997). Colloidal aspects of ice cream—a review. *International Dairy Journal, 7*(6-7), 363-373.

Goff, H. D. (2002). Formation and stabilisation of structure in ice-cream and related products. *Current opinion in colloid & interface science, 7*(5-6), 432-437.

Goff, H. D. (2006). *Ice cream*: Springer.

Goff, H. D., Verespej, E., & Smith, A. K. (1999). A study of fat and air structures in ice cream. *International Dairy Journal, 9*(11), 817-829.

Granger, C., Leger, A., Barey, P., Langendorff, V., & Cansell, M. (2005). Influence of formulation on the structural networks in ice cream. *International Dairy Journal, 15*(3), 255-262.

Guo, E., Zeng, G., Kazantsev, D., Rockett, P., Bent, J., Kirkland, M., Van Dalen, G., Eastwood, D. S., StJohn, D., & Lee, P. D. (2017). Synchrotron X-ray tomographic quantification of microstructural evolution in ice cream–a multi-phase soft solid. *Rsc Advances, 7*(25), 15561-15573.

Guo, Y., Zhang, X., Hao, W., Xie, Y., Chen, L., Li, Z., Zhu, B., & Feng, X. (2018). Nano-bacterial cellulose/soy protein isolate complex gel as fat substitutes in ice cream model. *Carbohydrate polymers, 198*, 620-630.

Guven, M., Karaca, O. B., & Kacar, A. (2003). The effects of the combined use of stabilizers containing locust bean gum and of the storage time on Kahramanmaraş-type ice creams. *International Journal of Dairy Technology, 56*(4), 223-228.

Güzeler, N., Kaçar, A., & Say, D. (2011). Effect of Milk Powder, Maltodextrin and Polydextrose Use on Physical and Sensory Properties of Low Calorie Ice Cream during Storage. *Academic Food Journal/Akademik GIDA*.

Javidi, F., Razavi, S. M. A., Behrouzian, F., & Alghooneh, A. (2016). The influence of basil seed gum, guar gum and their blend on the rheological, physical and sensory properties of low fat ice cream. *Food hydrocolloids, 52*, 625-633.

Ji, L., Orthmann, A., Cornacchia, L., Peng, J., Sala, G., & Scholten, E. (2022). Effect of different molecular characteristics on the lubrication behavior of polysaccharide solutions. *Carbohydrate Polymers, 297*, 120000.

Ji, L., Otter, D. d., Cornacchia, L., Sala, G., & Scholten, E. (2023). Role of polysaccharides in tribological and sensory properties of model dairy beverages. *Food hydrocolloids, 134*, 108065.

Jiang, J., Jing, W., Xiong, Y. L., & Liu, Y. (2019). Interfacial competitive adsorption of different amphipathicity emulsifiers and milk protein affect fat crystallization, physical properties, and morphology of frozen aerated emulsion. *Food hydrocolloids, 87*, 670-678.

Kokini, J. L., Kadane, J. B., & Cussler, E. L. (1977). Liquid texture perceived in the mouth 1. *Journal of Texture Studies, 8*(2), 195-218.

Lucca, P. A., & Tepper, B. J. (1994). Fat replacers and the functionality of fat in foods. *Trends in food science & technology, 5*(1), 12-19.

Mahdian, E., & Karazhian, R. (2013). Effects of fat replacers and stabilizers on rheological, physicochemical and sensory properties of reduced-fat ice cream. *Journal of Agricultural Science and Technology, 15*(6), 1163-1174.

Malone, M. E., Appelqvist, I. A. M., & Norton, I. T. (2003). Oral behaviour of food hydrocolloids and emulsions. Part 1. Lubrication and deposition

considerations. *Food hydrocolloids, 17*(6), 763-773.

Masselot, V., Bosc, V., & Benkhelifa, H. (2021). Influence of stabilizers on the microstructure of fresh sorbets: X-ray micro-computed tomography, cryo-SEM, and Focused Beam Reflectance Measurement analyses. *Journal of Food Engineering, 300*, 110522.

McClements, D. J. (2012). Crystals and crystallization in oil-in-water emulsions: Implications for emulsion-based delivery systems. *Advances in colloid and interface science, 174*, 1-30.

Méndez-Velasco, C., & Goff, H. D. (2012). Fat structure in ice cream: A study on the types of fat interactions. *Food hydrocolloids, 29*(1), 152-159.

Minhas, K. S., Sidhu, J. S., Mudahar, G. S., & Singh, A. K. (2002). Flow behavior characteristics of ice cream mix made with buffalo milk and various stabilizers. *Plant Foods for Human Nutrition, 57*, 25-40.

Mostafavi, F. S., Tehrani, M. M., & Mohebbi, M. (2017). Rheological and sensory properties of fat reduced vanilla ice creams containing milk protein concentrate (MPC). *Journal of Food Measurement and Characterization, 11*, 567-575.

Munk, M. B., Erichsen, H. R., & Andersen, M. L. (2014). The effects of low-molecular-weight emulsifiers in O/W-emulsions on microviscosity of non-solidified oil in fat globules and the mobility of emulsifiers at the globule surfaces. *Journal of Colloid and Interface Science, 419*, 134-141.

Muse, M. R., & Hartel, R. W. (2004). Ice cream structural elements that affect melting rate and hardness. *Journal of dairy science, 87*(1), 1-10.

Nagarawatta, G. U. (2000). Effect of fat and sucrose replacers on physical, chemical, and sensory properties of reduce calorie ice cream.

Nishinari, K., Zhang, H., & Ikeda, S. (2000). Hydrocolloid gels of polysaccharides and proteins. *Current opinion in colloid & interface science, 5*(3-4), 195-201.

Park, S. H., Jo, Y.-J., Chun, J.-Y., Hong, G.-P., Davaatseren, M., & Choi, M.-J. (2015). Effect of frozen storage temperature on the quality of premium ice cream. *Korean journal for food science of animal resources, 35*(6), 793.

Prindiville, E. A., Marshall, R. T., & Heymann, H. (2000). Effect of milk fat, cocoa butter, and whey protein fat replacers on the sensory properties of lowfat and nonfat chocolate ice cream. *Journal of dairy science, 83*(10), 2216-2223.

Roland, A. M., Phillips, L. G., & Boor, K. J. (1999a). Effects of fat content on the sensory properties, melting, color, and hardness of ice cream. *Journal of dairy science, 82*(1), 32-38.

Roland, A. M., Phillips, L. G., & Boor, K. J. (1999b). Effects of fat replacers on the sensory properties, color, melting, and hardness of ice cream. *Journal of dairy science, 82*(10), 2094-2100.

Rudge, R. E. D., Scholten, E., & Dijksman, J. A. (2019). Advances and challenges in soft tribology with applications to foods. *Current Opinion in Food Science, 27*, 90-97.

Sakurai, K. (1996). Effect of production conditions on ice cream melting resistance and hardness. *Milchwissenschaft, 51*, 451-454.

Salem, S. A., Hamad, E. M., & Ashoush, I. S. (2016). Effect of partial fat replacement by whey protein, oat, wheat germ and modified starch on sensory properties, viscosity and antioxidant activity of reduced fat ice cream. *Food and Nutrition Sciences, 7*(6), 397-404.

Sarkar, A., & Krop, E. M. (2019). Marrying oral tribology to sensory perception: A systematic review. *Current Opinion in Food Science, 27*, 64-73.

Segall, K. I., & Goff, H. D. (2002). A modified ice cream processing routine that promotes fat destabilization in the absence of added emulsifier. *International Dairy Journal, 12*(12), 1013-1018.

Selway, N., & Stokes, J. R. (2013). Insights into the dynamics of oral lubrication and mouthfeel using soft tribology: Differentiating semi-fluid foods with similar rheology. *Food Research International, 54*(1), 423-431.

Sharma, M., Singh, A. K., & Yadav, D. N. (2017). Rheological properties of reduced fat ice cream mix containing octenyl succinylated pearl millet starch. *Journal of food science and technology, 54*, 1638-1645.

Skryplonek, K., Henriques, M., Gomes, D., Viegas, J., Fonseca, C., Pereira, C., Dmytrów, I., & Mituniewicz-Małek, A. (2019). Characteristics of lactose-free frozen yogurt with κ-carrageenan and corn starch as stabilizers. *Journal of dairy science, 102*(9), 7838-7848.

Soukoulis, C., Chandrinos, I., & Tzia, C. (2008). Study of the functionality of selected hydrocolloids and their blends with κ-carrageenan on storage quality of vanilla ice cream. *LWT-Food Science and Technology, 41*(10), 1816-1827.

Subroto, E., Indiarto, R., Djali, M., & Rosyida, H. D. (2020). Production and application of crosslinking-modified starch as fat replacer: A review. *Int. J. Eng. Trends Technol, 68*(12), 26-30.

Sun, L., Chen, W., Liu, Y., Li, J., & Yu, H. (2015). Soy protein isolate/cellulose nanofiber complex gels as fat substitutes: rheological and textural properties and extent of cream imitation. *Cellulose, 22*, 2619-2627.

Surapat, S., & Rugthavon, P. (2003). Use of modified starch as fat replacer in reduced fat coconut milk ice cream. *Agriculture and Natural Resources, 37*(4), 484-492.

Surendra Babu, A., Parimalavalli, R., & Jagan Mohan, R. (2018). Effect of modified starch from sweet potato as a fat replacer on the quality of reduced fat ice creams. *Journal of Food Measurement and Characterization, 12*, 2426-2434.

Upadhyay, R., Aktar, T., & Chen, J. (2020). Perception of creaminess in foods. *Journal of Texture Studies, 51*(3), 375-388.

VanWees, S. R., & Hartel, R. W. (2018). Microstructure of ice cream and frozen dairy desserts. *Microstructure of dairy products*, 237-260.

Varela, P., Pintor, A., & Fiszman, S. (2014). How hydrocolloids affect the temporal oral perception of ice cream. *Food Hydrocolloids, 36*, 220-228.

Warren, M. M., & Hartel, R. W. (2014). Structural, compositional, and sensorial properties of United States commercial ice cream products. *Journal of food science, 79*(10), E2005-E2013.

Warren, M. M., & Hartel, R. W. (2018). Effects of emulsifier, overrun and dasher speed on ice cream microstructure and melting properties. *Journal of Food Science, 83*(3), 639-647.

Wildmoser, H., Scheiwiller, J., & Windhab, E. J. (2004). Impact of disperse microstructure on rheology and quality aspects of ice cream. *LWT-Food Science and Technology, 37*(8), 881-891.

Wu, B., Freire, D. O., & Hartel, R. W. (2019). The effect of overrun, fat destabilization, and ice cream mix viscosity on entire meltdown behavior. *Journal of food science, 84*(9), 2562-2571.

Yazici, F., & Akgun, A. (2004). Effect of some protein based fat replacers on physical, chemical, textural, and sensory properties of strained yoghurt. *Journal of Food Engineering, 62*(3), 245-254.

Yilsay, T. Ö., Yilmaz, L., & Bayizit, A. A. (2006). The effect of using a whey protein fat replacer on textural and sensory characteristics of low-fat vanilla ice cream. *European Food Research and Technology, 222*, 171-175.

Yu, B., Zeng, X., Wang, L., & Regenstein, J. M. (2021). Preparation of nanofibrillated cellulose from grapefruit peel and its application as fat substitute in ice cream. *Carbohydrate Polymers, 254*, 117415.

Zayas, J. F., & Zayas, J. F. (1997). Foaming properties of proteins. *Functionality of proteins in food*, 260-309.

Chapter 2

Effect of fat aggregate size and percentage on the melting properties of ice cream

Published as: Liu, X., Sala, G., & Scholten, E. (2022). Effect of fat aggregate size and percentage on the melting properties of ice cream. *Food Research International*, 160, 111709.

Abstract

In this study, we investigated the effect of fat aggregate size and percentage on fat network formation and, ultimately, on the melting properties of ice cream. To control fat destabilization degree and fat network formation, we varied fat and emulsifier content, and blended coconut oil with milk fat, obtaining three different sample series varying in: 1) fat content, 2) fat aggregate size, and 3) fat aggregate percentage. The degree of fat destabilization in terms of aggregate size and the percentage was measured by light scattering techniques. The distribution of the fat around the air cells and in the unfrozen serum phase was calculated based on the measured overrun. Overall, a similar overrun was found in the three series of ice cream. The fat percentage in the remaining phases was measured to verify how much fat and what type of fat aggregates were present in the fat network. The results show that fat destabilization degree is relatively more important than fat content in determining the melting behavior of ice cream with low overrun. Clear relations between different fat destabilization parameters and ice cream melting behavior were established, indicating that the melting behavior of ice cream is related to specific properties of the fat network. Controlling fat destabilization in the unfrozen ice cream phase may be used to alter the properties of ice cream, and could contribute as a fat reduction strategy in ice cream.

2.1 Introduction

Ice creams typically contain 10-16 % of fat, making it an important ingredient that affects product hardness, shape retention, and melting resistance after hardening (Mahdian & Karazhian, 2013). So, it can be stated that fat plays a key role in determining the texture of ice cream, and thereby also its specific sensory characteristics. It has been shown that as the fat content decreases, ice cream becomes less white, harder, and melts more quickly (Roland, Phillips, & Boor, 1999). Reduction of fat in ice cream can thus lead to textural defects such as iciness and coarseness, brittle body and shrinkage (Mahdian & Karazhian, 2013). During the whipping and freezing process, some of the fat in the mix is converted into aggregates, and then a three-dimensional aggregated fat network is formed, which provides structural integrity, a process known as fat destabilization (Goff & Hartel, 2013). Fat aggregates are mainly the result of three mechanisms: aggregation, partial coalescence and coalescence. Aggregation refers to the fact that individual fat droplets stick together during collisions caused by the shear forces in the dynamic freezing step. As the droplets are partially crystalline, their integrity is maintained, which limits the extent of true coalescence of the fat into larger droplets (Pawar, Caggioni, Hartel, & Spicer, 2012). To obtain coalescence, destabilization of the fat globules is required, which is often accomplished by the addition of emulsifiers that compete with proteins at the fat globule interface, leading to more emulsifier-rich domains. This results in a decrease in the strength of the protein layer adsorbed at the interface and a reduction of the steric repulsion among fat globules, which favors partial coalescence. Emulsifiers also interact with fat and influence the crystallization of emulsified fat by changing crystal growth, morphology and stiffness of the crystallized fat (Cheng, Dudu, Li, & Yan, 2020). For partial coalescence to occur, fat crystals protruding from the interfacial membrane of fat globules need to penetrate into other globules. The presence of these fat crystals is of course related to the solid fat content (SFC) at a specific temperature (Sung & Goff, 2010). Fat destabilization is necessary for the stabilization of the ice cream structure, as partially coalesced fat is mainly responsible for stabilizing the air cells and for the formation of a fat network in the unfrozen serum phase separating the air cells. The fat aggregates at the air cell interface and the fat network in the unfrozen serum phase also influence the melting behavior of ice cream (Koxholt, Eisenmann, & Hinrichs, 2001). To date, limited research has clarified the effect of the degree of fat destabilization and fat particle distribution on fat network formation and its relationship with melting behavior.

Melting behavior is an important quality parameter for ice cream, as it provides information on structural changing occurring during ice cream consumption. A few studies focusing on the structure of ice cream in relation to the melting properties have been conducted. The melting rate is especially related to milk fat, which plays an important role in the formation and stabilization of air cells. Research has shown that properties such as fat globule size and particle size distribution are related to melting rate, and if the size of fat agglomerates in the unfrozen phase was above a critical diameter, they will block the foam lamellae and impede the drainage, leading to significantly higher meltdown rate (Kokubo, Sakurai, Hakamata, Tomita, & Yoshida, 1996; Kokubo, Sakurai, Hattori, & Tomita, 1994; Kokubo, Sakurai, Iwaki, Tomita, & Yoshida, 1998; Koxholt et al., 2001). In general, a lower degree of fat destabilization (± 30%) results in faster melting and poor shape retention compared to ice cream with a high degree of fat destabilization (> 50%) (Muse & Hartel, 2004). Furthermore, it has been shown that ice cream with a high overrun has a lower melting rate than ice cream with a low overrun. Higher overrun is presumed to decrease the melting rate as air cells decrease the thermal diffusivity of the ice cream (Sofjan & Hartel, 2004).

Overall, fat destabilization and overrun have been identified as the main two factors that can affect the melting behavior of ice cream (Wu, Freire, & Hartel, 2019). However, the exact relation between the characteristics of the fat network and different melting parameters still remains unclear. To clarify the effect of specific structural features of ice cream on the melting behavior, it would be required to vary only one element at a time while keeping other variables constant. However, in most studies, multiple parameters are changed simultaneously, which makes it difficult to verify the effect of the individual structural features. For example, a greater extent of fat destabilization has been shown to reduce the melting rate, but in these studies the overrun also changed. It is known that the degree of fat destabilization and the apparent viscosity caused by dispersed fat or hydrocolloids can affect the overrun (Warren & Hartel, 2014, 2018; Wu et al., 2019). As all parameters influence each other, it is difficult to attribute the change in melting rate to either fat destabilization or overrun. Therefore, our study aimed to understand the individual contribution of different fat network properties on ice cream melting properties, by separately varying fat destabilization degree and network formation, while keeping the overrun similar.

We prepared three different series of simplified ice cream models without addition of hydrocolloids to minimize the additional effect of viscosity on the studied parameters. In one series, we varied the fat content to change both the degree of fat destabilization and fat network in the unfrozen serum phase. In the other two series, the total fat content was kept similar, and the degree of fat destabilization was systematically changed by varying the emulsifier concentration, or by changing the total SFC by blending milk fat with coconut oil. Two different parameters were used to identify the level of fat destabilization: (i) fat aggregate size, and (ii) fat aggregate percentage. The distribution of the fat particles around the air cells and in the unfrozen serum phase was estimated from theoretical calculations based on the measured overrun. The presence of the fat droplets in the frozen ice cream was observed using cryo-SEM. The melting behavior of the ice cream was determined by measuring: (1) lag time, (2) melting rate, and (3) melted percentage. We analyzed the fat percentages in molten ice cream (dripped phase) and remaining phase after melting to identify how much fat and what type of fat (individual fat droplets or aggregates) remained in the fat network. This information was used to establish correlations between the different fat destabilization parameters and ice cream melting behavior characteristics. This knowledge can be used to control the melting properties of ice cream, and to design fat reduction strategies while keeping similar melting behavior.

2.2 Materials and methods

2.2.1 Materials

Anhydrous milk fat (AMF) was obtained from FrieslandCampina (Wageningen, Netherlands). Coconut oil (CO) was purchased from Holland & Barrett (Wageningen, Netherlands). Sucrose and one of the emulsifiers, Tween 80, P4780, were purchased from Sigma-Aldrich (Netherlands). The other emulsifier, whey protein isolate (WPI, 88.8% protein content) was obtained from Davisco (USA). Ultrapure water, purified by a Millipore Milli-Q system (Darmstadt, Germany), was used for the preparation of all samples.

2.2.2 Ice cream mix preparation

The simplified ice cream models optimized for the present study contained only sugar, fat (AMF or mixtures of AMF and coconut oil) and emulsifiers (Tween 80 or mixtures of Tween 80 and WPI). Three series of ice cream mixes were made to vary the level

of fat destabilization: (i) a fat content series (FC), (ii) an emulsifier concentration series (EC), and a coconut oil series (CO).

Stock emulsions with different emulsifiers were prepared. All emulsions were prepared by pre-homogenization with an Ultra Turrax (T25 basic, IKA, Staufen, Germany) at a speed of 13000 rpm for 2 min, and then homogenized with a homogenizer (Delta Instruments LaboScope Homogenizer HU-3.0, USA) at 13 MPa for one cycle and 11 MPa for 3 cycles.

Fat content series (FC)

For the series with varying fat content (Tab. 2.1), a 20% AMF stock emulsion was prepared with Tween 80 as an emulsifier. AMF was melted at 65 °C and then added to a 0.5% (w/w) Tween 80 solution containing 15 % of sucrose and homogenized as described before. The Tween 80 stock emulsion was then diluted with a 23.3 % sugar solution to obtain fat levels ranging between 4 % and 20 %. The sugar content in the water phase was kept constant to guarantee that the ice creams had the same freezing point depression and therefore the same ice fraction. The ice cream mixes were stored at 4 °C overnight.

Emulsifier concentration series (EC)

For the emulsifier series (Tab. 2.1), a stock solution of 12 % AMF was prepared with WPI as an emulsifier. WPI (4%) was added to water while stirring and allowed to hydrate for 1 h at room temperature. AMF was melted at 65 °C and then added to the WPI solution containing a sucrose content of 15 %. The emulsion was made as described before. After homogenization, Tween 80 was added to achieve concentrations ranging from 0 to 0.25 %. The ice cream mixes were stored at 4 °C overnight to allow the emulsifiers to replace part of the WPI and induce aggregation and/or coalescence.

Coconut oil series (CO)

For the coconut oil series (Tab. 2.1), anhydrous milk fat and coconut oil were first heated at 65 °C and then mixed at percentages between 0 and 4.6 % coconut oil of the total fat content (12 %) to obtain fat with varying SFC. A 0.5 % Tween 80 solution containing 15 % sucrose was added to the heated oil mixtures, and the emulsions were

prepared as described above. The SFC values of the mixtures were calculated based on the fat fractions in the mixtures and the SFC of the individual fats at 4°C: 90% for coconut oil (Dhaygude, Soós, Zeke, & Somogyi, 2018), and 55 % for milk fat (Lopez, Briard-Bion, Camier, & Gassi, 2006). In these calculations, we neglected eutectic effects.

Tab. 2.1. Formulations of the three series of ice cream mixes.

Ingredients		Anhydrous milk fat (g)	Tween 80 (g)	Sucrose (g)	Water (g)	WPI (g)	Coconut oil (g)
FC-series	FC-4	4	0.1	18.09	77.81	0	0
	FC-8	8	0.2	17.32	74.48	0	0
	FC-12	12	0.3	16.55	71.15	0	0
	FC-16	16	0.4	15.78	67.82	0	0
	FC-20	20	0.5	15	64.5	0	0
EC-series	EC-0	12	0	15	69	4	0
	EC-0.1	12	0.1	15	69	4	0
	EC-0.15	12	0.15	15	69	4	0
	EC-0.2	12	0.2	15	69	4	0
	EC-0.25	12	0.25	15	69	4	0
CO-series	CO-55	12	0.5	15	72.5	0	0
	C0-58	10.9	0.5	15	72.5	0	1.1
	CO-62	9.7	0.5	15	72.5	0	2.3
	CO-65	8.6	0.5	15	72.5	0	3.4
	CO-68	7.4	0.5	15	72.5	0	4.6

2.2.3 Ice cream preparation

After overnight aging at 4 °C, 500 ml ice cream mix was transferred into an ice cream machine (Nemox Gelatissimo, Italy) precooled to -15 °C. The ice cream machine contained a barrel with a rotary scraper removing the frozen ice cream from the wall of the machine. The preparation of the ice cream lasted 15 min in total. The obtained ice cream was collected into plastic containers or rings of different sizes to form solid ice cream cylinders for different measurements and immediately hardened at -18 °C for 24 h.

2.2.4 Determination of overrun

The overrun of the ice cream was determined by first weighing a fixed volume of the aged pre-mix in a metal cup. Next, the same volume of ice cream was weighed in said cup directly after ice cream preparation (freezing step). The overrun was quantified as follows (Muse & Hartel, 2004):

$$\text{Overrun } (\%) = \frac{Weight\ of\ mix - weight\ of\ ice\ cream}{Weight\ of\ ice\ cream} \times 100 \quad (2.1)$$

2.2.5 Fat particle size distribution

The particle size distribution of the ice cream mix and molten ice cream samples was determined by static light scattering (Mastersizer 2000, UK.). Deionized water (refractive index, RI=1.33) was used to dilute the samples. The refractive index of milk fat (RI=1.46) was used for the dispersed phase. Measurements were performed at ambient temperature (20 °C) and repeated in triplicate. The particle size distribution of the ice cream mixes presented one peak; that of molten ice creams in which aggregation had occurred showed two peaks. The $D_{4,3}$ of the second peak separated from the first at 10 μm was taken as the size of the fat aggregates. The volume ratio between the two peaks was used to calculate the fat aggregate percentage, reflecting the degree of destabilization.

2.2.6 Microstructure

The microstructure of the ice creams was visualized using a cold-stage scanning electron microscope (SEM, FEI Magellan 400, USA). Small ice cream samples (inner diameter of sampling tube: 1 mm) were taken and rapidly frozen in liquid nitrogen. As the presence of fat aggregates could be covered by the ice crystals, the samples were further prepared by vacuum-sublimation of water at the surface of the fractured specimen to remove surface ice without damaging the ice cream structure. Then the samples were sputter-coated with platinum to create a thin conductive layer to improve the imaging. The ice cream samples were then observed by SEM at 35000x magnification to visualize the fat droplets and fat droplet aggregates. Two samples with different degrees of fat destabilization, i.e. EC-0 with single fat droplets and FC-12 with aggregated fat droplets, were selected from the studied samples.

2.2.7 Melting behavior

For the determination of the melting properties, samples with the same volume were prepared using plastic rings. The dimensions of these rings were 20 mm in height and 30 mm in radius. Prior to the measurement, the samples were stored in a freezer at -20 °C for a minimum of 12 h. The samples were then taken out of the rings and placed on a 136x136 mm metal grid with 5x5 mm openings with an area of 44 % of the total area. The starting weight of each sample was measured, and the samples were placed in a climate-controlled room with a constant temperature of 20 °C and 50 % air humidity. Underneath the mesh, a collection cup was placed on a measuring scale connected to a computer, which recorded the measured weight of the molten sample every 10 s, for a duration of 240 min. The measurements were performed in duplicate. From the recorded data, the following parameters were extracted to describe the melting behavior of the samples: (i) the melting rate (%/min), which corresponded to the slope of the curve representing weight versus time, (ii) the lag time (min), which was the time at which the first droplet hit the collection cup, and (iii) the melted percentage (%), which was taken as the loss of the ice cream (dripped phase) in percentage after complete melting.

2.2.8 Fat content of the different phases obtained after melting

The fat content of the dripped phase of the samples after the melting test was measured with a MilkoScan (MilkoScan FT120, type 71200, Denmark). The instrument was calibrated before use against a range of cow milk samples of known composition. Specimens of about 40 ml were collected and preheated to 40 °C in a water bath to melt the fat. After melting, they were filtered through a 90 µm sieve to avoid the presence of large solid particles. All samples were measured in duplicate and a mean value for the duplicate measurements was calculated automatically. The fat content in the dripped phase was measured for all samples to obtain the fat percentage in the dripped phase based on the original fat content in the ice cream. From this, the fat percentage in the remaining phase was also calculated (100 % - fat percentage in the dripped phase).

2.2.9 Statistical analysis

The data were analyzed with SPSS software (Version 25.0, IBM Corp). The means were compared using a Tukey's test at a 5 % level of significance using an analysis of variance (ANOVA).

2.3 Results and discussion

2.3.1 Fat particle size and overrun measurements

The fat particle size in the ice cream mixes was determined as a measure of the initial particle size before freezing. In these samples, only one peak could be observed and the mean fat particle diameter was around 1 – 1.6 µm for all three studied emulsions (Tab. 2.2). These droplets corresponded to single fat droplets.

Tab. 2.2 Overview of initial fat droplet size and overrun of the three different series of ice cream.

Ingredients		Initial droplet size (µm)	Overrun (%)
FC-series	FC-4	1.06 ± 0.03^{bc}	15.6 ± 1.1^{a}
	FC-8	1.03 ± 0.01^{bc}	17.2 ± 1.2^{a}
	FC-12	1.03 ± 0.01^{bc}	18.0 ± 1.1^{a}
	FC-16	1.01 ± 0.01^{c}	18.3 ± 1.0^{a}
	FC-20	1.04 ± 0.02^{bc}	19.0 ± 1.1^{a}
EC-series	EC-0	1.53 ± 0.13^{a}	17.2 ± 1.4^{a}
	EC-0.1	1.29 ± 0.21^{abc}	15.4 ± 1.1^{a}
	EC-0.15	1.59 ± 0.19^{a}	17.8 ± 1.3^{a}
	EC-0.2	1.46 ± 0.09^{ab}	17.3 ± 0.8^{a}
	EC-0.25	1.57 ± 0.26^{a}	16.4 ± 2.8^{a}
CO-series	CO-55	0.99 ± 0.03^{c}	19.1 ± 1.5^{a}
	C0-58	0.98 ± 0.04^{c}	18.4 ± 1.8^{a}
	CO-62	0.90 ± 0.01^{c}	20.5 ± 2.1^{a}
	CO-65	0.94 ± 0.06^{c}	20.0 ± 2.6^{a}
	CO-68	0.96 ± 0.04^{c}	18.9 ± 1.8^{a}

Values with different letters within the same column are significantly different ($P < 0.05$)

To investigate whether the differences in fat properties would influence the final

structure of the ice cream, we first focused on the overrun. As shown in Tab. 2.2, this parameter did not differ significantly among the series ($P > 0.05$), ranging from16 to 19 % in the fat content and emulsifier series, and from 18 % to 21 % in the coconut oil series. In general, a positive correlation has been found between overrun and the fat content or the degree of fat destabilization (Eisner, Wildmoser, & Windhab, 2005; Segall & Goff, 2002; Warren & Hartel, 2018), but this was not the case for our samples. This could be due to the fact that the ice creams in our study were produced with a batch freezer, instead of a continuous freezer, resulting in limited overrun development. This is consistent with the previous research by Muse & Hartel., (2004), in which it was shown that the use of a batch freezer did not allow for sufficient differences in overrun. Another possible cause of the low overrun could be the low viscosity of the mixes. As we did not add any hydrocolloids to the model recipes, the mixes thus had a lower ability to incorporate air cells during freezing. However, a limited variation in overrun represented a benefit for our study, as this allowed us to relate differences in melting properties to differences in the fat network.

2.3.2 Fat destabilization

The fat particle size in the molten ice creams was also determined as a measure of fat destabilization caused by the studied variations in fat properties. As shown in Fig. 2.1, we could only observe one peak (approximately 1 µm) in the ice cream mix of all three series, indicating that only single fat droplets were present in the ice cream mix. However, in most of the molten ice creams, a bimodal distribution could be found: one peak was present at 1-1.5 µm, referring to the single fat droplets, and an additional peak was visible starting at 10 µm, representing aggregated fat clusters, due to either aggregation or particle coalescence (Daw & Hartel, 2015). So, even though the overrun of the samples did not sensibly vary, the degree of fat destabilization and that of fat network formation were different.

To estimate the degree of destabilization, we used the mean size and volume percentage of the second peak to represent the fat aggregate size and percentage of fat aggregates, respectively (Warren & Hartel, 2018). For all three series, the size of fat aggregates and the percentage of fat aggregates are given in Tab. 2.3. For the fat content series, the fat aggregate size increased from 48.3 to 74.3 µm with increasing fat content. In addition, the percentage of fat aggregate also increased from 39 to 97 %. This effect of fat content on fat destabilization in ice cream is in good agreement with

previous findings, in which ice creams were formulated to contain 6-14 % fat, and for which the amount of fat destabilization increased from 35 % to 78 % (Rolon, Bakke, Coupland, Hayes, & Roberts, 2017). The larger degree of destabilization could be attributed to the higher number of fat droplets in the ice cream mix, providing a higher possibility of colliding with each other, resulting in more destabilization.

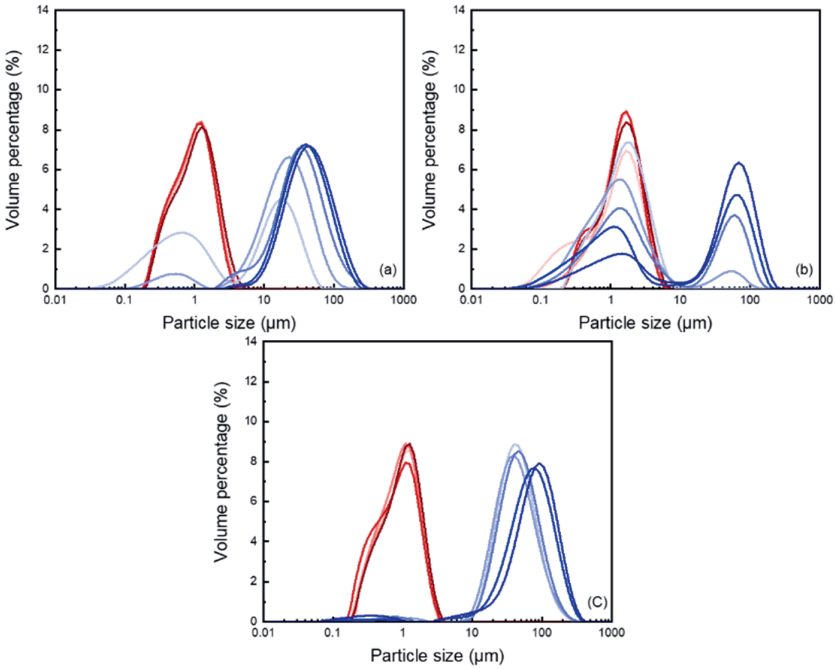

Fig. 2.1. Particle size distribution of ice cream mixes (red lines) and molten ice creams (blue lines) in a) FC-series, the colors of the line from light to dark refer to the fat content from 4 to 20 %, b) EC-series, the colors of the line from light to dark refer to the Tween 80 concentration from 0 to 0.25 %, and c) CO-series, the colors of the line from light to dark refer to the coconut oil concentration from 0 to 4.6 %.

In the emulsifier series, both the fat aggregate size (0-66 μm) and the fat aggregate percentage (0-66 %) increased with increasing emulsifier concentration. This was expected, as it is known that small molecular weight emulsifiers provide less stability against aggregation compared to proteins, which tend to form a thicker and more viscoelastic membrane at the oil/water interface (Fredrick, Walstra, & Dewettinck,

2010). In this series, WPI served as the emulsifier to stabilize the fat droplets, and T80 was added after the homogenization process. Thus, competitive adsorption of the emulsifiers decreases the strength of the adsorbed protein layer and induces fat particle destabilization (Munk, Erichsen, & Andersen, 2014). Without emulsifiers, WPI-stabilized emulsions were stable against aggregation and partial coalescence, as the fat particle size and fat aggregate percentage in EC-0 were 2 µm and 0 %, respectively. The maximum fat aggregate size (66.3 µm) and highest fat aggregate percentage (66 %) in this series were lower than the highest values in the fat content series (FC-20), which were 74 µm and 97 %, respectively. This means that the highest degree of fat destabilization in the EC series was lower than in FC-20.

Tab. 2.3. Overview of the parameters describing the degree of fat destabilization of the three studied series of ice cream.

Ingredients		Fat aggregate size (µm)	Fat aggregate percentage (%)
FC-series	FC-4	48.3 ± 2.3^{fg}	39.2 ± 3.1^{f}
	FC-8	52.0 ± 1.5^{def}	74.1 ± 3.3^{c}
	FC-12	55.2 ± 2.6^{d}	89.2 ± 2.5^{b}
	FC-16	62.4 ± 1.6^{c}	96.4 ± 2.6^{a}
	FC-20	74.3 ± 2.2^{b}	97.4 ± 1.9^{a}
EC-series	EC-0	$1..6 \pm 0.8^{j}$	0
	EC-0.1	7.8 ± 1.8^{i}	8.2 ± 1.6^{g}
	EC-0.15	36.4 ± 1.4^{h}	36.4 ± 1.4^{f}
	EC-0.2	48.8 ± 1.4^{efg}	49.3 ± 2.3^{e}
	EC-0.25	66.3 ± 1.3^{c}	66.1 ± 0.2^{d}
CO-series	CO-55	45.0 ± 0.3^{g}	98.2 ± 0.1^{a}
	C0-58	46.2 ± 0.5^{fg}	98.1 ± 0.9^{a}
	CO-62	54.4 ± 0.1^{de}	98.2 ± 0.3^{a}
	CO-65	75.9 ± 0.6^{b}	98.5 ± 1.2^{a}
	CO-68	89.2 ± 1.2^{a}	96.8 ± 0.8^{a}

Values with different letters within the same column are significantly different ($P < 0.05$)

In the coconut oil series, the total SFC was changed to vary the degree of partial coalescence. Compared with the other two series, the fat aggregate percentage in this series was consistently high (approximately 98 %) due to the extensive destabilization of the fat droplets, as they were stabilized by Tween 80 only and no proteins were

present. We also found that increasing the coconut oil content promoted an increase in fat aggregate size (45-89 μm), which can be attributed to the increased SFC. The increase in fat aggregate size with SFC has been described before (Rønholt et al., 2014).

In conclusion, the degree of fat destabilization in ice cream could be controlled by changing fat content and emulsifier concentration, or by changing the SFC. Both fat aggregate size and fat aggregate percentage increased with an increase in fat content and emulsifier concentration, while only fat aggregate size increased with increasing coconut oil content. Fat aggregate percentage was high and similar throughout the coconut oil series.

2.3.3 Fat particle distribution at the air cell interface and in the unfrozen serum phase

Due to different degrees of fat destabilization, the distribution of the fat particles within the frozen ice cream was expected to be different in the different series. To estimate how these particles were distributed within the system after the freezing process, the percentage of fat particles present around the air cells and in the unfrozen serum was calculated by taking the measured overrun and assuming complete surface coverage of the air bubbles by the fat droplets. From these values, the proportion of fat present in the unfrozen serum phase was then derived. For these estimations, we made some assumptions: the air cells were assumed to be stabilized only by single fat droplets, which could completely cover the air cell surface. Although it has been reported that the air cell interface included both discrete fat globules and clusters (Goff, Verespej, & Smith, 1999), it is hard to estimate the exact percentage of fat around the air cell interface. In this study, we use a more ideal situation in our estimations. The mean cell size was assumed to be 20 μm. This estimate is based on several studies, which have reported mean air cell sizes ranging from 12 to 30 μm (Muse & Hartel, 2004; Sofjan & Hartel, 2004; Warren & Hartel, 2018; Wu et al., 2019). As shown in Tab. 2.3, only single fat droplets (2 μm) were found in the EC-0 sample. Even though no fat aggregates were present, also this sample achieved an overrun similar to that of other samples containing fat aggregates, suggesting that both single fat droplets and fat aggregates could stabilize air cells. As mentioned above, the size of the fat droplets was measured to be approximately 1 μm in all series. The overrun was taken as 17 % in the fat content and emulsifier series, and 20 % in

the coconut oil series. This resulted in a fat content on the air cells of 3.6 % in the FC and EC series, and 4.8 % fat around the air cells in the CO series. These values were used to calculate the fat in the unfrozen serum phase. As shown in Tab. 2.4, for the fat content series, more fat droplets were present in the serum phase as the fat content increased. For example, in the sample with the lowest fat content of 4 %, nearly 94 % of fat droplets were adsorbed around the air cells, and only 6 % of fat remained in the serum phase. However, this value increased from 6 to 81 % in the ice cream with a fat content of 20 %. In the EC-series, 31 % of fat droplets were calculated to stabilize the air cells, and 69 % of fat was present in the serum phase. This was similar to the sample with 12% of the FC series. In the CO series with 12% fat, a slightly higher overrun (approximately 20 %) was observed, and therefore more fat droplets (40 %) were needed to stabilize the air cells.

Tab. 2.4. Distribution of the fat particles around the air cells and in the serum phase for the three series of ice cream.

Fat distribution	FC-series					EC-series	CO-series
	4 %	8 %	12 %	16 %	20 %		
Around the air cells (%)	94	47	31	23	19	31	40
In the unfrozen serum phase (%)	6	53	69	77	81	69	60

2.3.4 Observation of fat particles in the frozen ice cream (Cryo-SEM)

From the data obtained from the characterization of fat destabilization and our estimates of the distribution of fat within the ice cream, we found that fat droplets were mainly present as aggregated droplets, except for sample EC-0, which contained only single fat droplets. Therefore, EC-0 and FC-12 were selected to be further characterized by Cryo-SEM to visualize the difference between them, and to verify the presence of the aggregated fat droplets. Fig. 2.2a confirmed that the fat droplets in EC-0 did not aggregate and were only present as single particles. These results were consistent with the data from the fat aggregate size measurements. The fat structures in FC-12 fat are shown in Fig. 2.2b: in this ice cream, in which Tween 80 was the only emulsifier, the droplets were present in aggregated form. These aggregates were observed both at the air cell interface and within the unfrozen serum phase, in agreement with the result of others (Goff et al., 1999).

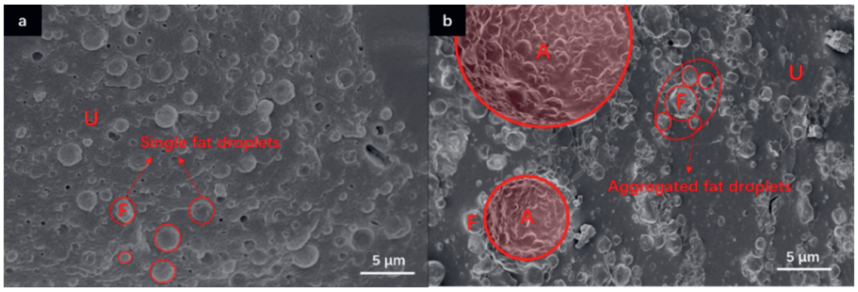

Fig. 2.2. SEM pictures of (a) EC-0 and (b) FC-12, in which both individual fat droplets and droplets at the surface of air cells are visible. Fat droplets (F), air cells (A) and unfrozen serum phase (U).

Based on the presented insights, in Fig. 2.3 we propose a schematic representation of the structures of the studied ice cream. In the case of WPI-stabilized emulsions (EC-0), single fat droplets were present around the air cells (31 %) and in the unfrozen serum phase (69 %). In the unfrozen serum phase of these samples, the single fat droplets without fat destabilization could not form a 3D fat network. For the sample with a higher degree of fat destabilization (FC-12), the higher amount of fat aggregates in the serum phase (around 69%) allowed the formation of a 3D network in the unfrozen serum phase. We assume that the aggregates were also interacting with the fat droplets attached to the interface. The air cells were therefore expected to be integrated within the network of the aggregated fat droplets.

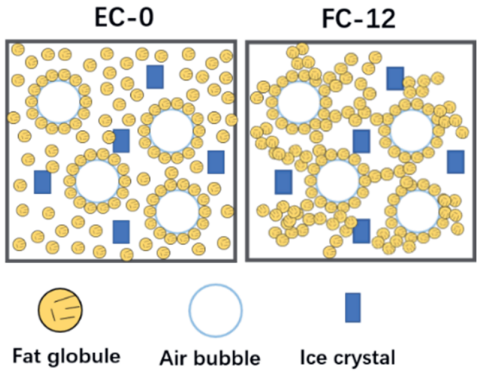

Fig. 2.3 Schematic representation of the fat destabilization in ice creams with the same fat content containing single fat droplets (EC-0) and aggregated fat droplets (FC-12).

2.3.5 Melting behavior

The effect of fat distribution and fat destabilization on the melting behavior of ice cream was clarified by analyzing the various parameters obtained during the melting test (melting rate, lag time, and melted percentage of the sample) for the different studied samples. In the fat content series (Fig. 2.4), a lower melting rate (from 1.7 to 0.6 %/min in Fig. 2.4a), a higher lag time (from 4 to 50 min in Fig. 2.4b), and a lower melted percentage (from 94 to 20 % in Fig. 2.4c) were observed with increasing fat content and degree of fat destabilization. These results were attributed to the formation of a stronger fat network within the ice cream. Increasing fat content led to a higher degree of fat destabilization and more fat droplets in the unfrozen serum phase, which resulted in the formation of a stronger fat network able to resist ice cream melting, which affected all three melting parameters. The results were consistent with previous studies in which it was shown that the melting rate was usually higher in low-fat ice cream (Akalın, Karagözlü, & Ünal, 2008; Akbari, Eskandari, Niakosari, & Bedeltavana, 2016; Sofjan & Hartel, 2004). In the other series, we kept the fat content constant (12%) and changed the degree of fat destabilization.

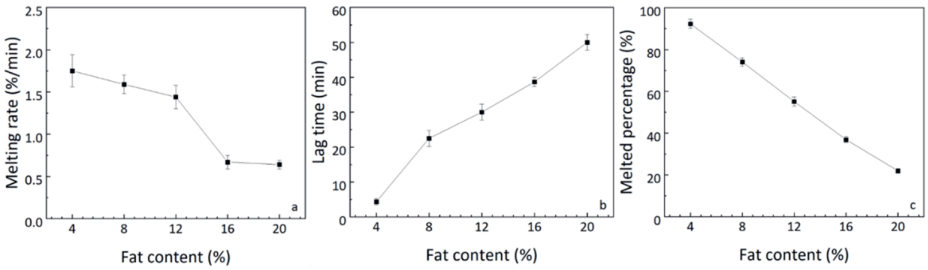

Fig. 2.4. Melting behavior as a function of fat content for the FC-series with a) melting rate (%/min), b) lag time (min), and c) melted percentage (%).

As shown in Fig. 2.5, with increasing emulsifier concentration (EC), both the melting rate and melting percentage decreased from 1.8 to 1.0 %/min and from 97 to 65 %, respectively. This shows that with increasing fat destabilization, the melting behavior changed even when the fat content was constant. These results indicate that degree of fat destabilization is more important than fat content in determining melting rate and melted percentage. However, the degree of fat destabilization displayed no apparent effect on lag time. This is inconsistent with previous findings, which showed that increasing fat destabilization increased the lag time (Wu et al., 2019). This

discrepancy is probably due to the fact that the fat destabilization degrees were relatively low in our EC-series, resulting in a relatively weak fat network compared with other series used in the literature. The weak network was probably not able to retard the initial loss of the serum phase. In addition, previous studies showed that in ice cream with a high overrun, melting was slower compared to low overrun samples, indicating that overrun is another factor affecting melting behavior (Warren & Hartel, 2018; Wu et al., 2019). The overrun in our samples was relatively low, and this may explain the fact that the lag time was similar for all samples. However, the overrun of the FC series was similar, but higher lag times were found, indicating that also for samples with low overruns, the fat network still had a significant effect on melting.

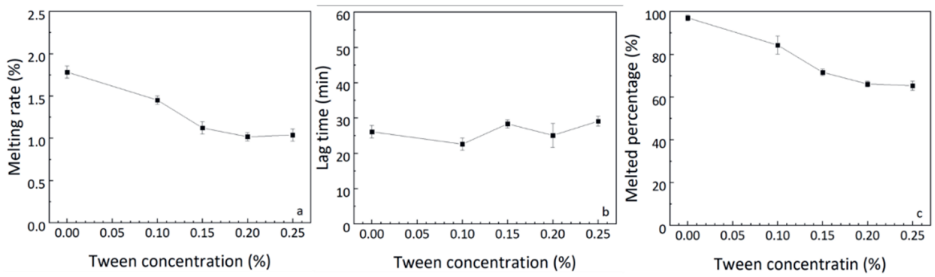

Fig. 2.5. Melting behavior as a function of tween concentration for the EC-series) with a) melting rate (%/min), b) lag time (min), and c) melted percentage (%).

The melting behavior of the coconut oil (CO) series is shown in Fig. 2.6. As the fat content was the same in all samples (12%), we expected the amount of fat aggregates present in the unfrozen serum phase (Tab. 2.4) to be similar to that of the EC series. However, a clear difference was found between the results of the EC series and those of the CO series. In the CO series, with increasing coconut oil content (i.e. increasing SFC) an increase in lag time, ranging from 33 to 48 min, was observed (Fig. 2.6b), whereas this was not observed in the EC-series. For the other two parameters, melting rate (Fig. 2.6a) and melting percentage (Fig. 2.6c), we did not observe an effect of the total SFC, which was also in contrast with the findings of the EC series. These results indicate that the amount of fat present in the unfrozen serum phase determines not only the melting properties, but also the specific characteristics of the fat aggregates and the network. As mentioned above, although the fat aggregate size increased from 45 to 89 µm in the CO-series, the fat aggregate percentage was very high and similar for all the samples of this series (approximately 98 %). We therefore expected that similar fat networks were formed in this series, resulting in similar melting rates and

melted percentages. In this case, the percentage of aggregates seems to be more important than the size of the aggregates in the formation of a 3D network. As these samples changed only in size of fat aggregates, but not in aggregates percentage, the lag time was mainly affected by the fat aggregate size. This would indicate that also the start of the melting depends on the fat network. Apparently, a larger aggregate size leads to a stronger initial network at the same level of aggregate percentage. This may be related to the SFC in the system. A higher SFC content could provide stronger interactions between the individual particles and the aggregates. In addition, the relation between fat aggregate size and lag time could also be attributed to the fact that the fat aggregate size also influences the ice crystal connectivity. In this case, the flow path of the serum phase as the ice melts would be more tortuous, as the fluid must travel around more obstacles (the numerous fat aggregates and ice crystals). This has been discussed to slow down the melting rate (Muse & Hartel, 2004).

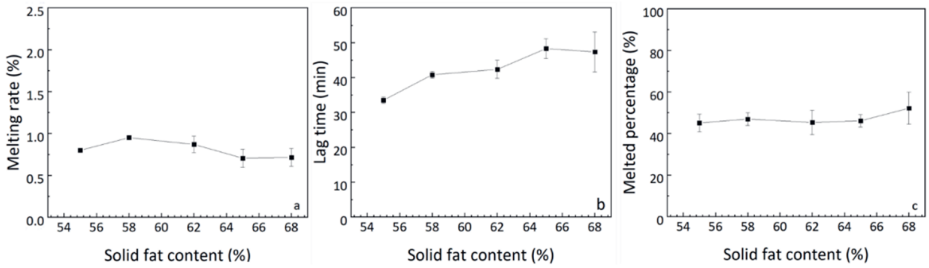

Fig. 2.6. Melting behavior as a function of SFC for the CO series with a) melting rate (%/min), b) lag time (min), and c) melted percentage (%)

By comparing the different results, we distinguished which features used to describe fat destabilization were the most dominant for a specific melting characteristic. An overview of these results is shown in Fig. 2.7. Taken together, both the degree of fat destabilization and the fat content appear to influence the melting behavior of the ice cream. From our results, we can conclude that the degree of fat destabilization or the fat network formed by the aggregated fat droplets seems to be more important than the fat content in affecting melting behavior. The lag time seems mostly related to the fat aggregate size, whereas melting rate and melted percentage seem more related to fat aggregate percentage.

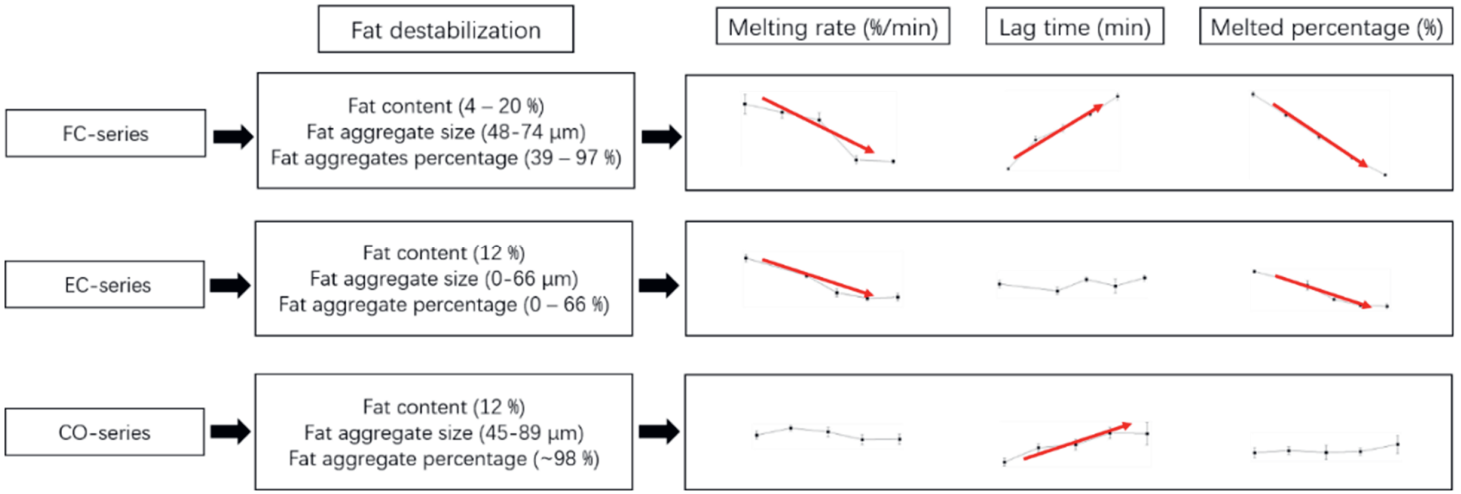

Fig. 2.7. Overview of the parameters describing the features used to characterize fat destabilization and their effect on the melting behavior of the three series of ice cream samples.

2.3.6 Fat distribution in the remaining phase

Our results show that the final amount of molten ice cream is inversely related to the extent of fat destabilization and network formation. Previous research has shown that the percentage of fat in the dripped portion during melting is a reliable indicator of the extent of destabilization (Goff & Spagnuolo, 2001). To identify how much fat and what type of fat particles (individuals or aggregates) were present in the fat network, we measured the percentage of fat in the dripped and remaining phases. In addition, at the end of the melting process, the size distribution of particles in the dripped phase was measured to identify which types of fat droplets were transferred during melting to the serum phase. In all studied samples, most of the particles were smaller than 1 μm (data not shown), indicating that during melting only single fat droplets dripped with the serum, whereas fat aggregates remained in the network.

To check a possible effect of the studied fat properties, we plotted for all three series the fat percentage in the remaining phase as a function of fat aggregate size and fat aggregate percentage (Fig. 2.8): with an increase in fat aggregate size, the percentage of fat in the remaining phase increased from 1 to 96 %. This confirms that larger aggregates are able to form a 3D network more easily. However, we also observed that an increase in fat aggregate size was not always necessary to incorporate more fat into the network. For example, with an increase in fat content from 4 to 12% in the FC series, the fat aggregate size increased only slightly, from 48 to 55 μm, whereas the fat percentage increased to a much larger extent, from 39 to 90 %. Oppositely, in the CO series, a fat percentage in the network of 98 % could be obtained already with a smaller fat aggregate size of 45 μm. So, a similar fat aggregate size did not lead to the same fat percentage in the remaining network. Interestingly, Fig. 2.8a shows that the fat percentage in the remaining phase was constant when the fat aggregates reached a certain critical size (approximately 45 μm). This indicates that a 3D fat network can be formed when the aggregates reach a specific size and are able to connect together. A critical size of fat aggregates of 1.15 μm was reported by Koxholt et al, (2001) to affect the melting properties to large extent. The authors attributed this to the ability of the fat aggregates to block the foam lamellae between the air cells, which impeded drainage, leading to a significantly lower meltdown rate. The critical size of fat aggregates found in our work indicates that fat aggregates formation depends on other characteristics of the ice cream structure and might be related to the thickness of the unfrozen serum phase, which can in turn be influenced by overrun

and composition of the unfrozen serum phase. In the research of Koxholt et. al., the overrun was 80 %, which resulted in thin lamellae between the air cells. Therefore, the critical size was small. In our study, the overrun of the samples was much lower (approximately 20 %), which led to thicker lamellae. Therefore, larger aggregates were formed and resulted in a thick network. Compared to our systems, the samples of Koxholt et. al. contained also other ingredients, such as non-fat milk solids, hydrocolloids and calcium. These additional ingredients may have also influenced the melting properties, and therefore a smaller critical size was already sufficient to provide a more stable structure. As we can see from Fig. 2.8b, a more linear relationship was found between fat aggregate percentage and the fat percentage in the remaining phases, indicating that a stronger fat network was formed when more fat droplets could aggregate. The amount of fat remaining in the network after melting was thus determined by the amount of fat that is initially present in aggregates.

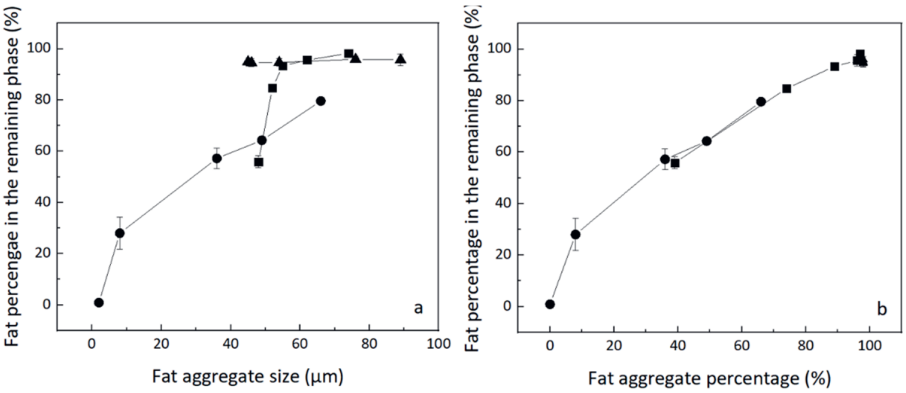

Fig. 2.8. Fat percentage in the remaining phase (FC-series (■), EC-series (●), CO-series (▲)): as a function of (a) fat aggregate size and (b) fat aggregate percentage.

In conclusion, fat distribution after melting depended on the fat destabilization degree, especially the fat aggregate percentage in the serum phase. Most of the single fat droplets dripped during melting, and the fat network mainly consisted of aggregated fat droplets. The percentage of fat aggregates was most likely related to the formation of a stronger fat network. In addition, the incorporation of the aggregates into the fat network seemed to be related to a certain critical fat aggregate size.

2.4 Conclusion

In this study, we controlled the fat destabilization degree and fat network formation of model ice cream by changing fat content (FC), emulsifier concentration (EC) and coconut oil content (CO). These factors were shown to have a significant influence on the melting behavior of ice cream. In all series, the overrun was similar, independently of the type of fat particles or fat network, indicating that both single fat droplets and fat aggregates can stabilize air cells. By investigating the effect of fat aggregate size and fat aggregate percentage on the microstructure and melting behavior, we showed the relative importance of fat destabilization and fat content on the melting properties of ice cream. Different fat destabilization parameters appeared to determine the melting behavior: the fat aggregate size was found to be the more dominant factor influencing the lag time, whereas the percentage of fat aggregates influenced the melting rate and melted percentage. The determination of the fat distribution showed that with an increase in fat aggregate size and aggregate percentage a stronger fat network was formed, and that the stability of the fat network was mainly determined by the percentage of fat aggregates. In addition, we found a critical size of the fat aggregates to form a 3D network, which is most likely related to the lamellae thickness between the air cells. The lamellae thickness depends on both the overrun and composition of ice cream. These results provide important insights into the role of fat on melting behavior, and can be used to design strategies for fat reduction in ice cream. Furthermore, to understand the effect of other structural features, also the effect of high overrun level, air cell distribution, and viscosity on the formation of fat network should be investigated.

References

Akalın, A. S., Karagözlü, C., & Ünal, G. (2008). Rheological properties of reduced-fat and low-fat ice cream containing whey protein isolate and inulin. *European Food Research and Technology, 227* (3), 889-895.

Akbari, M., Eskandari, M. H., Niakosari, M., & Bedeltavana, A. (2016). The effect of inulin on the physicochemical properties and sensory attributes of low-fat ice cream. *International Dairy Journal, 57*, 52-55.

Cheng, J., Dudu, O. E., Li, X., & Yan, T. (2020). Effect of emulsifier-fat interactions and interfacial competitive adsorption of emulsifiers with proteins on fat crystallization and stability of whipped-frozen emulsions. *Food Hydrocolloids, 101*, 105491.

Daw, E., & Hartel, R. W. (2015). Fat destabilization and melt-down of ice creams with increased protein content. *International Dairy Journal, 43*, 33-41.

Dhaygude, V., Soós, A., Zeke, I., & Somogyi, L. (2018). Comparison Between Static and Dynamic Analyses of the Solid Fat Content of Coconut Oil. *Hungarian Journal of Industry and Chemistry, 46* (2), 33-36.

Eisner, M. D., Wildmoser, H., & Windhab, E. J. (2005). Air cell microstructuring in a high viscous ice cream matrix. *Colloids and Surfaces A: Physicochemical and Engineering Aspects, 263* (1-3), 390-399.

Fredrick, E., Walstra, P., & Dewettinck, K. (2010). Factors governing partial coalescence in oil-in-water emulsions. *Advances in colloid and interface science, 153* (1-2), 30-42.

Goff, H. D., & Hartel, R. W. (2013). *Ice cream*: Springer Science & Business Media.

Goff, H. D., & Spagnuolo, P. (2001). ORIGINAL PAPERS-Effect of stabilizers on fat destabilization measurements in ice cream. *Milchwissenschaft, 56* (8), 450-453.

Goff, H. D., Verespej, E., & Smith, A. K. (1999). A study of fat and air structures in ice cream. *International Dairy Journal, 9* (11), 817-829.

Kokubo, S., Sakurai, K., Hakamata, K., Tomita, M., & Yoshida, S. (1996). The effect of manufacturing conditions on the de-emulsification of fat globules in ice cream. *Milchwissenschaft (Germany)*.

Kokubo, S., Sakurai, K., Hattori, M., & Tomita, M. (1994). Effect of drawing temperature at a freezer and overrun on de-emulsified fat of ice cream. *Nippon Shokuhin Kogyo Gakkaishi, 41* (5), 347-354.

Kokubo, S., Sakurai, K., Iwaki, S., Tomita, M., & Yoshida, S. (1998). Agglomeration

of fat globules during the freezing process of ice cream manufacturing. *Milchwissenschaft, 53* (4), 206-209.

Koxholt, M. M. R., Eisenmann, B., & Hinrichs, J. (2001). Effect of the fat globule sizes on the meltdown of ice cream. *Journal of dairy science, 84* (1), 31-37.

Lopez, C., Briard-Bion, V., Camier, B., & Gassi, J. Y. (2006). Milk fat thermal properties and solid fat content in emmental cheese: a differential scanning calorimetry study. *Journal of Dairy Science, 89* (8), 2894-2910.

Mahdian, E., & Karazhian, R. (2013). Effects of fat replacers and stabilizers on rheological, physicochemical and sensory properties of reduced-fat ice cream. *Journal of Agricultural Science and Technology, 15* (6), 1163-1174.

Munk, M. B., Erichsen, H. R., & Andersen, M. L. (2014). The effects of low-molecular-weight emulsifiers in O/W-emulsions on microviscosity of non-solidified oil in fat globules and the mobility of emulsifiers at the globule surfaces. *Journal of colloid and interface science, 419*, 134-141.

Muse, M. R., & Hartel, R. W. (2004). Ice Cream Structural Elements that Affect Melting Rate and Hardness. *Journal of Dairy Science, 87* (1), 1-10.

Pawar, A. B., Caggioni, M., Hartel, R. W., & Spicer, P. T. (2012). Arrested coalescence of viscoelastic droplets with internal microstructure. *Faraday discussions, 158* (1), 341-350.

Roland, A. M., Phillips, L. G., & Boor, K. J. J. J. o. D. S. (1999). Effects of fat content on the sensory properties, melting, color, and hardness of ice cream. *82* (1), 32-38.

Rolon, M. L., Bakke, A. J., Coupland, J. N., Hayes, J. E., & Roberts, R. F. (2017). Effect of fat content on the physical properties and consumer acceptability of vanilla ice cream. *Journal of Dairy Science, 100* (7), 5217-5227.

Rønholt, S., Buldo, P., Mortensen, K., Andersen, U., Knudsen, J. C., & Wiking, L. (2014). The effect of butter grains on physical properties of butter-like emulsions. *Journal of Dairy Science, 97* (4), 1929-1938.

Segall, K. I., & Goff, H. D. (2002). A modified ice cream processing routine that promotes fat destabilization in the absence of added emulsifier. *International Dairy Journal, 12* (12), 1013-1018.

Sofjan, R. P., & Hartel, R. W. (2004). Effects of overrun on structural and physical characteristics of ice cream. *International Dairy Journal, 14* (3), 255-262.

Sung, K. K., & Goff, H. D. (2010). Effect of solid fat content on structure in ice creams containing palm kernel oil and high-oleic sunflower oil. *Journal of food science, 75* (3), C274-C279.

Warren, M. M., & Hartel, R. W. (2014). Structural, compositional, and sensorial properties of United States commercial ice cream products. *Journal of food science, 79* (10), E2005-E2013.

Warren, M. M., & Hartel, R. W. (2018). Effects of emulsifier, overrun and dasher speed on ice cream microstructure and melting properties. *Journal of food science, 83* (3), 639-647.

Wu, B., Freire, D. O., & Hartel, R. W. (2019). The effect of overrun, fat destabilization, and ice cream mix viscosity on entire meltdown behavior. *Journal of food science, 84* (9), 2562-2571.

Chapter 3

Structural and functional differences between ice crystal-dominated and fat network-dominated ice cream

Published as: Liu, X., Sala, G., & Scholten, E. (2023). Structural and functional differences between ice crystal-dominated and fat network-dominated ice cream. *Food Hydrocolloids*, 138, 108466.

Abstract

In this study, we investigated the effect of overrun, fat destabilization degree and ice crystal size on viscoelastic behavior, hardness and melting properties of ice cream by changing only one parameter at a time. To vary the degree of fat destabilization, we changed the emulsifier type; to modify overrun and ice crystal size, we used either a batch freezer or liquid nitrogen freezing upon whipping. Fat destabilization degree, overrun and ice crystal size were measured to determine the structural differences between the studied samples. Furthermore, viscoelastic behavior upon increasing strain and temperature were evaluated by oscillatory rheology. Hardness and meltdown tests were performed to explore the role of different microstructural elements. Depending on the composition of the ice cream, we identified two main types of structures: one dominated by the ice crystals, and one dominated by a fat network. The results showed that the ice crystal-dominated structure contributed more than the fat network to viscoelastic behavior and hardness, whereas the fat network had a larger effect on the melting process. Only a limited effect of ice crystal size on the properties of the ice cream was seen, independently of the kind of dominated structure. In both types of ice cream, overrun had a large effect on mechanical properties, but only in ice crystal-dominated samples it also affected melting. This research provides a better understanding of the role of multiple structural elements in ice cream, which can be used for its reformulation.

3.1 Introduction

Ice cream is generally described as having "a complex microstructure consisting of air cells, ice crystals, and a network of coalesced fat droplets entrapped in a thick continuous phase" (Scholten, 2014). The structural elements in ice cream can be divided into four categories: (1) fat phase (fat content and degree of fat destabilization), (2) air phase (air cell size and overrun), (3) ice phase (ice crystal size and ice fraction), and (4) unfrozen serum phase. Among these structural elements, fat content and ice fraction can be easily controlled by adding different amounts of fat and varying the ratio between sugar and water, which also determines the final unfrozen serum phase. In addition, the concentration and the type of emulsifier influence the degree of fat destabilization. The addition of emulsifiers helps to destabilize the emulsion, as they are claimed to displace proteins from the interface, thereby creating a thinner interface favoring coalescence. This increases the extent of fat partial coalescence and also influences overrun (Warren & Hartel, 2018). However, many factors in ice cream do not just depend on the composition, but also on the production process. For example, the shear stresses exerted during the freezing process influence the size of the air cells (Chang & Hartel, 2002), that of the ice crystals (Russell, Cheney, & Wantling, 1999), and fat destabilization (Goff & Jordan, 1989). In addition, the rate of cooling leads to faster ice crystallization, which also has an effect on the final ice crystal size. The microstructure of ice cream depends therefore on both its composition and production process.

The microstructure of ice cream is responsible for its viscoelastic behavior, hardness and melting properties, which are important quality parameters. For example, the fat network formed by fat aggregates has been shown to greatly decrease the melting rate of ice cream and promote shape retention (Tharp, Forrest, Swan, Dunning, & Hilmoe, 1998; Warren & Hartel, 2014). Also the overrun and the ice crystal size can influence melting. The melting behavior is governed by the heat transfer from the warmer environment to the ice cream. As air is a good insulator, ice cream with low overrun has been found to melt quickly, whereas ice creams with high overrun have a good melting resistance (Warren, et al., 2018). However, this contradicts the results found by Muse & Hartel (2004), who showed that overrun did not appear to affect the melting rate. Heat transfer is also in part affected by the ice crystals, but also in this case conflicting results can be found in literature. Muse et al. (2004) found that the melting rate increased as ice crystal size increased, which was attributed to the less

tortuous flow path of the serum phase created by large ice crystals. However, no clear correlation could be found between ice crystal size and melting rate in the study of Amador et al. (2017). Even though many studies have been performed, the contradictory indications reported in literature show that there is still limited understanding of how the microstructural factors of ice cream influence melting. This is often related to the fact that in published studies many parameters are changed at the same time, which makes it challenging to extract their exact effects.

Besides melting, also hardness is an important quality parameter of ice cream. The hardness of ice cream is affected by overrun, ice crystal size and fat network. Also for hardness, contradictory results related to air content have been reported (Muse, et al., 2004; Prindiville, Marshall, & Heymann, 1999). This was attributed to differences in secondary effects (ice crystal size, etc.), highlighting again that information on the role of the individual microstructural features of ice cream is difficult to obtain. Also in the case of ice crystal size, conflicting results were found (Sakurai, 1996; Sofjan & Hartel, 2004). In some cases, larger ice crystals have been shown to increase hardness, while in others they lead to a decrease in hardness. Contradicting results have also been seen for the effect of the degree of fat destabilization. Destabilized fat was found to provide a network among the air cells in ice cream, thereby increasing hardness (Muse, et al., 2004). However, another research showed that no significant correlation was found between destabilized fat and hardness. This was again attributed to a secondary effect, as differences in ice crystal size were also found (Amador, et al., 2017). Overall, it is clear that each structural element (overrun, fat destabilization degree and ice crystal size), individually or in concomitance with others, affects viscoelastic behavior, hardness and melting properties of ice cream. However, it is difficult to gain insight into the relative importance of the different structural elements on these properties. For a better understanding of the physics of ice cream, these elements have to be controlled separately.

The main aim of this study was to unveil the individual role of fat network, overrun and ice crystal size in determining viscoelastic behavior, hardness and melting properties of ice cream by changing only one of these characteristics at a time, while keeping the others constant. To manipulate the degree of fat destabilization and thus alter the fat network, two different surfactants were chosen. Tween 80 served as the emulsifier to induce fat aggregation or partial coalescence. On the other hand, whey protein isolate (WPI) was used to strongly stabilize the fat droplets, resulting in

limited fat destabilization. Furthermore, two freezing methods, a batch freezer or freezing with liquid nitrogen, were used to manipulate overrun and ice crystal size. Fat content and viscosity of the unfrozen serum phase were kept constant. In addition, sugar type and ratio sugar: water were kept the same in all ice creams to guarantee that all samples had the same ice fraction. Fat destabilization degree, overrun and ice crystal size were measured separately to characterize the microstructural differences between the studied samples. X-Ray Tomography (XRT) was used to visualize the structural differences of ice creams with different overrun levels. Furthermore, we applied strain sweep and temperature sweep oscillatory rheology to identify the structure changes during small deformation and melting. Hardness tests were performed to explore the role of different microstructural elements at large deformation. The meltdown properties of samples were also determined to clarify the effect of different structural elements on melting.

3.2 Materials and methods

3.2.1 Materials

Anhydrous milk fat was kindly donated by FrieslandCampina (Wageningen, Netherlands). Whey protein isolate (WPI, 88.8 % protein content) was purchased from Davisco (USA). Tween 80 (P4780) and sucrose were both purchased from Signa-Aldrich (Netherlands). Kerosene was purchased from a local store (Action, Wageningen, Netherlands). Liquid nitrogen was obtained from SOL GROUP (the Netherlands). Ultrapure water, purified by a Millipore Milli-Q system (Darmstadt, Germany), was used for the preparation of all samples.

3.2.2 Mix preparation

Two emulsions containing either Tween 80 or WPI as emulsifier were prepared. For the Tween 80-stabilized emulsion, a stock emulsion of 12 % AMF was prepared. AMF was melted at 65 °C and then added to a 0.3 % (w/w) Tween 80 solution containing 16.55 % sucrose. For the WPI emulsion, WPI (4 %) was added to water while stirring and was allowed to hydrate for 1 h at room temperature. AMF was melted at 65 °C, and was added at a concentration of 12 % to the WPI solution containing 15.85 % sucrose. Both emulsions were prepared by pre-homogenization with an Ultra Turrax at a speed of 13000 rpm for 2 min and then homogenized by a homogenizer (Delta Instruments LaboScope Homogenizer HU-3.0, USA) at 13 MPa

for one cycle and 11 MPa for 3 cycles. The mixes were cooled to 25 °C and aged at 4 °C overnight.

3.2.3 Ice cream preparation

Ice cream samples were made with two freezing methods to vary the overrun and ice crystal size. According to the first method, the ice cream mix (1 L) was frozen in a batch freezer (Frigomat T4S-T5S, Italy) for 10 min to a drawing temperature of approximately -10 °C. The overrun was measured after freezing and the obtained ice cream was collected into 250 ml containers and hardened at -20 °C for 24 h. According to the second method, the ice cream mix (1 L) was first whipped with a milk frother (KitchenSpecials, Netherlands) with a fixed speed for 2 min, after which the mix was poured into a Mixer (Bosch MFQ36460, Netherlands). Liquid nitrogen was gradually added during shearing to gradually decrease temperature. During the process, samples with a constant volume were taken to determine the weight of the ice cream and the corresponding overrun. Ice creams with varying overrun (30, 60 and 90 %) were collected in plastic containers or rings of different sizes to form solid ice cream cylinders for different measurements and were hardened at -20 °C for 24 h. An overview of the studied ice cream samples is shown in Tab. 3.1. The samples are coded according to the process used (BF: batch freezer, LN: liquid nitrogen), overrun (30, 60 or 90 %) and the emulsifier used (WPI or T80).

Tab. 3.1. Overview of the studied ice cream samples.

Series		Sample code
WPI series	Ice cream mix	MIX-WPI
	LN series	LN-90-WPI
		LN-60-WPI
		LN-30-WPI
	BF series	BF-30-WPI
T80 series	Ice cream mix	MIX-T80
	LN series	LN-90-T80
		LN-60-T80
		LN-30-T80
	BF series	BF-30-T80

3.2.4 Overrun

The overrun of ice cream pre-mix foam (whipped ice cream mix) and frozen ice cream was determined by first weighing a fixed volume of the aged pre-mix in a metal cup. Next, the same volume of either whipped ice cream mix or ice cream was weighted in the cup directly after whipping or ice cream preparation. The overrun was quantified as (Muse et al., 2004):

$$\text{Overrun (\%)} = \frac{Weight\ of\ mix - weight\ of\ ice\ cream}{Weight\ of\ ice\ cream} \times 100 \quad (3.1)$$

3.2.5 Particle size distribution

The fat particle size distribution of the pre-mix and molten ice cream was measured with static light scattering (Mastersizer 2000, Malvern Instruments, Ltd, Malvern, Worcestershire, UK), using a refractive index of 1.46 and 1.33 for the fat and the water, respectively. The initial fat globule size was obtained from the peak of the pre-mix. From the bimodal distribution of the molten ice cream, we extracted two additional parameters, according to the results of **Chapter 2** (Liu, Sala, & Scholten, 2022). The mean particle size of each individual peak ($D_{4,3}$) was determined separately, and the volume percentage of the second peak was used to reflect the degree of fat destabilization as fat aggregate percentage. Measurements were performed at room temperature and repeated in triplicate.

3.2.6 Ice crystal size

The analysis of ice crystal size was modified according to the method described by Velásquez-Cock et al. (2019). A light microscope with a hot stage (Zeiss Axioskop 2 Plus, Germany) was used to observe the ice crystals. The temperature of the hot stage was set at -20 °C, and all tools, reagents and samples were kept at -20 °C before the samples were prepared. Five mg of ice cream were taken from the core section of each container with a sharp knife and deposited over a standard glass slide. One or two drops of kerosene were applied to disperse the ice crystals more evenly, and the glass slide was covered with a chilled cover slide. The ice crystals were spread out gently by tapping the cover slide with chilled tweezers. The whole sample preparation process was carried out in a -20 °C storage room to prevent the melting of the ice crystals. The radius of the ice crystals was determined from these images assuming the ice crystals to have a spherical shape. A circle was placed around the ice crystals

manually, from which the area and radius of the circle were determined by the software ZEN 2011. Ice crystal images were taken at 10x magnification to acquire at least 300 ice crystals to calculate the mean ice crystal radius and standard deviation of the samples.

3.2.7 Microstructure evaluation by X-ray Tomography

To visualize differences in structure, two samples (LN-30-T80 and LN-90-T80) were evaluated with X-ray Tomography (XRT). A cylindrically-shaped ice cream sample of 1.5-2 cm in height and 1 cm in diameter was extracted by pressing plastic tubes into the frozen ice cream. Samples were stored at -20 °C before measurements. An X-ray Tomograph (GE phoenix v[tome] x m 240, United States) fitted with a nano-focus head and a 100kV/10W transmission target was used to observe the three-dimensional structure of the frozen ice cream samples. A custom-made isolated sample holder equipped with an ice-filled bucket was cooled to -20 °C to keep the ice cream samples in a frozen state. The samples were loaded into the holder and scanned at 90 kV and 320 μA. Approximately 1800 projections were taken during a full rotation of 360° and the exposure time of each projection was 333 ms, with filtering turned off, and shift and auto scan optimizer enabled. The collected images were reconstructed into a three-dimensional representation using reconstruction software (GE Phoenix dataosx rec) with 1800x1800x1000 pixels. The mean size of the air cells and the thickness of the non-air phase were analyzed by Avizo 2019.4 after further processing.

3.2.8 Oscillatory rheology

The rheological evaluation of frozen ice cream was performed with a Physica MCR 501 rheometer (Anton Paar, Germany), using a plate-plate geometry (PP50/P2). A moveable hood covering the plate-plate geometry was connected to the cooling system to control the temperature of the plate. An air pump was also connected to the hood to prevent heat exchange with the environment. Ice cream tablets (-20 °C) of 5 mm height and 25 mm diameter were taken out of the metal rings using a cylindrical cutting tool and were transferred to the plate (PP50) immediately. The initial force was set at 5 N to guarantee that the upper plate touched the sample tightly before starting the measurements. The gap width between the plates was adjusted to a constant value of 3 mm, which was small enough to keep contact between the probe and the sample during the entire duration of the measurements. Strain sweeps were

carried out in a strain range from 0.0001 to 10 %, at a frequency of 1.6 Hz (which was in the linear viscoelastic regime) and at a temperature of -10 °C to keep the ice cream at the frozen state. Storage modulus (G') and loss modulus (G'') were measured and were plotted as a function of strain.

Temperature sweeps were used to characterize the melting process of studied ice cream with increasing temperature (-20 to 10 °C). Measurements were performed at a constant deformation of 0.005 % and a frequency of 1.6 Hz with a plate-plate geometry (PP50/P2). Prior to the measurement, the temperature of the plate was reduced to -20 °C. The temperature was increased from -20 to 10 °C with a heating rate of 0.5 °C/min. Sixty measuring points were recorded with 1 min between measuring points. At least two measurements for each ice cream sample were carried out. G' and G'' were plotted as a function of temperature.

3.2.9 Hardness

The hardness of the samples was measured with a Texture Analyzer (TA-TX plus, Stable Micro Systems, UK). Samples with the same volume were prepared using plastic rings. The dimensions of the samples were 25 mm in height and 60 mm in diameter. The samples were stored in a freezer at -20 °C for a minimum of 24 h. Prior to the measurement, a climate chamber was connected to the Texture Analyzer to maintain a temperature of -20 °C. The samples were taken out of the plastic rings using a cylindrical cutting tool and transferred to the climate chamber immediately. Then the samples were measured using an aluminum cylinder probe (10 mm in diameter) attached to a 50 kg load cell and were penetrated to a strain of 50 % at a speed of 2 mm/s. Instrumental hardness was defined as the maximum peak force during penetration of each sample.

3.2.10 Melting test at room temperature

The melting properties of the samples were measured at room temperature (20 °C). Samples with the same volume were prepared using plastic rings with 25 mm height and 60 mm diameter. Prior to measurements, the samples were stored overnight in a freezer at -20 °C. Then the samples were taken out of the rings and placed on a 136x136 mm metal grid with 5x5 mm holes representing 44 % of the total area of the metal grid. The starting weight of each sample was measured and a collection cup

was placed on a measuring scale underneath the mesh. The weight of the molten sample was measured every 10 s, at a temperature of 20 °C, for a duration of 240 min. Three phases could be identified during the whole melting process: (i) a lag phase, (ii) a fast-melting phase, and (iii) a plateau phase. The lag phase corresponds to the phase until the first droplet dripped, from which the lag time (min) was obtained. The fast-melting phase corresponds to the phase between the end of the lag phase and the beginning of plateau phase, from which the melting rate (%/min) was determined from the slope. From the plateau phase, representing the phase after complete melting, the melted percentage (%) was determined as the loss of total ice cream after complete melting. The measurements were performed in duplicate.

3.2.11 Statistical analysis

The data were analyzed by SPSS software (Version 25.0, IBM Corp). The means were compared using a Duncan's test at a 5 % level of significance using the analysis of variance (ANOVA).

3.3 Results and discussion

3.3.1 Variations in overrun

Variations in the overrun of the different samples were obtaining by applying different ice cream making procedures. In samples made with a batch freezer, the overrun increased within 3 min to around 30 % (data not shown) and then remained constant with increasing freezing time (10 min). This method allowed to obtain ice cream with constant overrun. On the other hand, the liquid nitrogen freezing process optimized for our research allowed to obtain samples with varying overrun. According to this process, liquid nitrogen was added into pre-whipped ice cream mixes. The gradual addition led to a decrease in temperature from 4 to -4 °C with a much slower cooling rate, as a limited amount of liquid nitrogen was added at a time (the ratio liquid nitrogen: pre-mix was kept around 1:30). This process resulted in higher overrun values, and with increasing processing time these values gradually decreased. Specifically, the overrun decreased from 240 to 30 % in the WPI series (Fig. 3.1a), while a less pronounced decrease, from 110 to 30 %, was seen in the T80 series (Fig. 3.1b). The difference in the evolution of the overrun can be attributed to the different stability of the air cells. In the WPI series, the air cells were mainly stabilized by fat droplets and whey protein, while in the T80 series the air cells were stabilized by fat

droplets, fat droplet aggregates and Tween 80. The higher ability of whey protein to stabilize air cells resulted in a higher initial overrun in the WPI series. As freezing proceeded, the air cells in the WPI series were progressively more destabilized and the overrun decreased. Although the initial overrun in the T80 series was lower, the aggregation of the fat droplets provided more stability to the air bubbles, and therefore the decrease in overrun was more limited. For both the WPI and T80 series, we could collect samples with different overrun (approximately 30, 60 and 90 %) by sampling at different times during processing, as indicated in Fig. 3.1 with red circles. At the moment of collection, the ice content was different, but after the hardening step, it was the same in all samples, as the ratio sugar: water was kept the same.

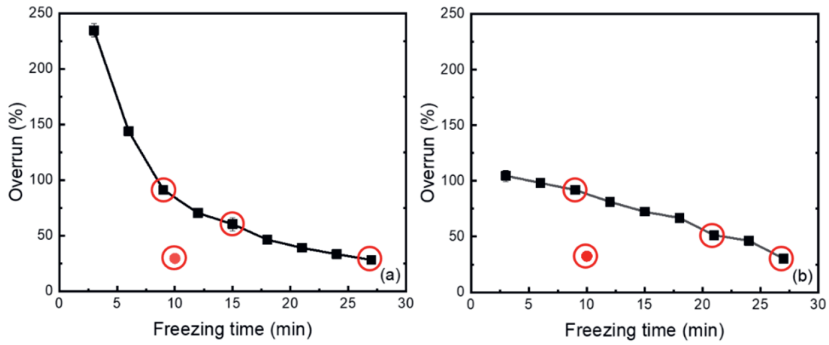

Fig. 3.1. Overrun changes in (a) WPI and (b) T80 ice cream series during freezing in a batch freezer (BF) and with liquid nitrogen (LN). LN: black squares, BF: red dot. The times of sample collection are highlighted with red circles.

3.3.2 XRT analysis for ice cream microstructure

To obtain information on the structural organization of the air cells and the non-air phase, we analyzed two representative ice cream samples with X-ray tomography. As this method relies on density differences between phases, we were only able to distinguish between the dispersed air phase and the non-air phase, but no information on the fat phase could be obtained. We selected a sample with 30 % overrun and one with 90 % overrun from the T80 series. The results are shown in Fig. 3.2. From the image reconstruction, the mean size of air cells and the mean distance between air cells (thickness of non-air phase) were quantified. The sample with low overrun was of course much denser, with a mean air cell size of 34 µm, and a mean thickness of the non-air (serum) phase between the air of 178 µm. For higher overrun (90 %), the

structure was more open, with a mean air cell size of 165 µm, and a much lower thickness of the non-air (serum) phase of 69 µm. Similar indications were reported by Koxholt, Eisenmann, & Hinrichs (2001), who showed that higher overrun leads to thinner lamellae between the air cells.

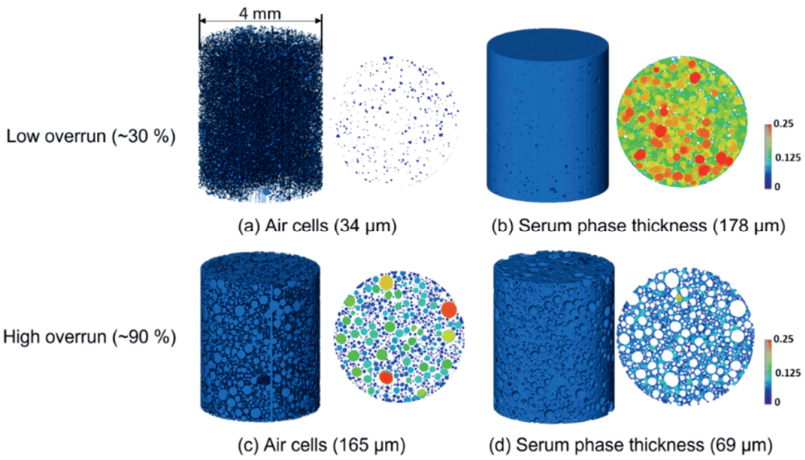

Fig. 3.2. Images of the 3D microstructure of ice creams with different overrun level from the T80 series. The air and non-air phase were examined for the mean size of the air cells, and the thickness of the (non-air) serum phase. The dimensions of the cylinders were 4.5 mm in height and 4 mm in diameter. The warmer (red) colors indicate higher values of air cell size or serum phase thickness and colder (blue) colors indicate lower values.

3.3.3 Variations in fat destabilization

The degree of fat destabilization in the WPI and T80 series was determined by measuring the fat particle size distribution of pre-mix and molten ice cream. As shown in Fig. 3.3, a bimodal distribution was found for both the WPI series (Fig. 3.3a) and the T80 series (Fig. 3.3b). The first peak (0.01 to 10 µm) corresponded to the single fat droplets, and the second peak to aggregated fat droplets with a size over 10 µm. From these results, two parameters were used to quantify the fat destabilization degree: (1) mean fat particle size ($D_{4,3}$), and (2) fat aggregate percentage (determined from the second peak), which are summarized in Tab. 3.2 for both series.

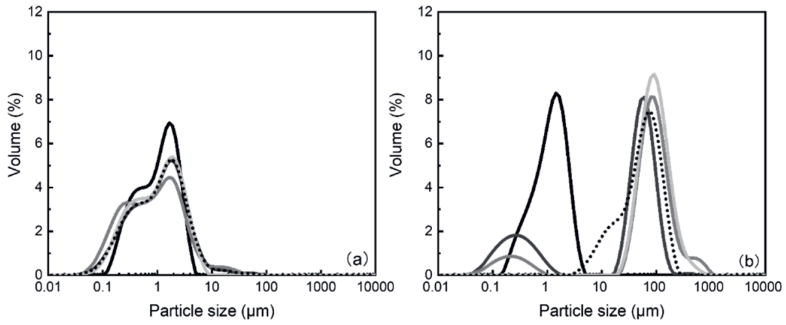

Fig. 3.3. Fat particle size distribution of the (a) WPI and (b) T80 ice cream series (including mix and molten ice cream). MIX: black line; LN-90: dark grey; LN-60: grey; LN-30: light grey; BF-30: black dotted line.

In the WPI series, limited fat destabilization took place, independently of the freezing process, and samples with different overruns also had similar particle size distribution (Fig. 3.3a). In the curves of Fig. 3.3, a small shoulder/ peak with a mean size around 0.2 μm could be observed, which could be attributed to whey protein aggregates present in the continuous phase. As shown in Tab. 3.2, the particle size ranged from 1.4 to 2.6 μm, and the fat aggregate percentage was less than 3.9 %. Comparatively, in the T80 series (Fig. 3.3b), a higher degree of fat destabilization was found for both freezing processes. This was expected, as it is known that small molecular weight emulsifiers (T80) provide less stability against aggregation compared to proteins, which tend to form a thicker and more viscoelastic membrane at the oil/water interface (Fredrick, Walstra, & Dewettinck, 2010). The mean fat particle size of the T80 ice creams made with liquid nitrogen ranged between 44 and 107 μm, and the percentage of fat aggregates ranged between 72 and 100 %. This can be explained by the increasing processing time, as it has been found that the degree of fat destabilization in ice cream is influenced by shear forces and freezing time (Chang, et al., 2002). Samples with higher overrun had a lower total freezing time, and showed therefore a lower degree of fat destabilization. In addition, in the T80 ice cream samples prepared with the batch freezer and low overrun (BF-30-T80), the $D_{4,3}$ and the percentage of fat aggregates were 62 μm and 94 %, respectively. These values were relatively low compared with those of the liquid nitrogen ice cream sample at the same overrun level (LN-30-T80), which were 107 μm and 100 %. This difference can also be attributed to the longer freezing time with the liquid nitrogen freezing process. Thus, both the emulsifier type and freezing time were used to control the degree of fat destabilization.

Tab. 3.2. Mean particle size and degree of fat destabilization of the WPI and T80 ice cream series.

Ingredients		Mean particle size, $D_{4,3}$ (μm)	Fat aggregate percentage (%)
WPI series	Mix	1.2 ± 0.1^{e}	0
	LN-90-WPI	2.6 ± 0.2^{e}	0
	LN-60-WPI	1.7 ± 0.1^{e}	3.1 ± 0.2^{e}
	LN-30-WPI	1.4 ± 0.1^{e}	3.9 ± 0.1^{e}
	BF-30-WPI	2.0 ± 0.1^{e}	2.4 ± 0.3^{ef}
T80 series	Mix	1.5 ± 0.1^{e}	0
	LN-90-T80	44 ± 2^{d}	72 ± 1^{d}
	LN-60-T80	85 ± 7^{b}	84 ± 2^{c}
	LN-30-T80	107 ± 9^{a}	100^{a}
	BF-30-T80	62 ± 1^{c}	94 ± 1^{b}

Values with a different letter within the same column are significantly different ($P < 0.05$).

3.3.4 Ice crystal size

The ice crystal size of the samples was expected to mainly be influenced by the freezing process. In fact, as shown in Tab. 3.3, for the WPI series, the average crystal radius was 22 μm for samples made with the batch freezer (BF-WPI), and approximately 41 μm for samples made with liquid nitrogen (LN-WPI), regardless of the overrun. For the T80 series, the ice crystal radii of samples made with the batch freezer (BF-T80) and liquid nitrogen (LN-T80) were 29 and 52 μm, respectively. For both series, the liquid nitrogen freezing process resulted in larger ice crystals than the batch freezer. These results were in contradiction with a previous study, in which liquid nitrogen provided smaller ice crystals (Goff & Hartel, 2013). These differences can be explained by the cooling rate. Although liquid nitrogen can lead to fast ice crystal nucleation due to its very low temperature, the cooling rate is actually determined by the ratio between pre-mix and liquid nitrogen. As we only added a very limited amount of liquid nitrogen at a time, the cooling rate was much lower than that in the batch freezer. A lower cooling rate thus resulted in larger ice crystals. In addition, the longer freezing time could be another reason for the inconsistency between our results and those of Goff & Hartel (2013), as a longer processing time has been shown to produce ice creams with larger ice crystals due to the greater extent of recrystallization (Drewett & Hartel, 2007; Russell, et al., 1999).

Tab. 3.3. Mean radius of the ice crystals in the T80 and WPI ice cream series.

Ingredients		Ice crystal radius (µm)
WPI series	LN-90-WPI	39 ± 6^{abc}
	LN-60-WPI	41 ± 9^{abc}
	LN-30-WPI	42 ± 6^{abc}
	BF-30-WPI	22 ± 6^{c}
T80 series	LN-90-T80	47 ± 12^{ab}
	LN-60-T80	52 ± 6^{a}
	LN-30-T80	57 ± 13^{a}
	BF-30-T80	29 ± 7^{bc}

Values with a different letter within the same column are significantly different ($P < 0.05$).

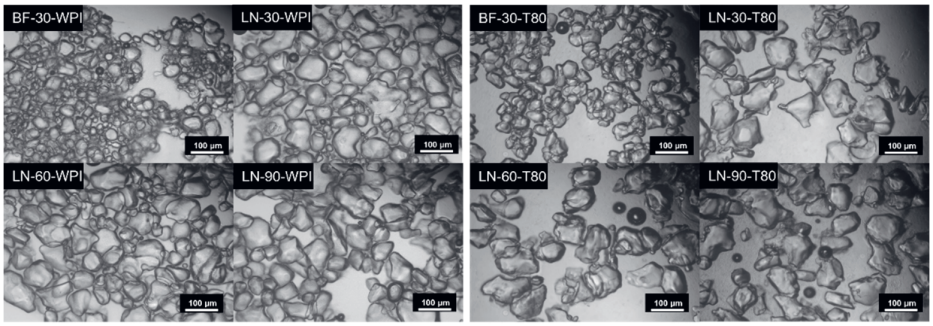

a. WPI series b. T80 series

Fig. 3.4. Images of ice crystals in the (a) WPI and (b) T80 ice cream series. Top left: samples prepared with a batch freezer (BF). Top right: samples made with liquid nitrogen (LN) with an overrun of 30 %. Bottom: samples made with LN with 60 % (left) and 90 % (right) overrun.

Some differences in ice crystal size could also be found between the T80 and the WPI series. Ice cream of the latter series (Fig. 3.4a) showed small ice crystals, whereas the T80 series contained slightly larger ice crystals (Fig. 3.4b). As the ice faction was the same in all studied samples, the number of ice crystals was higher in samples with smaller ice crystals. This most probably led to a higher ice connectivity in the WPI samples. As in the T80 series a fat network was formed by destabilized fat aggregates, we could also speculate that the contact frequency among ice crystals was reduced, resulting in lower ice connectivity and larger ice crystals. Therefore, samples with WPI had smaller ice crystals with higher ice connectivity, whereas T80 samples had

large ice crystals with low ice connectivity. These results showed that in our samples, next to overrun and fat destabilization degree, also ice crystal size could in fact be controlled.

3.3.5 Dominating structure in the two series

To get insights in the dominating structures present in the studied samples, we examined their shape retention after melting for 3 h, which is related to the formation of a fat network remaining behind at the end of the melting process (**Chapter 2**). As shown in Fig. 3.5, a significant difference in shape retention could be found between the two series. The samples of the WPI series presented a low ability to retain their structure due to a limited degree of fat destabilization, while the samples of the T80 series showed strong shape retention after melting. As both series had the same fat content, we can conclude that the main reason leading to the different shape retention was the different degree of fat destabilization, which resulted in a significantly different microstructure in the two series.

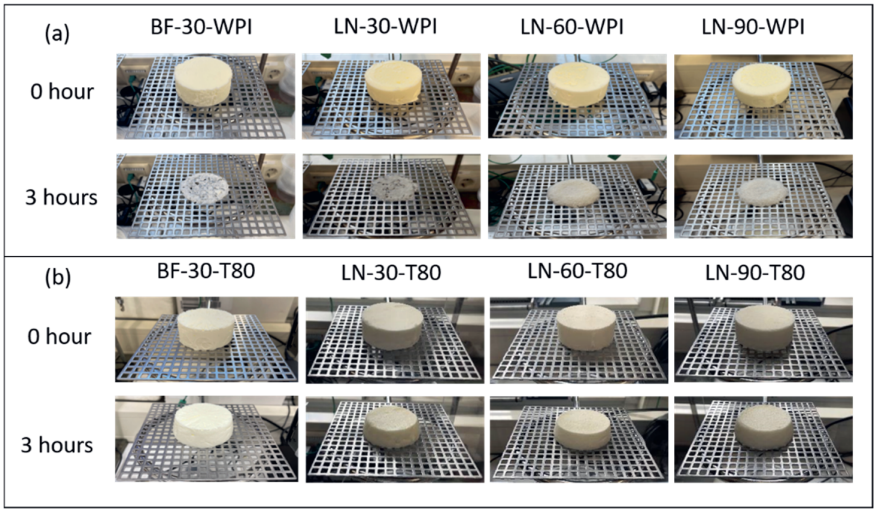

Fig. 3.5. Shape retention of the (a) WPI and (b) T80 ice cream series after 3 h melting at 20 °C. From left to right: samples prepared with the batch freezer (BF) with 30 % overrun, and samples prepared with liquid nitrogen (LN) with 30 %, 60 % and 90 % overrun.

Based on the results presented above, in Fig. 3.6 we propose a schematic

representation of the microstructure of the WPI and T80 ice creams. In the case of the WPI series, the dominant structure was formed by the ice crystals due to the limited degree of fat destabilization. The ice crystal structure was formed by the smaller ice crystals and a higher ice connectivity between the smaller crystals (Fig. 3.6a). In comparison, in the case of the T80 series, a high degree of fat destabilization resulted in a fat network-dominated structure, in which ice crystals and air cells acted as fillers (Fig. 3.6b). Thus, at the same fat content and ice fraction, ice creams with two significant different microstructures were identified, by which we could clarify the separate contribution of fat network, overrun and ice crystal size.

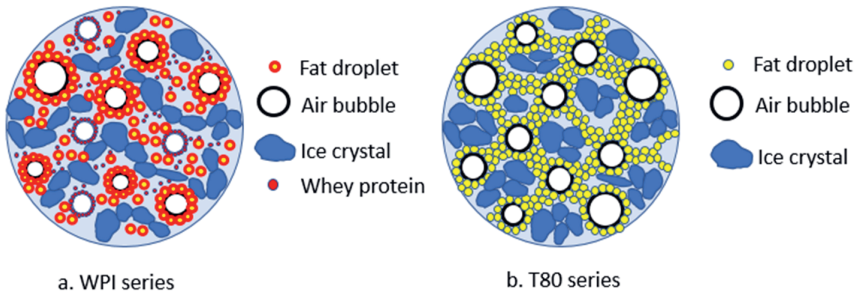

Fig. 3.6. Schematic representation of the (a) ice crystal-dominated structure (WPI series) and (b) fat network-dominated structure (T80 series). This figure is not drawn to scale.

3.3.6 Effect of structure on viscoelastic behavior

Using different ingredients and freezing processes, we were able to control the different microstructural elements of our samples. To unveil how their intrinsic arrangement and the interactions among them affected the viscoelastic behavior of the ice cream, we measured G' and G" as a function of the applied strain (Fig. 3.7). To gain insights in the role of the fat network, we compared BF-30-WPI (black circles) and BF-30-T80 (grey circles), which had a similar ice crystal size ($P > 0.05$) and the same overrun (30 %), but a different fat destabilization degree (Fig. 3.7a). BF-30-WPI, the sample with a lower degree of fat destabilization, showed a longer linear viscoelastic regime (LVR) than BF-30-T80. In addition, although the G' and G" were similar at low strain (lower than 0.002 %), they decreased less with increasing strain for BF-30-WPI than for BF-30-T80. The difference can be explained by the

difference in the dominating contribution. The sample with a higher contribution of the ice crystal structure and the weaker fat network (BF-30-WPI) presented the most solid like properties (higher G') upon increasing deformation.

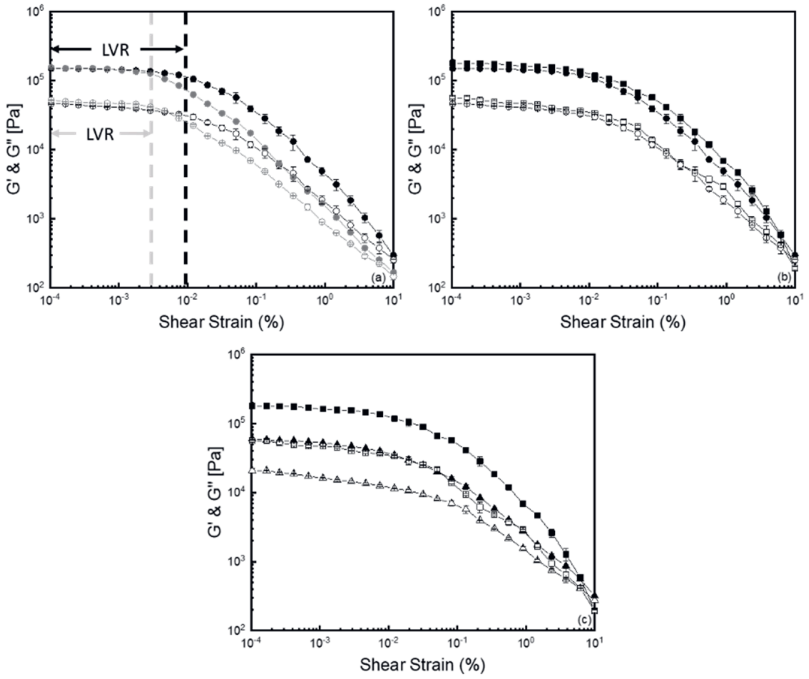

Fig. 3.7. Storage modulus (G') and loss modulus (G'') as a function of strain for samples with different structural elements. (a) Samples with varying fat destabilization degree: BF-30-WPI (black circles) and BF-30-T80 (grey circles); (b) samples with varying ice crystal size: LN-30-WPI (black squares) and BF-30-WPI (black circles); (c) samples with varying overrun: LN-30-WPI (black squares), and LN-90-WPI (black triangles). G' is provided as solid symbols, and G" as empty symbols. WPI series are shown as black color, and T80 series as grey color.

To clarify the effect of ice crystal size on the viscoelastic behavior of the WPI series, we compared the moduli of LN-30-WPI (black squares) and BF-30-WPI (black circles), which had similar limited degree of fat destabilization and overrun (30 %), but a different ice crystal size (42 and 22 μm). As shown in Fig. 3.7b, within the whole strain range, similar G' and G'' could be found for both samples. The solid-like properties were thus more determined by the total ice content, and the ice crystal size

or connectivity had limited effect. A similar trend could also be found in the T80 series (Fig. S3.1a in supplementary material): the sample LN-30-T80 with larger ice crystal size and a higher degree of fat destabilization showed similar G' and G'' as BF-30-T80 within the whole strain range. The fat aggregates could reduce the connectivity of the ice crystals even further, but the differences between the samples were limited.

In addition, by comparing the viscoelastic behavior of LN-30-WPI (black squares) and LN-90-WPI (light grey squares), which had a similar ice crystal size (approximately 40 μm) and degree of fat destabilization, but a different overrun of 30 and 90 %, respectively, the effect of overrun on the viscoelastic properties could be identified. As can be seen from Fig. 3.7c, within the whole strain range, LN-30-WPI showed higher values of G' and G'' than LN-90-WPI. The higher moduli for samples with lower overrun could be attributed to the formation of a more connected ice crystal structure in the LN-30-WPI sample. Ice cream with a lower overrun was expected to have a thicker serum phase, which would lead to more contacts among ice crystals. Similarly, LN-30-T80, with lower overrun but higher degree of fat destabilization, also showed higher values of G' and G'' than LN-90-T80 within the whole strain range, but the differences between these two samples decreased with increasing strain (Fig. S3.1b supplementary material). The smaller difference between G' and G" can be explained by the effect of the fat network on the ice crystal-dominated structure. The sample with a higher overrun had a lower degree of fat destabilization and thus a weaker fat network, which had a lower influence on ice crystal connectivity. Therefore, the difference in the connectivity between the ice crystals between low and high overrun samples was smaller. As discussed above, the viscoelastic properties of ice cream were dominated by the ice crystal structure, and, therefore, a smaller difference between G' and G'' was expected between LN-30-T80 and LN-90-T80 (Fig. S3.1b supplementary material), as both samples have a fat-dominated network. The effect of rheological and structural components (mix viscosity, overrun and fat destabilization) on the viscoelastic properties of ice cream was also reported by Freire, Wu, & Hartel (2020). In this article, $G'_{-15°C}$ was used to characterize the viscoelastic properties of the ice cream. In this paper, $G'_{-15°C}$ was strongly correlated with mix viscosity, but did not appear to significantly relate to overrun and fat destabilization. An inverse correlation was found between mix viscosity and $G'_{-15°C}$, and the authors attributed this to a loss in connectivity among ice crystals as a result of the presence of a serum phase in which the polysaccharides

were highly entangled (as result of freeze concentration of the serum phase). Due to the high viscosity of their samples, they did not see any effects of overrun and fat destabilization. However, when the effect of viscosity is reduced, which is the case in our study, a clear inverse correlation can be observed between overrun and G' in both the ice crystal-dominated and fat network- dominated series. As discussed above, this can be explained by a loss in connectivity among ice crystals due to high overrun values. In addition, although no clear effect of fat destabilization on G' and G'' could be found within the LVR, we could observe that fat destabilization had a negative effect on the G' and G'' with increasing strain, clarifying that fat destabilization mainly plays a role upon large deformation.

In conclusion, the viscoelastic properties of ice cream were mainly determined by the ice crystal structure. The effect of ice crystal size on the viscoelastic behavior of both series was limited. However, the overrun had a larger effect on the viscoelastic moduli of samples with an ice crystal-dominated structure, due to a secondary effect of the influence of the fat network on the connectivity between ice crystals. Increasing overrun weakened the structure of ice crystals and thus led to lower viscoelastic moduli. Although oscillatory rheology has not been extensively used in ice cream research, our results showed that this technique can provide valuable information on the structural organization of this food.

3.3.7 Hardness

As evidenced with oscillatory shear experiments, the different structural elements of the samples affected the strength of the structure and the resistance against collapse after melting of the ice fraction. The ice crystal-dominated structure was shown to contribute the most to the solid-like behavior, and was thus expected to strongly influence also the hardness of the ice cream. The hardness of both the WPI and the T80 series was determined by performing penetration tests. As shown in Fig. 3.8, in both series, samples with smaller ice crystals (BF samples, dark grey) had hardness similar ($P > 0.05$) to that of samples with the same overrun but larger ice crystals (LN-30, black), indicating that ice crystal size did not affect hardness. The connectivity among ice crystals, therefore, does not seem to affect ice cream structure at large deformation.

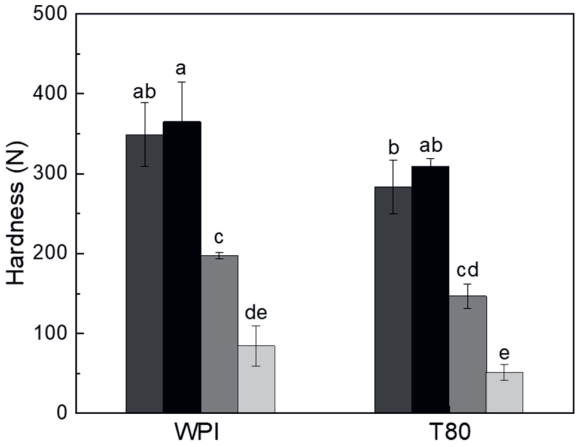

Fig. 3.8. Hardness of the WPI and T80 ice cream series. BF-30-WPI and BF-30-T80 (dark grey), LN-30-WPI and LN-30-T80 (black), LN-60-WPI and LN-60-T80 (grey), LN-90-WPI and LN-90-T80 (light grey). Values with a different letter above the bars are significantly different ($P < 0.05$).

A clear effect of overrun was observed in Fig. 3.8. For both the WPI and T80 series, the lowest hardness was observed in high overrun ice creams (90 %, light grey bars), and its value increased when the overrun decreased (30 %, black bars). This relationship has been reported by many researchers (Biasutti, Venir, Marino, Maifreni, & Innocente, 2013; das Graças Pereira, de Resende, de Abreu, de Oliveira Giarola, & Perrone, 2011; Syed, Anwar, Shukat, & Zahoor, 2018). Limited differences were observed between the WPI and T80 series, indicating that the type of dominated structure had a negligible effect on hardness. In both ice crystal-dominated and fat network-dominated structures, the effect of overrun on hardness was similar, by limiting the formation of either structure. In spite of this, we did see some effect of fat destabilization on hardness. Samples with a higher fat destabilization degree (T80 samples) and with similar overruns had a slightly lower hardness than samples without fat destabilization (WPI series). This could be attributed to the fact that the fat network (in T80 samples) was less solid compared with the ice crystal-dominated structure. In addition, a higher degree of fat destabilization could limit the formation of an ice crystal-dominated structure even further. The lower connectivity between ice crystals in T80 samples thus led to reduced hardness. This finding is consistent with the results found with oscillatory shear experiments, in which higher moduli were found with increasing strain in samples with a more extended ice crystal-

dominated structure (WPI samples). Therefore, it can be concluded that the ice crystal-dominated structure plays a major role in determining hardness.

3.3.8 Structure changes during melting

The results discussed above show that in our samples the ice crystal structure had the largest effect on hardness. The effect of the microstructure during melting was also evaluated by measuring G' and G" as a function of temperature. Fig. 3.9 shows the structural changes of ice creams with either an ice crystal-dominated (BF-30-WPI) or a fat network-dominated (BF-30-T80) structure. All measurements were carried out within the LVR, and in the obtained curves three zones can be identified; (1) zone I, from -20 to -3 °C: in this temperature range the solid behavior of the sample dominates the rheological properties as the ice cream is still in its frozen state; (2) zone II, between -3 to 4 °C: in this region, the moduli show a steep decrease, which indicates the fast-melting state of the ice cream; (3) zone III, from 4 to 10 °C: within this zone, the rheological behavior of ice cream is dominated by the microstructure of the molten ice cream (Eisner, Wildmoser, & Windhab, 2005).

As shown in Fig. 3.9, in zone I, similar G' and G'' were observed for the ice creams with different degrees of fat destabilization, indicating that ice crystals and a fat network had a similar contribution to the viscoelastic properties at small deformation. This result was consistent with the data from the strain sweep within the LVR (Fig. 3.7a). Although in the frozen state the effect of microstructure was limited, larger effects were seen in the fast-melting state (zone II). A fast and early decrease of both G' and G" was seen for the sample dominated by an ice crystal structure (black symbols). However, for samples dominated by a fat network, the decrease in G' and G'' occurred mainly at higher temperature, which corresponded to a slower melting. This result indicated that the formation of a fat network had a significant influence on the melting process. In addition, the fat network was also able to entrap the serum phase, which was reflected by the relatively lower melting rate and melted percentage (Fig. 3.5). As a matter of fact, when fat droplets are present as a 3D network, drainage of the serum phase is prevented. This result is in agreement with studies by other authors (Warren, et al., 2014, 2018). In zone III, all samples melted completely. Due to the 3D network of fat particles, G' and G" were still high in samples with a fat network dominated structure, whereas samples with an ice crystal-dominated structure showed much lower G' and G", as limited fat destabilization was present.

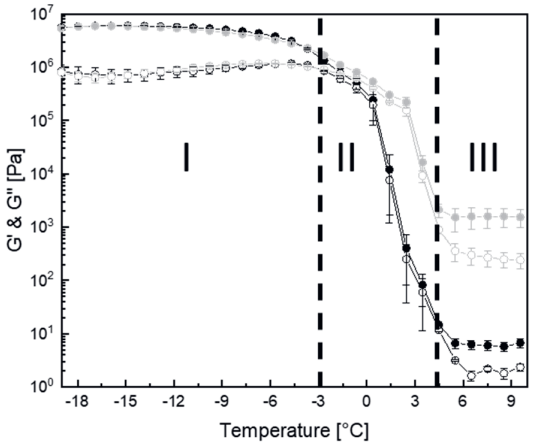

Fig. 3.9. Storage modulus (G') and loss modulus (G'') as a function of temperature for samples with two different structures as a result of different fat destabilization degree. Ice crystal-dominated structure: BF-30-WPI (black circles); fat network-dominated structure, BF-30-T80 (grey circles). G' is provided as solid symbols, and G'' as empty symbols.

To clarify the effect of ice crystal size on structure changes during melting, we compared samples of both the WPI (Fig. 3.10a) and T80 series (Fig. 3.10b) with a low overrun of 30 %, prepared with either a batch freezer (BF) or liquid nitrogen (LN), and thus with different ice crystal size. As shown in Fig. 3.10a, for WPI samples, similar G' and G'' were observed in ice creams with different ice crystal size in all three zones. These results showed that ice crystal size did not have a significant influence on the melting process. As also concluded from the results of the oscillatory shear experiments, the structure of the ice crystals was dominated by ice content, and ice crystal size had limited influence. Also for the T80 samples (Fig. 3.10b), where the fat network was more prominent, similar G' and G'' were found. However, at higher temperatures, differences in G' and G'' started to appear, especially in zone III. Higher values were found for samples with larger ice crystals. This could be attributed to the fact that the fat aggregate percentage was also higher in the sample with a larger ice crystal size. As the ice crystals melted, the 3D fat network slowed down the melting process. Due to the disappearance of the ice crystals and their connectivity, the contribution of the fat network became more relevant.

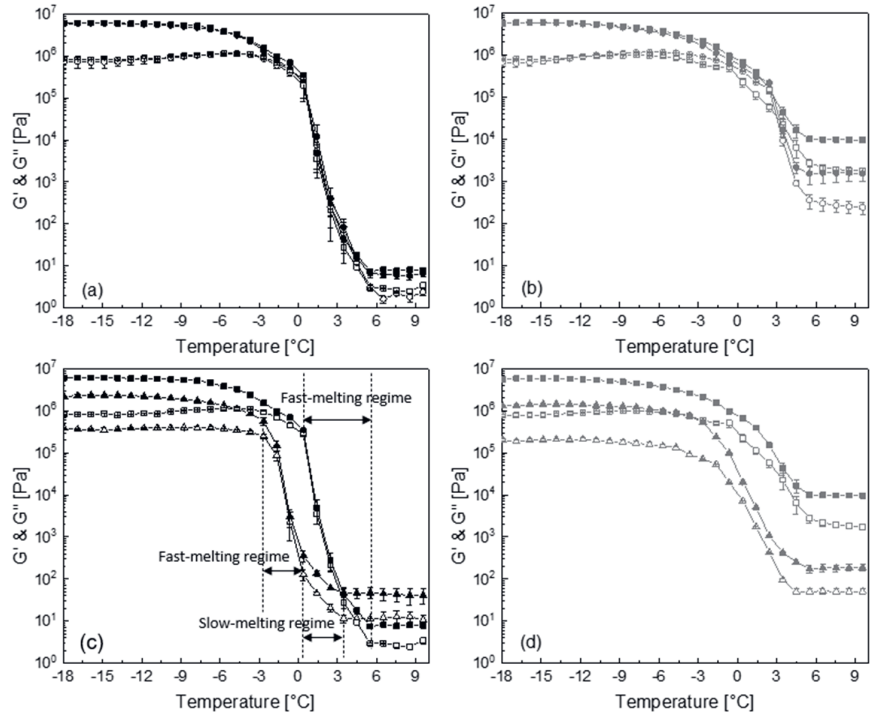

Fig. 3.10. Storage modulus (G') and loss modulus (G'') as a function of temperature for samples with different structural elements. Samples with varying ice crystal size; (a) WPI series: LN-30-WPI (black squares) and BF-30-WPI (black circles) and (b) T80 series: LN-30-T80 (grey squares) and BF-30-T80 (grey circles). Sample with varying overrun; (c) WPI series: LN-30-WPI (black squares), and LN-90-WPI (black triangles), and (d) T80 series: LN-30-T80 (grey squares) and LN-90-T80 (grey triangles). G' is provided as solid symbols, and G" as empty symbols.

The effect of overrun could be clarified by comparing samples with different overrun (30 % and 90 %) in both the ice crystal- and fat-dominated series. As shown in Fig. 3.10c, for WPI samples with higher overrun (triangles), lower values for G' and G'' were observed in zone I. As discussed in section 3.3.4, the overrun significantly influenced the thickness of the lamellae between air cells: a higher overrun corresponded to larger air cell size, leading to thinner lamellae. This negatively affected the connectivity among ice crystals, which explained the lower values of the moduli. Due to the lower connectivity between the ice crystals, the moduli also started to decrease at a lower temperature, i.e. melting started earlier. However, at higher

temperature, the melting slowed down, and therefore, two different melting regimes (fast-melting and slow-melting regime) were seen in zone II for the sample with high overrun. The low overrun sample (squares) showed only one fast-melting regime, but the melting started later (higher temperature). Although many results in literature claim that air is a good insulator and slows down the rate of heat transfer to the ice cream (Sofjan, et al., 2004; Wu, Freire, & Hartel, 2019), our results clarified that the structure obtained by the ice crystals seems to be more important for initial melting than the overrun, and that the overrun mainly slows down melting at a later stage. The differences between our results and those of other authors concerning the effect of overrun on melting may be explained by differences in serum phase viscosity. In studies of other authors, polysaccharides were often added to the recipe and thus led to a high serum phase viscosity, which could stabilize the air cells during the melting process. However, in our study, no polysaccharides were used. The lower serum phase viscosity provided lower stability to the air cells, leading to a faster escape once the structure determined by the ice crystals collapsed. In the T80 series with a fat network-dominated structure, only one melting regime was found in zone II (Fig. 3.10d) and the melting was much slower. This again shows that the fat network had a strong influence on the melting rate. In these samples, overrun had a larger effect. The sample with higher overrun (triangles) started to melt at lower temperature and faster (higher slope of moduli curves). The faster melting is consistent with the samples of the WPI series, and contradicts the findings by others. For example, Warren et al. (2018) showed that ice creams with high overrun had a good melting resistance, due to the good insulating properties of air. These results show that not only the overrun is important, but that the network or structure in which the air is incorporated plays a larger role. In the study of Warren, the sample with higher overrun also corresponded with a higher level of fat partial coalescence. However, in our case, a lower degree of fat destabilization was found in the high overrun sample. As shown in Fig. 3.2, the thickness of the lamellae between air cells was 178 µm for the low overrun sample, and 69 µm for the high overrun sample, and the fat aggregate size was 107 and 44 µm, respectively (Tab. 3.2). These results show that the stronger fat network in the thicker serum phase had a higher ability to resist melting, even though these samples have a lower overrun. The effect of air is thus very much dependent on the specific structure of the sample. In zone III, higher values of G' and G'' were found for the high overrun WPI sample, indicating the air cells were able to provide some structural integrity when molten. However, higher values were found for the T80 samples with lower overrun, as it had a stronger fat network.

3.3.9 Melting properties

We also measured the melting properties of the different ice creams using a common test carried out at room temperature during which three melting parameters were determined: melting rate, lag time, and melted percentage of ice cream. Ice crystal-dominated samples (WPI series) exhibited a significantly different melting behavior than fat network-dominated samples (T80 series). As shown in Tab. 3.4, for the fat network-dominated series, longer lag time, lower melting rate and lower melted percentage were found compared to the samples in which ice crystals were more dominant ($P < 0.05$). These results were consistent with the melting behavior obtained from temperature sweep measurements, where samples of the T80 series showed a higher initial temperature and a lower melting rate. This confirmed that in our sample a fat network played a larger role in affecting the melting process than the structure obtained by the ice crystals.

Tab. 3.4. Overview of melting parameters of ice creams in WPI and T80 series.

Samples		Lag time (min)	Melting rate (% / min)	Melted percentage (%)
WPI series	LN-90-WPI	12.2 ± 1.7^{d}	2.3 ± 0.3^{a}	97.6 ± 2.0^{a}
	LN-60-WPI	12.8 ± 2.1^{d}	2.3 ± 0.1^{a}	98.4 ± 0.9^{a}
	LN-30-WPI	16.2 ± 0.7^{c}	2.2 ± 0.1^{a}	99.2 ± 0.6^{a}
	BF-30-WPI	17.9 ± 1.8^{c}	2.1 ± 0.1^{a}	98.0 ± 0.4^{a}
T80 series	LN-90-T80	18.0 ± 0.2^{c}	1.2 ± 0.2^{b}	40.6 ± 1.0^{c}
	LN-60-T80	23.2 ± 0.9^{b}	1.0 ± 0.1^{bc}	41.2 ± 1.8^{c}
	LN-30-T80	29.4 ± 1.3^{a}	0.7 ± 0.1^{c}	44.8 ± 0.5^{b}
	BF-30-T80	29.9 ± 0.8^{a}	1.1 ± 0.1^{b}	46.7 ± 1.2^{b}

Values with a different letter within the same column are significantly different ($P < 0.05$).

In the WPI series, dominated by the structure of ice crystals, ice crystal size (comparing LN-30-WPI and BF-30-WPI) did not appear to have a significant effect on melting rate, lag time and melted percentage ($P > 0.05$). These results were consistent with the observations in zone II in Fig. 3.10a, and contradict those obtained by Muse et al. (2004), who reported that the melting rate increased as ice crystal size increased. However, in their study, these samples varied also in degree of fat destabilization and overrun, making it difficult to draw firm conclusions on the role of ice crystal size. In our samples, only ice crystal size varied, and therefore, a direct

link with the melting behavior could be made. Our results show that ice crystal size itself has limited influence, and that the structure obtained by the ice crystals or fat network plays a more important role. The limited influence of ice crystal size was also seen in the T80 series, where lag time and melting percentage ($P > 0.05$) for sample LN-30-T80 and BF-30-T80 were similar. However, a small effect of ice crystal size on melting rate was observed. We propose that this was an indirect effect of difference in the fat network.

The overrun had a larger effect on the melting properties. In ice crystal-dominated systems, by comparing LN-90-WPI and LN-30-WPI, it could be concluded that increasing overrun decreased the lag time from 16.2 to 12.2 min. This result was in line with the findings in zone II in Fig. 3.10c. As discussed before, the lower lag time could be attributed to a lower connectivity between ice crystals. These results thus confirmed that in our samples the ice crystal-dominated structure was more important than the overrun for the start of the melting process, even though overrun has always been claimed to slow down melting. However, samples with different overrun showed similar melting rate and melted percentage, which seemed to be inconsistent with the observations in Fig. 3.10c. This was probably due to the different conditions during the melting process. When ice cream melts on a mesh screen, air cells can easily escape due to the collapse of the structure obtained by connecting ice crystals. However, during rheology measurements, the structure is more confined, leading to a slow-melting regime in Fig. 3.10c. For fat network-dominated systems, the effect of overrun was more pronounced. For samples with higher overrun (LN-90-T80), lag time decreased and melting rate increased. These results were consistent with the observations in Fig. 3.10d. A stronger fat network formed in the sample with a lower overrun (LN-30-T80) significantly delayed the melting process, which confirmed that the fat network is more important than overrun in resisting the melting.

By combining data obtained on a mesh screen with those derived from temperature sweeps, we could conclude that the presence of a fat network played a dominant role in determining the melting behavior. For fat network-dominated ice cream, all melting parameters were determined by the degree of fat destabilization, and overrun played a limited role. For ice crystal-dominated ice cream, the ice crystal structure was also more important than the overrun, but only at an early melting stage. At later stages when the structure of connecting ice crystals disappeared, the overrun could slow down the melting if air cells were well stabilized.

3.4 Conclusion

In this study, the role of fat destabilization degree, overrun and ice crystal size in determining the viscoelastic behavior, hardness and melting properties of ice cream was investigated. The structural factors were altered independently, which allowed us to extract the role of the individual factors. Due to differences in fat destabilization, ice creams with two significantly different microstructures were identified: an ice crystal-dominated structure and a fat network-dominated structure. For the ice crystal-dominated ice cream, changing ice crystal size had limited influence on viscoelastic moduli, hardness and melting behavior. Increasing overrun induced a loss of connectivity between ice crystals and thus led to lower viscoelastic moduli and hardness. The lower connectivity between ice crystals also caused earlier melting of the ice cream in the initial melting stage. At later stages of melting, higher overrun was able to slow down the melting process, leading to a two-step melting process. The ice crystal-dominated structure was shown to contribute more than the fat network to the solid-like properties of ice cream. For fat network-dominated structures, ice crystal size had limited effect. Overrun did affect hardness, but to a lesser extent than for the ice crystal-dominated samples. However, the fat network played a more dominant role in the melting properties. As a higher overrun disrupted the fat network, higher values of this parameter led to faster melting, even though overrun is generally assumed to slow down melting. These results revealed that the effect of the fat network on the melting behavior was more prominent than the effect of overrun.

References

Amador, J., Hartel, R., & Rankin, S. (2017). The effects of fat structures and ice cream mix viscosity on physical and sensory properties of ice cream. Journal of food science, 82(8), 1851-1860.

Biasutti, M., Venir, E., Marino, M., Maifreni, M., & Innocente, N. (2013). Effects of high pressure homogenisation of ice cream mix on the physical and structural properties of ice cream. International Dairy Journal, 32(1), 40-45.

Chang, Y., & Hartel, R. W. (2002). Development of air cells in a batch ice cream freezer. Journal of Food Engineering, 55(1), 71-78.

das Graças Pereira, G., de Resende, J. V., de Abreu, L. R., de Oliveira Giarola, T. M., & Perrone, I. T. (2011). Influence of the partial substitution of skim milk powder for soy extract on ice cream structure and quality. European Food Research and Technology, 232(6), 1093-1102.

Drewett, E. M., & Hartel, R. W. (2007). Ice crystallization in a scraped surface freezer. Journal of Food Engineering, 78(3), 1060-1066.

Eisner, M. D., Wildmoser, H., & Windhab, E. J. (2005). Air cell microstructuring in a high viscous ice cream matrix. Colloids and Surfaces A: Physicochemical and Engineering Aspects, 263(1-3), 390-399.

Fredrick, E., Walstra, P., & Dewettinck, K. (2010). Factors governing partial coalescence in oil-in-water emulsions. Advances in colloid and interface science, 153(1-2), 30-42.

Freire, D. O., Wu, B., & Hartel, R. W. (2020). Effects of structural attributes on the rheological properties of ice cream and melted ice cream. Journal of food science, 85(11), 3885-3898.

Goff, H. D., & Hartel, R. W. (2013). Ice cream: Springer Science & Business Media.

Goff, H. D., & Jordan, W. K. (1989). Action of emulsifers in promoting fat destabilization during the manufacture of ice cream. Journal of dairy science, 72(1), 18-29.

Koxholt, M. M. R., Eisenmann, B., & Hinrichs, J. (2001). Effect of the fat globule sizes on the meltdown of ice cream. Journal of dairy science, 84(1), 31-37.

Liu, X., Sala, G., & Scholten, E. (2022). Effect of fat aggregate size and percentage on the melting properties of ice cream. Food Research International, 111709.

Muse, M. R., & Hartel, R. W. (2004). Ice cream structural elements that affect melting rate and hardness. Journal of dairy science, 87(1), 1-10.

Prindiville, E. A., Marshall, R. T., & Heymann, H. (1999). Effect of milk fat on the

sensory properties of chocolate ice cream. Journal of dairy science, 82(7), 1425-1432.

Russell, A. B., Cheney, P. E., & Wantling, S. D. (1999). Influence of freezing conditions on ice crystallisation in ice cream. Journal of Food Engineering, 39(2), 179-191.

Sakurai, K. (1996). Effect of production conditions on ice cream melting resistance and hardness. Milchwissenschaft, 51, 451-454.

Sofjan, R. P., & Hartel, R. W. (2004). Effects of overrun on structural and physical characteristics of ice cream. International Dairy Journal, 14(3), 255-262.

Syed, Q. A., Anwar, S., Shukat, R., & Zahoor, T. (2018). Effects of different ingredients on texture of ice cream. Journal of Nutritional Health & Food Engineering, 8(6), 422-435.

Tharp, B. W., Forrest, B., Swan, C., Dunning, L., & Hilmoe, M. (1998). Basic factors affecting ice cream meltdown. International Dairy Federation Special Issue(3), 54-64.

Velásquez-Cock, J., Serpa, A., Vélez, L., Gañán, P., Hoyos, C. G., Castro, C., Duizer, L., Goff, H. D., & Zuluaga, R. (2019). Influence of cellulose nanofibrils on the structural elements of ice cream. Food Hydrocolloids, 87, 204-213.

Warren, M. M., & Hartel, R. W. (2014). Structural, compositional, and sensorial properties of United States commercial ice cream products. Journal of food science, 79(10), E2005-E2013.

Warren, M. M., & Hartel, R. W. (2018). Effects of emulsifier, overrun and dasher speed on ice cream microstructure and melting properties. Journal of food science, 83(3), 639-647.

Wu, B., Freire, D. O., & Hartel, R. W. (2019). The effect of overrun, fat destabilization, and ice cream mix viscosity on entire meltdown behavior. Journal of food science, 84(9), 2562-2571.

Supplementary material

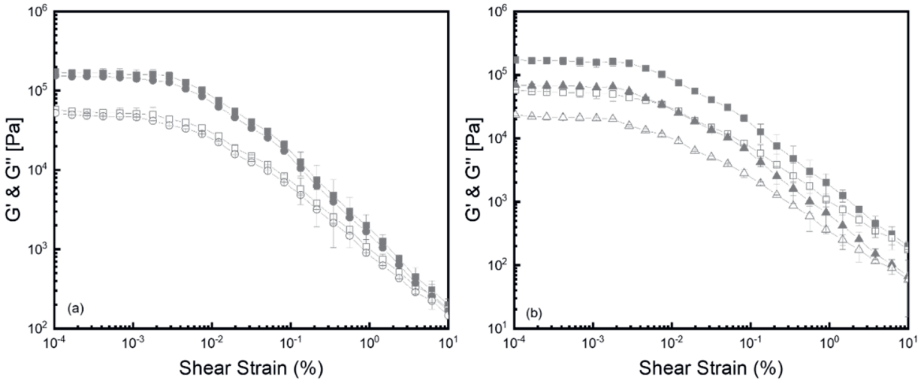

Fig. S3.1. Storage modulus (G') and loss modulus (G'') for the fat-network dominated samples with different structural elements as a function of strain: (a) varying ice crystal size: LN-30-T80 (grey squares) and BF-30-T80 (grey circles), and (b) varying overrun: LN-30-T80 (grey squares), and LN-90-T80 (grey triangles). G' is provided as solid symbols, and G'' as empty symbols.

Chapter 4

Role of polysaccharide structure in the rheological, physical and sensory properties of low-fat ice cream

Published as: Liu, X., Sala, G., & Scholten, E. (2023). Role of polysaccharide structure in the rheological, physical and sensory properties of low-fat ice cream. *Current Research in Food Science*, *7*, 100531.

Abstract

Polysaccharides can be used as fat replacers in ice cream, as they contribute to an increase of viscosity. However, no research has clarified the exact role of viscosity from that of the structure of the polysaccharides on the properties of ice cream. In this study, the effect of polysaccharide structure on different properties of low-fat ice cream was investigated. The polysaccharides taken into consideration varied from flexible (locust bean gum and guar gum) to rigid (xanthan gum and iota carrageenan). Relationships between rheological properties of ice cream mixes and microstructural characteristics and sensory perception of the final ice cream were established. To separate the effect of the polysaccharide structure from that of viscosity, two series of ice cream were prepared: one in which the mix viscosity of the various samples was similar (approximately 68.3 mPa·s), and one in which the serum phase viscosity was similar (approximately 15563 mPa·s). Flexible polysaccharides showed a lower degree of shear-thinning and a more liquid-like viscoelastic behavior compared with rigid polysaccharides. In addition, flexible polysaccharides led to higher overrun (47-58%) than other samples (approximately 30%), which resulted in lower hardness of the ice cream (< 3.2 MPa). Rigid polysaccharides caused gelation of the serum phase, which made the ice cream more difficult to scoop. Based on the results of the sensory evaluation, flexible polysaccharides could provide higher softness and creaminess-related properties, while rigid polysaccharides resulted in higher coldness and grittiness. Therefore, polysaccharides with a flexible structure are a better choice for improving the textural and sensory properties of low-fat ice cream.

4.1 Introduction

Ice cream is a popular dessert and is highly liked by consumers. However, it contains high amounts of fat, and an excessive consumption of high-fat foods is linked nowadays to obesity and cardiovascular disease, diabetes and cancer. The microstructure of ice cream is rather complex, consisting of air cells, ice crystals, and a network of coalesced fat droplets entrapped in a thick continuous phase (Scholten, 2014). Commercial ice cream contains 10-16 % dairy fat, which is an important component in affecting melting rate, shape retention after melting, overrun, creaminess and mouthcoating, which can be attributed to the formation of a fat network in the unfrozen serum phase and the lubricating effect of fat (Liu, Sala, & Scholten, 2022; Milani & Koocheki, 2011; Roland, Phillips, & Boor, 1999; Rolon, Bakke, Coupland, Hayes, & Roberts, 2017). Although low-fat ice creams are already available on the market, such products still have lower quality. Therefore, fat reduction in ice cream while retaining the sensory quality of the full-fat product still remains a challenge, and requires ingredients able to replace the functionalities of fat.

Based on their composition, fat replacers are mainly categorized into three groups: lipid-, protein- and carbohydrate-based (Akbari, et al., 2019). Carbohydrate-based fat replacers are most common, and many polysaccharides have already been used also in ice cream. These polysaccharides contribute largely to viscosity enhancement and give ice cream a creamy and full mouthfeel (Akbari, et al., 2019). Many studies have shown that the addition of polysaccharides in low-fat ice cream can be an effective way to improve the physical and sensory properties of low-fat or fat-free ice cream (Javidi, Razavi, Behrouzian, & Alghooneh, 2016; Kurt, Cengiz, & Kahyaoglu, 2016; Mahdian & Karazhian, 2013; Soukoulis, Chandrinos, & Tzia, 2008). Up to now, mainly polysaccharides have been subject of investigation for their effect on the rheological properties of ice cream mixes, and mix viscosity is considered to be the main factor in affecting the ice cream microstructure and sensory properties. For example, an increase in viscosity has been shown to have a positive effect on overrun, melting resistance and sensory properties (BahramParvar, Tehrani, & Razavi, 2013; Mahdian, et al., 2013; Milani, et al., 2011). In addition, shear thinning and thixotropy of ice cream mixes have been related to an enhancement of creaminess and a reduction of coldness and coarseness (Javidi, et al., 2016). However, in these studies the viscosity of the ice cream mixes with similar concentration was not constant, as the structure of the polysaccharides has an influence on the rheological profile. This

makes it difficult to distinguish the exact role of viscosity from that of the structure of the polysaccharides in the different structural and physical properties of ice cream. For a better understanding of these aspects, mix viscosity should be kept constant by varying the concentration of different polysaccharides. In addition, the structure of polysaccharides may also affect serum phase viscosity, which refers to the viscosity of the unfrozen continuous phase excluding air cells and ice crystals. The serum phase viscosity originates from the mix viscosity and undergoes a significant increase during the freezing process, as the concentration of different soluble components within the unfrozen phase becomes more and more pronounced due to ice crystallization. However, for sensory perception, the viscosity of the serum phase resulting from freeze concentration may become more relevant than mix viscosity, as the mouthfeel of ice cream is more related to its frozen form (Goff & Hartel, 2013). To clarify the exact role of both mix viscosity and serum phase viscosity on the different properties of ice cream, samples with the same serum phase viscosity should also be compared.

Besides viscosity, the sensory perception of ice cream may also be related to the lubrication properties of the different polysaccharides. Even though studies on the tribological properties of individual polysaccharides have been carried out (Ji, et al., 2022; Stokes, Macakova, Chojnicka-Paszun, de Kruif, & de Jongh, 2011; Taira & McNamee, 2014), the lubrication functionality of these molecules in ice cream is still unclear. It has been reported that rigid polysaccharides like xanthan provide better lubrication than flexible polymers like guar gum, although the viscosity of the samples was the same (Ji, et al., 2022). It is not clear how these differences may affect the perception of ice cream, and which sensory attributes may be influenced by lubrication. A better understanding of the exact role of the structure of the polysaccharides in structural, tribological, rheological and sensory properties of ice cream is still required.

Our study aimed to shed light on the described issues by investigating the addition of a set of polysaccharides varying in molecular flexibility in fat-reduced ice cream. Two reference samples with 1 % and 10 % fat were used. Four polysaccharides differing in structure were used to gain insight in how both mix and serum phase viscosity relates to different structural and sensory aspects: locust bean gum, guar gum, xanthan gum and iota-carrageenan. Both locust bean gum (LBG) and guar gum (GG) have a random coil conformation, with a persistence length of approximately 3 nm, and are

therefore considered flexible polysaccharides (Picout, Ross-Murphy, Jumel, & Harding, 2002). Xanthan gum (XG) has a rigid-rod conformation, with a persistence length of 5-35 nm, and is therefore more rigid than LBG and GG. Iota-Carrageenan (IC) has a rigid conformation, with a persistence length of 23-26 nm (Thrimawithana, Young, Dunstan, & Alany, 2010). Our samples set thus included two random coil polysaccharides (LBG and GG) and two rigid polysaccharides (XG and IC). The differences in morphology of these four polysaccharides have been widely discussed in literature (Dogan, Aslan, & Gurmeric, 2018; Ferdiansyah, Abdassah, Zainuddin, Rachmaniar, & Chaerunisaa, 2023; Hadinugroho, Martodihardjo, Fudholi, & Riyanto, 2021). To be able to isolate the effect of polysaccharide structure, we prepared two series of ice cream, one in which the mix viscosity was matched, and one in which the serum phase viscosity of the ice cream was matched. We determined the rheological behavior of these different polysaccharides (consistency coefficient, flow behavior index, and loss factor) in ice cream mixes, which was then linked to the structure of the obtained ice creams (overrun, air cell size, ice crystal size, serum phase viscosity). The ice cream structure was subsequently linked to different rheological (G' and G" upon temperature increase), textural (hardness and scoopability), lubrication, and sensory properties (such as hardness, coldness and creaminess) of the samples.

4.2 Materials and methods

4.2.1 Materials

Organic carrageenan-free cream (33 % fat, 3 % lactose, 2.4 % protein, 0.08 % minerals), organic skimmed milk (5 % lactose, 3.5 % protein, 0.1 % minerals) and sucrose were purchased from a local supermarket (Jumbo Wageningen, Netherlands). Locust bean gum (LBG, ~310 kDa), guar gum (GG, ~4000 kDa), xanthan gum (XG, ~4000 kDa), iota carrageenan (IC, ~120 kDa) were purchased from Sigma-Aldrich Chemie GmbH (Steinheim, Germany). Vanillin (100%) was purchased from Royal Polak Spices (Steenwijk, Netherlands).

4.2.2 Ice cream mix preparation

Two different series of low-fat ice cream (1% fat) were prepared by using different polysaccharides. In one series, we matched the mix viscosity measured at 50 s^{-1} by varying the concentration of different polysaccharides (0.55% LBG, 0.3% GG, 0.2%

XG and 0.2% IC). In the other series, the serum phase viscosity measured at the mentioned shear rate and at -20 °C was matched in the same way (0.55% LBG, 0.3% GG, 0.4% XG and 0.55% IC). The sugar concentration in the continuous phase of both series was kept the same (~15%) to guarantee constant freezing point depression and ice fraction. Vanillin (0.1%) was added to all samples. In addition, two reference samples were prepared, both without polysaccharides: a low-fat ice cream with 1 % fat, and a high-fat ice cream with 10% fat. An overview of the model ice cream recipes is shown in Tab. 4.1.

Tab. 4.1. Ice cream formulations of the studied samples (LBG: locust bean gum; GG: guar gum, XG: xanthan gum; IC: iota carrageenan).

Ingredients (%)	10 % fat	1 % fat	LBG	GG	XG		IC	
Cream	30	3.0	2.98	2.99	2.99	2.99	2.99	2.98
Skimmed milk	56.2	81.9	81.47	81.67	81.75	81.59	81.75	81.47
Sucrose	13.8	15.0	14.90	14.94	14.96	14.93	14.96	14.90
Vanillin	0.1	0.1	0.1	0.1	0.1	0.1	0.1	0.1
Polysaccharide (similar mix viscosity)	0	0	0.55	0.3	0.2	0	0.2	0
Polysaccharide (similar serum phase viscosity)	0	0	0.55	0.3	0	0.4	0	0.55

For the preparation of the ice cream mixes, sugar and skimmed milk were first mixed with a magnetic stirrer for 30 min. Then, different amounts of polysaccharides and vanillin were added slowly upon stirring at approximately 25 °C for 1.5 h. The mixed systems were then heated in a water bath at 85 °C for 30 min, to achieve complete dissolution of the polysaccharides. The mixes were cooled to room temperature (approximately 25 °C) and cream was added upon stirring for 1 h before ice cream preparation. The mixes were aged at 4 °C overnight.

4.2.3 Ice cream preparation

Ice cream samples (3 L) were frozen in a batch freezer (Frigomat T4S-T5S, Italy) for 8 min and the draw temperature was approximately -5 °C. The ice cream was collected into different containers depending on the determination to be carried out: plastic rings of 25 mm in height and 70 mm in diameter for hardness and scoopability measurements, metal rings of 5 mm in height and 25 mm in diameter for rheological

characterization, and 60 mL containers for sensory evaluation. These samples were first hardened at -20 °C for 24 h to solidify further before measurement.

4.2.4 Ice cream mix viscosity

The viscosity of ice cream mixes was measured using a rheometer (MCR 501, Anton Paar, Germany) equipped with a concentric cylinder geometry (probe CC17/Ti; cup CC17/Ti). A sample of 4.7 ml was added to the geometry and the temperature was set at 20 °C. The viscosity was measured at a shear rate ranging from 0.1 to 300 s^{-1} in a time frame of 5 min. The flow behavior of the ice cream mix was described by a power law model as:

$$\sigma = K\gamma^n \quad (4.1)$$

where σ is the shear stress (Pa), K is the consistency coefficient (Pa·s^n, equal to viscosity when n = 1), γ is the shear rate (s^{-1}) and n, the flow behavior index, is a dimensionless number reflecting the shear-thinning behavior. Lower values of n represent a higher degree of shear-thinning behavior. The measurements were repeated three times for each sample.

4.2.5 Viscoelastic properties of ice cream mix

The viscoelastic properties (G' and G") of the ice cream mixes were measured with a rheometer (MCR 501, Anton Paar, Germany). Prior to measurements, the samples (2 ml) were placed into a PP50 plate/plate geometry and allowed to equilibrate at 20 °C for 120 s. The strain was set at 0.5% and the frequency at 1.6 Hz. Storage modulus (G') and loss modulus (G") were measured during a time frame of 5 min. The measurements were repeated three times for each sample. The mean value of G' of the ice cream mix and the mean value of loss factor of mix (G"/G') were extracted to characterize the viscoelastic behavior of ice cream mixes.

4.2.6 Overrun of frozen ice cream

The overrun of frozen ice cream was determined by first weighing a fixed volume (30 ml) of the aged pre-mix in a metal cup. Next, the same volume of ice cream was weighted in the cup directly after preparation. The overrun was quantified as (Muse & Hartel., 2004):

$$\text{Overrun } (\%) = \frac{Weight\ of\ mix - weight\ of\ ice\ cream}{Weight\ of\ ice\ cream} \times 100 \quad (4.2)$$

4.2.7 Ice crystal and air cell size of frozen ice cream

The analysis of ice crystal size and air cell size was performed according to the methods described by Velásquez-Cock et al. (2019) and Muse et al. (2004), respectively, with slight modifications. A light microscope with a hot stage (Zeiss Axioskop 2 Plus, Germany) was used, which allowed to control the temperature of the microscope at -20 °C. For the analysis of ice crystal size, all tools, reagents and samples were kept at -20 °C before sample preparation. Five mg of ice cream sample were taken from the core section of each container with a sharp knife and deposited over a standard glass slide. One or two drops of kerosene (approximately -20 °C) were applied to disperse the ice crystals more evenly, and the glass slide was covered with a chilled cover slide. Ice crystals were spread out gently by tapping the cover slide with chilled tweezers. The whole sample preparation process was carried out in a -20 °C storage room to prevent melting of the ice crystals.

For the analysis of air cell size, a small sample of ice cream was placed on a prechilled microscope slide within an area delimited by a plastic frame (65 µl, 1.5 x 1.6 cm) to create a space to prevent the deformation of air cells. The slides were sealed with a cover slide to smear the sample into a thin layer and prevent the escape of air cells. The temperature of the hot stage was adjusted to -6 °C, and at this temperature the air cells were sufficiently buoyant to rise to the bottom of the top slide for size determination.

Images of both ice crystals and air cells were taken at 10x magnification to include at least 300 ice crystals or air cells to calculate mean size and standard deviation. The size of ice crystals and air cells was determined by placing a circle around an ice crystal or air cell manually, from which the area and radius were calculated using the software ZEN 2011 assuming that the crystals and air cells were of spherical shape.

4.2.8 Serum phase viscosity of frozen ice cream

The serum phase viscosity in ice cream cannot be measured directly in the frozen state. Therefore, the serum phase of the various samples was mimicked taking into account the amount of polysaccharides, sugar and other ingredients in the non-frozen fraction. First, the amount of unfrozen water was calculated based on the measured ice fraction. The ice fraction as determined by the Differential Scanning Calorimetry (DSC) was approximately 62% in all samples. Based on this, the concentrations of

water-soluble ingredients (polysaccharides, sucrose, lactose, protein and salt) in the unfrozen serum phase were calculated. These concentrations were used to recreate the unfrozen serum phase. The exact recipes of the recreated serum phase of all samples can be seen in Tab. 4.2.

Tab. 4.2. Unfrozen serum phase formulations of the studied samples. (LBG: locust bean gum; GG: guar gum, XG: xanthan gum; IC: iota carrageenan).

Ingredients (%)	10% fat	1% fat	LBG	GG	XG		IC	
Sucrose	38.59	38.65	38.12	38.35	38.45	38.26	38.45	38.12
SMP	21.76	21.64	21.34	21.47	21.53	21.42	21.53	21.34
Water	39.65	39.71	39.16	39.41	39.51	39.31	39.51	39.16
Polysaccharide (similar mix viscosity)	0	0	1.40	0.77	0.51	0	0.51	0
Polysaccharide (similar serum phase viscosity)	0	0	1.40	0.77	0	1.02	0	1.40

The serum phase viscosity measurements were performed using a rheometer MCR 501 equipped with a CC17/Ti geometry. During the measuring process, the temperature was decreased from 4 to -20 °C with a cooling rate of 0.5 °C/min. The shear rate was kept constant at 50 s^{-1}. In some cases, ice crystal formation and growth were still observed, and therefore not all samples could be measured over the entire temperature range. In these cases, the serum phase viscosity was estimated by extrapolation of the results to -20 °C.

4.2.9 Evaluation of network formation in the serum phase

To evaluate the formation of a fat network, the particle size distribution of ice cream mix and molten full-fat ice cream was measured with static light scattering (Mastersizer 3000, Malvern Instrument, Ltd, Malvern, Worcestershire, UK), using a refractive index of 1.46 and 1.33 for the fat and the water, respectively. A bimodal distribution was observed in the molten ice cream, and according to our previous work (**Chapter 2**), the second peak with a particle size higher than 10 µm could be regarded as aggregated fat clusters. The mean particle size of ice cream mix and molten ice cream ($D_{4,3}$) was determined separately, and the volume percentage of the aggregated fat clusters was used to reflect the degree of fat destabilization as fat

aggregate percentage. To evaluate possible changes in microstructure due to the formation of a polysaccharide, the viscosity of the molten ice cream was compared to viscosity measured before ice cream preparation. The viscosity of the molten ice cream samples was measured at a shear rate between 0.1 and 100 s^{-1} with a rheometer (Physica MCR 501, Anton Paar, Germany) equipped with the cup geometry (CC17/T200/Ti). The temperature was set at 20 °C and the total measuring time was set at 5 min. The measurements were repeated three times for each sample. Based on our measurements, both the viscosity of the ice cream mix and that of the molten ice cream showed shear-thinning behavior, indicating that the structure of the samples changed during the shearing process. We took the viscosity of both the mix and molten ice cream at low shear rate (0.1 s^{-1}) to represent the structure of the samples, and their ratio was used to characterize network formation by fat aggregates or polysaccharides, with low values indicating a higher degree of network formation.

4.2.10 Hardness and scoopability of frozen ice cream

Hardness and scoopability of the samples were measured with a Texture Analyzer (TA-TX plus, Stable Micro Systems, UK). Samples with fixed volume were prepared using plastic rings of 25 mm in height and 70 mm in diameter. The samples were stored in a freezer at -20 °C for a minimum of 24 h. Prior to measurement, a climate chamber was connected to the Texture Analyzer to maintain a temperature of -20 °C. For hardness determination, the samples were taken out of the plastic rings and were transferred to the climate chamber immediately (-20 °C). Then they were penetrated with an aluminum cylinder probe (5 mm in diameter) attached to a 50 kg load cell to a strain of 50% at a speed of 2 mm/s. Hardness was taken as the maximum stress of the stress-strain curve.

To measure scoopability, a scooping spoon probe in combination with an ice cream sample holder was used (see Fig. 4.1), which were mounted in a climate chamber hold at a temperature of -20 °C with liquid nitrogen. The scooping spoon was forced into the ice cream with a constant velocity of 3 mm/s over a distance of 25 mm. We used the total area under the curve to determine the scooping energy (N · mm), which we used as a measure for scoopability: the larger the scooping energy, the lower the scoopability. Both hardness and scoopability measurements were done in triplicate to obtain average value and standard deviation.

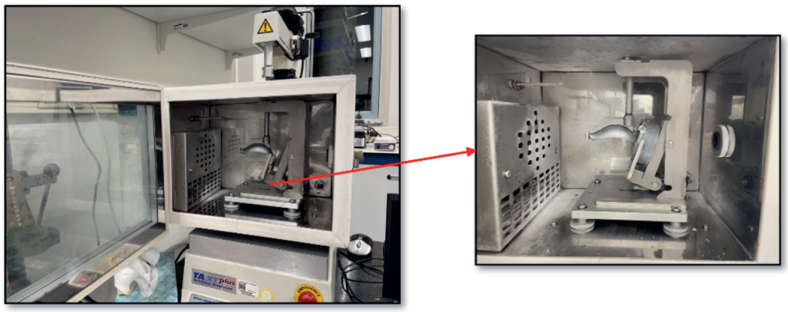

Fig. 4.1. Climate chamber with the scoopability measurement setup. The dimensions of the ring: 25 mm in height and 70 mm in diameter; dimensions of the spoon: 63 x 33 x 25 mm. Angle of the ring: 65°.

4.2.11 Melting properties of frozen ice cream

Temperature sweeps were performed to explore the melting process of the studied ice cream samples by increasing the temperature from -20 to 10 °C. Measurements were performed using a rheometer (MCR 301, Anton Paar, Germany) at a constant strain of 0.005% and a frequency of 1.6 Hz with a plate-plate geometry (PP50/P2). A moveable hood covering the plate-plate geometry was connected to the cooling system to control the temperature. An air pump was also connected to the hood to prevent heat exchange with the environment. Prior to the measurement, the initial temperature of the plate was reduced to -20 °C using a Peltier element, and then the temperature was increased to 10 °C with a heating rate of 0.5 °C/min. Sixty measuring points were recorded and the total measuring time was 60 min. Storage modulus (G') and loss modulus (G'') were measured. Three zones could be identified during the whole process (Wildmoser, Scheiwiller, & Windhab, 2004) and two parameters were extracted after the measurements: (1) the mean value of G' in the frozen state (zone I, G'ZI), and (2) the slope of G' during the melting stage (zone II, SZII) , which is an indicator for the speed of melting (Eisner, Wildmoser, & Windhab, 2005). Ice cream samples were measured at least twice to obtain average values.

4.2.12 Lubrication behavior of molten ice cream

Tribology measurements were carried out to evaluate the lubrication properties of molten ice cream samples. Measurements were performed with a MCR 301 rheometer equipped with a tribology accessory (T-PTD 200, BC 12.7, Anton Paar,

Austria). The set-up was based on a glass ball-on-three-pins principle, consisting of a spherical glass ball (d = 12.7 mm) and three PDMS pins (d = 6 mm, roughness 0.2 μm ± 0.03). The temperature of the tribology cup was set at 20 °C and a normal force of 1 N was applied. Samples with a volume of 0.6 ml were poured into the tribology cup, and the friction coefficient was measured as a function of sliding speed. The measurements consisted of two runs in total with increasing and decreasing sliding speed between 0.01 and 470 mm/s, in 7.5 min per run. The data of the second run with increasing speed showed good repeatability and were selected for further analysis. The measured friction coefficient was plotted versus sliding speed. Two regimes could be identified: a boundary regime at low sliding speed, and a mixed regime at intermediate sliding speeds. A hydrodynamic regime was not obtained as the viscosities of the samples were not high enough. The mean friction coefficient in the boundary regime (FCB) and the slope of friction coefficient over sliding speed in the mixed regime (SMR) were used to represent different lubrication properties of molten ice cream samples.

4.2.13 Sensory analysis

A sensory study was performed using an untrained panel (n = 80 participants; gender: 43 female, 37 male; age range: 18 - 32). Participants were recruited from the campus of Wageningen University & Research. They all had good general and oral health, good/normal tasting and smelling abilities, used no medication and had no allergies or intolerances towards the ingredients used in the samples. A consent form was signed by the participants and they were given a financial compensation upon completion of the study.

A rate-all-that-apply (RATA) methodology was applied, based on previous works in which structural aspects were related to sensory perception for foods in which differences were limited (Fuhrmann, Sala, Scholten, & Stieger, 2020; Ji, den Otter, Cornacchia, Sala, & Scholten, 2023; Meyners, Jaeger, & Ares, 2016). The samples were stored in the freezer (-20 °C) and coded with 3-digit numbers according to a random design. Each sample was supplied in individual plastic containers of 60 ml and kept at room temperature (approximately 25 °C) for 5 min before serving. For logistics reasons, the participants were divided into 8 groups, and the serving order of samples was randomized for each group using a Latin Square design to prevent presentation order effects. The provided attribute list and definition are shown in Tab.

4.3. Attributes and definitions were taken from previous works (Alvarez, 2009; Pintor, Escalona-Buendía, & Totosaus, 2017; Thompson, Chambers, & Chambers Iv, 2009) and adjusted when necessary. The participants selected the attributes that were applicable to their samples (creaminess, softness, coldness, grittiness, thickness, stickiness, mouth coating, meltdown, off-flavor) and when selected, these attributes were scored on a 1-to-9 scale, with anchors "weak" to "strong". In addition, participants were also asked to rate their overall liking of each sample using a 9-point hedonic scale ("Dislike extremely" to "Like extremely"). Between samples, the participants were instructed to drink water to remove the residue of the previous sample from the mouth.

Tab. 4.3. Sensory attributes and definitions for the sensory test.

Attribute	Definition
Creaminess	Refers to the intensity of the "fatty" feeling in the mouth when the sample is manipulated between the tongue and the palate; perceived fat content
Softness	The ease of compressing the sample between the tongue and palate
Coldness	The feeling of cold in the mouth/upper gastrointestinal tract upon eating or swallowing the sample
Grittiness	The immediate perception of crystal-like particles within the sample
Thickness	The pressure necessary to move the sample between the tongue and the palate
Stickiness	The elasticity between the tongue and the palate when coated with the sample
Mouth coating	A sensation of having a coating on the tongue and other mouth surfaces
Meltdown	The time required for the product to melt in the mouth when continuously pressed by the tongue against the palate
Off-flavor	An unpleasant or unusual flavor that is not typically associated with ice cream
Overall liking	How much was the sample liked

4.2.14 Statistical analysis

The data obtained from rheological, tribological and textural measurements were analyzed with SPSS software (Version 25.0, IBM Corp). The means were compared with a Tukey's test at a 5% level of significance using an analysis of variance (ANOVA). Moreover, RATA data and overall liking were analyzed using linear mixed models using RStudio with the additional packages LmerTest and Emmeans (RStudio, Inc., Version 4.0.2). Significance level of $P < 0.05$ was chosen. Additionally, the results obtained from rheological, physical and sensory measurements were analyzed by Principal Component Analysis (PCA) and correlation matrices were established for the different properties. In addition, biplots obtained from PCA were used to visually represent sample grouping and differentiation. PCA analyses were performed using XLSTAT software (Addinsoft, Paris, France).

4.3 Results and discussion

4.3.1 Effect of polysaccharide structure on rheological properties of ice cream mix and serum phase

We first investigated the effect of polysaccharides on the rheological properties of ice cream mixes. As shown in Tab. 4.4, both the high-fat sample and the low-fat sample, without polysaccharides, had a lower viscosity of 6.8 and 3.3 mPa·s, respectively. Upon addition of polysaccharides, the viscosity increased, and the extent of the increase depended on the type of polysaccharide. For the series with mix viscosity matched at 50 s^{-1}, 0.55% of LBG and 0.3% of GG were used to obtain a viscosity of approximately 70 mPa·s, whereas only 0.2% of XG and IC were needed to achieve the same viscosity value. This can be explained by the molecular weight and structure of the various polysaccharides. Both LBG and GG have a flexible structure, but the GG used for our research had a molecular weight higher (~4000 kDa) than that of LBG (~310 kDa). Therefore, a lower concentration of GG was required to achieve the desired viscosity. However, the polysaccharide structure seemed to be more important than molecular weight in affecting viscosity. As a matter of fact, a comparable low concentration for XG and IC was required to obtain the desired viscosity (70 mPa·s), even though their molecular weight was quite different (XG: 4000 kDa; IC: 120 kDa). Both XG and IC are more rigid than GG and LBG, they were more effective in increasing viscosity, and therefore their concentration was lower. However, even though the viscositv values were matched, consistency

coefficient (K) and flow behavior index (n) were very different, indicating a different shear-thinning behavior for the different polysaccharides. A higher K could be observed in the XG and IC samples, which also proved the higher ability of these polysaccharides to increase viscosity. In addition, smaller n values were found in the samples containing rigid polysaccharides, indicating a greater degree of shear thinning (Rosti & Takagi, 2021). This can be explained by the fact that rigid polysaccharides can be more easily aligned in the direction of the shear flow (Bai, et al., 2017). The difference in structure also had an influence on serum phase viscosity. Even though the mix viscosity was similar, the serum phase viscosity of ice creams with rigid polysaccharides was lower. This may be attributed to changes in solvent quality. Upon freezing, the concentration of polysaccharides and all solutes (such as ions and milk proteins) in the serum phase increased. This may lower the solvent quality for both XG and IC, reducing their ability to contribute to viscosity. In addition, screening of the charged groups by ions might reduce the rigidity of anionic polysaccharides, although this is not commonly observed for rigid molecules. Such a change in solubility or rigidity would explain the decrease in serum phase viscosity. This result is in contradiction with the statement of Amador et al. (2017), who reported that serum phase viscosity was expected to be higher in samples with rigid polysaccharides. However, in their study, they did not measure the serum phase viscosity, but based their expectation on extrapolations. Our results show that such extrapolation cannot be used, and that the structure of the polysaccharides plays a large role in these phenomena.

To obtain the series with matched serum viscosity, we adjusted the concentrations of the polysaccharides. We took the sample containing 0.55% LBG as a reference. Since the molecule flexibility of GG is similar to that of LBG, the serum phase viscosity of samples containing these ingredients was also similar, and the concentration of GG did not have to be adjusted. However, in the case of XG and IC, to achieve a comparable serum phase viscosity as LBG and GG, their concentration had to be increased to 0.4% and 0.55%, respectively. Based on our findings, we can conclude that the serum phase viscosity and the link between mix viscosity and serum phase viscosity mainly depend on the structure of the polysaccharides.

Tab. 4.4. Rheological properties of ice cream mix samples with different polysaccharides. The notation of the samples includes the name of the polysaccharide and the concentration used. For example, LBG055 refers to a sample with 0.55% LBG.

Ice cream mix	Mix viscosity (mPa·s)	Serum phase viscosity (mPa·s)	Mix consistency coefficient (K)	Mix flow behavior index (n)	Mix G' (Pa)	Mix loss factor (G"/G')
1% fat	3.3 ± 0.4^{d}	2579 ± 655^{c}	3.8 ± 0.3^{f}	0.98 ± 0.02^{a}	0.9 ± 0.3^{d}	0.83 ± 0.02^{b}
10% fat	6.8 ± 0.1^{d}	2608 ± 496^{c}	10.8 ± 1.1^{f}	0.92 ± 0.02^{a}	7.5 ± 0.5^{bcd}	0.61 ± 0.07^{c}
LBG055*,**	68.3 ± 1.9^{c}	15563 ± 2338^{a}	137.2 ± 8.2^{e}	0.80 ± 0.01^{b}	4.2 ± 0.7^{bcd}	0.97 ± 0.01^{a}
GG03*,**	70.6 ± 1.4^{c}	16741 ± 1478^{a}	237.9 ± 7.3^{d}	0.67 ± 0.03^{c}	2.7 ± 0.5^{cd}	0.91 ± 0.02^{ab}
XG02*	66.6 ± 1.8^{c}	7666 ± 1306^{b}	424.9 ± 10.2^{c}	0.51 ± 0.04^{d}	9.0 ± 1.1^{bc}	0.48 ± 0.02^{d}
IC02*	68.1 ± 2.1^{c}	4136 ± 641^{bc}	760.2 ± 9.8^{b}	0.42 ± 0.02^{d}	12.1 ± 0.5^{b}	0.28 ± 0.04^{e}
XG04**	398.5 ± 2.5^{a}	14669 ± 1517^{a}	3221.5 ± 14.5^{a}	0.41 ± 0.02^{d}	20.3 ± 3.1^{a}	0.36 ± 0.04^{de}
IC055**	211.2 ± 3.1^{b}	15388 ± 2145^{a}	2544.1 ± 13.9^{a}	0.37 ± 0.01^{d}	21.5 ± 0.5^{a}	0.25 ± 0.04^{e}

Values with a different letter within the same column are significantly different ($P < 0.05$).

*Group of ice cream mixes with similar mix viscosity.

**Group of ice cream mixes with similar serum phase viscosity.

The storage modulus (G') and loss factor (G"/G') of ice cream mixes were also measured to characterize the viscoelastic properties of ice cream mixes. As shown in Tab. 4.4, ice cream mixes with flexible polysaccharides (LBG055 and GG03) showed a relatively lower G' and a significantly higher loss factor than mixes with rigid polysaccharides (XG and IC), indicating that more flexible polysaccharides gave a more liquid-like behavior. In contrast, XG and especially IC showed higher G', i.e., more solid-like properties, which were most likely related to the ability of these stiff polysaccharides to form a gel at the chosen concentrations (Petri, 2015; Thrimawithana, et al., 2010). This could be partly explained by their negative charge. As both cream and skim milk contain divalent calcium ions, a XG or IC network may have formed through salt bridges.

4.3.2 Microstructural characteristics

As shear-thinning behavior and viscoelastic properties of the ice cream mixes were expected to directly affect the structure of the frozen ice cream (air phase, ice phase and serum phase), overrun, air cell size, ice crystal size and serum phase viscosity were analyzed, and the results are summarized in Tab. 4.5. To quantify a possible network formation during the freezing process due to fat aggregation or polysaccharide gelation, we also compared the viscosity of the final molten ice cream with that of the initial ice cream mix at a low shear rate.

Compared with the low-fat (1%) reference, increasing fat content and degree of fat destabilization did not appear to influence the overrun. This was consistent with our previous research, which also showed that fat content and degree of fat destabilization did not appear to have a significant effect on the overrun values. This had probably to do with a dominant effect of the freezing process on overrun in our model systems (**Chapters 2 and 3**). For the samples with polysaccharides, the overrun of ice cream with XG and IC was similar to that of the low-fat reference (approximately 30%), while the overrun of LBG055 and GG03 was significantly higher, between 47 to 58% ($P < 0.05$). Flexible polysaccharides thus have a higher ability to incorporate air cells than rigid polysaccharides. A similar result was found in the study of Salahi & Mohebbi. (2021), which showed that GG and LBG led to higher overrun in soy milk foams than XG. This could be attributed to the lower shear-thinning behavior or more liquid-like viscoelastic behavior of samples with flexible polysaccharides. During ice cream preparation, shear stresses are experienced by the samples. In the case of ice

cream with flexible polysaccharides, a higher viscosity is maintained at such higher stresses, which allows to retain the air in the sample. Under these conditions, the lower viscosity of samples with rigid polysaccharides as a result of the larger shear thinning behavior might lead to an easier escape of the air. In addition, the more liquid-like viscoelastic behavior of the flexible polysaccharides might provide sufficient molecular flexibility at the air-serum interfaces, which can result in more expansion of the air cells. Furthermore, we would like to highlight that the increase in mix viscosity resulting from adding polysaccharides did not always contribute to an increase in overrun, as samples with rigid polysaccharides showed overrun similar to that of the low-fat reference without polysaccharides. Instead, the structure of the polysaccharide appeared to play a significant role in determining the development of overrun.

Tab. 4.5. Microstructural characteristics of ice cream samples with different polysaccharides The notation of the samples includes the name of the polysaccharide and the concentration used. For example, LBG055 refers to a sample with 0.55% LBG.

Ice cream	Overrun (%)	Air cell size (μm)	Ice crystal size (μm)	Mix viscosity / viscosity of molten ice cream
1 % fat	34 ± 4^{cd}	50 ± 27^{a}	55 ± 18^{a}	0.87 ± 0.08^{a}
10 % fat	32 ± 1^{d}	60 ± 27^{a}	57 ± 17^{a}	< 0.01
LBG055*,**	47 ± 2^{b}	52 ± 22^{a}	51 ± 19^{a}	0.91 ± 0.05^{a}
GG03*,**	58 ± 1^{a}	49 ± 24^{a}	56 ± 17^{a}	0.85 ± 0.04^{a}
XG02*	34 ± 1^{cd}	48 ± 22^{a}	46 ± 15^{a}	0.68 ± 0.05^{b}
IC02*	29 ± 3^{d}	42 ± 17^{a}	53 ± 18^{a}	0.52 ± 0.07^{c}
XG04**	28 ± 4^{d}	39 ± 14^{a}	48 ± 18^{a}	0.39 ± 0.01^{cd}
IC055**	30 ± 4^{d}	52 ± 25^{a}	58 ± 17^{a}	0.36 ± 0.02^{d}

Values with a different letter within the same column are significantly different ($P < 0.05$).
*Group of ice cream mixes with similar mix viscosity.
**Group of ice cream mixes with similar serum phase viscosity.

In the present study, no significant differences were found in air cell size and ice crystal size among the studied samples ($P > 0.05$). In other studies, the size distribution of air pockets was influenced by the viscosity of the ice cream mix (Chang & Hartel, 2002; Sofjan & Hartel, 2004), which was not the case in our research. Small differences were observed, but they were not statistically significant.

These results could be explained by our process conditions. It has been reported that the size of air cells and ice crystals can be strongly affected by the freezing conditions, including shear force, shear speed and drawing time etc. (Chang, et al., 2002; Eisner, et al., 2005; Muse, et al., 2004; Scholten, 2014). As our samples were prepared with the same freezing process, the similar air cell and ice crystal size suggests that the freezing conditions might have played a more dominant role in determining air cell size and ice crystal size than small differences in viscosity. However, a significant difference was found in the ratio between the viscosity of ice cream mix and that of the molten ice cream, indicating that for some of the samples network formation occurred during freezing. An extremely low ratio (< 0.01) was observed in high-fat molten ice cream. In addition, based on the fat particle size distribution in ice cream mix and molten high-fat ice cream (Fig S4.1 of supplementary material), the $D_{4,3}$ of the fat particles increased during ice cream preparation from 6.0 µm (ice cream mix) to 47.2 µm (molten ice cream). This value was larger than the critical fat aggregate size (approximately 45 µm) needed to provide a stable 3D fat network, which was obtained from our previous work (**Chapter 2**). In addition, the fat aggregate percentage increased from 7% to 90%, which was also high enough to indicate fat network formation (**Chapter 2**). These data indicate that a fat network was thus present in this sample. This network formation has been reported in previous studies (Granger, Leger, Barey, Langendorff, & Cansell, 2005; Liu, et al., 2022). In comparison, limited network formation was obtained in the sample with 1% fat, as the viscosity ratio was 0.87. Such high values were also found for samples containing flexible polysaccharides, i.e., 0.55% LBG and 0.3% GG. However, a lower viscosity ratio between mix and molten ice cream was observed for samples with 0.2% xanthan gum and 0.2% iota carrageen, which can be attributed to a certain degree of gel network formation. In addition, more solid like properties were also obtained in samples with 0.4% xanthan and 0.55% iota carrageenan, which provided an additional indication that these samples most likely formed a network.

To clarify which properties of the mix were related to the structure of ice cream, correlations between rheological properties of ice cream mixes and different microstructural characteristics of the final ice creams were determined. As shown in Fig. 4.2, overrun was highly correlated with the loss factor of the mix (0.816). The liquid-like behavior of the ice cream mix is thus the most important factor for incorporation of air cells. A lower correlation was found between overrun and mix viscosity (-0.416), indicating that the structural characteristics of the polysaccharides

were more important in affecting overrun than mix viscosity. Both the air cell size and ice crystal size did not appear to be significantly (< -0.562) correlated with the rheological properties of ice cream mixes. As mentioned before, the freezing conditions, including scraper blade speed and drawing time, could play more important roles in the development of air cells and ice crystals. The viscosity ratio was negatively correlated with K (-0.891) and G' (-0.973), but positively correlated with n (0.891) and loss factor (0.946). The formation of a gel network is reflected by the rheological properties of ice cream mixes: an ice cream mix with a higher shear-thinning behavior and a more solid-like viscoelastic behavior had a higher ability to form a gel network in the serum phase during the freezing process.

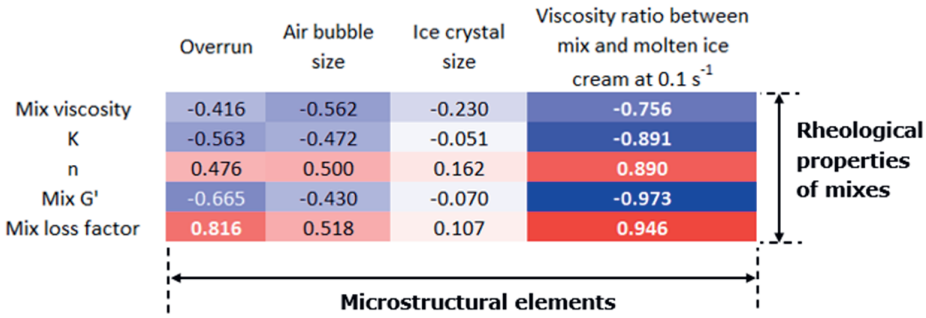

Fig. 4.2. Heatmap of correlation matrix (Pearson coefficients) between rheological properties of ice cream mixes and microstructural elements of frozen ice cream (without high-fat sample). Blue indicates negative correlation and red indicates positive correlation.

In conclusion, ice cream mixes with flexible polysaccharides showed a higher ability to incorporate air cells due to their low shear sensitivity and molecular flexibility. Rigid polysaccharides provided a more solid-like behavior and tended to form a gel network in the serum phase, which was linked to less air incorporation.

4.3.3 Rheological tribological, and textural properties

Viscoelastic behavior upon increasing temperature (G' at zone I (G'ZI) and slope of zone II (SZII)), tribological parameters (mean friction coefficient of the boundary regime (FCB) and slope of the mixed regime (SMR)), and textural properties (hardness and scooping energy) of the ice cream samples were determined, as they are important features relating to both the ice cream structure and sensory perception.

As shown in Tab. 4.6, no significant differences could be found in G'ZI and hardness between the references with low and high fat content. The reason why fat content had limited effect on these parameters was most likely the dominant effect of ice and air cells on hardness. As both the low-fat and high-fat references had the same ice fraction and similar overrun and ice crystal size, they thus had similar G'ZI and hardness. These results are consistent with the studies of Roland et al. (1999) and Rolon et al. (2017), in which it was also shown that the fat content did not significantly affect hardness. The addition of rigid polysaccharides (XG and IC) did not significantly affect G'ZI and hardness, but LBG055 and GG03 showed significantly lower hardness compared to the other samples, likely due to their higher overrun. An inverse relationship between hardness and overrun has been observed by many researchers (Biasutti, Venir, Marino, Maifreni, & Innocente, 2013; Muse, et al., 2004; Sofjan, et al., 2004). However, the overrun did not appear to affect scoopability, as we did not observe a higher scoopability, i.e., lower values of scooping energy, in LBG055 and GG03. However, XG04 and IC055 showed much higher values of scooping energy, and were thus more difficult to scoop. This could be due to the higher degree of gel network formation by XG and IC, which made it more difficult for a spoon to cut through the dense structure.

The reference with high fat content (10% fat) and the samples with higher serum phase viscosity (LBG055, GG03, XG04 and IC055, denoted with **) showed significantly lower values of SZ II, indicating that they melted more slowly. The lower melting in the high-fat (10%) reference could be attributed to the formation of a fat network formed by fat aggregates, which could block the continuous phase between air cells and create a more tortuous path for the serum phase to escape (**Chapter 2**). In addition, the highly viscous serum phase created by the addition of polysaccharides also appeared to contribute to a slower melting rate. The high serum phase viscosity probably led to slow drainage of the serum becoming more and more diluted upon melting. However, the formation of a more solid-like network in the samples XG and IC did not have an additional contribution to melting, as their values of SZII were similar to those of LBG055. Therefore, the viscosity of the serum phase itself seemed to be more dominant.

Tab. 4.6. Rheological (G' at zone I and slope of zone II), tribological (mean friction coefficient of boundary regime and slope of the mixed regime) and textural properties (hardness and scooping energy) of ice creams with different polysaccharides. The notation of the samples includes the name of the polysaccharide and the concentration used. For example, LBG055 refers to a sample with 0.55% LBG.

Ice cream	G' at zone I (10^6 Pa, G'ZI)	Slope of zone II (SZII)	Mean friction coefficient of boundary regime (FCB)	Slope of the mixed regime (SMR)	Hardness (MPa)	Scooping energy (N · mm)
1 % fat	5.4 ± 1.5^{a}	-1.23 ± 0.01^{d}	0.31 ± 0.01^{ab}	-0.27 ± 0.01^{d}	11.2 ± 1.8^{a}	437 ± 24^{c}
10 % fat	5.8 ± 1.7^{a}	-0.87 ± 0.03^{a}	0.25 ± 0.01^{cd}	-0.21 ± 0.01^{c}	9.3 ± 0.4^{a}	565 ± 98^{bc}
LBG055*,**	4.8 ± 1.4^{a}	-0.83 ± 0.01^{a}	0.24 ± 0.01^{d}	-0.16 ± 0.01^{a}	3.2 ± 0.2^{b}	564 ± 123^{bc}
GG03*,**	4.7 ± 1.2^{a}	-1.05 ± 0.01^{b}	0.28 ± 0.01^{bc}	-0.19 ± 0.01^{ab}	2.8 ± 1.0^{b}	605 ± 90^{bc}
XG02*	5.7 ± 1.7^{a}	-1.25 ± 0.02^{d}	0.27 ± 0.01^{cd}	-0.20 ± 0.01^{bc}	6.9 ± 1.1^{ab}	504 ± 63^{c}
IC02*	5.9 ± 1.6^{a}	-1.14 ± 0.01^{c}	0.32 ± 0.01^{a}	-0.18 ± 0.01^{ab}	10.9 ± 2.3^{a}	538 ± 68^{bc}
XG04**	5.4 ± 1.5^{a}	-0.89 ± 0.02^{a}	0.26 ± 0.01^{cd}	-0.20 ± 0.01^{bc}	7.6 ± 0.7^{ab}	915 ± 68^{ab}
IC055**	5.6 ± 1.5^{a}	-0.85 ± 0.02^{a}	0.25 ± 0.01^{cd}	-0.17 ± 0.01^{ab}	9.2 ± 1.0^{a}	1156 ± 195^{a}

Values with a different letter within the same column are significantly different ($P < 0.05$).

*Group of ice cream mixes with similar mix viscosity.

**Group of ice cream mixes with similar serum phase viscosity.

We also observed differences in lubrication properties among samples. As expected, the 10% fat sample had a significantly lower friction coefficient in the boundary regime (FCB) and a lower slope of the mixed regime (SMR) compared with the 1% fat sample. As known, fat is a good lubricant, the addition of polysaccharides to the low fat (1%) sample decreased the friction coefficient, especially in the mixed regime. Also a significantly lower slope of the mixed regime was found after adding polysaccharides. In the case of the polysaccharides, the flexible LBG provided the lowest FCB and SMR. However, the lubricating capacity of the flexible polysaccharides (LBG and GG) was not significantly different from that of the rigid polysaccharides (XG and IC). This was unexpected, as it has been reported that stiff and charged polysaccharides provide better lubrication than flexible polysaccharides (Garrec & Norton, 2012). This could be attributed to the presence of various ingredients in the ice cream. Ice cream is a complex system, and the various ingredients and the interactions among them can affect the lubrication properties of the whole system, and overshadow the lubrication effect of the polysaccharides themselves.

Correlation coefficients were determined to evaluate how microstructural elements affected the rheological and physical properties of ice cream with different polysaccharides (Fig. 4.3). Overrun was negatively correlated with G'ZI (-0.891) and hardness (-0.837): samples with a higher overrun had a more open structure, and were thus softer. Serum phase viscosity was negatively correlated to hardness (-0.748): in the mix viscosity series, samples prepared with flexible polysaccharides had a higher serum phase viscosity and a higher overrun. However, the correlation between these two parameters was not significant (0.478, data not shown). Scoopability (scooping energy) appeared to be negatively correlated with the viscosity ratio (-0.778): the formation of a gel network resulted in a more dense network, and therefore more energy was needed during scooping. All rheological parameters thus seemed more related to the structure of the polysaccharides than to their direct contribution to viscosity.

The melting properties were correlated to the serum phase viscosity, but was less affected by the type of polysaccharide. SZII showed a strong correlation with serum phase viscosity (0.818), but a relatively low correlation with the viscosity ratio, i.e., network formation (-0.307). No microstructural elements showed strong correlations with FCB and SMR. So, next to the fact that the type of polysaccharide was not linked

to lubrication properties, also other microstructural elements of ice cream did not directly affect the lubrication behavior.

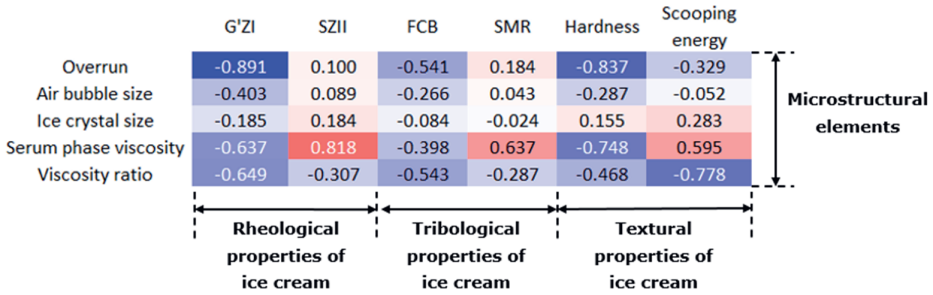

Fig. 4.3. Heatmap of correlation matrix (Pearson coefficients) between microstructural elements and rheological, tribological and textural properties of the studied samples (without high-fat sample). Blue indicates negative correlation and red indicates positive correlation.

4.3.4 Sensory properties of ice cream

The results of the sensory evaluation are shown in Tab. 4.7. Significant differences in all sensory attributes could be found among studied samples, as all P values were lower than 0.05. To identify common features of the samples, we also present a biplot obtained with Principal Components Analysis (PCA) (Fig. 4.4a). The first two principal components explained 86.13% of the variation. The first factor (F1, 63.26%) was mainly related to textural properties (creaminess, softness, coldness, grittiness, thickness, stickiness, mouth coating and meltdown), while the second factor (F2, 22.87%) was mainly linked to off-flavor and overall liking. The eight experimental samples were grouped into three groups, which are shown in different colors (Fig. 4.4a). The first one included the 10% fat reference and LBG055, and they were related to mouth coating, creaminess, thickness, stickiness and meltdown; the second group consisted of GG03 only, which had the strongest off-flavor; the third group included the 1 % fat reference, XG02, XG04, IC02, and IC055, and they were most linked to grittiness and coldness. The fact that F2 was mainly related to flavor and overall liking only shows that off-flavor played a dominant role in determining the overall appreciation of the samples. The polysaccharide guar gum was mostly responsible for this off flavor. To better understand the effect of polysaccharides on sensory properties apart from the off-flavor, we removed off-flavor and overall liking from

the analysis, and the obtained biplot is shown in Fig. 4.4b. We found that GG03 could then be categorized into the same group of LBG055 and 10% fat, indicating that LBG and GG had a similar effect on the texture of ice cream. Both flexible polysaccharides could provide textural properties similar to those of the high-fat sample, although the scores of the ice cream with LBG were closer to those of the full fat sample (Tab. 4.7). These samples were related to higher scores for mouth coating, creaminess, stickiness and thickness. On the other hand, the low-fat sample and the samples with rigid polysaccharides were located in the opposite direction, and showed the highest scores for grittiness and coldness. It has been reported before by Ares et al. (2010) that grittiness and coldness could be considered drivers of disliking, while creaminess is strongly related to liking. Flexible polysaccharides thus have a higher ability to improve the sensory properties of low-fat ice cream than rigid polysaccharides.

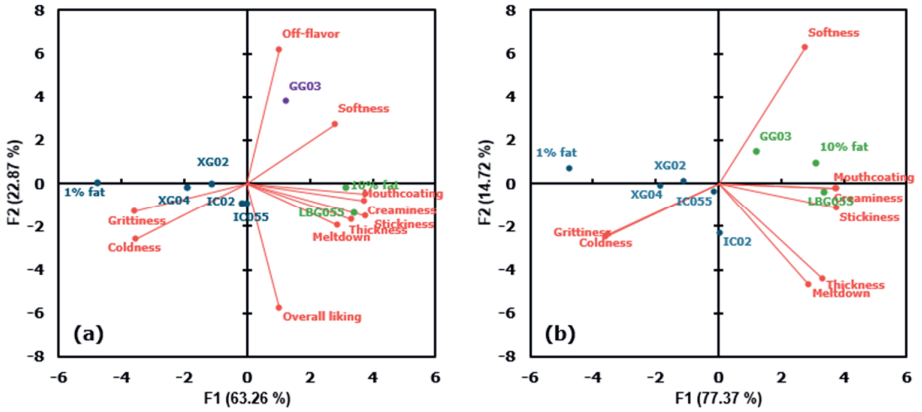

Fig. 4.4. Principal Components Analysis of the studied ice cream samples with (a) all sensory attributes and (b) all sensory properties without off-flavor and overall liking, where the red points with lines refer to the different sensory properties and the dots with the other colors refer to the studied samples. Different colors of points indicate different groups.

Tab. 4.7. Scores for the sensory properties of the studied samples. The notation of the samples includes the name of the polysaccharide and the concentration used. For example, LBG055 refers to a sample with 0.55% LBG.

Attributes	1% fat	10% fat	LBG055	GG03	XG02	IC02	XG04	IC055	F value	P Value
Creaminess	3.3 ± 1.9^{d}	4.7 ± 1.9^{ab}	5.2 ± 1.8^{a}	4.3 ± 2.0^{bc}	4.2 ± 2.2^{bc}	4.1 ± 2.2^{bc}	3.8 ± 2.0^{cd}	4.1 ± 1.9^{bc}	7.65	< 0.01***
Softness	3.1 ± 1.8^{cd}	4.8 ± 2.2^{a}	4.1 ± 2.2^{bc}	4.5 ± 1.9^{ab}	3.5 ± 2.1^{bc}	2.7 ± 1.9^{d}	3.4 ± 2.0^{bc}	3.6 ± 1.9^{bc}	10.98	< 0.01***
Coldness	6.6 ± 1.7^{a}	5.3 ± 1.9^{d}	5.5 ± 1.8^{cd}	5.2 ± 1.5^{d}	5.9 ± 1.9^{bc}	5.9 ± 1.6^{bc}	6.3 ± 1.5^{ab}	6.0 ± 1.9^{bc}	10.30	< 0.01***
Grittiness	5.1 ± 2.3^{a}	3.0 ± 2.3^{c}	3.6 ± 2.3^{bc}	3.5 ± 2.3^{bc}	4.3 ± 2.6^{ab}	4.3 ± 2.3^{ab}	4.1 ± 2.5^{ab}	4.0 ± 2.5^{ab}	9.04	< 0.01***
Thickness	3.3 ± 1.9^{c}	4.2 ± 1.9^{b}	4.6 ± 1.9^{a}	4.0 ± 1.9^{bc}	3.8 ± 2.0^{c}	4.5 ± 2.3^{ab}	3.7 ± 2.0^{c}	4.0 ± 1.9^{bc}	5.84	< 0.01***
Stickiness	2.1 ± 1.6^{d}	3.4 ± 2.2^{ab}	3.6 ± 2.2^{a}	2.8 ± 2.0^{bc}	2.6 ± 2.1^{cd}	2.9 ± 2.3^{bc}	2.4 ± 2.0^{cd}	2.9 ± 1.8^{bc}	8.50	< 0.01***
Mouth coating	3.3 ± 1.9^{c}	4.5 ± 2.0^{ab}	4.9 ± 2.0^{a}	4.2 ± 2.1^{ab}	3.7 ± 2.0^{bc}	4.0 ± 2.1^{bc}	3.6 ± 2.0^{bc}	4.0 ± 1.9^{bc}	7.60	< 0.01***
Meltdown	3.9 ± 2.2^{b}	4.7 ± 2.1^{a}	4.6 ± 1.8^{a}	4.4 ± 1.9^{ab}	4.4 ± 2.1^{ab}	4.8 ± 2.3^{a}	4.5 ± 2.2^{ab}	4.6 ± 2.0^{a}	2.27	0.02*
Off-flavor	1.3 ± 1.8^{b}	1.7 ± 1.9^{b}	1.4 ± 1.8^{b}	4.0 ± 3.0^{a}	1.6 ± 2.0^{b}	1.6 ± 2.1^{b}	1.4 ± 1.9^{b}	1.3 ± 1.7^{b}	24.43	< 0.01***
Overall liking	4.6 ± 1.8^{ab}	5.2 ± 2.0^{a}	5.3 ± 2.0^{a}	3.5 ± 2.1^{c}	4.7 ± 1.9^{ab}	4.5 ± 1.9^{ab}	4.6 ± 1.8^{ab}	5.0 ± 1.8^{a}	10.20	< 0.01***

Values with a different letter within the same row are significantly different ($P < 0.05$).

To get a better understanding of how the sensory attributes were related to the properties of the ice cream, correlation coefficients between physicochemical characteristics and sensory properties are shown in Fig. 4.5. Off-flavor and overall liking were omitted from the analysis.

Some strong correlations were found between ice cream characteristics and sensory properties. As expected, overrun was strongly correlated with softness (0.862). This also explained the high negative correlation between G'ZI and softness (-0.878). In addition, overrun was negatively linked to coldness (-0.800). As air is a bad heat conductor, higher overrun leads to slower melting, which has been discussed before by Sofjan et al. (2004). Therefore, we also expected a high negative correlation between overrun and meltdown. However, a low correlation (-0.109) was found. This result is consistent with the findings of Wu et al. (2019) and Freire et al. (2020), who also found that overrun can only affect the meltdown under certain conditions. For example, Wu et al. (2019) found that overrun only had an effect on meltdown when no stabilizers were added. In our case, the low correlation between overrun and meltdown could be attributed to the addition of polysaccharides. Furthermore, the fast melting of our ice cream during consumption could be another reason for the difficulty to distinguish differences among samples. These results could indicate that coldness is not only related to the meltdown behavior, but also to other characteristics of the ice cream, such as the connectivity among ice crystals or structural changes of the serum phase. As overrun was related to the structure of the polysaccharides, we can conclude that polysaccharide structure also influences sensory perception.

Serum phase viscosity was highly correlated with softness (0.808) and grittiness (-0.869). Therefore, these attributes did not seem to be influenced much by the type of polysaccharides, but just by the viscosity of the serum phase. The positive correlation between serum phase viscosity and softness could be attributed to the fact that a higher serum phase viscosity seemed to be linked to a higher overrun. In addition, the fact that grittiness was inversely related to serum viscosity could be explained by the fact that a more viscous serum phase can mask the detection of ice crystals during oral processing (Clarke, 2015). Although grittiness is often related to larger ice crystal sizes (Clarke, 2003), we did not see a correlation between these two parameters. This is however logical, as the ice crystal size in our samples was not significantly different, and therefore other aspects became more important.

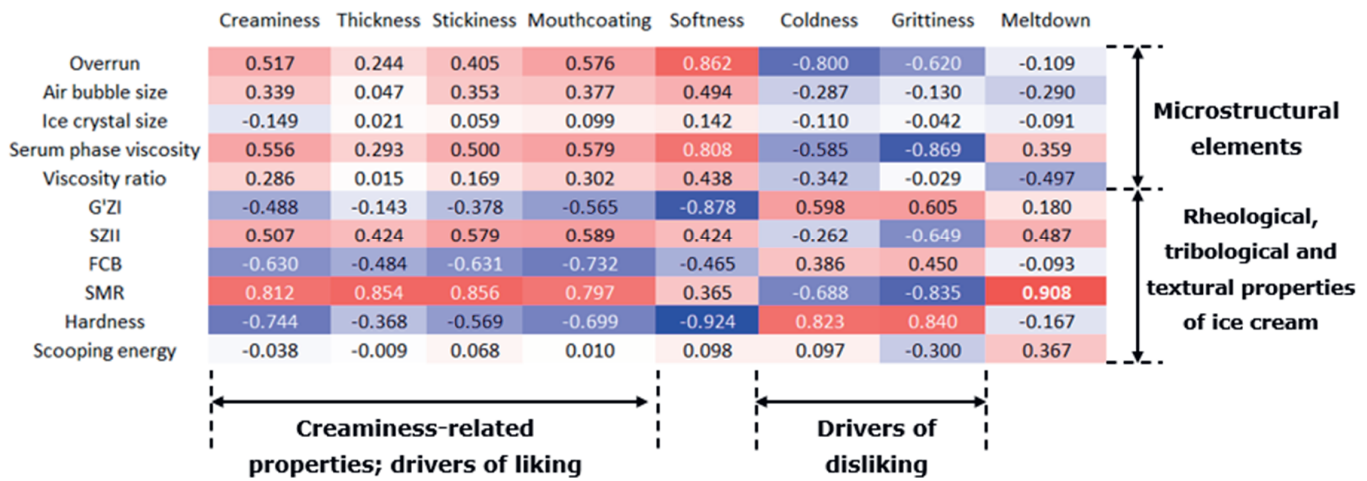

Fig. 4.5. Heatmap of correlation matrix (Pearson coefficients) between physicochemical characteristics and sensory properties of the studied ice cream samples (without high-fat sample and the attributes off-flavor and overall liking). Blue indicates negative correlation and red indicates positive correlation.

Although the lubrication properties were not directly linked to structural changes in the ice cream, they were correlated with several sensory attributes. The slope of the mixed regime (SMR) was positively correlated with creaminess (0.812), thickness (0.854), stickiness (0.856), and mouth coating (0.797). These are sensory attributes for which lubrication properties indeed play a role. However, it is worth noting that the friction coefficient in the boundary regime (FCB) did not appear to be closely correlated with any of these sensory attributes, indicating that SMR seems to be more relevant. In previous studies, sensory attributes have always been linked to friction coefficients at a specific velocity, i.e. FCB, and correlations have indeed been observed (Chojnicka-Paszun, Doussinault, & De Jongh, 2014; Fan, Shewan, Smyth, Yakubov, & Stokes, 2021; Upadhyay & Chen, 2019). However, our results showed that this is not the case for ice cream, which may be related to its complex structure. Ji et al. (2022) also found that sensory perception cannot always be explained based on one single friction coefficient extracted from a Stribeck curve, and that dynamic changes in the friction coefficient during different stages of oral processing should also be taken into account. Such dynamic changes are represented in the parameter SMR. As the structure of ice cream during oral processing is affected by the melting of the ice crystals and a dilution of the serum phase and subsequent decrease in viscosity, it is not surprising that the parameter SMR correlates better with sensory perception than FCB. Although we expected a high correlation between thickness and serum phase viscosity, and melting rate and sensory meltdown, these correlations were rather low (0.293 and 0.487, respectively). These results could indicate that thickness and meltdown are affected by multiple factors, which need further investigation.

In conclusion, flexible polysaccharides showed a higher ability to improve the sensory properties of low-fat ice cream than rigid polysaccharides. This seems mostly related to an increased overrun, which was directly correlated to increased softness and reduced coldness. Grittiness perception did not seem to be affected by the type of polysaccharides, but was mainly affected by serum phase viscosity. Attributes as creaminess, thickness and mouthcoating were more related to lubrication aspects (SMR), but could not be linked to the structure of the polysaccharides.

4.4 Conclusion

In this study, we investigated the effect of polysaccharide structure on the rheological, tribological, textural and sensory properties of ice cream. Flexible polysaccharides (LBG and GG) were less shear-thinning and showed a more liquid-like viscoelastic behavior compared with rigid polysaccharides (XG and IC), which was reflected in differences in the properties of the ice cream mix. Mixes with flexible polysaccharides showed a higher ability to incorporate air cells, while rigid polysaccharides provided a more solid-like behavior and tended to form a gel network in the serum phase, related to less air incorporation. The higher overrun of samples containing flexible polysaccharides led to lower hardness, while ice creams with rigid polysaccharides were harder to scoop. Overrun and scoopability were thus affected by the type of polysaccharide. However, melting rate was not related to the type of polysaccharide, but to serum phase viscosity. Also, no link between polysaccharide type and lubrication performance was found, nor did other structural ice cream characteristics directly link to lubrication parameters. Based on sensory evaluation, two main groups were found: ice creams with flexible polysaccharides were closer to the full-fat reference ice cream, while those with rigid polysaccharides were closer to the low-fat reference ice cream. Ice creams with flexible polysaccharides were associated with higher softness and creaminess-related properties, while rigid polysaccharides were related to higher coldness. Some attributes did not seem to be directly related to the type of polysaccharide, but to other characteristics. For example, grittiness was more related to serum viscosity, while creaminess, thickness and mouthcoating were related to changes in the friction coefficient. These results indicate that flexible polysaccharides can be considered more suitable fat replacers for improving the sensory properties of low-fat ice cream than rigid polysaccharides.

References

Akbari, M., Eskandari, M. H., & Davoudi, Z. (2019). Application and functions of fat replacers in low-fat ice cream: A review. *Trends in food science & technology, 86*, 34-40.

Alvarez, V. B. (2009). Ice cream and related products. *The sensory evaluation of dairy products*, 271-331.

Amador, J., Hartel, R., & Rankin, S. (2017). The effects of fat structures and ice cream mix viscosity on physical and sensory properties of ice cream. *Journal of food science, 82*(8), 1851-1860.

Ares, G., Giménez, A., Barreiro, C., & Gámbaro, A. (2010). Use of an open-ended question to identify drivers of liking of milk desserts. Comparison with preference mapping techniques. *Food Quality and Preference, 21*(3), 286-294.

BahramParvar, M., Tehrani, M. M., & Razavi, S. M. A. (2013). Effects of a novel stabilizer blend and presence of κ-carrageenan on some properties of vanilla ice cream during storage. *Food Bioscience, 3*, 10-18.

Bai, L., Liu, F., Xu, X., Huan, S., Gu, J., & McClements, D. J. (2017). Impact of polysaccharide molecular characteristics on viscosity enhancement and depletion flocculation. *Journal of Food Engineering, 207*, 35-45.

Biasutti, M., Venir, E., Marino, M., Maifreni, M., & Innocente, N. (2013). Effects of high pressure homogenisation of ice cream mix on the physical and structural properties of ice cream. *International Dairy Journal, 32*(1), 40-45.

Chang, Y., & Hartel, R. W. (2002). Development of air cells in a batch ice cream freezer. *Journal of Food Engineering, 55*(1), 71-78.

Chojnicka-Paszun, A., Doussinault, S., & De Jongh, H. H. J. (2014). Sensorial analysis of polysaccharide–gelled protein particle dispersions in relation to lubrication and viscosity properties. *Food Research International, 56*, 199-210.

Clarke, C. (2003). The physics of ice cream. *Physics education, 38*(3), 248.

Clarke, C. (2015). *The science of ice cream*: Royal Society of Chemistry.

Dogan, M., Aslan, D., & Gurmeric, V. (2018). The rheological behaviors and morphological characteristics of different food hydrocolloids ground to sub-micro particles: in terms of temperature and particle size. *Journal of Food Measurement and Characterization, 12*, 770-780.

Eisner, M. D., Wildmoser, H., & Windhab, E. J. (2005). Air cell microstructuring in

a high viscous ice cream matrix. *Colloids and Surfaces A: Physicochemical and Engineering Aspects, 263*(1-3), 390-399.

Fan, N., Shewan, H. M., Smyth, H. E., Yakubov, G. E., & Stokes, J. R. (2021). Dynamic Tribology Protocol (DTP): Response of salivary pellicle to dairy protein interactions validated against sensory perception. *Food Hydrocolloids, 113*, 106478.

Ferdiansyah, R., Abdassah, M., Zainuddin, A., Rachmaniar, R., & Chaerunisaa, A. Y. (2023). Effects of Alkaline Solvent Type and pH on Solid Physical Properties of Carrageenan from Eucheuma cottonii. *Gels, 9*(5), 397.

Freire, D. O., Wu, B., & Hartel, R. W. (2020). Effects of structural attributes on the rheological properties of ice cream and melted ice cream. *Journal of food science, 85*(11), 3885-3898.

Fuhrmann, P. L., Sala, G., Scholten, E., & Stieger, M. (2020). Influence of clustering of protein-stabilised oil droplets with proanthocyanidins on mechanical, tribological and sensory properties of o/w emulsions and emulsion-filled gels. *Food Hydrocolloids, 105*, 105856.

Garrec, D. A., & Norton, I. T. (2012). The influence of hydrocolloid hydrodynamics on lubrication. *Food Hydrocolloids, 26*(2), 389-397.

Goff, H. D., & Hartel, R. W. (2013). Ice cream structure. *Ice cream*, 313-352.

Granger, C., Leger, A., Barey, P., Langendorff, V., & Cansell, M. (2005). Influence of formulation on the structural networks in ice cream. *International Dairy Journal, 15*(3), 255-262.

Hadinugroho, W., Martodihardjo, S., Fudholi, A., & Riyanto, S. (2021). Preparation of Citric Acid-Locust Bean Gum (CA-LBG) for the Disintegrating Agent of Tablet Dosage Forms. *Journal of Pharmaceutical Innovation*, 1-16.

Javidi, F., Razavi, S. M. A., Behrouzian, F., & Alghooneh, A. (2016). The influence of basil seed gum, guar gum and their blend on the rheological, physical and sensory properties of low fat ice cream. *Food Hydrocolloids, 52*, 625-633.

Ji, L., den Otter, D., Cornacchia, L., Sala, G., & Scholten, E. (2023). Role of polysaccharides in tribological and sensory properties of model dairy beverages. *Food Hydrocolloids, 134*, 108065.

Ji, L., Orthmann, A., Cornacchia, L., Peng, J., Sala, G., & Scholten, E. (2022). Effect of different molecular characteristics on the lubrication behavior of polysaccharide solutions. *Carbohydrate Polymers, 297*, 120000.

Kurt, A., Cengiz, A., & Kahyaoglu, T. (2016). The effect of gum tragacanth on the rheological properties of salep based ice cream mix. *Carbohydrate Polymers,*

143, 116-123.

Liu, X., Sala, G., & Scholten, E. (2022). Effect of fat aggregate size and percentage on the melting properties of ice cream. *Food Research International*, 111709.

Mahdian, E., & Karazhian, R. (2013). Effects of fat replacers and stabilizers on rheological, physicochemical and sensory properties of reduced-fat ice cream. *Journal of Agricultural Science and Technology, 15*(6), 1163-1174.

Meyners, M., Jaeger, S. R., & Ares, G. (2016). On the analysis of rate-all-that-apply (RATA) data. *Food Quality and Preference, 49*, 1-10.

Milani, E., & Koocheki, A. (2011). The effects of date syrup and guar gum on physical, rheological and sensory properties of low fat frozen yoghurt dessert. *International Journal of Dairy Technology, 64*(1), 121-129.

Muse, M. R., & Hartel, R. W. (2004). Ice cream structural elements that affect melting rate and hardness. *Journal of dairy science, 87*(1), 1-10.

Petri, D. F. S. (2015). Xanthan gum: A versatile biopolymer for biomedical and technological applications. *Journal of Applied Polymer Science, 132*(23).

Picout, D. R., Ross-Murphy, S. B., Jumel, K., & Harding, S. E. (2002). Pressure cell assisted solution characterization of polysaccharides. 2. Locust bean gum and tara gum. *Biomacromolecules, 3*(4), 761-767.

Pintor, A., Escalona-Buendía, H. B., & Totosaus, A. (2017). Effect of inulin on melting and textural properties of low-fat and sugar-reduced ice cream: optimization via a response surface methodology. *International Food Research Journal, 24*(4), 1728.

Roland, A. M., Phillips, L. G., & Boor, K. J. (1999). Effects of fat content on the sensory properties, melting, color, and hardness of ice cream. *Journal of dairy science, 82*(1), 32-38.

Rolon, M. L., Bakke, A. J., Coupland, J. N., Hayes, J. E., & Roberts, R. F. (2017). Effect of fat content on the physical properties and consumer acceptability of vanilla ice cream. *Journal of dairy science, 100*(7), 5217-5227.

Rosti, M. E., & Takagi, S. (2021). Shear-thinning and shear-thickening emulsions in shear flows. *Physics of Fluids, 33*(8), 083319.

Salahi, M. R., & Mohebbi, M. (2021). Development of soy milk in the form of wet foam in the presences of whey protein concentrate and polysaccharides at different whipping temperatures: Study of physical, rheological and microstructural properties. *LWT, 137*, 110444.

Scholten, E. (2014). Ice cream. In *Particulate Products* (pp. 273-294): Springer.

Sofjan, R. P., & Hartel, R. W. (2004). Effects of overrun on structural and physical

characteristics of ice cream. *International Dairy Journal, 14*(3), 255-262.

Soukoulis, C., Chandrinos, I., & Tzia, C. (2008). Study of the functionality of selected hydrocolloids and their blends with κ-carrageenan on storage quality of vanilla ice cream. *LWT-Food Science and Technology, 41*(10), 1816-1827.

Stokes, J. R., Macakova, L., Chojnicka-Paszun, A., de Kruif, C. G., & de Jongh, H. H. J. (2011). Lubrication, adsorption, and rheology of aqueous polysaccharide solutions. *Langmuir, 27*(7), 3474-3484.

Taira, Y., & McNamee, C. E. (2014). Polysaccharide films at an air/liquid and a liquid/silicon interface: effect of the polysaccharide and liquid type on their physical properties. *Soft Matter, 10*(42), 8558-8572.

Thompson, K. R., Chambers, D. H., & Chambers Iv, E. (2009). Sensory characteristics of ice cream produced in the USA and Italy. *Journal of Sensory Studies, 24*(3), 396-414.

Thrimawithana, T. R., Young, S., Dunstan, D. E., & Alany, R. G. (2010). Texture and rheological characterization of kappa and iota carrageenan in the presence of counter ions. *Carbohydrate Polymers, 82*(1), 69-77.

Upadhyay, R., & Chen, J. (2019). Smoothness as a tactile percept: Correlating 'oral'tribology with sensory measurements. *Food Hydrocolloids, 87*, 38-47.

Velásquez-Cock, J., Serpa, A., Vélez, L., Gañán, P., Hoyos, C. G., Castro, C., Duizer, L., Goff, H. D., & Zuluaga, R. (2019). Influence of cellulose nanofibrils on the structural elements of ice cream. *Food Hydrocolloids, 87*, 204-213.

Wildmoser, H., Scheiwiller, J., & Windhab, E. J. (2004). Impact of disperse microstructure on rheology and quality aspects of ice cream. *LWT-Food Science and Technology, 37*(8), 881-891.

Wu, B., Freire, D. O., & Hartel, R. W. (2019). The effect of overrun, fat destabilization, and ice cream mix viscosity on entire meltdown behavior. *Journal of food science, 84*(9), 2562-2571.

Supplementary material

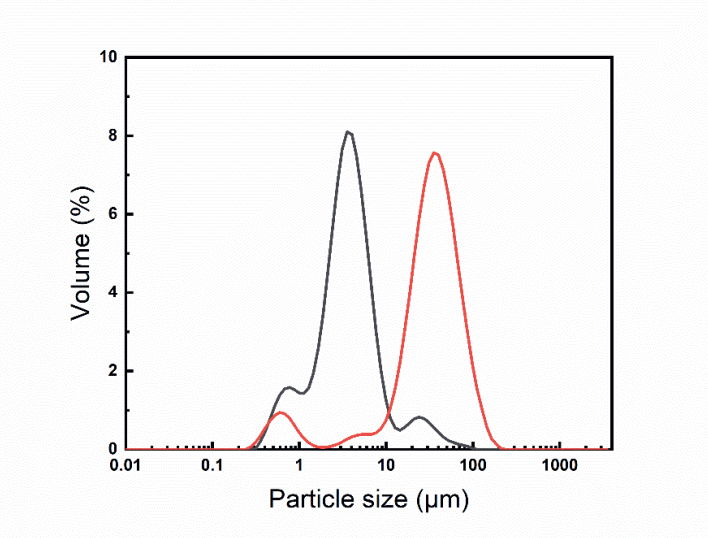

Fig. S4.1. Fat particle size distribution of ice cream mix (black line) and molten high-fat ice cream (red line). The D4,3 of ice cream mix and molten ice cream was 6.0 and 47.2 µm, and the fat aggregate percentage was 7% and 90%, respectively.

Chapter 5

Impact of soy protein dispersibility on the structural and sensory properties of fat-free ice cream

Published as: Liu, X., Sala, G., & Scholten, E. (2023). Impact of soy protein dispersibility on the structural and sensory properties of fat-free ice cream. *Food Hydrocolloids,* 109340.

Abstract

Soy protein can be an effective fat replacer in ice cream due to its contribution to the viscosity and foaming ability. In this study, we investigated the individual effect of soy protein particle size and mix viscosity on the physical, rheological, tribological and sensory properties of fat-free ice cream. Particle size was varied by homogenization and subsequent separation of the dispersible and non-dispersible fractions. Three series of ice cream mixes were made in which (i) particle size and viscosity were varied, (ii) particle size was varied with a constant viscosity, and (iii) the ratio between the dispersible and non-dispersible protein fractions, particle size and viscosity were varied. The results showed that dispersible protein particles (0.25 μm) led to lower hardness and higher scoopability as their presence was related to increased overrun and reduced non-air thickness between the air cells. In comparison, large non-dispersible particles (3.8-145 μm) enhanced the melting resistance and stability of ice cream by forming a network in the serum phase. Therefore, the size of the protein particles determined their functionality in ice cream. Based on sensory evaluation, samples with a protein particle size of approximately 4 μm showed a relatively denser texture, a lower melting rate and better lubrication behavior (lower friction), as well as a sensory profile similar to that of full-fat ice cream. This study indicates that both textural and sensory properties of fat-free ice cream can be improved by manipulating the size of plant proteins and mix viscosity.

5.1 Introduction

With today's consumers being more and more health-conscious in their food choices, low-fat or fat-free food products are becoming increasingly popular. An example of a food with high fat content is ice cream, containing 10-16% fat (Wang, et al., 2022). Ice cream has a complex microstructure consisting of air cells, ice crystals, and fat droplets entrapped in a thick continuous phase (Scholten, 2014). Fat can be present in different forms as result of the process of fat destabilization, which is linked to the properties of ice cream. When the fat droplets are present as single droplets, their main function is to adsorb at the air cell interface, but limited stability is provided. However, when the fat droplets are partially coalesced or aggregated with each other, they can contribute to the formation of a fat network. Our previous work has shown that large fat aggregates could block the lamellae between the air cells, thereby providing higher air stability by reducing the merging of the air cells and entrapping the serum phase (**Chapter 2**). Due to its multiple functionalities, reducing fat will cause many defects to ice cream, including a fast melting and a loss of creaminess and mouth coating (Liu, et al., 2022; Mostafavi, 2019; Mostafavi, Tehrani, & Mohebbi, 2017). Therefore, it is difficult to reduce the fat content but still retain the physical performance and sensory quality of ice cream.

In the search for solutions to mitigate defects that might arise from fat reduction, several fat replacers have been investigated in low-fat and fat-free ice creams. Based on the composition, fat replacers can be divided into three categories: lipid-, protein- and carbohydrate-based (Akbari, Eskandari, & Davoudi, 2019; Guo, et al., 2018; Liu, Wang, Liu, Wu, & Zhang, 2018; Yilsay, Yilmaz, & Bayizit, 2006). Although various fat replacers have been used, it has been shown that such non-fat ice creams do not meet the requirements of full-fat ice cream in terms of texture, flavor and appearance. It is for example known that milk fat can reduce the thermal diffusivity of ice cream, and that the presence of a fat network provides a better shape retention during storage and consumption (Amador, Hartel, & Rankin, 2017; Liu, et al., 2022; Wu, Freire, & Hartel, 2019). Fat replacers do not always have the capacity to provide these characteristics. Proteins are often used for their foaming and gelling abilities, which indicate their capability to adsorb at the air cell interface and form a network between the air cells (Alves, Martha, Casanova, & Tavares, 2022; Jian, et al., 2016; Morales, Martínez, Ruiz-Henestrosa, & Pilosof, 2015; Song, Zhou, Fu, Chen, & Wu, 2013; Sorgentini, Wagner, & Anón, 1995). Studies involving protein-based fat replacers

have so far mainly been focused on proteins of animal origin and mainly ascribed their contribution to the viscosity of the mix or serum phase. It has been shown that whey proteins and milk protein concentrate (including whey and casein) could partially replace fat due to their positive effect on viscosity. The presence of protein slowed down the melting rate and improved the sensory properties of low-fat ice cream, providing lower coldness and higher smoothness (Mostafavi, et al., 2017; Yilsay, et al., 2006). However, these fat-reduced ice cream did not have the same sensory quality as the full-fat ice cream.

With an increasing concern about environmental sustainability, plant-based proteins are gaining more interest from the food industry. However, research on the replacement of fat by plant proteins in ice cream is limited. Soy protein isolate is a commonly used plant protein due to its high availability and multiple functionalities, such as foaming ability and aggregation behavior (Biswas, Chakraborty, & Choudhuri, 2002; Dervisoglu, Yazici, & Aydemir, 2005; Friedeck, Aragul-Yuceer, & Drake, 2003; Puppo, et al., 2008). Although some studies have been conducted with soy protein as a fat replacer, this protein was often used in combination with a polysaccharide in the form of a complex. For example, complexes of nano-bacterial cellulose and soy protein isolate (Guo, et al., 2018) and complexes of xanthan gum and soy protein hydrolysate have been investigated (Liu, et al., 2018). With this strategy, the fat content (Liu, et al., 2018) or the cream content (Guo, et al., 2018) could be reduced by 50% and 30%, respectively, without detrimental effect on the textural properties compared to full-fat ice cream. As these studies focused on complexes rather than the protein itself, it is difficult to distinguish the role of the polysaccharide from that of the protein. In many cases, polysaccharides have also been shown to function as good fat replacers by themselves, by affecting the ice cream microstructure, physical, rheological and sensory properties (Javidi, Razavi, Behrouzian, & Alghooneh, 2016; Kurt, Cengiz, & Kahyaoglu, 2016; Liu, Sala, & Scholten, 2023a; Mahdian & Karazhian, 2013; Soukoulis, Chandrinos, & Tzia, 2008). Currently, it is not known whether soy proteins alone can be used as fat replacers, and which characteristics are important for their functionality. The particle size of commercial soy protein preparations can vary substantially, as the extraction and isolation from the original crop have a large effect on protein aggregation/agglomeration. Low level of aggregation often leads to high dispersibility of commercial protein isolates, whereas high level of aggregation leads to poor dispersibility. In other words, in different commercial soy protein preparations the ratio between dispersible and non-

dispersible fractions can vary remarkably. It is still not clear how particle size and dispersibility affect the structure of ice cream, and how the sensory characteristics can be linked to the properties of the proteins and changes in viscosity.

Our study aimed to investigate the effect of protein dispersibility (represented by particle size and viscosity) on the textural and sensory properties of fat-free ice cream. In our preliminary test, fat-free ice cream was initially planned as a control, but we found that the sample was too hard, which made it impossible to measure the relevant physical parameters. Therefore, it was excluded from the sample series. A sample containing 10% fat was used as a full-fat reference. We selected commercial soy protein isolate (SPI) as a representative plant protein and prepared three different series to vary dispersibility: a particle size series, a dispersible fraction series and a viscosity series. First, the impact of size, dispersibility and viscosity on different structural elements (overrun, air cell size and morphology, ice crystal size and morphology, non-air thickness), textural and rheological properties (hardness, scoopability, melting behavior, viscoelastic) was determined. These parameter were then linked to nine sensory attributes, which were evaluated using a rate-all-that-apply (RATA) methodology. Besides the textural and rheological parameters, we also linked the sensory attributes to the friction coefficients of the systems, as lubrication properties have also been acknowledged to play a role in sensory perception (Fuhrmann, Sala, Scholten, & Stieger, 2020; Ji, den Otter, Cornacchia, Sala, & Scholten, 2023; Schädle, Bader-Mittermaier, & Sanahuja, 2022).

5.2 Materials and methods

5.2.1 Materials

Organic cream (chosen because of the absence of carrageenan as a stabilizer and containing 33% fat, 3% lactose, 2.4% protein, 0.08% salt), organic skimmed milk (5% lactose, 3.5% protein, 0.1% salt) and sucrose were purchased from a local supermarket (Jumbo Wageningen, The Netherlands). Soy protein isolate (protein content: 90%, fat: 1.5%, carbohydrate: 1.8%, salt: 0.5%) was purchased from Myprotein (Magnice, Poland). Locust bean gum (LBG) from Ceratonia siliqua seeds with molecular weights (Mw) of ~310 kDa was purchased from Sigma-Aldrich Chemie GmbH (Steinheim, Germany). Vanillin (100%) was purchased from Royal Polak Spices (Steenwijk, The Netherlands).

5.2.2 Ice cream mix preparation

Three different series of fat-free ice creams were prepared using a model recipe containing sucrose, skimmed milk, locust bean gum, vanillin and SPI. For all series, both locust bean gum and vanillin were added at a low concentration (0.1% and 0.2%) to improve the overall sensory perception. The sugar concentration in the continuous aqueous phase of all series was kept the same (~17.4%) to guarantee constant freezing point depression and resulting ice fraction. In all series, SPI was added to the model recipe, but it was treated in different ways before addition to vary the properties of the samples. An overview of the formulations, with details on the applied processing conditions, is shown in Tab. 5.1. As a reference sample, a recipe with 10% fat was used. The sample codes are explained in the next sections. Briefly, H refers to homogenization, S refers to the dispersible fraction, IS the non-dispersible fraction, and the number at the end of each code refers to the protein concentration.

Before the series were made, we examined how much SPI was present as a dispersible fraction and how much was present as large aggregates as an non-dispersible fraction. Briefly, skimmed milk and SPI were mixed at approximately 25 °C for 2 h, and then heated upon stirring in a water bath at 80 °C for 30 min to achieve a proper dispersion of the SPI. Subsequently, the sample was centrifuged at 15500 rpm for 20 min at 20 °C. Both the supernatant and pellet were collected, and the supernatant was placed in a Binder oven (Drying Binder oven E28, VONMARCKEN, The Netherlands) and dried overnight at 105 °C. The percentage of dispersible (supernatant) and non-dispersible fraction (pellet) were evaluated by determining the amount of solid material that remained in the supernatant after centrifugation. The percentage of non-dispersible protein increased from 0 to 64% with increasing SPI content from 0 to 10% (Fig. S5.1 in supplementary material). Overall, three series of samples were made to clarify the role of soy protein particle size and dispersibility in the properties of ice cream: (i) a particle size series, in which protein particle size was varied by homogenization, (ii) a dispersible fraction series, in which the dispersible and non-dispersible fractions were first separated by centrifugation and remixed in different ratios, and (iii) a viscosity series, in which both concentration and homogenization pressure were changes simultaneously to vary particle size, while keeping viscosity the same. Detailed information for each series is shown below.

Tab. 5.1. Ice cream formulations of the studied samples. The sample codes refer to the details of the preparation methodology and the concentration of the proteins used.

Sample series		Ref	Particle size series			Dispersible fraction series			Viscosity series		
Sample codes		Fat-10	H-4	H150-4	H450-4	S-4	S50-4	IS-4	H-4	H450-5	H860-6
Ingredients (%)	Sucrose	13.3	14.2						14.2	14.05	13.90
	Skimmed milk	56.4	81.5						81.5	80.65	79.79
	Cream	30	0						0	0	0
	LBG	0.1	0.1						0.1	0.1	0.1
	Vanillin	0.2	0.2						0.2	0.2	0.2
	SPI	0	4						4	5	6

Particle size series

To adjust the particle size of dispersed SPI, we used different homogenization pressures to decrease the average particle size (Particle size series, Tab. 5.1). First, a stock solution of ice cream mix containing 4% SPI was prepared. This concentration was selected based on preliminary sensory testing of samples containing 1 to 6% SPI, and was considered to be the best concentration for comparison. Sugar and skimmed milk were first mixed with a mechanical blender for 30 min. Then LBG, vanillin and SPI were added slowly upon stirring at approximately 25 °C for 2 h. The average particle size of the SPI dispersion was around 145 µm, indicating the presence of extensive agglomeration in this commercial SPI. The mixed systems were then heated upon stirring in a water bath at 80 °C for 30 min, to achieve complete dissolution of sugar and LBG and proper dispersion of the SPI. The mixes were then cooled to room temperature (approximately 25 °C) before further treatment. One sample, denoted as "H-4", was used without homogenization and the dispersibility was 74% (Fig. 3 in supplementary material). A second sample, denoted as "H150-4", was homogenized with a homogenizer (PandaPlus, Niro Soavi, Parma, Italy) at 150 bar for 3 cycles, and a third sample, denoted as "H450-4", at 450 bar for 3 cycles. Some denaturation of protein may have occurred during homogenization (Song, et al., 2013; Sun, et al., 2022; Zhang, et al., 2022). However, as the used protein was already extensively denatured, we expected that further denaturation would not influence its functionality. After homogenization, the ice cream mixes were stored at 4 °C overnight.

Dispersible fraction series

To gain more insight in the functionality of the dispersible and non-dispersible fractions, a second "Dispersible fraction series" (Tab. 5.1) was prepared, with one sample containing only the dispersible fraction (small protein particles), one sample only the non-dispersible fraction (agglomerated protein particles), and another sample a combination of the two, all with a total protein concentration of 4%. To obtain samples with only a dispersible or non-dispersible fraction, skimmed milk and SPI were first mixed at approximately 25 °C for 2 h. Based on the results of dispersibility measurements, we adjusted the initial SPI content to 8% (dispersible percentage: ~50%) in the skimmed milk to obtain a dispersible fraction of 4% protein. The mix was then centrifuged at 15500 rpm for 20 min at 20 °C. After centrifugation, the supernatant was collected and diluted with a mixture containing skimmed milk, sugar, LBG and vanillin, to obtain a final concentration of 4% dispersible SPI in the

mix; this sample was denoted as "S-4". To obtain a sample with only the non-dispersible fraction, denoted as "IS-4", we collected the precipitate (pellet) containing non-dispersible protein aggregates, which was redispersed in the mixture (skimmed milk, sugar, LBG and vanillin) with an Ultra Turrax at a speed of 13000 rpm for 5 min to obtain a final SPI concentration of 4%. For both samples, the diluted solutions containing skimmed milk, sugar, LBG and vanillin were prepared as described in the particle size series, in which sugar, LBG and vanillin were added slowly upon stirring at approximately 25 °C for 2 h, and then heated upon stirring in a water bath at 80 °C for 30 min. In addition, we also mixed the two samples in a 50:50 ratio to obtain a sample with both a dispersible and non-dispersible fraction, denoted as "S50-4". The ice cream mixes were stored at 4 °C overnight.

Viscosity series

To exclude the effect of viscosity, we also created a series for which the viscosity was matched, referred to as the "Viscosity series" (Tab. 5.1). As viscosity decreased with decreasing particle size due to homogenization, we adjusted the SPI concentration to obtain the same viscosity, while changing homogenization pressure. We aimed for a viscosity around 31 mPa·s, similar to the viscosity of the sample H-4 (31.2 mPa·s, containing both the non-dispersible and dispersible fraction). Homogenization was again used and the concentration was adjusted to gain a similar viscosity. By changing homogenization pressure and concentration at the same time, we selected another two mixes containing 5% SPI homogenized at 450 bar for 3 cycles, and 6% SPI homogenized at 860 bar for 3 cycles, denoted as "H450-5" and "H860-6", respectively. After homogenization, the ice cream mixes were stored at 4 °C overnight before ice cream preparation.

5.2.3 Ice cream preparation

Ice cream samples (4 L) were frozen in a batch freezer (Frigomat T4S-T5S, Italy) for 8 min. The overrun was measured directly after taking the sample out of the machine. The ice cream was collected into different containers depending on the determination to be carried out: rings of different sizes for rheological characterization, and 60 mL containers for sensory evaluation. These samples were first hardened at -20 °C for 24 h to solidify further before measurements were performed.

5.2.4 Protein particle size distribution and observation

The particle size distribution of protein particles in the ice cream mix was determined by static light scattering (Mastersizer 3000, UK). Deionized water (refractive index, RI=1.33) was used to dilute the samples. The refractive index of 1.46 and 1.45 were used for fat and soy protein, and 1.33 for water. Measurements were performed at ambient temperature (20 °C) and repeated in triplicate. The $D_{4,3}$ was used to represent the mean particle size of all dispersions. The protein particles were visualized using a Zeiss Axio light microscope (AxioSkop 2 plus, Carl Zeiss GMBH, Oberkochen, Germany). Samples were diluted 10 times and were observed by an objective of 10x.

5.2.5 Ice cream mix viscosity

The viscosity of ice cream mixes was measured using a rheometer (MCR 501, Anton Paar, Germany) equipped with a cup geometry (CC17/T200/Ti). A sample of 4.7 ml was pipetted into the cup and equilibrated at 20 °C for 1 min before the measurements started. The shear rate increased from 0.1 to 100 s^{-1} in a time frame of 5 min. All measurements were performed in duplicate and the value of viscosity at 50 s^{-1} was selected as a representative.

5.2.6 Overrun

The determination of the overrun of frozen ice cream was conducted based on the measurement of a fixed volume of the aged mix in a metal cup, followed by the measurement of the same volume of ice cream in the same cup immediately after preparation. The overrun was quantified as (Muse & Hartel, 2004):

$$\text{Overrun } (\%) = \frac{Weight\ of\ mix - weight\ of\ ice\ cream}{Weight\ of\ ice\ cream} \times 100 \quad (5.1)$$

5.2.7 Ice crystal and air cell size and morphology

The analysis of ice crystal size and air cell size was carried out utilizing the methodologies outlined by Velásquez-Cock et al. (2019) and Muse & Hartel. (2004), respectively, with slight modifications. Ice crystal size and air cell size were analyzed using a Zeiss Axioskop 2 Plus light microscope equipped with a hot stage, allowing precise temperature control at -20 °C. To maintain the low temperature, all tools, reagents, and samples were kept at -20 °C prior to sample preparation. A total of 5

mg of ice cream sample was taken from the core section of each container using a sharp knife and deposited onto a standard glass slide. To promote even dispersion of ice crystals, one or two drops of kerosene at approximately -20 °C were applied, followed by covering the glass slide with a chilled cover slide. Gentle tapping with chilled tweezers was used to spread out the ice crystals. Notably, the entire sample preparation process was conducted in a -20 °C storage room to prevent melting of the ice crystals.

To analyze the air cell size, a small sample of ice cream was precisely placed on a prechilled microscope slide within a defined area delimited by a plastic frame (65 µl, 1.5 x 1.6 cm), which created a space to minimize air cell deformation. The slides were carefully sealed with a cover slide to prevent the escape of air cells. Subsequently, the hot stage of the microscope was adjusted to -6 °C, a temperature at which the air cells were buoyant enough to rise to the surface of the cover slide, enabling accurate size determination.

Images of both ice crystals and air cells were taken at 20x magnification to include at least 300 ice crystals or air cells to calculate mean size and standard deviation. The size of ice crystals and air cells was determined by manually placing a circle around each individual ice crystal or air cell, and subsequently calculating the area and radius using ZEN 2011 software. It was assumed that the crystals and air cells possessed a spherical shape during the analysis.

5.2.8 Microstructure evaluation by X-Ray Tomography

To visualize differences in structure, samples with a significant difference in overrun were selected for characterization with X-Ray Tomography (XRT), as this method is only able to distinguish between the dispersed air phase and the non-air phase. A cylindrically-shaped ice cream sample of 1.5-2 cm in height and 1 cm in diameter was extracted by pressing plastic tubes into the frozen ice cream. Samples were stored at -20 °C before measurement. An X-Ray Tomograph (GE phoenix v[tome] x m 240, United States) fitted with a nano-focus head and a 100kV/10W transmission target was used to observe the three-dimensional structure of the frozen ice cream samples. A custom-made isolated sample holder equipped with an ice-filled bucket was cooled to -20 °C to keep the ice cream samples in a frozen state. The samples were loaded into the holder and scanned at 90 kV and 320 µA. Approximately 1800 projections

were taken during a full rotation of 360° and the exposure time of each projection was 333 ms, with filtering turned off, and shift and auto scan optimizer enabled. The collected images were reconstructed into a three-dimensional representation using reconstruction software (GE Phoenix dataosx rec) with 1800 x 1800 x 1000 pixels. The mean size of the air cells and the thickness of the non-air phase were analyzed by Avizo 2019.4 after further processing.

5.2.9 Hardness and scoopability

The assessment of hardness and "scoopability" of the ice cream samples was conducted using a Texture Analyzer (TA-TX plus, Stable Micro Systems, UK). Samples with fixed volume were prepared by employing plastic rings measuring 25 mm in height and 70 mm in diameter. These samples were subsequently stored in a freezer at -20 °C for a minimum of 24 h. Prior to the measurement, a climate chamber was connected to the Texture Analyzer to maintain a temperature of -20 °C, achieved by utilizing liquid nitrogen. For the determination of hardness, the samples were carefully removed from the plastic rings using a cylindrical cutting tool, and promptly transferred to the climate chamber. Subsequently, a penetration test was carried out with an aluminum cylindrical probe (5 mm in diameter) attached to a 50 kg load cell, with a strain of 50% applied at a speed of 2 mm/s. Hardness was taken as the maximum stress of the stress-strain curve. For scoopability, a scooping spoon probe in combination with an ice cream sample holder was used, as explained in our previous work (**Chapter 4**). The scooping spoon was forced into the ice cream with a constant velocity of 3 mm/s over a distance of 25 mm. We used the area under the curve (AUC) as a measure of spooning energy: the larger the scooping energy, the lower the scoopability. Both hardness and scoopability measurements were done in triplicate to obtain average values and standard deviations.

5.2.10 Changes of viscoelastic properties during melting

Temperature sweep experiments (-20 to 10 °C) were performed to determine the viscoelastic properties of the studied ice cream samples during the melting process. Measurements were performed using a rheometer (MCR 301, Anton Paar, Germany) at a constant strain of 0.005% and a frequency of 1.6 Hz with a plate-plate geometry (PP50/P2). A moveable hood covering the plate-plate geometry was connected to the cooling system to control the temperature. An air pump was connected to the hood to prevent heat exchange with the environment. Prior to the measurement, the initial

temperature of the plate was reduced to -20 °C using a Peltier element, and then the ice cream specimens (-20 °C) of 5 mm height and 25 mm diameter were taken out of the metal rings using a cylindrical cutting tool and were transferred to the plate immediately. The initial force was set at 5 N to guarantee that the upper plate touched the sample tightly before starting the measurements. The gap width between the plates was adjusted to a constant value of 3 mm, which was small enough to keep contact between the probe and the sample during the entire duration of the measurements. The temperature was increased to 10 °C with a heating rate of 0.5 °C/min. Sixty measuring points were recorded and the total measuring time was 60 min. Storage modulus (G') and loss modulus (G'') were recorded (Fig. S5.2 in supplementary material). Three zones could be identified during the whole process (Wildmoser, Scheiwiller, & Windhab, 2004) and three parameters were extracted after the measurements: (1) the value of G' at -15 °C (zone I, G'_{-15}), (2) the slope of G' during the melting stage (zone II, SZII), and (3) the value of G' at 5°C (zone III, G'_{5}), which is related to the structure stability after complete melting. Ice cream samples were measured at least twice to obtain average values.

5.2.11 Lubrication behavior

Tribology measurements were carried out to evaluate the lubrication properties of different samples with a MCR 301 rheometer equipped with a tribology accessory (T-PTD 200, BC 12.7, Anton Paar, Austria). The set-up was based on a glass ball-on-three-pins principle, consisting of a spherical glass ball (d = 12.7 mm) and three PDMS pins (d = 6 mm, roughness = 0.2 µm ± 0.03). The temperature of the tribology cup was set at 20 °C and a normal force of 1 N was applied. Molten ice creams with a volume of 0.6 ml were poured into the tribology cup, and the friction coefficient was measured as a function of sliding speed. One measurement consisted of 2 cycles in total with increasing and decreasing sliding speed between 0.01 and 470 mm/s, in 7.5 min per run (total of 4 runs). The data of the third run with increasing speed showed good repeatability and were selected for further analysis. The measured friction coefficient was plotted versus sliding speed (Fig. S5.3 in supplementary material). Two regimes could be identified: a boundary regime at low sliding speed, and a mixed regime at intermediate sliding speeds. A hydrodynamic regime was not obtained as the viscosities of the samples were not high enough. The friction coefficient in the boundary regime of 1 mm/s (FCB) and the slope of the friction coefficient over sliding speed in the mixed regime (SMR) were used to represent

different lubrication behavior of different samples.

5.2.12 Determination of sensory properties

A sensory study was performed using an untrained panel (n = 78 participants; gender: 46 female, 32 male; age range: 18 - 45) using a rate-all-that-apply (RATA) methodology (Fuhrmann, et al., 2020; Ji, et al., 2023; Santagiuliana, Christaki, Piqueras-Fiszman, Scholten, & Stieger, 2018). Participants were recruited from the campus of Wageningen University & Research. All participants in the study were found to have good general and oral health, normal tasting and smelling abilities, did not use any medication, and reported no allergies or intolerances towards the ingredients of the ice cream samples. All participants signed a consent form, and upon completion of the study, they were provided with appropriate financial compensation.

Nine samples (Tab. 5.1) were stored in the freezer (-20 °C) and coded with 3-digit numbers according to a random design. Each sample was supplied in individual plastic containers of 60 ml and kept at 4 °C for 30 min and room temperature (approximately 25 °C) for 5 min before serving. For logistics reasons, the participants were divided into 8 groups, and the serving order of samples was randomized for each group using a Latin Square design to prevent presentation order effects. The participants evaluated the 9 ice cream samples for 8 attributes (creaminess, softness, coldness, grittiness, denseness, mouth coating, melting time and beany flavor). The provided attribute list and definitions are chosen and adjusted based on previous studies (Pang, Bourouis, & Liu, 2022; Thompson, Chambers, & Chambers Iv, 2009; Wang, et al., 2022) and are shown in Tab. 5.2. The participants first selected the attribute(s) that were applicable for their samples. Once selected, they were asked to score the chosen attributes on a 9-point scale labeled from “lowest intensity” (= 1) to “highest intensity” (= 9). In addition, the overall liking was also rated based on a 9-point hedonic scale. Data were collected online using a questionnaire made in Qualtrics (2023). Between samples, the participants were instructed to drink water to remove the residue of the previous sample from their mouth.

Tab. 5.2. Sensory attributes and definitions for the sensory test.

Attribute	Definition
Creaminess	Refers to the intensity of a smooth, velvety and thick feeling in the mouth when the sample is manipulated between the tongue and the palate
Softness	The ease of compressing the sample between the tongue and palate
Coldness	The feeling of cold in the mouth/upper gastrointestinal tract upon eating or swallowing the sample
Grittiness	The immediate perception of particles within the sample
Denseness	The thickness of the samples and the lack of air
Mouth coating	A sensation of having a coating on the tongue and other mouth surfaces
Melting time	The time required for the product to melt in the mouth when continuously pressed by the tongue against the palate
Beany flavor	An unpleasant or unusual beany flavor that is not typically associated with ice cream
Overall liking	How much was the sample liked

5.2.13 Statistical analysis

The data, apart from those obtained by the sensory study, were analyzed with SPSS software (Version 25.0, IBM Corp). The means were compared with a Duncan's test at a 5% level of significance using an analysis of variance (ANOVA). RATA data and overall liking obtained from the sensory study were analyzed by a linear mixed model using RStudio (RStudio, Inc., Version 4.0.2), having both the sample and panelist as independent factors. Additionally, the results obtained from physical, rheological, tribological and sensory measurements were analyzed by Principal Component Analysis (PCA) and correlation matrices were established for the different properties. In addition, biplots obtained from Principal Component Analysis (PCA) were used to visually represent sample grouping and differentiation. PCA analyses were performed using XLSTAT software (Addinsoft, Paris, France).

5.3 Results and discussion

5.3.1 Particle size, particle morphology and ice cream mix viscosity

We first investigated the particle size distribution of the protein particles of the mixes of the different samples. As shown in Fig. 5.1, four groups could be identified among all fat-free samples based on the different mean particle sizes: (1) a sample with mean particle size lower than 1 µm (black: S-4); (2) samples with mean particle size from 4 to 7 µm (red from light to dark: H450-5, H450-4 and H860-6); (3) a sample with mean particle size of approximately 23 µm (green: H150-4); and (4) samples with mean particle size higher than 100 µm (blue from light to dark: S50-4, IS-4 and H-4). A bimodal distribution could be found for the second group, in which samples were treated with high pressure homogenization (> 450 bar). Under these conditions, large non-dispersible agglomerates were broken into two ranges of particles, one with particles smaller than 1 µm, and one with particles larger than 1 µm. In addition, the corresponding protein dispersibility also increased compared with the sample without homogenization. For example, the dispersibility of H-4 increased from 74% to 90% (H450-4) after homogenization. The mean particle size and percentage of dispersible fraction of all fat-free samples are shown in Tab. 5.3.

When commercial soy protein was used, a mean particle size of 145 µm was observed in H-4, which in the graph of Fig. 5.1 presented only one peak (darkest blue). Although this sample also contained dispersible proteins (74%), the particle size distribution was dominated by the size of the non-dispersible protein agglomerates. This is logical, as the $D_{4,3}$ is based on a volume-based measurement, and therefore the larger particles have a much greater contribution to the light scattering signal. In the first series, the applied pressure of 150 bar (H150-4) decreased the particle size to 23.2 µm, and slightly increased the dispersible fraction from 74 to 79%. When pressure was increased to 450 bar (H450-4), the particle size decreased further to 4.1 µm, and the dispersible fraction increased to 90%. High mechanical shearing during homogenization partially disrupted the non-dispersible protein agglomerates into smaller particles, which has also been shown by others (Sun, et al., 2022; Yu, et al., 2018). Homogenization thus led to a series with particle size varying from 4.1 to 145 µm. With a decrease in particle size, the corresponding mix viscosity also decreased from 31.2 to 17.1 mPa·s. This result is qualitatively in agreement with the study of Song et al. (2013), who showed that increasing homogenizing pressure could reduce the particle size of a soy protein suspension and its viscosity.

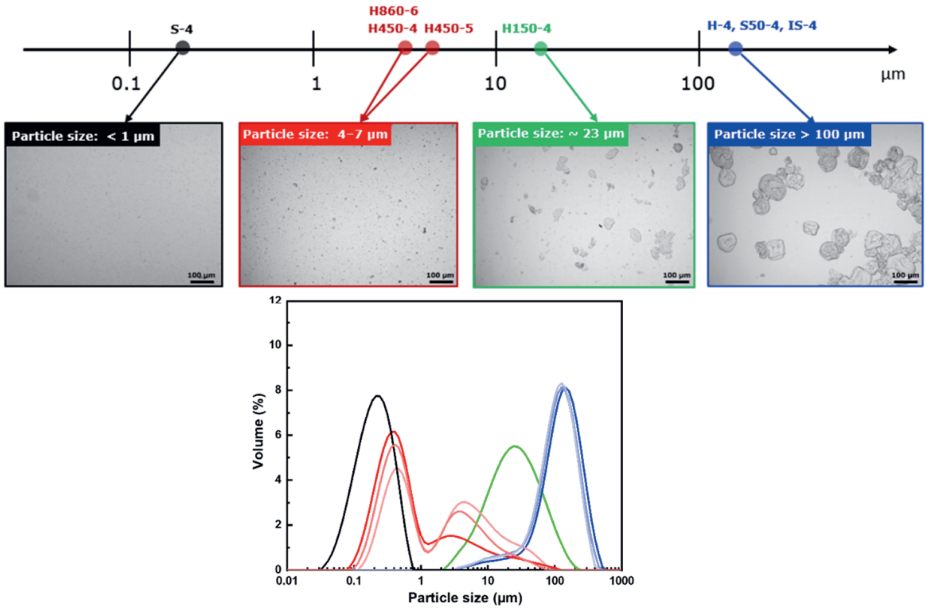

Fig. 5.1. Overview of the particle size distribution of the mixes of the studied samples characterized with light microscopy and static light scattering. The scale bar in the figures represents 100 µm. Different colors refer to different ranges of mean particle size: black (S-4); red from light to dark (H450-5, H450-4 and H860-6); green (H150-4) and blue from light to dark (S50-4, IS-4 and H-4).

In the dispersible fraction series, we separated the dispersion with commercial soy protein into a dispersible fraction (S-4) and a non-dispersible fraction (IS-4), and from these fractions we prepared new dispersions both with a concentration of 4%. The dispersible fraction had a mean particle size of 0.25 µm (Tab. 5.3), whereas the non-dispersible fraction showed a much larger size of 137 µm, close to the initial size of 145 µm. To investigate the relative contribution of these fractions to the properties of ice cream, a sample was prepared with a 50/50 ratio of these fractions (S50-4), which showed a particle size distribution very similar to that of the sample made with the non-dispersible fraction (IS-4). The contribution of the small dispersible protein fraction was not visible (Fig. 5.1), similarly to what was obtained for sample H-4. In this series, the mix viscosity significantly increased from 11.4 to 199 mPa·s with decreasing proportion of dispersible fraction from 100 to 0%, indicating that non-dispersible agglomerates contributed more to viscosity. An increase in viscosity as a

result of aggregation is a common phenomenon for proteins (Hong, Iwashita, & Shiraki, 2018). The obtained viscosities were thus higher than those of the samples of the particle size series.

Tab. 5.3. Overview of protein particle characteristics and viscosity of the mixes of the studied samples.

Sample series	Sample codes	$D_{4,3}$ (μm)	Percentage of dispersible fraction (%)	Mix viscosity (mPa·s)
Ref	Fat-10	16.0 ± 0.2^{c}	-	20.1 ± 0.1^{d}
Particle size series	H-4	145 ± 5^{a}	74	31.2 ± 1.1^{b}
	H150-4	23.2 ± 0.5^{c}	79	26.8 ± 0.3^{c}
	H450-4	4.1 ± 0.1^{de}	90	17.1 ± 0.1^{e}
Dispersible fraction series	S-4	0.25 ± 0.01^{e}	100	11.4 ± 0.2f
	S50-4	139 ± 5^{ab}	50	31.7 ± 2.1^{b}
	IS-4	137 ± 6^{ab}	0	199 ± 2^{a}
Viscosity series	H-4	145 ± 5^{a}	74	31.2 ± 1.1^{b}
	H450-5	6.9 ± 0.2^{d}	82	30.8 ± 0.4^{b}
	H860-6	3.8 ± 0.1^{e}	88	32.1 ± 0.9^{b}

Values with a different letter within the same column are significantly different ($P < 0.05$).

To exclude the effect of viscosity and focus on the effect of particle properties only, we prepared a third series with viscosity similar to that of H-4 by varying the protein concentration and homogenization pressure (that is why H-4 is thus present in series 1 and 3). In the sample with 5% SPI (H450-5), an applied pressure of 450 bar was needed to obtain a viscosity of 31 mPa·s. The corresponding particle size decreased to 6.9 μm, and the dispersibility increased from 68% (Fig. S5.1 in supplementary material) to 82%. When the protein content was increased to 6%, a higher applied pressure of 860 bar was needed to obtain a viscosity of 31 mPa·s, and the sample H860-6 showed a particle size of 3.8 μm and a dispersibility of 88%. Overall, we were able to create three sample sets that differed in viscosity and/or particle size/number to investigate how parameters influence the properties of ice cream.

5.3.2 Characteristics of the ice cream samples

As the particle size distribution and the viscosity of the mixes were expected to directly affect the different structural elements of the ice cream, we measured overrun, air cell size and morphology, ice crystal size and morphology, and non-air thickness of all ice cream samples. The results are provided in Tab. 5.4.

The overrun of the reference sample (10% fat) was 32%, consistently with values of samples of our previous study (**Chapter 3**). Compared with the reference, samples containing protein particles showed a higher overrun, ranging from 43 to 71%. The highest overrun (71%) was found in sample S-4, which had the lowest particle size (0.25 µm) compared with others (> 3.8 µm). This indicates the importance of the size of protein particles for air incorporation. As the air cell size in our samples was approximately 30 µm (Tab. 5.4), it might be hypothesized that to stabilize air cells in ice cream the size of protein particles should roughly be ten times smaller than such value. The proteins in the dispersible fraction could thus rapidly absorb at the water-air interface during ice cream preparation. In addition, a positive correlation between viscosity and overrun was observed in the particle size series, in which the overrun decreased from 55 to 44% with a decrease in viscosity from 31.2 to 17.1 mPa·s. When the viscosity was matched at around 31 mPa·s, a similar high overrun of approximately 53% was found in the concentration series. In addition, the sample S50-4 with the viscosity of 31.7 mPa·s also showed high overrun of 63%, indicating the importance of the viscosity in air incorporation.

In the present study, no significant differences could be found in air cell size among studied samples (Tab. 5.4). However, some differences were found in the air cell morphology. As shown in Fig. 5.2, some irregular air cells were observed in the samples containing fat aggregates (Fat-10) or non-dispersible protein aggregates (IS-4, S50-4 and H-4). The large particles in the non-air (serum) phase may have physically hindered the air cells in acquiring a spherical shape. In addition, in sample S-4 a higher amount of large air cells was observed, corresponding with the highest overrun (71%). This could potentially be attributed to a higher degree of coalescence of the air cells in this sample, as the absence of large particles may have allowed for closer contact of the air cells due to smaller non air-phase thickness.

Tab. 5.4. Microstructural characteristics of the studied ice cream samples.

Sample series	Sample codes	Overrun (%)	Air cell size (µm)	Ice crystal size (µm)	Overrun based on XRT (%)	Non-air thickness (µm)
Ref	Fat-10	32 ± 2^{f}	35 ± 13^{a}	50 ± 14^{a}	24.0	152
Particle size series	H-4	55 ± 1^{c}	29 ± 13^{a}	50 ± 12^{a}	40.5	111
	H150-4	50 ± 2^{cd}	26 ± 11^{a}	52 ± 11^{a}	35.8	120
	H450-4	44 ± 3^{de}	33 ± 16^{a}	51 ± 15^{a}	32.1	139
Dispersible fraction series	S-4	71 ± 4^{a}	28 ± 16^{a}	47 ± 13^{a}	55.5	87
	S50-4	63 ± 2^{b}	33 ± 7^{a}	54 ± 15^{a}	48.8	98
	IS-4	43 ± 2^{e}	30 ± 13^{a}	43 ± 12^{a}	32.8	138
Viscosity series	H-4	55 ± 1^{c}	29 ± 13^{a}	50 ± 12^{a}	40.5	111
	H450-5	52 ± 4^{c}	30 ± 16^{a}	48 ± 13^{a}	39.8	113
	H860-6	53 ± 4^{c}	25 ± 9^{a}	48 ± 15^{a}	38.6	112

Values with a different letter within the same column are significantly different ($P < 0.05$).

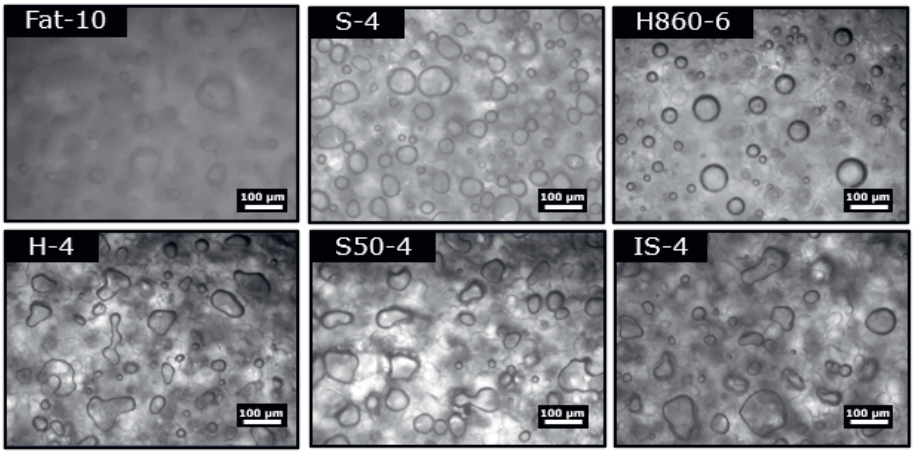

Fig. 5.2. Micrographs illustrating air cell morphology of representative samples (10x).

To obtain further information on the air cell morphology and size distribution, we investigated the 3D structure of ice cream by X-Ray Tomography. This method relies on the density differences between phases and is able to distinguish between the dispersed air phase and the non-air phase. We analyzed four samples representative of groups with different ranges of overrun. The results are shown in Fig. 5.3. From the image reconstruction, the air volume (overrun) was calculated based on the ratio air volume/total volume (air plus solid volume), and the distance between air cells (non-air thickness) was also quantified. The results are summarized in Tab. 5.4. The overrun values ranged from 24 to 56%. These values are slightly lower than those determined with a gravimetric method reported in Tab. 5.4. The discrepancy can be explained with the differences in the determination methods. To start, we cannot exclude that during the determination with the gravimetric method extra air is inserted in the samples when scooping the ice cream in the measuring cylinder. Secondly, the resolution of the XRT method (10 µm) might lead to the fact that the smallest air cells in the ice cream are not included in the quantification of the overrun. These aspects would explain why XRT provides lower values. Samples with high overrun corresponded with a lower non-air thickness. For example, sample S-4 with the highest overrun (56%) showed the lowest non-air thickness of 87 µm, while sample Fat-10 with the lowest overrun (24%) had the highest non-air thickness of 152 µm. Similar indications were also found in our previous research (**Chapter 3**), in which we reported that higher overrun leads to lower thickness between air cells. The negative correlation between overrun and non-air thickness is logical, as the air cells

were all of similar size. When more air is incorporated, less non-air (serum) phase is present in a fixed sample volume, and thickness is consequently lower.

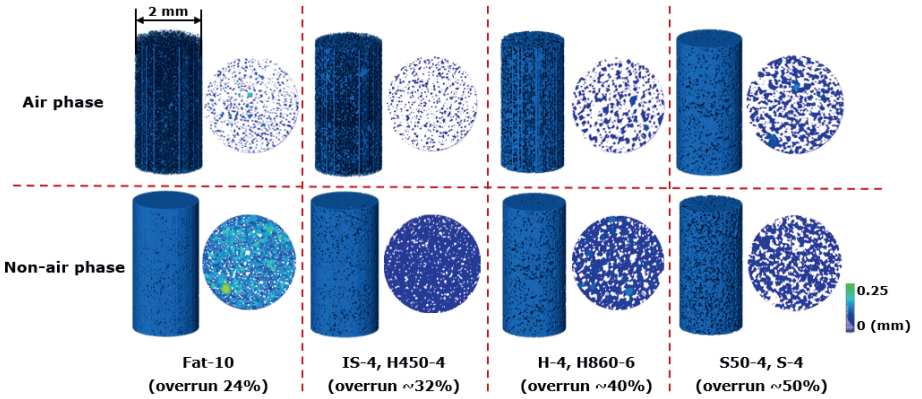

Fig. 5.3. Images of the 3D microstructure of ice creams with different overrun level. The dimensions of the cylinders were 4.5 mm in height and 2 mm in diameter. In both air and non-air phase, the warmer (green) colors indicate higher values of air cell size or non-air thickness, and colder (blue) colors indicate lower values.

Similarly to what was discussed for the air cell size, no significant difference could be found in the ice crystal size of the studied samples (Tab. 5.4), which ranged from 43 to 54 μm. To unveil possible variations in the morphology of ice crystals, we carried out microscopy observations. As shown in Fig. 5.4, the crystals' morphology was also similar, indicating that differences in proteins particles size and mix viscosity did not appear to affect this structural feature. This could be attributed to the dominant effect of freezing conditions on the formation of ice crystals, as discussed in many papers (Adapa, Schmidt, Jeon, Herald, & Flores, 2000; Cook & Hartel, 2010; Muse and Hartel, 2004). As the same freezing process was used for all samples, similar ice crystal size and morphology could be expected.

In conclusion, small protein particles present in the dispersible centrifugation fraction showed a significant ability to adsorb at the air cell interface, resulting a higher overrun values of ice cream samples (S-4 and S50-4). In comparison, large non-dispersible agglomerates were most likely present in the non-air phase among air cells, modifying the shape of the air cells. For large particles, a lower overrun and a higher non-air thickness was found.

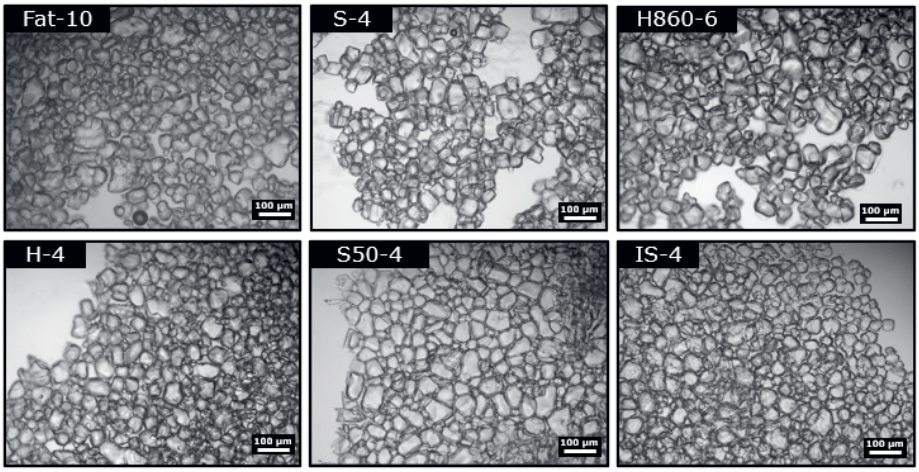

Fig. 5.4. Observation of ice crystal morphology of representative samples by light microscope (10x).

5.3.3 Textural and melting properties

To investigate how the structure of the samples affected their textural properties, hardness, scoopability and melting behavior were determined. The results are summarized in Tab. 5.5.

The reference sample with 10% fat showed a hardness of 8.0 MPa, while all fat-free samples had a lower hardness (1.0 – 5.6 MPa), apart from IS-4 (9.5 MPa). The relatively higher hardness of Fat-10 could be attributed to the lower overrun value (32%), as overrun has been negatively correlated with hardness (Muse & Hartel, 2004; Sofjan & Hartel, 2004; Wilbey, Cooke, & Dimos, 1998). The lowest hardness of 1.0 MPa for sample S-4 in the dispersible fraction series can easily be explained by the fact that this sample had the highest overrun (71%). In addition, we also found that in the particle size series, overrun was not negatively correlated with hardness. This could be attributed to a secondary effect of mix viscosity on hardness, for which higher viscosity leads to higher hardness. The variations in scooping energy were similar to those of hardness, indicating that scooping energy was also influenced by overrun and mix viscosity.

Tab. 5.5. Textural and melting properties of ice cream samples with different protein particle size and viscosity.

Sample series	Sample codes	Hardness (MPa)	Scooping energy (N · mm)	Lag time (min)	Melting rate (%/min)
Ref	Fat-10	8.0 ± 0.2^{b}	454 ± 69^{b}	35 ± 1.8^{b}	0.76 ± 0.03^{e}
Particle size series	H-4	5.2 ± 0.3^{cd}	388 ± 22^{bc}	28 ± 0.2^{cd}	2.16 ± 0.04^{b}
	H150-4	4.4 ± 0.9^{de}	356 ± 25^{c}	19 ± 0.3^{ef}	2.17 ± 0.01^{b}
	H450-4	3.6 ± 0.4^{ef}	309 ± 18^{cd}	16 ± 0.4^{f}	2.11 ± 0.03^{b}
Dispersible fraction series	S-4	1.0 ± 0.3^{g}	108 ± 24^{e}	20 ± 0.9^{ef}	2.72 ± 0.01^{a}
	S50-4	2.9 ± 0.5^{f}	257 ± 15^{d}	33 ± 0.5^{bc}	1.86 ± 0.07^{c}
	IS-4	9.5 ± 0.4^{a}	572 ± 43^{a}	48 ± 3.3^{a}	1.07 ± 0.10^{d}
Viscosity series	H-4	5.2 ± 0.3^{cd}	388 ± 22^{bc}	28 ± 0.2^{cd}	2.16 ± 0.04^{b}
	H450-5	5.6 ± 0.2^{cd}	395 ± 33^{bc}	23 ± 0.3^{de}	2.22 ± 0.03^{b}
	H860-6	5.3 ± 0.2^{cd}	359 ± 65^{c}	18 ± 0.1^{ef}	2.25 ± 0.05^{b}

Values with a different letter within the same column are significantly different ($P < 0.05$).

We also observed significant differences in melting behavior among samples. As shown in Tab. 5.5, the reference sample (Fat-10) had a significantly lower melting rate (0.76 %/min) compared with the reduced-fat samples (1.07 – 2.72 %/min). This could be attributed to the formation of a fat network, which could hold the structural integrity and resist the dripping of the molten phase (**Chapter 2**). Some differences in melting performance could be found in fat-free samples. For example, in the dispersible fraction series, a significantly higher lag time (48 min) and lower melting rate (1.07 %/min) were found for IS-4, which had a low overrun (43%) and a high mix viscosity (199 mPa·s). In contrast, sample S-4 with a higher overrun (71%) and low viscosity (11.4 mPa·s) had a much lower lag time (20 min) and a higher melting rate (2.72 %/min). Although it has been reported that air is a good insulator and can decrease the melting process (Liu, et al., 2023b; Muse & Hartel, 2004; Sofjan, et al., 2004), in our samples mix viscosity seemed to be more important than overrun in determining the melting behavior. In both the homogenization and viscosity series, with small differences in overrun and viscosity, we could observe similar melting rate but significant differences in lag time. Differences in lag time may be more related to differences in particle size. In both series, the sample H-4, with large particles of 145 μm, showed a higher lag time than the other samples with smaller particles (< 23.2 μm). This may be due to the formation of a temporary protein network with a higher

ability to retain the non-air serum phase. However, this temporary network will break down due to the dilution of the serum phase during melting. Therefore, no significant differences could be found in the melting rate.

In conclusion, small dispersible protein particles lead to lower hardness and higher scoopability due to their contribution to overrun, whereas non-dispersible particles contribute more to the melting resistance due to their positive effect on mix viscosity and higher ability to form a network in the serum phase. Mix viscosity appeared to be the dominant factor in affecting the melting rate, while particle size appeared to be the dominant factor in affecting the lag time.

5.3.4 Rheological and tribological properties

The viscoelastic behavior upon increasing temperature and the tribological parameters were determined to unveil the effect of different structural elements on these properties. From the curves of the viscoelastic behavior upon increasing temperature (Fig. S5.2, supplementary material), three parameters were extracted: storage modulus at -15°C, G'_{-15}, storage modulus at 5°C, G'_{5}, and slope in the melting zone, SZII. As shown in Tab. 5.6, similar values of G'_{-15} could be found in the reference sample (8.2 MPa) and IS-4 (7.9 MPa), which were significantly higher than other fat-free samples (5.5 – 7.1 MPa). This could be partly attributed to their lower overrun values (32% and 43%, respectively). In the frozen state, the ice network should be the dominant factor in affecting G'. The presence of air cells could reduce the contact among ice crystals, and thus, a weaker ice crystal network could be formed. However, we also found some differences in G'_{-15} for some samples with similar overrun, indicating that also other aspects were relevant. For example, at a similar overrun (43%), IS-4 showed significantly higher G'_{-15} (7.9 MPa) than H450-4 (6.0 MPa). This may be related to the high viscosity of the IS-4 samples, which was also reflected in the highest hardness (9.5 MPa). The relation between G'_{-15} and hardness was also reported by other studies (Balthazar, et al., 2017; Leahu, Ropciuc, & Ghinea, 2022; Liu, et al., 2023b).

Tab. 5.6. Viscoelastic and tribological properties of the three series of ice cream samples.

Sample series	Sample codes	G'_{-15} (MPa)	SZII	G'_5 (Pa)	FCB (at 1 mm/s)	SMR
Ref	Fat-10	8.2 ± 0.7^{a}	-0.76 ± 0.02^{a}	10765 ± 571^{a}	0.11 ± 0.01^{e}	-0.85 ± 0.01^{g}
Particle size series	H-4	6.7 ± 0.5^{bcd}	-0.64 ± 0.03^{cde}	11.1 ± 1.7^{d}	0.46 ± 0.01^{b}	-1.96 ± 0.03^{d}
	H150-4	6.3 ± 0.6^{cde}	-0.60 ± 0.01^{def}	2.5 ± 0.4^{e}	0.44 ± 0.01^{bc}	-1.97 ± 0.03^{d}
	H450-4	6.0 ± 0.3^{def}	-0.53 ± 0.01^{f}	0.3 ± 0.1^{e}	0.44 ± 0.01^{bc}	-2.09 ± 0.01^{c}
Dispersible fraction series	S-4	5.5 ± 0.1^{f}	-0.59 ± 0.01^{ef}	0.2 ± 0.1^{e}	0.50 ± 0.01^{a}	-2.27 ± 0.01^{a}
	S50-4	5.9 ± 0.4^{ef}	-0.62 ± 0.04^{cde}	24.1 ± 2.2^{c}	0.46 ± 0.01^{b}	-2.15 ± 0.01^{b}
	IS-4	7.9 ± 0.4^{a}	-0.73 ± 0.02^{ab}	132 ± 20^{b}	0.41 ± 0.01^{d}	-1.96 ± 0.01^{d}
Viscosity series	H-4	6.7 ± 0.5^{bcd}	-0.64 ± 0.03^{cde}	11.1 ± 1.7^{d}	0.46 ± 0.01^{b}	-1.96 ± 0.03^{d}
	H450-5	7.1 ± 0.3^{b}	-0.67 ± 0.05^{bcd}	1.2 ± 0.1^{e}	0.42 ± 0.01^{cd}	-1.79 ± 0.01^{e}
	H860-6	7.0 ± 0.1^{bc}	-0.68 ± 0.01^{bc}	0.5 ± 0.1^{e}	0.40 ± 0.01^{d}	-1.72 ± 0.03^{f}

Values with a different letter within the same column are significantly different ($P < 0.05$).

In the melting zone, defined by SZII, the full-fat reference (Fat-10) showed the highest SZII (-0.76), which could be explained by the fat network. Nearly all three series of fat-free ice creams showed a lower SZII (from -0.53 to -0.68), apart from IS-4 (-0.73), which showed a SZII comparable to that of the full-fat reference. This result suggests that when large non-dispersible protein agglomerates were concentrated enough in the serum phase, they could partly mimic the function of the fat network in the melting process by forming a protein particle network, as also supported by the result of melting tests. The effect of the network formation could also be observed in zone III, in which G' is a result of the structural organization of molten ice cream. The reference containing a fat network and the fat-free sample containing non-dispersible aggregates showed significantly higher G'_5. Therefore, we concluded that the viscoelastic behavior of the molten ice cream was mainly related to the protein particle size: large agglomerates showed a significantly higher ability to form a structure in the serum phase.

Besides the viscoelastic behavior, protein particle properties were expected to affect the lubrication behavior of molten ice cream. Lubrication has been shown to correlate with several sensory attributes, such as creaminess and mouth coating (De Wijk, Terpstra, Janssen, & Prinz, 2006; Ji, et al., 2023; Krop, Hetherington, Miquel, & Sarkar, 2019). Reduced lubrication, i.e. increased friction coefficient, has been associated with the reduced sensation of creaminess. Attributes such as creaminess and mouthcoating are relevant at late stages of oral processing just before swallowing, during which the ice cream is already mostly melted. Thus, we measured the lubrication properties of molten samples, and the results are shown in Tab. 5.6. For all samples, two regimes could be found (Fig. S5.3 in supplementary material), and the friction coefficient in the boundary regime at 1 mm/s (FCB) was used to represent the lubrication properties of the different samples. A significantly lower friction coefficient in the boundary regime (FCB, 0.11) was found in the full-fat reference sample, which could be attributed to the good lubrication ability of fat (Chojnicka-Paszun, De Jongh, & De Kruif, 2012). For all fat-free samples, higher friction coefficients (> 0.40) were found. This could be attributed to the specific lubrication mechanisms of protein particles. Due to its hydrophobic nature, fat is able to form a layer on the PDMS surface (film lubrication) based on the so-called plate-out mechanism (Ji, Cornacchia, Sala, & Scholten, 2022; Schädle, et al., 2022). Instead, large protein particles provide lubrication via particle lubrication, by reducing the contact between the interacting surfaces (Ji, Cornacchia, et al., 2022; Rudge, Van De

Sande, Dijksman, & Scholten, 2020). The higher FCB in fat-free samples indicates that protein particles were less effective in providing lubrication than the fat particles, which has been discussed in other papers as well (Ji, Cornacchia, et al., 2022; Ningtyas, Tam, Bhandari, & Prakash, 2021; Nourmohammadi, Austin, & Chen, 2023). Differences were found in the fat-free samples, as the efficiency of protein particles largely depends on the particle characteristics, such as particle size and shape (Ji, Cornacchia, et al., 2022; Nourmohammadi, et al., 2023). A significantly higher FCB of 0.50 was observed in S-4, which only contained dispersible small protein particles. In comparison, a lower FCB of 0.41 was found in IS-4, which contained non-dispersible large agglomerates. This can be explained by the different gap sizes caused by the presence of small and large particles. Large particles caused a larger gap size between surfaces, and the lower contact between surfaces thus lead to lower friction. This effect of particle size has been discussed in several studies (Rudge, et al., 2020; Stribiţcaia, Krop, Lewin, Holmes, & Sarkar, 2020). In addition, when both dispersible and non-dispersible particles were present in the systems (particle size series), decreasing particle size from 145 to 4 µm did not appear to affect the FCB, indicating that a size of 4 µm might be sufficient to separate the two sliding surfaces, probably also because a higher number of particles was present (as a similar total protein content was used). Comparing samples with similar particle size (4 µm) but different protein content, we observed that sample H860-6 with a higher protein content (6%) showed a friction coefficient (0.40) lower than sample H450-4 (0.44) with a protein content of 4%, due to an increased number of particles between the surfaces. Such effect of concentration has also been reported in previous studies (Chojnicka, de Jong, de Kruif, & Visschers, 2008; Rudge, et al., 2020). The high friction coefficient (0.50) was related to the highest value of SMR (-2.27), while the lowest friction (0.40) was related to the lowest SMR (-1.72). So even though large particles were more efficient at small gap sizes, they were less efficient when speed and gap size increased. This may be related to differences in the rolling ability of the particles. It is known that irregularly-shaped particles have interlocking events with the surfaces (Ji, Zhang, Cornacchia, Sala, & Scholten, 2022), and therefore the lubrication efficiency is reduced. Overall, we see that the particle size has an influence on the lubrication properties.

5.3.5 Correlation between structural and physical properties

To clarify how the compositional and structural characteristics were related to the physical, rheological and tribological properties of the studied ice creams, correlation coefficients were determined by Principal Components Analysis (PCA) and are shown in Fig. 5.5.

Variables	Hardness	Scoopability	Lag time	Melting rate	G'_{-15}	SZII	G'_5	FCB	SMR
Particle size	0.401	0.409	**0.818**	-0.653	0.305	-0.407	0.605	0.047	-0.137
Mix viscosity	**0.841**	**0.764**	**0.876**	**-0.897**	**0.762**	-0.705	**0.986**	-0.460	0.151
Overrun	**-0.752**	**-0.820**	-0.197	0.617	-0.656	0.214	-0.408	**0.772**	-0.527
Air cell size	-0.073	-0.025	0.307	-0.334	-0.183	0.297	0.192	0.194	-0.453
Ice crystal size	-0.587	-0.442	-0.444	0.339	-0.645	0.641	-0.625	0.311	-0.233
Non-air thickness	0.684	**0.743**	0.226	-0.637	0.555	-0.100	0.464	-0.652	0.337

Fig. 5.5. Heatmap of correlation matrix (Pearson coefficients) between structural elements and textural, rheological and tribological properties of the studied samples (without high-fat sample). Blue indicates negative correlation and red indicates positive correlation.

Both the hardness and scooping energy were highly correlated with mix viscosity (0.841 and 0.764), overrun (-0.752 and -0.820) and non-air thickness (0.684 and 0.743). This is consistent with our discussion above: the structure of a sample with a higher viscosity and a lower overrun is more dense, with thicker non-air areas, leading to higher hardness and scooping energy. A positive correlation between mix viscosity and hardness and an inverse correlation between overrun and hardness have been reported by many studies (Amador, et al., 2017; Muse, et al., 2004; Sofjan, et al., 2004). Viscosity was also highly correlated to lag time (0.876), and no correlation was found between overrun and lag time (-0.197). This confirms the more important role of mix viscosity in affecting the lag time. A positive correlation could also be found between lag time and particle size (0.818). As discussed previously, larger particles may have a higher ability to form a network structure in the serum phase, and may hold the serum phase better and delay the dripping of the serum phase. However, the structure formed by the protein particles could not keep the shape retention during melting, and, therefore, melting rate was not closely correlated with particle size (-0.653), but more related to the viscosity (-0.897). Similarly, SZII was correlated only with mix viscosity (-0.705), which is logical, as SZII also characterizes the melting rate. In addition, mix viscosity also showed strong

correlations with G'_5 (0.986), indicating that the mix viscosity also played an important role in determining the structure of molten ice cream. Both the particle size and mix viscosity were not closely correlated with lubrication parameters (FCB and SMR). As discussed above, this is mainly because the lubrication behavior of molten ice cream was not only determined by protein particle size, but also by particle shape and number. To explore how different properties of ice cream would affect the sensory perception of ice cream, a sensory test was carried out and different sensory attributes were correlated with different ice cream properties.

5.3.6 Sensory properties of ice cream

The data of the sensory assessment of the studied samples are summarized in Tab. 5.7. Significant differences among different samples could be found for all attributes ($P < 0.05$). Larger differences were observed for creaminess, grittiness, denseness and beany flavor ($F > 15$). Sample S-4, with only dispersible particles, showed the lowest values of creaminess (3.8), denseness (3.8) and mouth coating (3.7), but the highest softness (5.2), coldness (5.7) and grittiness (4.7). This could be related to its lowest non-air thickness and viscosity, leading to ice crystals that were more easily perceived. In comparison, sample IS-4, with only non-dispersible agglomerates, had the highest values for creaminess (6.8), denseness (6.7) and mouth coating (5.7) and the lowest coldness (4.5) and grittiness (1.5). This was most likely related to the high viscosity and high non-air thickness. In presence of both dispersible and non-dispersible particles, in both the particle size and viscosity series, the attributes creaminess, denseness and mouth coating scored higher values when protein particle size decreased from 145 to 4 μm, independently of the viscosity. Scores for coldness and grittiness appeared to decrease with a decrease in protein particle size. These results indicate that protein particle size played an important role in determining the sensory properties of the final products.

Tab. 5.7. Scores for the sensory attributes of the studied samples.

Sample series	Ref	Particle size series			Dispersible fraction series			Viscosity series		*F* value	*P* value
Sample codes	Fat-10	H-4	H150-4	H450-4	S-4	S50-4	IS-4	H450-5	H860-6		
Creaminess	5.1 ± 1.6^{c}	4.2 ± 1.6^{d}	4.7 ± 1.9^{c}	4.9 ± 1.5^{c}	3.8 ± 2.0^{d}	4.9 ± 2.0^{c}	6.8 ± 1.7^{a}	5.6 ± 1.9^{b}	5.9 ± 1.9^{b}	22.0	< 0.01***
Softness	3.8 ± 2.0^{c}	4.4 ± 2.2^{bc}	4.6 ± 2.2^{abc}	4.0 ± 2.0^{bc}	5.2 ± 2.3^{a}	4.2 ± 2.1^{bc}	4.5 ± 2.5^{c}	4.8 ± 2.3^{ab}	4.6 ± 2.3^{ab}	2.9	< 0.01**
Coldness	4.6 ± 1.3^{cd}	5.4 ± 1.7^{a}	5.3 ± 1.9^{ab}	5.1 ± 1.2^{abc}	5.7 ± 1.8^{a}	5.5 ± 1.5^{a}	4.5 ± 2.0^{d}	5.2 ± 1.8^{abc}	4.8 ± 1.9^{bcd}	7.2	< 0.01***
Grittiness	2.8 ± 1.3^{cd}	3.6 ± 2.5^{b}	2.8 ± 2.1^{c}	2.1 ± 1.5^{bc}	4.7 ± 2.6^{a}	2.7 ± 2.0^{cd}	1.5 ± 1.8^{e}	2.1 ± 1.9^{de}	1.7 ± 1.7^{e}	22.0	< 0.01***
Denseness	5.9 ± 2.1^{bc}	5.2 ± 2.2^{c}	5.4 ± 1.7^{bc}	5.4 ± 1.8^{bc}	3.8 ± 2.0^{d}	5.6 ± 1.7^{bc}	6.7 ± 2.0^{a}	5.7 ± 1.7^{bc}	6.2 ± 1.8^{ab}	16.1	< 0.01***
Mouth coating	4.6 ± 2.3^{bc}	4.1 ± 2.2^{cd}	4.7 ± 1.8^{cd}	4.6 ± 1.7^{bc}	3.7 ± 2.2^{d}	4.5 ± 2.1^{c}	5.7 ± 2.0^{a}	4.8 ± 2.0^{bc}	5.3 ± 1.9^{ab}	9.2	< 0.01***
Melting time	5.4 ± 2.0^{a}	5.1 ± 1.9^{ab}	5.2 ± 1.8^{a}	5.3 ± 1.9^{a}	4.5 ± 2.3^{b}	5.3 ± 1.7^{a}	5.4 ± 1.9^{a}	5.0 ± 1.8^{ab}	5.4 ± 1.8^{a}	2.0	0.04*
Beany flavor	1.7 ± 2.3^{d}	4.9 ± 2.7^{ab}	5.0 ± 2.6^{ab}	4.4 ± 2.4^{b}	2.9 ± 2.3^{c}	4.8 ± 2.5^{ab}	5.6 ± 2.7^{a}	4.9 ± 2.5^{ab}	4.4 ± 2.6^{b}	30.6	< 0.01***
Overall liking	5.3 ± 2.4^{a}	4.1 ± 1.6^{b}	4.4 ± 1.8^{b}	4.9 ± 1.5^{b}	4.6 ± 1.8^{b}	4.2 ± 1.5^{b}	4.3 ± 2.1^{b}	4.6 ± 1.7^{b}	5.2 ± 1.7^{a}	5.2	< 0.01***

Values with a different letter within the same row are significantly different ($P < 0.05$).

To further clarify the correlations between different sensory attributes, a PCA biplot is shown (Fig. 5.6). The two principal components could explain 83.97% of the variation, in which the first factor (F1, 61.95%) was related to creaminess, coldness, grittiness, denseness, mouth coating and melting time, and the second factor (F2, 22.02%) was more related to the beany flavor and overall liking. Beany flavor and overall liking were in opposite direction, indicating that beany flavor had a significantly negative effect on overall liking. The reference sample (Fat-10) that did not contain any soy protein had the highest score of overall liking (5.3), which is most likely related to the lowest beany flavor (1.7) and the high fat content. Other studies have also reported that dairy products with SPI or SPC were rated significantly lower in overall flavor liking and overall acceptance than dairy products without plant proteins (Drake, Gerard, & Chen, 2001; Friedeck, Aragul-Yuceer, & Drake, 2003). Fat-free samples H860-6 and H450-4 were closest to the high-fat reference (colored by green in Fig. 5.6). This was most likely due to the fact that both H860-6 and H450-4 were close to the attributes creaminess, denseness, mouth coating and melting time, and were opposite of coldness, grittiness and beany flavor. Noteworthy, both H860-6 and H450-4 had a protein particle size of 4 μm, indicating that samples with particle size of 4 μm were more preferred. These particles thus have more potential to act as good fat replacers.

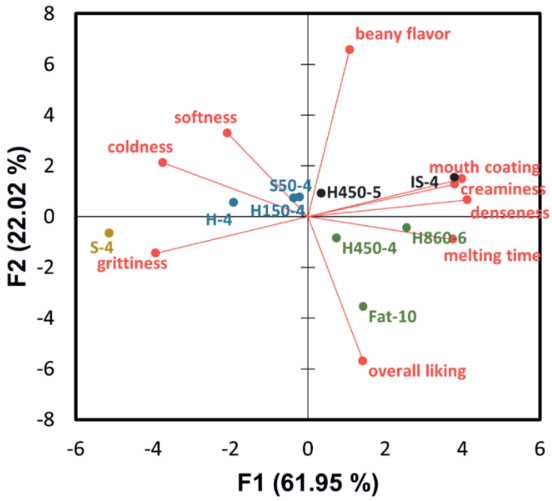

Fig. 5.6. PCA biplot of the sensory properties of the studied ice cream samples using RATA ($n_{participant}$=78), where the red points with lines refer to the different sensory properties and the dots with the other colors refer to the studied samples. Different colors for samples indicate different groups.

To get a better understanding of how sensory properties were affected by the ice cream properties, a heatmap representing the correlation matrix obtained from PCA is shown in Fig. 5.7. The full-fat sample was omitted to isolate the effect of protein particle size. In addition, beany flavor and overall liking were also omitted from the analysis.

Variables	creaminess	softenss	coldness	grittiness	denseness	mouth coating	melting time
Hardness	**0.848**	-0.197	**-0.869**	**-0.717**	**0.855**	**0.838**	0.611
Scoopability	**0.800**	-0.319	**-0.830**	**-0.742**	**0.869**	**0.814**	0.680
Lag time	0.541	-0.139	-0.431	-0.272	0.512	0.452	0.313
Melting rate	**-0.761**	0.467	**0.719**	0.656	**-0.798**	**-0.746**	-0.691
G'-15	**0.856**	-0.048	**-0.846**	-0.699	**0.827**	**0.822**	0.524
SZII	**-0.735**	-0.235	0.619	0.449	-0.658	-0.662	-0.303
G'5	0.682	-0.121	-0.656	-0.415	0.587	0.624	0.381
FCB	**-0.885**	0.286	**0.882**	**0.940**	**-0.913**	**-0.926**	**-0.766**
SMR	0.612	-0.027	-0.610	-0.664	0.678	0.647	0.498

Fig. 5.7. Heatmap of the correlation matrix (Pearson coefficients) between different sensory attributes and physical (hardness, scooping energy, lag time and melting rate), rheological (G'_{-15}, SZII and G'_5) and tribological (FCB and SMR) properties of the studied ice cream samples (without the reference and the attributes beany flavor and overall liking). Blue indicates negative correlation and red indicates positive correlation.

Most of the sensory attributes were shown to correlate to several ice cream properties. Creaminess, denseness and mouth coating were positively correlated with hardness, scooping energy and G'_{-15}, while coldness and grittiness were negatively correlated with these physical properties. These results indicate that ice cream with a denser structure was perceived more creamy and less gritty and cold. This could be explained by the high non-air thickness and high viscosity. Melting rate was negatively correlated with creaminess (-0.766), denseness (-0.803) and mouth coating (-0.753), but positively associated with coldness (0.726), indicating that ice cream with a lower melting rate would be more creamy and less cold. This is in agreement with previous studies (Javidi, et al., 2016; Varela, Pintor, & Fiszman, 2014). In addition, some strong correlations were also found between the lubrication parameter and sensory attributes. FCB was shown to be negatively correlated with creaminess (-0.887), denseness (-0.916) and mouth coating (-0.930). Several studies have also reported that samples with a better lubrication behavior corresponded with a more creamy and denser mouthfeel (Chojnicka-Paszun, et al., 2012; De Wijk, et al., 2006; Sonne, Busch-Stockfisch, Weiss, & Hinrichs, 2014; Stokes, Boehm, & Baier, 2013).

However, SMR did not appear to be strongly correlated with creaminess (0.618), indicating that the friction in the boundary regime is more important than the changes in the mixed regime in affecting the sensory attributes. Overall, the liking of the sample with a relatively denser structure and a better lubrication behavior could be expected to be higher, which could be achieved by the addition of medium-sized (approximately 4 μm) protein particles. Apparently, this size is large enough to block the lamellae between air cells, but also small enough to provide a homogeneous structure and a better lubrication behavior.

5.4 Conclusion

In this study, the role of plant protein particle size ranging from 0.25 to 145 µm on different properties of ice cream was investigated by separating the effect of particle size from that of mix viscosity itself. We created three series of ice creams that differed in protein dispersibility, represented by differences in viscosity and/or particle size/number, to investigate how different parameters affect the ice cream structure and properties. Small dispersible particles (0.25 µm) were able to significantly increase air incorporation (overrun), and led to lower hardness and higher scoopability. On the other hand, large non-dispersible agglomerates (145 µm) were mainly present in a thicker serum phase between the air cells, and contributed more to the melting resistance due to their ability to form a network and their positive effect on mix viscosity. When both dispersible and non-dispersible particles were present, mix viscosity appeared to be the dominant factor in affecting the melting rate, while particle size had a larger effect on melting lag time. In addition, the lubrication property of molten ice cream was shown to be mainly related to protein particle characteristics instead of mix viscosity. Finally, ice creams with a relatively denser structure, lower melting rate and lower friction provided higher creaminess, denseness and mouth coating, and lower coldness and grittiness. In this study, addition of protein particles with medium size of 4 µm had a positive effect on the properties of fat-free ice cream, resulting in sensory attributes and overall liking comparable to those of full-fat ice cream. This indicates that medium-sized protein particles have a higher potential to act as a suitable fat replacer for improving the textural and sensory properties of fat-free ice cream.

References

Adapa, S., Schmidt, K. A., Jeon, I. J., Herald, T. J., & Flores, R. A. (2000). Mechanisms of ice crystallization and recrystallization in ice cream: a review. *Food Reviews International, 16*(3), 259-271.

Akbari, M., Eskandari, M. H., & Davoudi, Z. (2019). Application and functions of fat replacers in low-fat ice cream: A review. *Trends in food science & technology, 86*, 34-40.

Alves, A. C., Martha, L., Casanova, F., & Tavares, G. M. (2022). Structural and foaming properties of whey and soy protein isolates in mixed systems before and after heat treatment. *Food Science and Technology International, 28*(6), 545-553.

Amador, J., Hartel, R., & Rankin, S. (2017). The effects of fat structures and ice cream mix viscosity on physical and sensory properties of ice cream. *Journal of food science, 82*(8), 1851-1860.

Balthazar, C. F., Silva, H. L. A., Cavalcanti, R. N., Esmerino, E. A., Cappato, L. P., Abud, Y. K. D., Moraes, J., Andrade, M. M., Freitas, M. Q., & Sant'Anna, C. (2017). Prebiotics addition in sheep milk ice cream: A rheological, microstructural and sensory study. *Journal of Functional Foods, 35*, 564-573.

Biswas, P. K., Chakraborty, R., & Choudhuri, U. R. (2002). Effect of blending of soy milk with cow milk on sensory, textural and nutritional qualities of Chhana analogue. *Journal of Food Science and Technology -Mysore-, 39*, 702-704.

Chojnicka-Paszun, A., De Jongh, H. H. J., & De Kruif, C. G. (2012). Sensory perception and lubrication properties of milk: Influence of fat content. *International Dairy Journal, 26*(1), 15-22.

Chojnicka, A., de Jong, S., de Kruif, C. G., & Visschers, R. W. (2008). Lubrication properties of protein aggregate dispersions in a soft contact. *Journal of Agricultural and Food Chemistry, 56*(4), 1274-1282.

Cook, K. L. K., & Hartel, R. W. (2010). Mechanisms of ice crystallization in ice cream production. *Comprehensive reviews in food science and food safety, 9*(2), 213-222.

De Wijk, R. A., Terpstra, M. E. J., Janssen, A. M., & Prinz, J. F. (2006). Perceived creaminess of semi-solid foods. *Trends in food science & technology, 17*(8), 412-422.

Dervisoglu, M., Yazici, F., & Aydemir, O. (2005). The effect of soy protein concentrate addition on the physical, chemical, and sensory properties of strawberry flavored ice cream. *European Food Research and Technology, 221*(3), 466-470.

Drake, M. A., Gerard, P. D., & Chen, X. Q. (2001). Effects of sweetener, sweetener concentration, and fruit flavor on sensory properties of soy fortified yogurt. *Journal of sensory studies, 16*(4), 393-405.

Friedeck, K. G., Aragul-Yuceer, Y. K., & Drake, M. A. (2003). Soy Protein Fortification of a Low-fat Dairy-based Ice Cream. *Journal of Food Science, 68*(9), 2651-2657.

Fuhrmann, P. L., Sala, G., Scholten, E., & Stieger, M. (2020). Influence of clustering of protein-stabilised oil droplets with proanthocyanidins on mechanical, tribological and sensory properties of o/w emulsions and emulsion-filled gels. *Food Hydrocolloids, 105*, 105856.

Guo, Y., Zhang, X., Hao, W., Xie, Y., Chen, L., Li, Z., Zhu, B., & Feng, X. (2018). Nano-bacterial cellulose/soy protein isolate complex gel as fat substitutes in ice cream model. *Carbohydrate polymers, 198*, 620-630.

Hong, T., Iwashita, K., & Shiraki, K. (2018). Viscosity control of protein solution by small solutes: a review. *Current Protein and Peptide Science, 19*(8), 746-758.

Javidi, F., Razavi, S. M. A., Behrouzian, F., & Alghooneh, A. (2016). The influence of basil seed gum, guar gum and their blend on the rheological, physical and sensory properties of low fat ice cream. *Food hydrocolloids, 52*, 625-633.

Ji, L., Cornacchia, L., Sala, G., & Scholten, E. (2022). Lubrication properties of model dairy beverages: Effect of the characteristics of protein dispersions and emulsions. *Food Research International, 157*, 111209.

Ji, L., den Otter, D., Cornacchia, L., Sala, G., & Scholten, E. (2023). Role of polysaccharides in tribological and sensory properties of model dairy beverages. *Food Hydrocolloids, 134*, 108065.

Ji, L., Zhang, H., Cornacchia, L., Sala, G., & Scholten, E. (2022). Effect of gelatinization and swelling degree on the lubrication behavior of starch suspensions. *Carbohydrate polymers, 291*, 119523.

Jian, H., Qiao, F., Yang, P., Guo, F., Huang, X., Adhikari, B., & Chen, J. (2016). Roles of soluble and insoluble aggregates induced by soy protein processing in the gelation of myofibrillar protein. *International Journal of Food Science & Technology, 51*(2), 480-489.

Krop, E. M., Hetherington, M. M., Miquel, S., & Sarkar, A. (2019). The influence of oral lubrication on food intake: a proof-of-concept study. *Food Quality and Preference, 74*, 118-124.

Kurt, A., Cengiz, A., & Kahyaoglu, T. (2016). The effect of gum tragacanth on the rheological properties of salep based ice cream mix. *Carbohydrate polymers, 143*, 116-123.

Leahu, A., Ropciuc, S., & Ghinea, C. (2022). Plant-Based Milks: Alternatives to the

Manufacture and Characterization of Ice Cream. *Applied Sciences, 12*(3), 1754.

Liu, R., Wang, L., Liu, Y., Wu, T., & Zhang, M. (2018). Fabricating soy protein hydrolysate/xanthan gum as fat replacer in ice cream by combined enzymatic and heat-shearing treatment. *Food Hydrocolloids, 81*, 39-47.

Liu, X., Sala, G., & Scholten, E. (2022). Effect of fat aggregate size and percentage on the melting properties of ice cream. *Food Research International, 160*, 111709.

Liu, X., Sala, G., & Scholten, E. (2023a). Role of polysaccharide structure in the rheological, physical and sensory properties of low-fat ice cream. *Current Research in Food Science*, 100531.

Liu, X., Sala, G., & Scholten, E. (2023b). Structural and functional differences between ice crystal-dominated and fat network-dominated ice cream. *Food Hydrocolloids*, 108466.

Mahdian, E., & Karazhian, R. (2013). Effects of fat replacers and stabilizers on rheological, physicochemical and sensory properties of reduced-fat ice cream. *Journal of Agricultural Science and Technology, 15*(6), 1163-1174.

Morales, R., Martínez, K. D., Ruiz-Henestrosa, V. M. P., & Pilosof, A. M. R. (2015). Modification of foaming properties of soy protein isolate by high ultrasound intensity: Particle size effect. *Ultrasonics sonochemistry, 26*, 48-55.

Mostafavi, F. S. (2019). Evaluating the effect of fat content on the properties of vanilla ice cream using principal component analysis. *Journal of Food Measurement and Characterization, 13*(3), 2417-2425.

Mostafavi, F. S., Tehrani, M. M., & Mohebbi, M. (2017). Rheological and sensory properties of fat reduced vanilla ice creams containing milk protein concentrate (MPC). *Journal of Food Measurement and Characterization, 11*, 567-575.

Muse, M. R., & Hartel, R. W. (2004). Ice cream structural elements that affect melting rate and hardness. *Journal of dairy science, 87*(1), 1-10.

Ningtyas, D. W., Tam, B., Bhandari, B., & Prakash, S. (2021). Effect of different types and concentrations of fat on the physico-chemical properties of soy protein isolate gel. *Food Hydrocolloids, 111*, 106226.

Nourmohammadi, N., Austin, L., & Chen, D. (2023). Protein-based fat replacers: a focus on fabrication methods and fat-mimic mechanisms. *Foods, 12*(5), 957.

Pang, Z., Bourouis, I., & Liu, X. (2022). Function of saliva in creaminess perception during food oral processing: In perspective of lubrication. *Journal of Agriculture and Food Research, 10*, 100377.

Puppo, M. C., Beaumal, V., Chapleau, N., Speroni, F., de Lamballerie, M., Añón, M.

C., & Anton, M. (2008). Physicochemical and rheological properties of soybean protein emulsions processed with a combined temperature/high-pressure treatment. *Food Hydrocolloids, 22*(6), 1079-1089.

Rudge, R. E. D., Van De Sande, J. P. M., Dijksman, J. A., & Scholten, E. (2020). Uncovering friction dynamics using hydrogel particles as soft ball bearings. *Soft Matter, 16*(15), 3821-3831.

Santagiuliana, M., Christaki, M., Piqueras-Fiszman, B., Scholten, E., & Stieger, M. (2018). Effect of mechanical contrast on sensory perception of heterogeneous liquid and semi-solid foods. *Food Hydrocolloids, 83*, 202-212.

Schädle, C. N., Bader-Mittermaier, S., & Sanahuja, S. (2022). Characterization of reduced-fat mayonnaise and comparison of sensory perception, rheological, tribological, and textural analyses. *Foods, 11*(6), 806.

Scholten, E. (2014). Ice Cream. In (Vol. 19, pp. 273-294).

Sim, J. Y., Enteshari, M., Rathnakumar, K., & Martínez-Monteagudo, S. I. (2021). Hydrodynamic cavitation: Process opportunities for ice-cream formulations. *Innovative Food Science & Emerging Technologies, 70*, 102675.

Sofjan, R. P., & Hartel, R. W. (2004). Effects of overrun on structural and physical characteristics of ice cream. *International Dairy Journal, 14*(3), 255-262.

Song, X., Zhou, C., Fu, F., Chen, Z., & Wu, Q. (2013). Effect of high-pressure homogenization on particle size and film properties of soy protein isolate. *Industrial Crops and Products, 43*, 538-544.

Sonne, A., Busch-Stockfisch, M., Weiss, J., & Hinrichs, J. (2014). Improved mapping of in-mouth creaminess of semi-solid dairy products by combining rheology, particle size, and tribology data. *LWT-Food Science and Technology, 59*(1), 342-347.

Sorgentini, D. A., Wagner, J. R., & Anón, M. C. (1995). Effects of thermal treatment of soy protein isolate on the characteristics and structure-function relationship of soluble and insoluble fractions. *Journal of Agricultural and Food Chemistry, 43*(9), 2471-2479.

Soukoulis, C., Chandrinos, I., & Tzia, C. (2008). Study of the functionality of selected hydrocolloids and their blends with κ-carrageenan on storage quality of vanilla ice cream. *LWT-Food Science and Technology, 41*(10), 1816-1827.

Stokes, J. R., Boehm, M. W., & Baier, S. K. (2013). Oral processing, texture and mouthfeel: From rheology to tribology and beyond. *Current Opinion in Colloid & Interface Science, 18*(4), 349-359.

Stribiţcaia, E., Krop, E. M., Lewin, R., Holmes, M., & Sarkar, A. (2020). Tribology and rheology of bead-layered hydrogels: Influence of bead size on sensory perception. *Food Hydrocolloids, 104*, 105692.

Sun, D., Wu, M., Bi, C., Gao, F., Wei, W., & Wang, Y. (2022). Using high-pressure homogenization as a potential method to pretreat soybean protein isolate: Effect on conformation changes and rheological properties of its acid-induced gel. *Innovative Food Science & Emerging Technologies, 82*, 103195.

Thompson, K. R., Chambers, D. H., & Chambers Iv, E. (2009). Sensory characteristics of ice cream produced in the USA and Italy. *Journal of sensory studies, 24*(3), 396-414.

Varela, P., Pintor, A., & Fiszman, S. (2014). How hydrocolloids affect the temporal oral perception of ice cream. *Food Hydrocolloids, 36*, 220-228.

Velásquez-Cock, J., Serpa, A., Vélez, L., Gañán, P., Hoyos, C. G., Castro, C., Duizer, L., Goff, H. D., & Zuluaga, R. (2019). Influence of cellulose nanofibrils on the structural elements of ice cream. *Food Hydrocolloids, 87*, 204-213.

Wang, W., Wang, M., Xu, C., Liu, Z., Gu, L., Ma, J., Jiang, L., Jiang, Z., & Hou, J. (2022). Effects of soybean oil body as a milk fat substitute on ice cream: Physicochemical, sensory and digestive properties. *Foods, 11*(10), 1504.

Wilbey, R. A., Cooke, T., & Dimos, G. (1998). Effects of solute concentration, overrun and storage on the hardness of ice cream. In: International Dairy Federation.

Wildmoser, H., Scheiwiller, J., & Windhab, E. J. (2004). Impact of disperse microstructure on rheology and quality aspects of ice cream. *LWT-Food Science and Technology, 37*(8), 881-891.

Wu, B., Freire, D. O., & Hartel, R. W. (2019). The effect of overrun, fat destabilization, and ice cream mix viscosity on entire meltdown behavior. *Journal of Food Science, 84*(9), 2562-2571.

Yilsay, T. Ö., Yilmaz, L., & Bayizit, A. A. (2006). The effect of using a whey protein fat replacer on textural and sensory characteristics of low-fat vanilla ice cream. *European Food Research and Technology, 222*, 171-175.

Yu, C., Cha, Y., Wu, F., Xu, X., Qin, Y., Li, X., & Du, M. (2018). Effects of high-pressure homogenisation on structural and functional properties of mussel (Mytilus edulis) protein isolate. *International Journal of Food Science & Technology, 53*(5), 1157-1165.

Zhang, A., Wang, L., Song, T., Yu, H., Wang, X., & Zhao, X.-h. (2022). Effects of high pressure homogenization on the structural and emulsifying properties of a vegetable protein: Cyperus esculentus L. *LWT, 153*, 112542.

Supplementary material

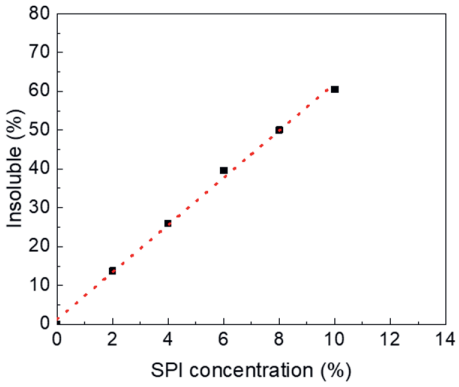

Fig. S5.1. Percentage of dray-basis insoluble material determined after centrifugation of samples containing 0 - 10% soy protein isolate.

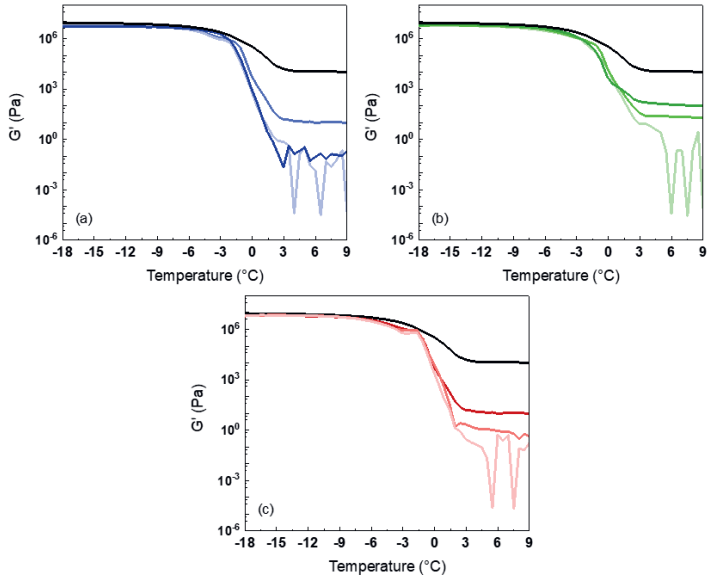

Fig. S5.2. Storage modulus (G') and loss modulus (G") as a function of temperature for samples with different particle size and soluble fraction. (a) Samples in homogenization series (from dark to light blue: H-4, H150-4, H450-4); (b) Samples in fraction series (from dark to light green: IS-4, S50-4, S-4); (c) Samples in concentration series (from dark to light red: H-4, H450-5, H860-6). Black line in all three figures refers to the full-fat sample).

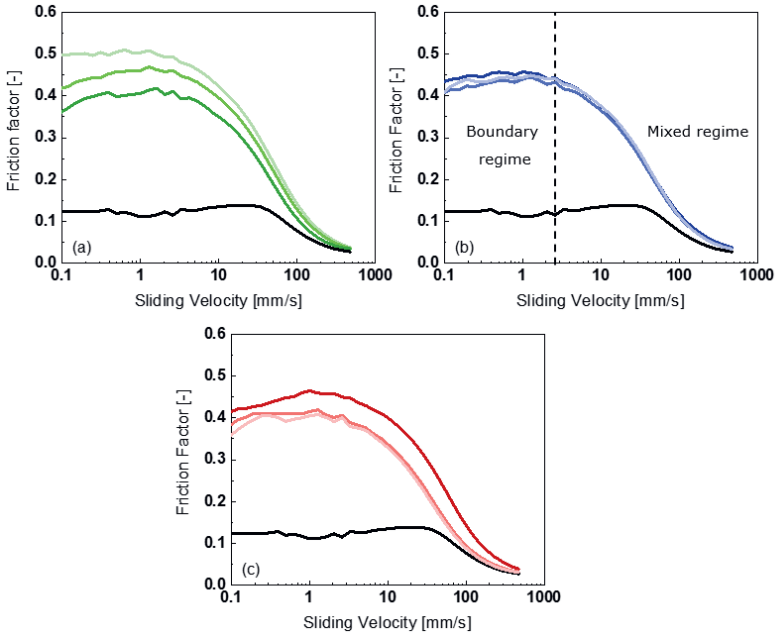

Fig. S5.3. Lubrication curves of samples with different particle size and soluble fraction. (a) Samples in homogenization series (from dark to light blue: H-4, H150-4, H450-4); (b) Samples in fraction series (from dark to light green: IS-4, S50-4, S-4); (c) Samples in concentration series (from dark to light red: H-4, H450-5, H860-6). Black line in all three figures refers to the full-fat sample (Fat-10).

Chapter 6

Lubrication of ice cream: effect of different structural elements

To be submitted as: Liu, X.*, Ji, L.*, Sala, G., & Scholten, E. Lubrication of ice cream: effect of different structural elements.
(* the authors have contributed equally to this work)

Abstract

Lubrication properties are considered to be closely related to complex sensorial attributes such as creaminess and smoothness. In ice cream, these properties can be presumed to be partly linked to the melting of the product network. It is still unclear how to measure the lubrication properties of ice cream during the melting process and which ice cream characteristics affect lubrication. In this study, a new method was developed to measure the lubrication properties of ice cream both during melting and in a molten state. Different structural elements, including fat content, ice fraction, fat aggregation, viscosity and overrun, were modified to identify the main factors that influence lubrication. Representative tribological parameters were extracted from the tribological curves and were correlated with ice cream characteristics. Using a tribometer with adjustable probe height, we were able to measure the lubrication properties during the entire melting process. The results showed that the lubrication properties of ice cream during melting were influenced by different structural elements, in which ice fraction mainly had a positive effect on the lubrication at the initial stage of melting, while fat content dominated the lubrication behavior at the later stage and in molten ice cream. A higher fat content provided better lubrication. Fat aggregation, serum phase viscosity and overrun did not appear to have a significant effect on the lubrication properties during melting. In addition, the penetration distance of the probe into the ice cream samples strongly correlated with hardness, and can likely be used as an alternative method to characterize the melting profile in terms of changes in hardness. This study indicates that different structural features determine the lubrication properties of ice cream in different melting regimes.

6.1 Introduction

Ice cream is a complex food colloidal system, containing dispersed air cells, ice crystals and partially coalesced fat droplets in a continuous viscous serum phase. Different structural elements, including ice fraction, fat content, degree of fat aggregation, viscosity and overrun have a large effect on the ice cream structure and thus influence sensory perception. For example, fat influences perception by providing lubrication and a creamier mouthfeel. This happens with the formation of a lubricating layer on the tongue, affecting also mouthcoating characteristics (Nagarawatta, 2000; Prindiville, Marshall, & Heymann, 1999; Roland, Phillips, & Boor, 1999). A higher ice fraction has been shown to provide a denser structure in ice cream, which leads to a higher perception of iciness (Goff & Hartel, 2013). The denseness of ice cream is decreased by the presence of air. Ice cream with a higher overrun has a lower hardness, reducing the feeling of iciness and coldness, and increasing creaminess (Sofjan & Hartel, 2004; Warren & Hartel, 2018; Wu, Freire, & Hartel, 2019). A higher overrun also leads to higher smoothness. Besides overrun, polysaccharides can also affect sensory attributes such as creaminess and smoothness. Polysaccharides increase the viscosity of the serum phase and provide a lubrication layer, therewith contributing to a creamier and fuller mouthfeel (Guven, Karaca, & Kacar, 2003; Javidi, Razavi, Behrouzian, & Alghooneh, 2016; Milani & Koocheki, 2011).

Both viscosity and lubrication characteristics can thus influence the sensory profile and specific attributes. In many food products, correlations between lubrication aspects and surface-related sensorial attributes, such as creaminess, mouthcoating and smoothness have already been shown (Chojnicka-Paszun, De Jongh, & De Kruif, 2012; Morell, Chen, & Fiszman, 2017; Sarkar & Krop, 2019; Shewan, Pradal, & Stokes, 2020). The lubrication properties of fat have been characterized in milk, yogurt, cheese, model emulsions and emulsion-filled gels (Chojnicka-Paszun, et al., 2012; Malone, Appelqvist, & Norton, 2003; Selway & Stokes, 2013). Besides fat, also other ingredients, such as polysaccharides and proteins have been shown to influence lubrication. However, for ice cream, it is not known how the structural features of this complex food influences lubrication aspects, and how they can be linked to sensory perception. In our previous study, we measured the lubrication properties of molten ice cream and found that the high-fat sample possessed a significantly better lubrication behavior (**Chapter 4**). However, we could only measure the lubrication behavior of molten ice cream (liquid state). For sensory perception, the changes of lubrication behavior during ice cream melting may also be

relevant, as the structure of ice cream changes dramatically upon melting during oral consumption. No studies have shown how to measure the lubrication properties of ice cream during the melting process (from solid to liquid states). To better understand how sensory attributes can be linked to structure and lubrication, an appropriate method needs to be developed to measure the lubrication properties during ice cream melting and the relation between structure and lubrication should be clarified.

Currently, many commercial tribometers are used in the field of food science to perform tribological measurements (Rudge, Scholten, & Dijksman, 2019; Sarkar, et al., 2019; Shewan, et al., 2020). Most of the tribological measurements are performed with a rheometer equipped with a tribology accessory (Chojnicka-Paszun, et al., 2012; Ji, Orthmann, et al., 2022; Ningtyas, Bhandari, Bansal, & Prakash, 2018; Vlădescu, et al., 2021). This geometry performs rotary movements, and can only be used for small amounts of liquid samples (< 1 ml), but not for solid materials. Therefore, it can only be used to measure the lubrication properties of molten ice cream. In this study, to measure changes in the lubrication behavior of ice cream upon melting, we examined the suitability of a different type of tribometer, which applies an oscillation linear movement, and contains a sample holder also suitable to hold solid foods with a large volume (> 10 ml). In addition, we aimed to identify how different structural features of ice cream influence the lubrication properties at different melting stages. Tests were conducted to optimize the measuring parameters to ensure reproducibility of the measurements, and define a good protocol to measure ice cream during the complete melting process. After a suitable method was developed, the effect of structure was examined. Five different structural elements, including fat content, ice fraction, fat aggregation degree, viscosity and overrun, were systematically changed by varying composition or freezing method. The individual contribution of these structural features was determined. Tribological curves for the different ice creams were obtained during melting and in the molten state, and representative parameters were extracted to represent lubrication properties during different stages. These parameters were linked to the different structural elements, but also to hardness and melting rate.

6.2 Materials and methods

6.2.1 Materials

Organic carrageenan-free cream (33 % fat, 3 % lactose, 2.4 % protein, 0.08 % minerals), organic skimmed milk (5 % lactose, 3.5 % protein, 0.1 % minerals) and sucrose were purchased from a local supermarket (Jumbo Wageningen, Netherlands). Guar gum (GG, ~4000 kDa) and xanthan gum (XG, ~4000 kDa) was purchased from Sigma-Aldrich Chemie GmbH (Steinheim, Germany).

6.2.2 Ice cream mix preparation

Ice cream mixes with different compositions were used to control the ice fraction, viscosity and fat content. To vary the ice fraction, two samples with different sugar content were prepared. For the sample containing skim milk only (denoted as "HIF"), a higher ice fraction was obtained than for the sample containing skim milk and 15% sucrose (denoted as "LIF"). The sample LIF was used as a reference sample, which was also compared to ice creams containing an additional 0.5% guar gum (denoted as "HV"), to investigate the effect of viscosity. The fat content was varied by adding cream while maintaining the same ratio between sugar and water of sample LIF, and therefore a similar ice fraction was present. Fat aggregation degree and overrun were varied by the freezing method, described in the next section.

6.2.3 Ice cream preparation

Ice cream samples (2 L) were frozen in a batch freezer (Frigomat T4S-T5S, Italy) for 8 min or a liquid nitrogen freezing process for 5 min, as described in **Chapter 3**. The liquid nitrogen freezing process was used to control the degree of fat destabilization or the overrun. An overview of the different samples is shown in Tab. 6.1. The overrun was measured directly after taking the sample out of the freezing machine. The ice cream was collected into different containers depending on the determination to be carried out: plastic rings with 20 mm in height and 60 mm in diameter for hardness and melting measurements, and metal rings with 7 mm height and 25 mm in diameter for tribological measurements with a tribometer. These samples were first hardened at -20 °C for 24 h to solidify the ice cream further before measurements were performed.

Tab. 6.1. Ice cream formulations and freezing methods investigated in this study.

Sample	Composition	Freezing method
High ice fraction (HIF)	Skim milk	Batch freezer
Low ice fraction (LIF)	Skim milk + 15% sucrose	Batch freezer
High viscosity-1 (HV1)	Skim milk + 14.93% sucrose + Guar gum 0.5%	Batch freezer
High fat with aggregation (FA)	Skim milk + sucrose + 33% cream	Batch freezer
High fat without aggregation (FNA)	Skim milk + sucrose + 33% cream	Liquid nitrogen
Low overrun (LO)	Skim milk	Liquid nitrogen

6.2.4 Ice fraction

The ice fraction of the different samples was measured with Differential Scanning Calorimetry (DSC, Discovery DSC25, TA Instrument, New Castle, USA). Approximately 13 mg sample was added to an aluminum Tzero pan and covered with a hermetic lid. The same pan and lid with 13 mg Milli-Q water was used as a blank. The samples were first cooled to -80 °C at a rate of 10 °C/min to initiate the crystallization of water into ice. The temperature was then increased to -18 °C to partly melt the ice crystals and kept constant at this temperature for 30 min. After that, the samples were heated to room temperature at a heating rate of 1 °C/min, during which the heat flow was measured. The ice fraction at -18 °C was calculated by dividing the measured enthalpy by the enthalpy of pure water (380.2 J/g). The measurements were done in triplicate to obtain average values and standard deviations.

6.2.5 Fat particle distribution

The particle size of the fat droplets in ice cream mix and molten ice cream samples was determined by static light scattering (Mastersizer 3000, UK.). Deionized water (refractive index. RI = 1.33) was used to dilute the samples. The refractive index of milk fat (RI = 1.46) was used for the dispersed phase. Measurements were performed at ambient temperature (20 °C) and repeated in triplicate. The $D_{4,3}$ was used to characterize the degree of fat destabilization, (**Chapters 2-5**). The measurements were done in triplicate to obtain average values and standard deviations.

6.2.6 Mix viscosity

The viscosity of ice cream mixes was measured using a rheometer (MCR 501, Anton Paar, Germany) equipped with a concentric cylinder geometry (probe CC17/Ti; cup CC17/Ti). A sample of 4.7 ml was added to the geometry and the temperature was set at 20 °C. The samples were equilibrated in the cup for 2 min before the measurement started. The viscosity was measured at a shear rate ranging from 0.1 to 300 s^{-1} in a time frame of 5 min. The viscosity at 0.5 s^{-1} was selected to characterize the mix viscosity. The measurements were done in triplicate to obtain average values and standard deviations.

6.2.7 Overrun

The overrun of the ice cream samples was determined by first weighing a fixed volume of the aged pre-mix in a metal cup. Next, the same volume of ice cream was weighted in said cup directly after ice cream preparation. The overrun was quantified based on the following formula (Muse & Hartel, 2004):

$$\text{Overrun } (\%) = \frac{Weight\ of\ mix - weight\ of\ ice\ cream}{Weight\ of\ ice\ cream} \times 100 \qquad (6.1)$$

The measurements were done in triplicate to obtain average values and standard deviations.

6.2.8 Determination of hardness

The hardness measurement was conducted using a Texture Analyzer (TA-TX plus, Stable Micro Systems, UK). Samples with fixed volume were prepared using plastic rings of 25 mm in height and 60 mm in diameter. The samples were stored in a freezer at -20 °C for a minimum of 24 h. Prior to the measurement, a climate chamber was connected to the Texture Analyzer to maintain a temperature of -20 °C, achieved by utilizing liquid nitrogen. For the determination of hardness, the samples were carefully removed from the plastic rings using a cylindrical cutting tool, and promptly transferred to the climate chamber. Subsequently, a penetration test was carried out with an aluminum cylindrical probe (5 mm in diameter) attached to a 50 kg load cell, with a strain of 50% applied at a speed of 2 mm/s. Hardness was taken as the maximum stress of the stress-strain curve. The measurements were done in triplicate to obtain average values and standard deviations.

6.2.9 Determination of melting properties

To determine melting properties, samples with fixed volume were prepared using plastic rings of 25 mm in height and 60 mm in diameter. The samples were stored in a freezer at -20 °C for a minimum of 24 h, and then they were taken out of the rings and placed on a 136x136 mm mesh screen with 5x5 mm openings with an area of 44% of the total area. The starting weight of each sample was measured, and the samples were melted at room temperature (25 °C). Underneath the mesh, a collection cup was placed on a measuring scale connected to a computer, which recorded the measured weight of the molten sample every 10 s, for a duration of 240 min. From the recorded data, the melting rate (%/min) was calculated based on the slope of the curve representing weight versus time (**Chapters 2 and 3**). The measurements were done in triplicate to obtain average values and standard deviations.

6.2.10 Determination of tribological measurements

Tribological measurements were performed according to the method described by Ji et al. (2022) on a TriboLab (UMT, Bruker, Billerica USA) with an oscillation linear movement to determine the lubrication properties of ice cream during melting and for molten ice cream, separately. The tribo-pair consisted of a spherical glass ball (R = 12.7 mm) as probe and a PDMS substrate (L x W x H=60 x 45 x 4 mm). The PDMS substrate (SYLGARDTM 184, Silicone Elastomer Kit, Dow Inc., USA) was made by mixing a base and curing agent, i.e. dimethyl vinylated and trimethylated silica, respectively, in a ratio of 10:1. After stirring, the mixture was poured into a plastic petri dish with sandpaper (180, CAMI-standard) glued on the bottom of it to create a rough surface on the PDMS substrate. The PDMS mixture was de-aired with a vacuum pump and afterwards was put into an oven overnight at 60 °C to solidify. Subsequently, the PDMS substrate was cut to fit into a metal container connected to a motor able to apply an oscillating movement in a linear direction. The spherical glass ball was inserted into a holder connected to a force sensor.

For the measurement of ice cream, a sample with a volume of 15-16 mm^3 was taken out of the metal rings and put on top of the PDMS substate to cover the entire surface (Fig. 6.1a). A normal force of 0.2 N was applied to induce contact between the probe and the ice cream sample. The friction coefficient was measured at a constant sliding speed of 10 mm/s over 9 min to record the change of friction coefficient during the melting period. The data were processed with the software UMT Text Viewer (UMT, Bruker, Billerica USA). The friction coefficient generated from each step was used for further analysis. Each sample was measured 5 times to obtain an averaged value. For the measurement of molten ice cream, a similar process was used, but some

parameters were slightly adjusted. The sample volume was decreased to 10 ml to create a thinner layer, and the normal force was increased to 0.5 N to provide a closer contact between probe and PDMS substrate (Fig. 6.1b). In addition, the total measuring time was 4 min for each measurement. Each sample was analyzed 3 times to obtain averaged values of the friction coefficient.

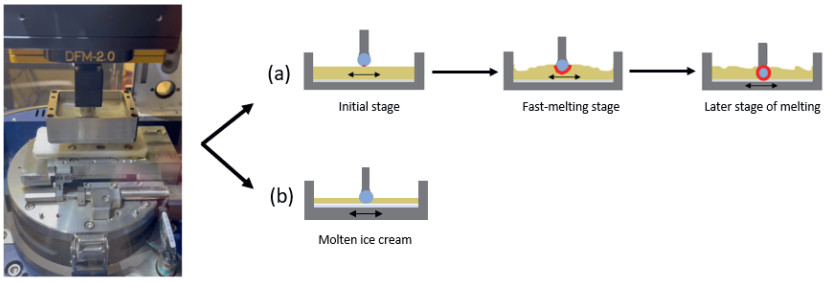

Fig. 6.1. Tribological measurements of (a) ice cream during melting and (b) for molten ice cream placed on a rough PDMS substrate. Measurements were performed with a Bruker tribometer.

6.2.11 Statistical analysis

The data were analyzed with SPSS software (Version 25.0, IBM Corp). The means were compared with a Duncan's test at a 5% level of significance using an analysis of variance (ANOVA). Additionally, the correlations between different ice cream features and tribological properties were analyzed by Principal Component Analysis (PCA). PCA analyses were performed using XLSTAT software (Addinsoft, Paris, France).

6.3. Results and discussion

6.3.1 Tribological measurements in different tribometer set-ups

In our previous studies, tribological measurements were conducted with an MCR 302 Rheometer equipped with a tribo-cell to evaluate the lubrication properties of molten ice cream samples (**Chapter 4**). In this work, we initially attempted to use the same method to measure the lubrication behavior of both ice cream and molten ice cream. However, some limitations were identified during the measurements. When measuring samples LIF and FA, the limited volume (< 1 ml) caused the sample to melt even before the measurement started. As a result, the rheometer proved impractical for measuring changes in the lubrication behavior of ice cream during

melting. Furthermore, although the lubrication properties of most molten samples could be measured, some undesirable phenomena were observed in specific cases. For example, when measuring samples with large fat aggregates (FA), the fat tended to further cluster together in the tribo-cell and was expelled from it during the measurement, as shown in Fig. 6.2. Therefore, the friction coefficient for samples containing fat aggregates could not be measured accurately. Considering these limitations, a tribometer with the ability to hold a larger volume and a linear sliding movement was considered to be more suitable for the tribological characterization of ice cream. For this purpose, a Bruker Tribometer was used, which fulfills the mentioned requirements.

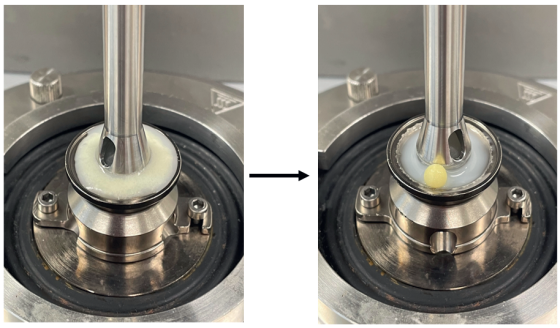

Fig. 6.2. Example of phenomena occurring during the tribological measurement of molten ice cream by the Anton Paar rheometer, leading to the formation of small fat spheres.

6.3.2 Method development for measuring lubrication of ice cream with a Bruker tribometer

Preliminary tests were first conducted to ensure the reproducibility of the measurements. Two main factors were identified as crucial in affecting the reproducibility of the results: sample height and normal force. Phenomena affecting the reproducibility in a negative way were observed when the sample height or the normal force exceeded specific values. When measuring the changes of friction in the sample LIF with a height of approximately 13 mm (volume of approximately 30 ml) and a normal force was 0.5 N, six separate measurements for the same sample showed deviating results (Fig. 6.3a). For some measurements, a sudden decrease in the friction coefficient (COF) was observed as a result of the breakdown of the sample during testing. This led to a large error band for the same sample (Fig. 6.3c, grey). This issue was prevented by optimizing the sample height and normal force. By

decreasing the sample height to 8 mm and reducing the normal force to 0.2 N, no breakdown of the samples was observed anymore, and the results became more reproducible (Fig. 6.3b). Consequently, the error band was much smaller (Fig. 3c, red). For further measurements, all samples had a height lower than 8 mm, and the applied force was set to 0.2 N.

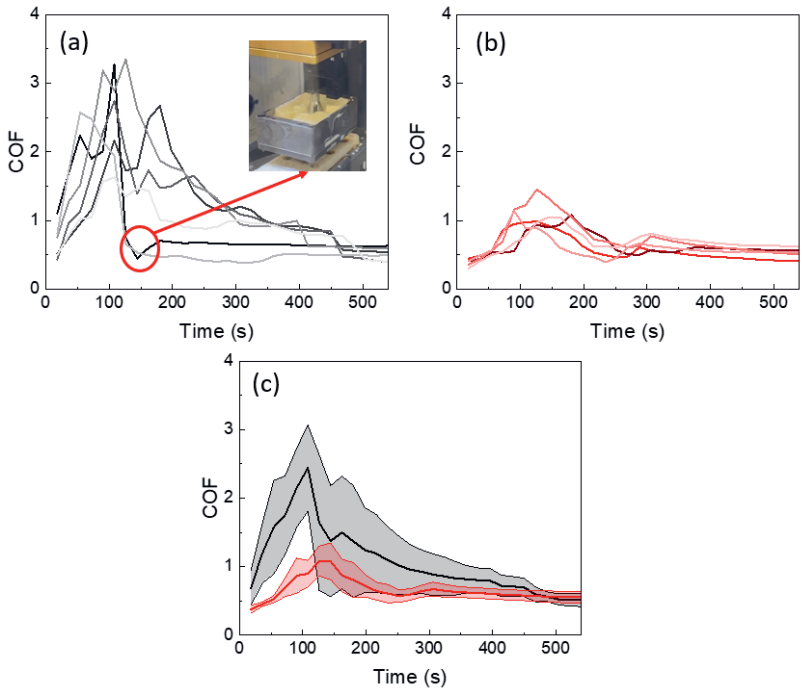

Fig. 6.3. Examples of tribological curves of ice cream (LIF) during melting. (a) Preliminary tests with large variations in results due to the breakdown of the sample (black lines); (b) Optimized results by adjusting sample height and normal force (red lines); (c) A comparison of the error bands before (grey) and after (red) optimization.

The measured friction coefficient (COF) is normally based on the assumption that the area of contact between sample and probe does not change. However, during melting, the contact between the probe and the sample changed, as the probe was able to enter the sample during the melting process when it became softer, as illustrated in Fig. 6.4 (red area). To correct for the changes in contact area, the friction coefficient was normalized by dividing the COF by the surface area of the probe, denoted as "COF/SA". The area was calculated based on:

$$\frac{COF}{SA} = COF/2\Pi Rd \qquad (6.2)$$

where R is the radius of the spherical glass ball (constant value: 6.35 mm) and d refers to the depth of the probe in the sample. The latter parameter was obtained from the distance of the probe in relation to the location of the substrate, which was measured simultaneously with the friction coefficient.

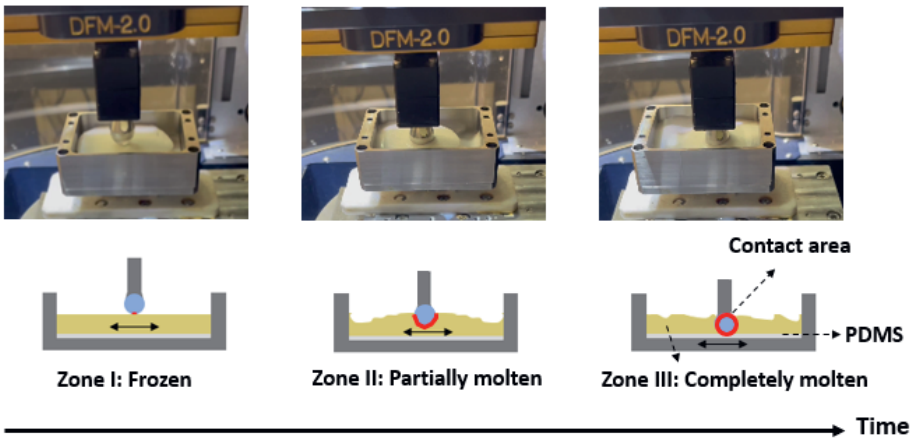

Fig. 6.4. Changes of contact area (red) between probe and sample due to the melting of ice cream during the tribological measurement.

Based on the results of Fig. 6.3b, the changes in the probe position were characterized by plotting the penetration distance as a function of measuring time (Fig. 6.5a). Interestingly, the pattern of the distance curve was similar to that of the melting curves observed in our previous studies (**Chapters 2 and 3**), suggesting that the penetration distance may be used to describe the melting behavior of the samples. To verify this, we also compared these data to data obtained with a gravimetric melting test, which will be discussed in a later section. By converting the data to COF/SA, as shown in Fig. 6.5b for sample LIF, two different zones could be identified. In zone I, the COF/SA significantly decreased with increasing measuring time, which was mainly related to the melting of the ice cream and therefore to the increase of the contact area between probe and sample. In zone II, the COF/SA reached its lowest value and remained constant. This could be attributed to the fact that the sample had completely melted, and the friction coefficient remained thus the same.

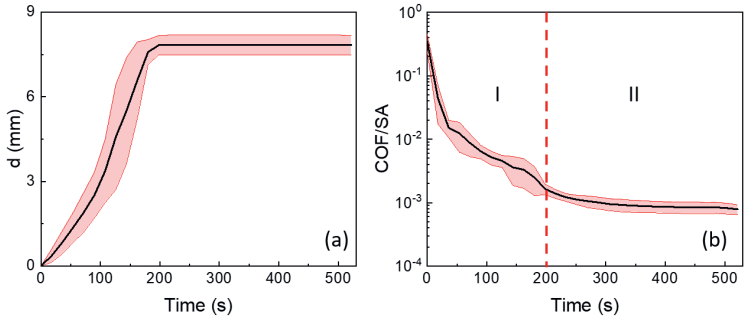

Fig. 6.5. Example of changes of (a) penetration distance and (b) normalized friction coefficient using the surface area with increasing measuring time.

6.3.3 Lubrication of molten ice cream

Besides the lubrication curve of melting ice cream, we also investigated the lubrication curve of molten ice cream. As different samples had different melting performances, it was hard to define the end of melting for all samples. Therefore, we put the samples at 4 °C overnight, and we created thereafter a thinner layer between the probe and the PDMS substrate to achieve complete contact. A sample volume of 10 ml was poured into the holder, and a normal force of 0.5 N was applied. The contact area between the sample and the probe was constant in this case. When measuring the sample LIF, as shown in Fig. 6.6, the friction coefficient remained constant as the measuring time increased, indicating a consistent lubrication behavior after melting.

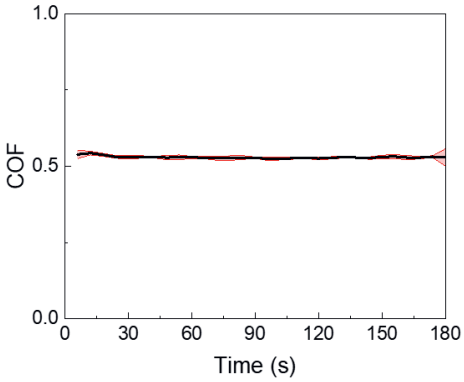

Fig. 6.6. Example of lubrication curve of molten ice cream (LIF).

6.3.4 Effect of different structural elements on the lubrication behavior of ice cream and molten ice cream

To explore how different structural elements affect the lubrication properties during ice cream melting, we first made 6 samples varying in ice fraction, overrun, viscosity, fat content and degree of fat aggregation. The ice fraction was controlled by varying the ratio between sugar and water, leading to a sample with a high ice fraction of 87% (HIF) and one with a lower ice fraction of 59% (LIF). The viscosity was varied by the addition of guar gum (0.5%), which increased the viscosity to 85.3 mPa·s, a value much higher than that (2.8 mPa·s) of the sample with no polysaccharides added (LIF). The fat content of the sample was changed by the addition of cream, which increased the fat content to 10% (FA and FNA). For one of the samples with 10% fat, also the degree of fat aggregation was increased by a different preparation method, which increased the size of the fat particles present in the molten ice cream from 8.9 (FNA) to 114 µm (FA). A different preparation method was also used to create a sample with a low air content of 20% (LO). The effect of structural elements was investigated by comparing samples differing in specific structural elements but similar in the others. An overview of the sample characteristics is shown in Tab. 6.2.

Tab. 6.2. Overview of the different structural elements and measured physical properties of the studies samples.

Sample	Ice fraction (%)	Fat content (%)	Fat aggregate size (µm)	Mix Viscosity (mPa·s)	Overrun (%)	Hardness (MPa)	Melting rate (%/min)
HIF	87 ± 1^{a}	< 0.1	0.25 ± 0.01^{c}	1.6 ± 0.3^{d}	74 ± 1^{a}	8.6 ± 1.5^{b}	$1.04 \pm .006^{b}$
LIF	59 ± 4^{b}	< 0.1	0.25 ± 0.01^{c}	2.8 ± 0.4^{d}	58 ± 5^{b}	2.6 ± 0.4^{d}	1.28 ± 0.06^{a}
HV	60 ± 3^{b}	< 0.1	0.25 ± 0.01^{c}	85.3 ± 1.0^{a}	78 ± 5^{a}	2.9 ± 0.5^{cd}	1.06 ± 0.08^{b}
FA	61 ± 1^{b}	10	114 ± 2^{a}	36.4 ± 6.8^{b}	31 ± 3^{c}	4.8 ± 0.7^{c}	0.61 ± 0.03^{e}
FNA	61 ± 5^{b}	10	8.9 ± 0.6^{b}	7.9 ± 1.3^{c}	34 ± 2^{c}	4.6 ± 0.7^{c}	1.32 ± 0.06^{a}
LO	87 ± 1^{a}	< 0.1	0.25 ± 0.01^{c}	1.6 ± 0.3^{d}	20 ± 1^{d}	18.6 ± 4.0^{a}	0.78 ± 0.05^{d}

Values with a different letter within the same column are significantly different ($P < 0.05$).

6.3.5 Effect of fat content (LIF vs FNA)

To gain insight into the effect of fat content on lubrication, we compared samples with (FNA) and without fat (LIF). As depicted in Fig. 6.7a, the ice cream sample with a high-fat content (10%) contained fat particles with a mean size of 8.9 µm, corresponding with a limited degree of fat aggregation, and thus the effect of fat aggregates on lubrication could be neglected. Tribological measurements showed that the friction coefficients of both fat-free and high-fat samples decreased with increasing time. To be more specific, during the initial measurement stage (Fig. 6.7b), i.e. the first 150 s, no significant difference in friction coefficients was found between fat-free and high-fat samples (error bands). However, a transition point could be seen at around 150 s, where the friction coefficient leveled off to a more constant value. As expected, at a later stage the friction coefficient of the high-fat sample was lower than that of the low-fat sample (Fig. 6.7b, 200 - 500s), indicating that a higher fat content positively contributes to lubrication in this phase, in line with what observed for many food products (Chojnicka-Paszun, et al., 2012; Milani, et al., 2011; Rahimi, Khosrowshahi, Madadlou, & Aziznia, 2007).

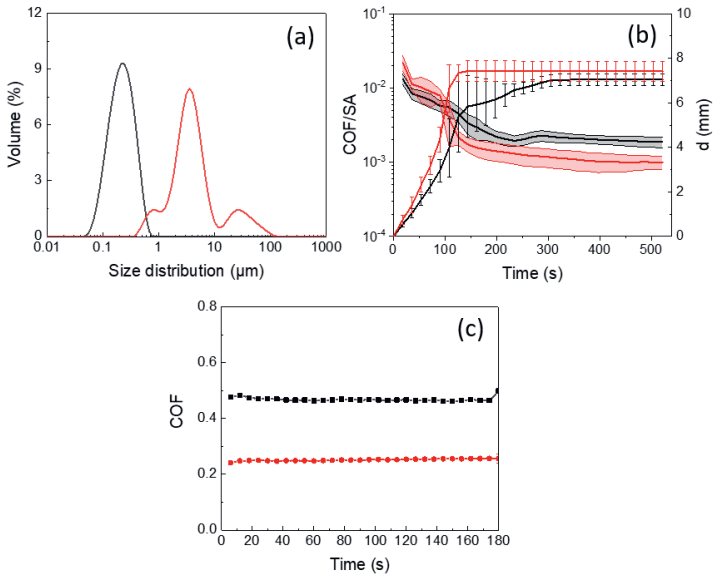

Fig. 6.7. (a) Particle size distribution of LIF (0% fat) and FNA (10% fat) ice cream; (b) Friction curves during melting (lines with error bands refer to COF/SA, and lines with the error bars represent the penetration distance); (c) Friction curve of molten ice cream. Black refers to the fat free (LIF) sample, while red refers to the high-fat (FNA) sample.

The transition point occurred when the penetration distance reached a constant value, which happened as soon as the probe touched the PDMS substrate as a result of the complete melting of the ice cream. The superior lubricating capacity of high-fat ice cream became even more evident when only the molten ice cream was measured (Fig. 6.7c). In many fat-containing foods, the good lubrication properties of fat have been attributed to its hydrophobic nature, which facilitates the spreading on the hydrophobic PDMS substrates (Schmid, Montmitonnet, Laugier, & Legrand, 2013). Fat can provide a lubrication fat layer on the PDMS surface, which more effectivly separates the two contacting surfaces, leading to lower friction. Thus, we could conclude that fat was not the main factor affecting the tribology of ice cream in the initial frozen state, but started to dominate the lubrication behavior upon melting in the later stage, where a fat layer was formed on the PDMS surface.

6.3.6 Effect of fat network formation (FA vs FNA)

We also compared the samples with the same fat content but different degrees of fat aggregation. Fig. 6.8a shows that the sample with fat aggregation (FA) had large particle size, and that aggregation did not significantly affect the frictional behavior (Fig. 6.8b).

So, fat aggregation did not appear to have a significant effect on the friction coefficient during melting. At the same fat content, the degree of fat aggregation had a limited effect on the formation of a fat layer on the PDMS surface, which also means that fat content is more important than fat aggregation for the lubrication properties in ice cream. Although no differences were seen during melting, a significant difference was observed when the molten ice cream was measured in a separate measurement (Fig. 6.8c). The friction coefficient of the ice cream without fat aggregation (FNA) remained constant at a constant sliding speed (10 mm/s), whereas the sample containing fat aggregates (FA) showed a small increase in friction coefficient over time. This observation might be explained by the fact that a further aggregation in the tribo-cell resulted in less fat able to form a lubricating layer on the PDMS substrate. Fat aggregation thus negatively affected the lubrication properties in the case of molten ice cream. Although the values for COF/SA were not affected, fat aggregation did show an effect on the penetration distance: the sample with a higher degree of fat aggregation had a slower change in the distance. This was most likely due to a lower melting rate or a higher hardness.

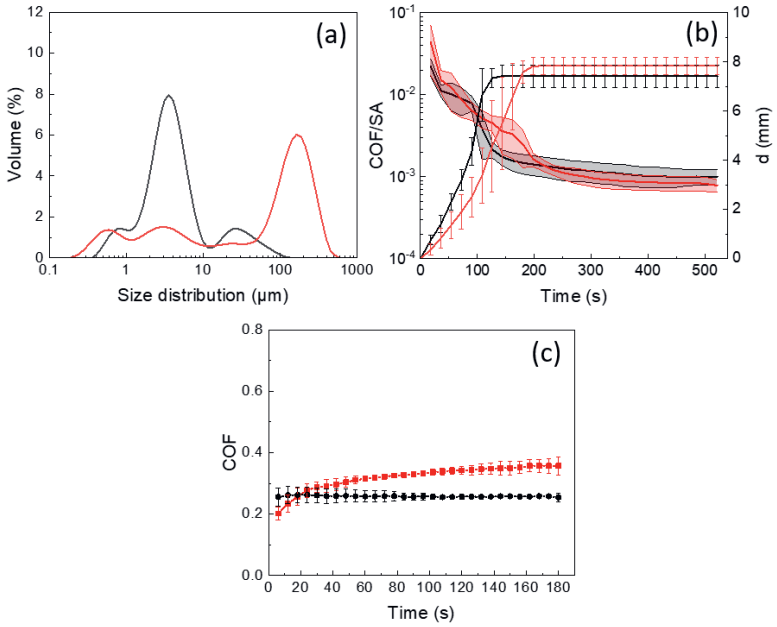

Fig. 6.8. (a) Particle size distribution of the FNA (8.9 μm) and FA (114 μm) samples; (b) Friction curves during melting (lines with error bands refer to COF/SA, and lines with the error bars represent the penetration distance); (c) Friction curve of molten ice cream. Black refers to the sample with limited fat aggregation (FNA), while red refers to the sample with a high degree of fat aggregation (FA).

6.3.7 Effect of ice fraction (HIF vs LIF)

To understand the effect of ice fraction on the lubrication properties of ice cream, two samples were prepared with ice fractions of 59% (LIF) and 87% (HIF), respectively (Fig. 6.9a). Samples with a high ice fraction (HIF) exhibited a faster decrease in friction coefficient during the first 200 s and a lower coefficient value (Fig. 6.9b), indicating that ice fraction played a role in affecting the lubrication properties at the initial stage of melting. This was probably due to their difference in melting rate and hardness, which have been shown to be much affected by ice content (Muse, et al., 2004).

The penetration distance of the sample with a higher ice fraction changed significantly more slowly than for the sample with a lower ice fraction, indicating a lower melting rate or a lower changes of hardness upon melting, and thus confirming a large difference in melting rate. As expected, no difference in friction coefficient

could be found at the later stage of melting (Fig. 6.9b), as the ice crystals were completely melted. Interestingly, for the molten ice cream, the sample LIF generated lower friction coefficients compared to the HIF (Fig. 6.9c). As this could not be due to differences in ice content, it may be related to a difference in sucrose content. The sample LIF contained more sugar, which is able to form a more viscous lubrication layer on the interacting surface and increase the lubrication of the molten ice cream. The lubrication ability of sugar has been shown before by Tian et al. (2022).

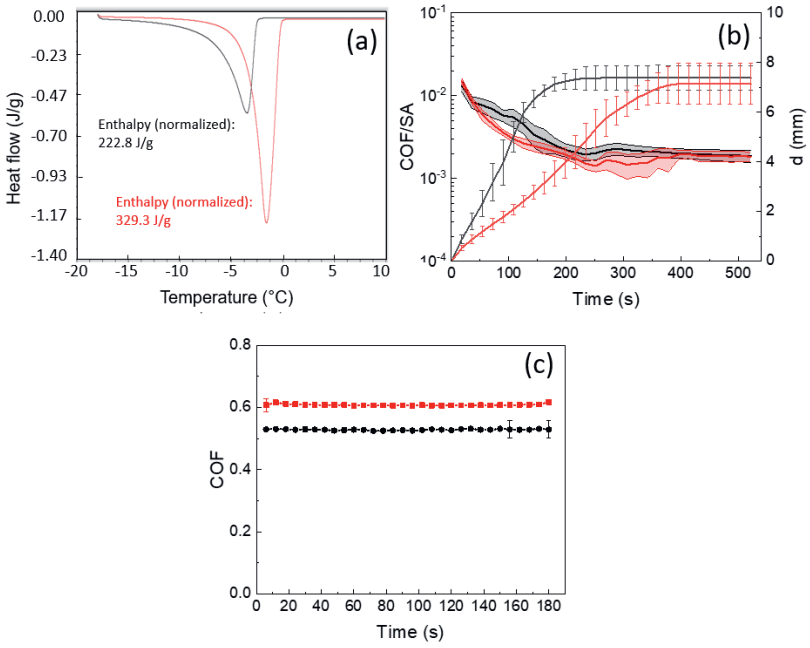

Fig. 6.9. (a) Enthalpy of HIF (329.3 J/g) and LIF (222.8 J/g) at -18 °C; (b) Friction curves during melting (lines with error bands refer to COF/SA, and lines with the error bars represent the penetration distance); (c) Friction curve of molten ice cream. Black refers to the sample with a low ice fraction (LIF), while red refers to the sample with a high ice fraction (HIF).

6.3.8 Effect of serum phase viscosity (LIF vs HV)

To assess the impact of serum phase viscosity on lubrication behavior, two samples were used: the reference ice cream mix with a viscosity of 2.8 mPa·s (LIF, without polysaccharide), and a sample (HV) prepared with GG, which had a viscosity of 85.3 mPa·s. The viscosity as a function of shear rate is presented in Fig. 6.10a. Although we did not measure the serum phase viscosity of the samples (which is difficult to

do), we assumed that the large differences in mix viscosity were also reflected in large differences in the serum phase viscosity, as the freeze concentration in the two samples was the same. It was observed that viscosity did not have any significant effects on the lubrication behavior of ice creams (Fig. 6.10b). This was unexpected, as it is known from literature that high viscosity provides better lubrication due to the formation of a viscous layer (Cassin, Heinrich, & Spikes, 2001; de Vicente, Stokes, & Spikes, 2006). Apparently, the effect of structure on lubrication was still dominated by the solid properties of the ice crystals. However, also for the molten ice cream, the difference in viscosity did not provide large differences in the friction coefficient, although the coefficient of the high-viscosity sample (HV) was slightly lower than that of the low-viscosity sample (LIF) (Fig. 6.10c). Apparently, the friction coefficient was not much affected by the viscosity of the molten ice cream. This may be related to the fact that other ingredients were also present in the sample. It has already been observed before that in more complex mixtures the lubrication properties are more dominated by the structure of the sample, and not by the lubrication ability of the individual components (Ji, Cornacchia, Sala, & Scholten, 2022).

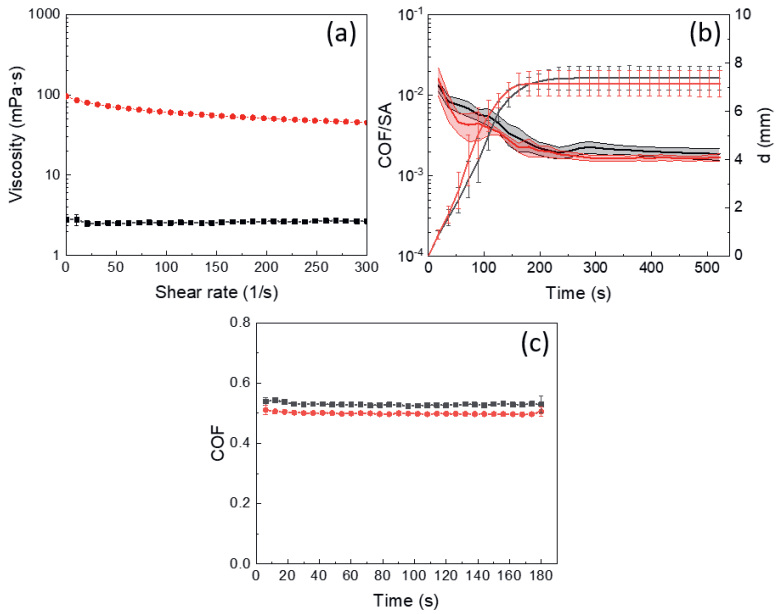

Fig. 6.10. (a) Mix viscosity of LIF (2.8 mPa·s) and HV (85.3 mPa·s) as a function of shear rate; (b) Friction curves during melting (lines with error bands refer to COF/SA, and lines with the error bars represent the penetration distance); (c) Friction curve of molten ice cream. Black refers to the sample with a low viscosity (LIF), while red refers to the sample with a high viscosity (HV).

6.3.9 Effect of overrun (HIF vs LO)

To examine the impact of overrun on frictional behavior, samples with an overrun of 74% (HIF) and 20% (LO) were compared. The low overrun sample exhibited a denser structure (Fig. 6.11a), and the friction coefficient of the high overrun sample decreased with increasing measurement time and remained constant after 200 s (Fig. 6.11b). However, the friction coefficient of the low overrun sample decreased continuously throughout the measurement time. This was consistent with the continuous change in the distance of the probe, indicating a slower melting of the sample with lower overrun. The continuous change in friction coefficient thus seemed to be more related to the slower melting of the sample. Another possibility is that lubrication is closely related to the hardness, as the hardness also continuously decreased with the melting of the ice cream. For the molten ice cream, no significant difference in friction coefficient was observed between the two samples (Fig. 6.11c), suggesting a loss of air cells during the melting process.

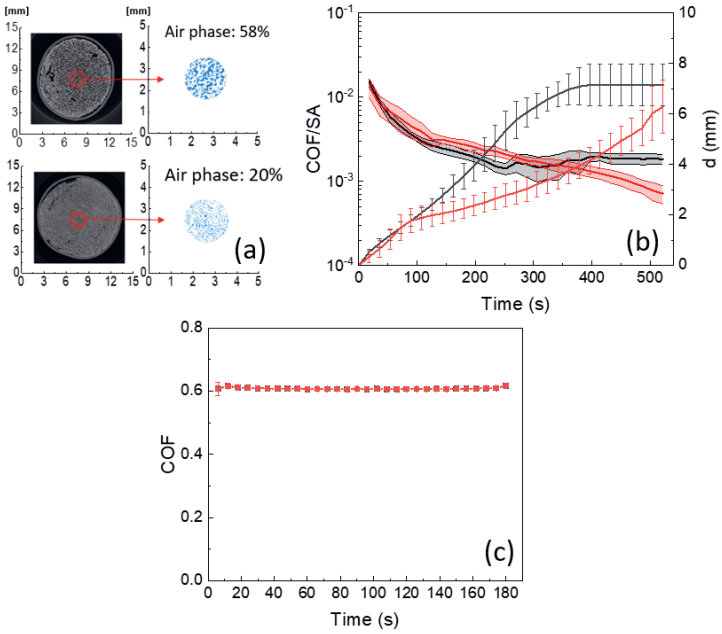

Fig. 6.11. (a) Structure observation of HIF (74% overrun) and LO (20% overrun); (b) Friction curves during melting (lines with error bands refer to COF/SA, and lines with the error bars represent the penetration distance); (c) Friction curve of molten ice cream. Black refers to the sample with a high overrun (HIF), while red refers to the sample with a low overrun (LO).

6.3.10. Extraction of friction parameters and their correlations with ice cream characteristics

Based on the results discussed above, some typical curves were identified, which are schematically depicted in Fig. 6.12.

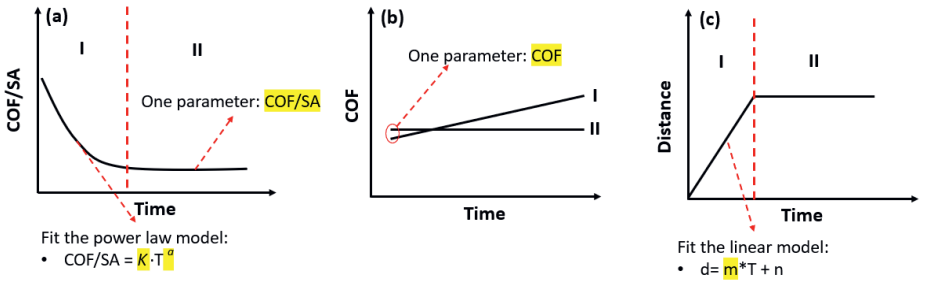

Fig. 6.12. Typical curves of (a) friction changes of ice cream during melting, (b) friction changes of molten ice cream, and (c) penetration distance during melting.

A representative tribological curve of all studied ice cream samples during melting is shown in Fig. 6.12a. Two regimes can be distinguished according to its shape: (1) regime I, in which the COF/SA decreased fast with increasing measurement time, and (2) regime II, in which COF/SA remained constant with measurement time. In the first stage, the curve could be fitted with the following power law model:

$$COF/SA = K \cdot T^{a} \quad (6.3)$$

where COF/SA is the friction coefficient normalized with the surface area, k is the consistency index, T is the melting time and a refers to how fast the friction coefficient decreases as a function of measuring time. The fitting curves are shown in the Fig. S6.1 of the supplementray material. An overview of the parameters of the best fit to the experimental data points is summarized in Tab. 6.3.

FA and FNA had significantly higher values for K (1.54 and 1.13) than other samples ($K < 0.18$). As both FA and FNA had higher fat content, the higher values of K indicate that fat particles did not contribute to the lubrication at the initial stage. However, FA and FNA also showed higher values of a (-1.23 and -1.26) compared to other samples (a < -0.87), indicating that the friction coefficient of high-fat content samples decreased faster during the fast-melting phase. The result of COF/SA refers to the friction coefficient at the later phase of the melting process. The lowest value for FA (0.00009) and FNA (0.00108) demonstrated the positive effect of fat content on lubrication, in line with the results of section 6.3.5.

Tab. 6.3. Overview of the parameters obtained from the best fit of the typical curves of friction changes of ice cream during melting, of molten ice cream and of the penetration distance during melting.

Sample	*K*	*a*	COF/SA at the later phase of melting	COF for molten ice cream	S_d
HIF	0.18	-0.87	0.0018	0.61	0.06
LIF	0.12	-0.71	0.00209	0.53	0.13
HV	0.12	-0.72	0.00219	0.50	0.14
FA	1.54	-1.23	0.00009	0.33	0.13
FNA	1.13	-1.26	0.00108	0.26	0.19
LO	0.11	-0.71	0.00149	0.61	0.03

Fig. 6.12b represents a typical tribological curve of molten ice cream, relating friction to structural changes of the sample. Most of the measured samples showed a type II curve, indicating a consistent lubrication behavior after melting. The increase in friction coefficient (type I curve) was obtained only for samples containing fat aggregates, which could be attributed to the accumulation of the fat aggregates as the sample is moved to the sides by the probe during the sliding movement. The mean values of COF for molten ice cream are also provided in Table 4. For these samples, it is clear that fat content contributed the most to these values (0.33 and 0.26). Other samples had similar higher values (0.5 ~0.6), due to small differences in composition after melting.

A representative curve of penetration distance is represented in Fig. 6.12c. Also for this curve two regimes were recognized: (1) regime I, in which the distance changed fast due to melting of the samples, and (2) regime II, in which the distance kept constant as result of complete melting. The slope in regime I could be fitted with a linear model, and the slope of the curve, S_d, was used to represent the melting rate or the changes of hardness during melting of the measured samples. The slope of regime I is shown in Tab. 6.3. The samples HIF and LO showed significantly lower values of S_d (0.06 and 0.03) than other samples (> 0.13), suggesting that the sample with a high ice fraction and low overrun melted more slowly, and, thus, that the hardness decreased more slowly during the melting process. The positive effect of ice fraction and the negative effect of overrun on hardness have been reported by many studies (Granger, Leger, Barey, Langendorff, & Cansell, 2005; Liu, et al., 2023b; Muse, et al., 2004; Sofjan, et al., 2004; Warren & Hartel, 2014). These results thus show that melting and hardness can be measured in different ways. As force is also applied to

ice cream during consumption, this new method may be more related to the melting in mouth.

Correlation coefficients between physicochemical characteristics and lubrication parameters of both ice cream and molten ice cream were calculated (Fig. 6.13).

Variables	*K*	*a*	COF/SA	COF	S_h
Ice fraction	-0.386	0.306	0.144	0.687	**-0.884**
Fat particle size	**0.935**	-0.759	**-0.884**	-0.540	0.184
fat content	**0.897**	**-0.956**	**-0.862**	**-0.943**	0.627
viscosity	0.092	0.044	0.093	-0.164	0.363
Overrun	-0.466	0.418	0.683	0.367	0.076
Hardness	-0.269	0.274	-0.040	0.512	-0.808
Melting rate	-0.473	0.248	0.589	-0.096	0.492
K	**1**	**-0.934**	**-0.949**	-0.772	0.404
a	**-0.934**	**1**	**0.894**	**0.839**	-0.487
COF/SA	**-0.949**	**0.894**	**1**	0.668	-0.190
COF	-0.772	**0.839**	0.668	**1**	**-0.845**
S_h	0.404	-0.487	-0.190	**-0.845**	**1**

Fig. 6.13. Heatmap of correlation matrix (Pearson coefficients) between ice cream characteristics and lubrication parameters. Blue indicates negative correlation and red indicates positive correlation.

K was strongly positively correlated with fat particle size (0.935) and fat content (0.897), and did not show any correlation with other structural elements. This suggests that fat content is the dominant factor in determining *K*, and samples with higher fat content provided higher initial friction coefficient at the initial stage of melting. However, *a* was negatively correlated with fat aggregate size (-0.759) and fat content (-0.956), indicating that the fat particles easily produced deformation during sliding movement and the friction coefficient decreased faster in the samples with high-fat content along with melting. Also at the later stage of melting and for ice cream in the molten state, fat content was negatively linked to COF/SA (-0.862) and COF (-0.943), suggesting that a higher fat content is more effective in improving the lubrication properties for both ice cream and molten ice cream. The COF/SA was strongly correlated with *a* (0.894) and COF (0.668), indicating that the sample with a higher lubrication during the fast-melting stage also had a better lubrication after being completely molten. With respect to the penetration distance, ice fraction (-0.884) and hardness (-0.808) were highly correlated to it. With higher ice fraction and hardness, the probe penetrated into the sample more slowly, corresponding to a lower melting rate. This result suggests that the penetration distance is a possible indicator of melting rate or of the changes of hardness during the melting process, providing new possibilities to measure the melting behavior or the hardness during melting.

6.4 Conclusion

In this study, a new method to measure the lubrication properties of ice cream during melting and in molten state was developed. Using a tribometer with an oscillatory linear movement and a large sample volume holder, the measuring parameters were optimized by adjusting the sample height and contact force between interacting surfaces, resulting in measurements with improved reproducibility. The obtained results show that it is possible to measure friction coefficients of ice cream during the melting process. Five parameters were extracted by establishing typical curves of tribological measurements, which were correlated to specific structural features of the ice cream, such as fat content, ice fraction, fat aggregation, serum phase viscosity and overrun. The lubrication behavior of ice cream during melting was mainly affected by ice fraction, fat content and overrun, although all at different stages of melting. Ice fraction was found to have a significant influence in affecting the lubrication properties of ice cream at the initial melting stage, while fat content and overrun dominated the lubrication behavior of ice cream at the later stages of melting. Interestingly, fat aggregation and viscosity did not appear to affect lubrication. The distance of the probe into the ice cream samples during melting was found to be mainly correlated with ice fraction and hardness, and was affected by fat content, ice fraction and overrun. Such distance can be used as an indication of melting behavior or hardness, which may provide more realistic results for melting in the mouth than currently used melting tests. However, the exact significance of the obtained data to describe changes in lubrication upon melting and how these data would be related to sensory perception need to be confirmed.

References

Cassin, G., Heinrich, E., & Spikes, H. A. (2001). The Influence of Surface Roughness on the Lubrication Properties of Adsorbing and Non-Adsorbing Biopolymers. *Tribology Letters, 11*(2), 95-102.

Chojnicka-Paszun, A., De Jongh, H. H. J., & De Kruif, C. G. (2012). Sensory perception and lubrication properties of milk: Influence of fat content. *International Dairy Journal, 26*(1), 15-22.

de Vicente, J., Stokes, J. R., & Spikes, H. A. (2006). Soft lubrication of model hydrocolloids. *Food hydrocolloids, 20*(4), 483-491.

Goff, H. D., & Hartel, R. W. (2013). Ice cream structure. *Ice cream*, 313-352.

Granger, C., Leger, A., Barey, P., Langendorff, V., & Cansell, M. (2005). Influence of formulation on the structural networks in ice cream. *International Dairy Journal, 15*(3), 255-262.

Guven, M., Karaca, O. B., & Kacar, A. (2003). The effects of the combined use of stabilizers containing locust bean gum and of the storage time on Kahramanmaraş-type ice creams. *International Journal of Dairy Technology, 56*(4), 223-228.

Javidi, F., Razavi, S. M. A., Behrouzian, F., & Alghooneh, A. (2016). The influence of basil seed gum, guar gum and their blend on the rheological, physical and sensory properties of low fat ice cream. *Food hydrocolloids, 52*, 625-633.

Ji, L., Cornacchia, L., Sala, G., & Scholten, E. (2022). Lubrication properties of model dairy beverages: Effect of the characteristics of protein dispersions and emulsions. *Food Research International, 157*, 111209.

Ji, L., Orthmann, A., Cornacchia, L., Peng, J., Sala, G., & Scholten, E. (2022). Effect of different molecular characteristics on the lubrication behavior of polysaccharide solutions. *Carbohydrate Polymers, 297*, 120000.

Ji, L., Otter, D. d., Cornacchia, L., Sala, G., & Scholten, E. (2023). Role of polysaccharides in tribological and sensory properties of model dairy beverages. *Food hydrocolloids, 134*, 108065.

Liu, X., Sala, G., & Scholten, E. (2022). Effect of fat aggregate size and percentage on the melting properties of ice cream. *Food Research International, 160*, 111709.

Liu, X., Sala, G., & Scholten, E. (2023a). Role of polysaccharide structure in the rheological, physical and sensory properties of low-fat ice cream. *Current Research in Food Science, 7*, 100531.

Liu, X., Sala, G., & Scholten, E. (2023b). Structural and functional differences between ice crystal-dominated and fat network-dominated ice cream. *Food*

hydrocolloids, 138, 108466.

Malone, M. E., Appelqvist, I. A. M., & Norton, I. T. (2003). Oral behaviour of food hydrocolloids and emulsions. Part 1. Lubrication and deposition considerations. *Food hydrocolloids, 17*(6), 763-773.

Milani, E., & Koocheki, A. (2011). The effects of date syrup and guar gum on physical, rheological and sensory properties of low fat frozen yoghurt dessert. *International Journal of Dairy Technology, 64*(1), 121-129.

Morell, P., Chen, J., & Fiszman, S. (2017). The role of starch and saliva in tribology studies and the sensory perception of protein-added yogurts. *Food & Function, 8*(2), 545-553.

Muse, M. R., & Hartel, R. W. (2004). Ice cream structural elements that affect melting rate and hardness. *Journal of dairy science, 87*(1), 1-10.

Nagarawatta, G. U. (2000). Effect of fat and sucrose replacers on physical, chemical, and sensory properties of reduce calorie ice cream.

Ningtyas, D. W., Bhandari, B., Bansal, N., & Prakash, S. (2018). Texture and lubrication properties of functional cream cheese: Effect of β-glucan and phytosterol. *Journal of Texture Studies, 49*(1), 11-22.

Prindiville, E. A., Marshall, R. T., & Heymann, H. (1999). Effect of milk fat on the sensory properties of chocolate ice cream. *Journal of dairy science, 82*(7), 1425-1432.

Rahimi, J., Khosrowshahi, A., Madadlou, A., & Aziznia, S. (2007). Texture of low-fat Iranian white cheese as influenced by gum tragacanth as a fat replacer. *Journal of dairy science, 90*(9), 4058-4070.

Roland, A. M., Phillips, L. G., & Boor, K. J. (1999). Effects of fat content on the sensory properties, melting, color, and hardness of ice cream. *Journal of dairy science, 82*(1), 32-38.

Rudge, R. E. D., Scholten, E., & Dijksman, J. A. (2019). Advances and challenges in soft tribology with applications to foods. *Current Opinion in Food Science, 27*, 90-97.

Sarkar, A., & Krop, E. M. (2019). Marrying oral tribology to sensory perception: A systematic review. *Current Opinion in Food Science, 27*, 64-73.

Schmid, S. R., Montmitonnet, P., Laugier, M., & Legrand, N. (2013). Lubrication with Emulsions. In Q. J. Wang & Y.-W. Chung (Eds.), *Encyclopedia of Tribology* (pp. 2151-2158). Boston, MA: Springer US.

Selway, N., & Stokes, J. R. (2013). Insights into the dynamics of oral lubrication and mouthfeel using soft tribology: Differentiating semi-fluid foods with similar rheology. *Food Research International, 54*(1), 423-431.

Shewan, H. M., Pradal, C., & Stokes, J. R. (2020). Tribology and its growing use

toward the study of food oral processing and sensory perception. *Journal of Texture Studies, 51*(1), 7-22.

Sofjan, R. P., & Hartel, R. W. (2004). Effects of overrun on structural and physical characteristics of ice cream. *International Dairy Journal, 14*(3), 255-262.

Tian, Q., Jia, X., Zhang, Y., Zhang, Y., Yang, J., Wang, S., Li, Y., Shao, D., Feng, L., & Song, H. (2022). In-situ growth of amorphous carbon on sucrose-assisted exfoliated boron nitride nanosheets: Exceptional water dispersibility and lubrication performance. *Tribology International, 173*, 107647.

Vlădescu, S.-C., Bozorgi, S., Hu, S., Baier, S. K., Myant, C., Carpenter, G., & Reddyhoff, T. (2021). Effects of beverage carbonation on lubrication mechanisms and mouthfeel. *Journal of Colloid and Interface Science, 586*, 142-151.

Warren, M. M., & Hartel, R. W. (2014). Structural, compositional, and sensorial properties of United States commercial ice cream products. *Journal of food science, 79*(10), E2005-E2013.

Warren, M. M., & Hartel, R. W. (2018). Effects of emulsifier, overrun and dasher speed on ice cream microstructure and melting properties. *Journal of food science, 83*(3), 639-647.

Wu, B., Freire, D. O., & Hartel, R. W. (2019). The effect of overrun, fat destabilization, and ice cream mix viscosity on entire meltdown behavior. *Journal of food science, 84*(9), 2562-2571.

Supplementary material

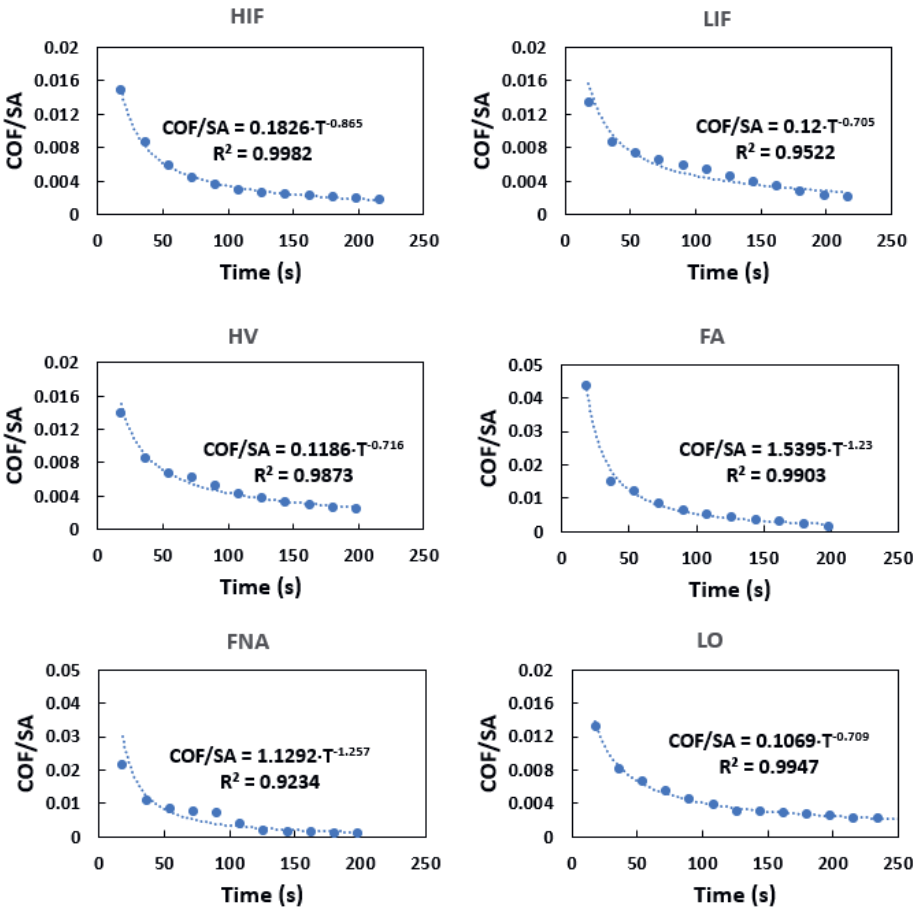

Fig. S6.1. COF/FA as a function of measuring time in regime I. The dotted lines refer to the best fit through the experimental data points.

Chapter 7

General discussion

7.1 Introduction

Reducing the fat content poses a challenging task due to the significant role that it plays in shaping the ice cream characteristics. For example, fat plays an important role in the formation and stabilization of air cells, which consequently affects the melting rate (Goff, Hartel, Goff, & Hartel, 2013; Rios, Pessanha, Almeida, Viana, & Lannes, 2014). In general, a lower degree of fat destabilization (< 30%) results in faster melting and poor shape retention compared with ice cream with a high degree of fat destabilization (> 50%) (Muse & Hartel, 2004). However, it is difficult to attribute the change in melting rate to fat destabilization itself or to secondary effects that fat stabilization has on other structural features of ice cream, such as the overrun. In addition, contradictory results have been seen for the effect of fat destabilization on hardness. Muse et. al (2004) reported that destabilized fat increased hardness, whereas another study showed that fat destabilization had limited effect on hardness (Roland, Phillips, & Boor, 1999b). The difference in results was attributed to differences in secondary effects (overrun, ice crystal size, etc.). The contradictory indications reported in the literature show that there is still a limited understanding of the exact role of fat in ice cream melting and textural properties. This is mainly due to the fact that in previous studies many parameters were changed at the same time, which makes it challenging to extract the individual effect of separate parameters. Therefore, in this research systematic variations in the composition of ice cream were done to first understand the exact functionality of fat on different ice cream properties (structure, rheological and tribological properties, and sensory profile) by changing only one property at a time, while keeping the others constant. Based on the exact role of fat in ice cream properties, different fat-replacing strategies were developed. First, the individual contribution of fat to the melting properties of ice cream was evaluated (**Chapter 2**). Subsequently, the properties of a fat-dominated network were compared to ice cream dominated by a network of ice crystals (without fat), to gain insight into the role of the fat in the textural and viscoelastic properties (**Chapter 3**). Based on the results obtained from these two chapters, two different fat-replacing strategies were proposed: in **Chapter 4,** polysaccharides were used to replace fat, and plant proteins were used in **Chapter 5**. To link the sensory profile of the ice creams to their structure and texture, both the rheological and lubrication properties of molten ice cream were measured in **Chapters 4 and 5.** To also be able to measure lubrication properties in the frozen state and during melting, a new method was developed in **Chapter 6**.

7.2 Main findings and conclusions

The individual contribution of fat to the melting, textural and viscoelastic properties of ice cream was clarified in **Chapter 2.** The specific relationship between fat properties (fat content and fat destabilization degree) and ice cream melting properties was explained. At a similar fat content, varying fat destabilization degree affected the melting behavior, which was related to specific properties of the fat network: the fat aggregate size was found to be the more dominant factor influencing the melting lag time, whereas the percentage of fat aggregates influenced the melting rate and melted percentage. A critical size of the fat aggregates (approximately 45 μm) was needed to form a 3D network, which was able to retain the structure of the ice cream after melting. Depending on the degree of fat destabilization, we identified two main types of structures in ice cream (**Chapter 3**): one dominated by ice crystals and one dominated by a fat network. In this chapter, the individual contribution of different structural elements, including fat network, overrun and ice crystal size, on the melting, textural and viscoelastic properties of the two different types of ice cream was investigated. It was observed that in fat network-dominated structures the degree of destabilization was the dominant factor in affecting melting, while the overrun did not contribute much to it. Instead, the overrun was responsible for slowing down the melting process in the ice crystal-dominated structure. Moreover, shape retention could only be observed in fat network-dominated samples. In both types of ice cream, the overrun showed a significant influence on viscoelastic behavior and hardness, but ice crystal size showed limited effect on these properties **(Chapter 3)**. A summary of the role of fat in different properties of ice cream is shown in Fig. 7.1.

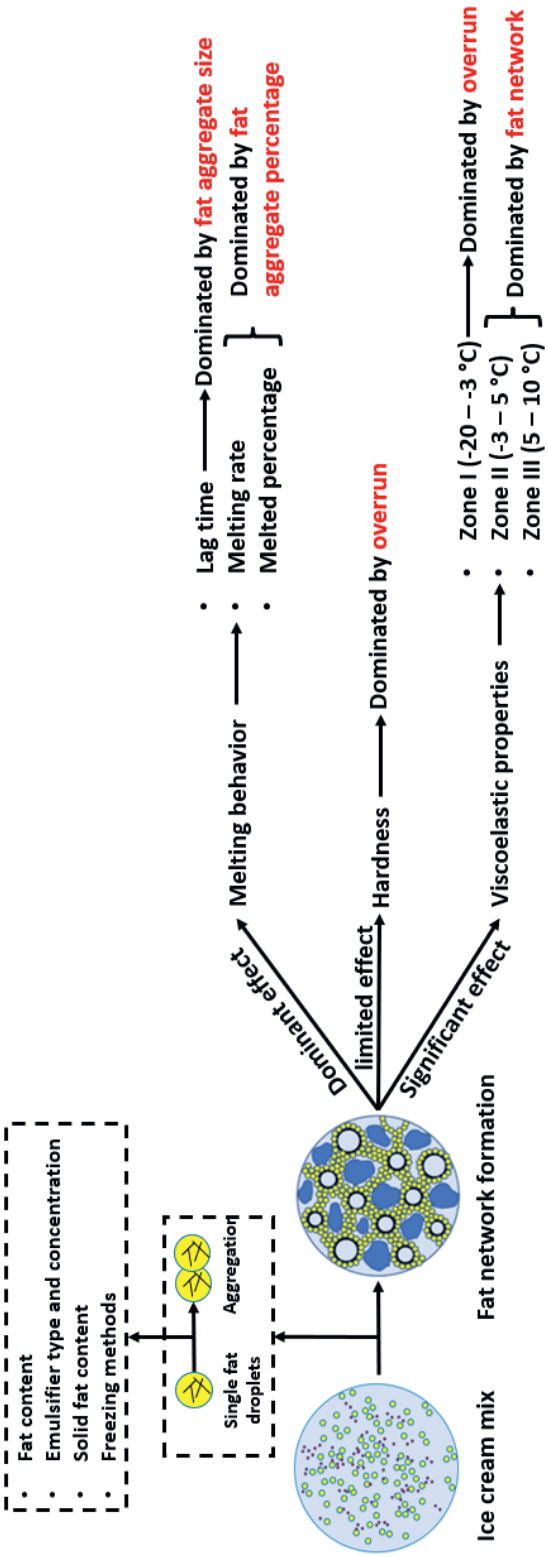

Fig. 7.1. Overview of the role of fat in different properties of ice cream.

As the fat network in the unfrozen serum phase resulted to be important for the ice cream characteristics, various fat replacers were used to mimic the function of the fat network in **Chapters 4 and 5**. An overview of the main results is shown in Fig. 7.2. In **Chapter 4**, polysaccharides were considered, as they have the ability to increase viscosity and provide a network in the unfrozen serum phase. Results showed that flexible polysaccharides (LBG and GG) had a lower degree of shear-thinning and a more liquid-like viscoelastic behavior compared to rigid polysaccharides (XG and IC). The flexible structure led to higher overrun, lower hardness and higher creaminess-related sensory perception, while rigid polysaccharides caused lower overrun, lower scoopability and higher coldness and grittiness. Therefore, flexible polysaccharides are a better choice for improving the quality of low-fat ice cream. In a second strategy, we used protein particles (**Chapter 5**) to provide structural features in the serum phase. Particle size and dispersibility of the added protein particles were varied. Dispersible particles of 250 nm led to higher overrun, which provided lower hardness and higher scoopability. In contrast, large, non-dispersible particles with a size between 3.8 and 145 µm resulted in lower overrun but enhanced the melting resistance and stability of the ice cream. Sensory evaluation indicated that samples with a protein particle size of approximately 4 µm provided a sensory profile similar to that of full-fat ice cream. Therefore, the quality of fat-free ice cream can also be improved by manipulating the size of protein particles added as fat-replacers. In both **Chapters 4 and 5**, the sensory perception was also shown to be related to the lubrication properties of molten ice cream. As we believed that changes in lubrication properties upon consumption are also relevant for perception, in **Chapter 6** we aimed to develop a new method to measure such properties during melting. This aim was achieved by using a Bruker tribometer with the option to include a large volume of frozen ice cream in the sample holder. With this new method, we also examined the effect of different structural elements on the lubrication behavior. Ice fraction was shown to be the main factor that contributed to the lubrication at the initial stage of melting, while fat content dominated the lubrication behavior at the later stage and in the molten state. Other structural elements, including fat aggregation, viscosity and overrun, did not appear to affect lubrication properties during melting.

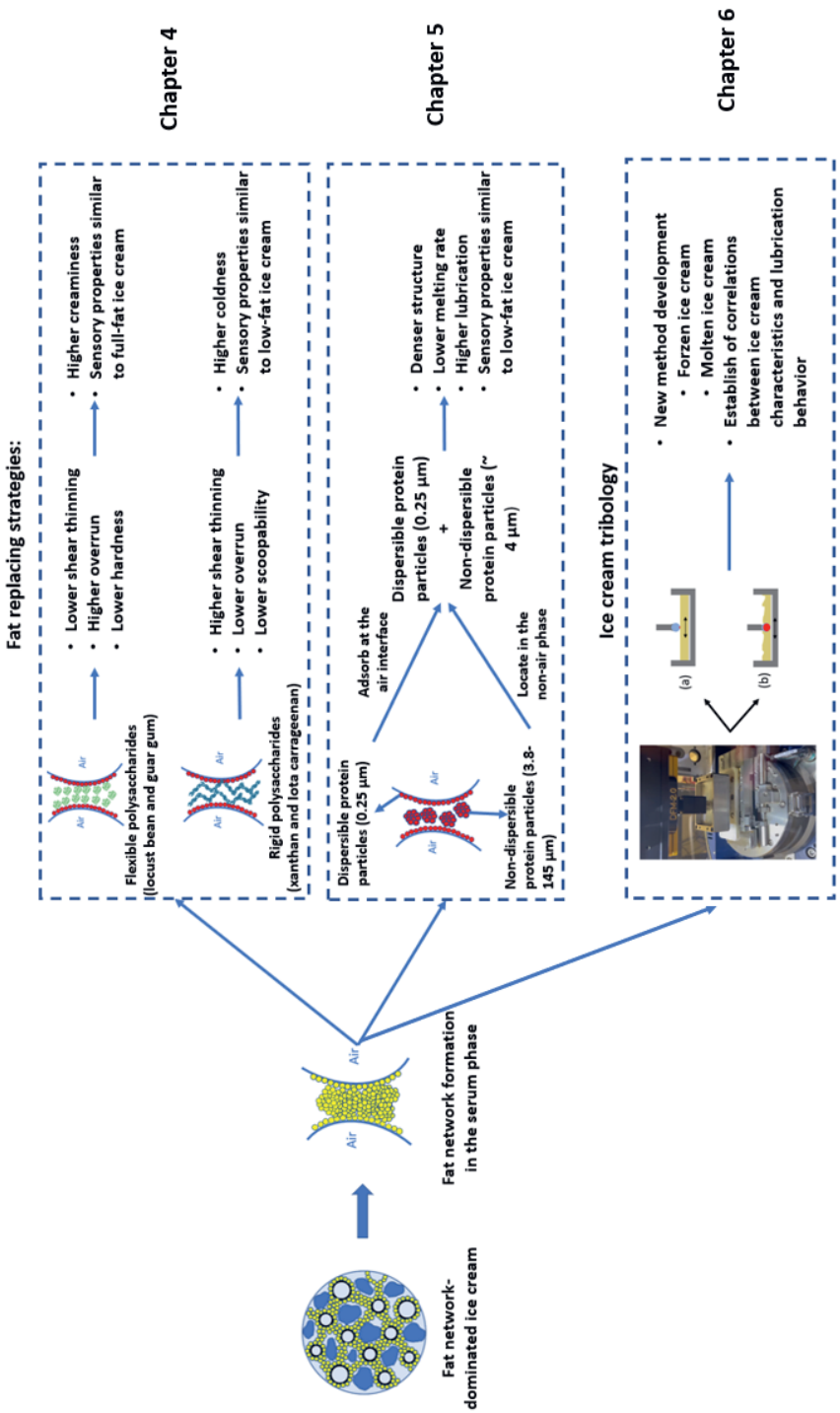

Fig. 7.2. Overview of the fat replacing strategies and ice cream tribology.

7.3 Discussion

7.3.1 Key determinants of ice cream melting

It has been reported that the formation of a fat network has a significant effect on melting behavior, which is an important quality parameter for ice cream (Amador, Hartel, & Rankin, 2017; Mahdian & Karazhian, 2013; Muse, et al., 2004; Warren & Hartel, 2018; Wildmoser, Scheiwiller, & Windhab, 2004b). However, only limited literature has discussed how to control the fat network formation and what properties of the fat network are responsible for melting (Amador, et al., 2017; Cheng, Dudu, Li, & Yan, 2020; Wu, Freire, & Hartel, 2019). Based on the results of **Chapter 2**, it becomes more clear that the formation of the fat network can be controlled by varying different parameters, including fat content, emulsifier concentration and type and solid fat content. In this work, we have clarified that different melting parameters are related to different properties of the fat network. For example, melting lag time is mainly determined by the size of fat aggregates, while melting rate and melted percentage are more influenced by the percentage of fat aggregates. The degree of fat aggregation shows a dominant effect on the melting behavior; the main structure of ice cream dominated by the fat network showed a significantly lower melting rate. However, in samples with a limited fat aggregation, melting properties were mainly determined by overrun and serum phase viscosity; the sample with a higher overrun and serum phase viscosity melts slower. Although many studies have reported that overrun can affect melting (Sofjan & Hartel, 2004; Warren, et al., 2018; Wu, et al., 2019), it seems to be mainly important for ice creams with lower fat contents or with limited degree of fat aggregation (**Chapter 3**). However, besides overrun, also the viscosity of both of the mix and unfrozen serum phase influences melting rate to a large extent, as was shown in **Chapters 4 and 5**. In literature, only the mix viscosity has been discussed, which has been shown to have a positive effect on melting resistance (Freire, Wu, & Hartel, 2020; Muse, et al., 2004; Roland, Phillips, & Boor, 1999a; Velásquez-Cock, et al., 2019; Warren, et al., 2018). However, due to freeze concentration, the viscosity of the serum phase increases to a large extent, and serum phase viscosity may become more relevant than the mix viscosity, as the melting of ice cream during consumption starts from its frozen form. In **Chapter 4** the more important role of the serum phase viscosity was confirmed by a strong negative correlation between serum phase viscosity and melting rate. It is worth mentioning that all samples in **Chapters 2-5** had a similar ice fraction, as we kept the ratio between sugar and water constant. When ice fraction is also varied, different melting behavior can be found, as discussed in **Chapter 6**. Samples with a higher ice fraction

showed a lower melting rate. This result was inconsistent with a previous study reported by Muse et al. (2004), in which ice fraction did not appear to affect melting. This is probably due to the secondary effect of other components.

7.3.2 Methods for the characterization of ice cream melting

In this thesis, different methods were used to measure the melting behavior of ice cream. In **Chapter 4**, melting was measured on a mesh screen at room temperature (**gravimetric test of melting**). This is the most commonly used method in literature (Muse, et al., 2004; Roland, et al., 1999a; Sakurai, 1996; Warren, et al., 2018). Alternatively, melting properties can also be extracted from the results of oscillatory measurements (**oscillatory melting test**), which reflect changes in the viscoelastic properties during a temperature sweep. A steeper decrease of the moduli indicates a fast-melting of the ice cream (Eisner et al., 2005). We found a strong correlation between the melting rate from gravimetric test and the slope of the fast-melting zone from the oscillatory test. However, we also found slight differences due to the different conditions during the melting process, especially for samples with different overrun values. When ice cream melted on a mesh screen, samples with different overruns showed similar melting rates, while the effect of overrun on the melting was more pronounced in the oscillatory measurement. In this case, samples with a higher overrun had a lower melting rate. The different effects of overrun mainly depend on the measuring conditions. Air cells can easily escape due to the collapse of the structure on a mesh screen at room temperature, but the structure of sample is more confined during rheology measurement. The bubbles are thus maintained within the sample structure. Based on this, oscillatory test of melting seems to be a more suitable method to measure the samples with high overrun values.

In fact, neither method reflects real melting during oral processing, in which a certain force is applied to the sample and a certain movement is used. Therefore, we developed a third method to characterize the melting behavior using tribological measurements (**tribology test of melting**), in which changes in penetration of a probe into the sample during melting were measured. We found that the penetration distance could easily be measured, and from this a 'melting profile' could be obtained. The penetration distance was mainly correlated with ice fraction and hardness, and the obtained curve was similar to the melting curve of the gravimetric test. Therefore, changes in penetration distance can be considered a promising indicator of melting rate (**Chapter 6**). However, it still needs to be confirmed how the penetration distance would be related to the sample melting during oral perception. Overall, the

gravimetric melting test can distinguish samples with significantly different melting properties, while the oscillatory test is a more accurate method to measure small differences. In comparison, the tribology test seems to be more related to the melting during oral perception.

7.3.3 Key determinants of ice cream texture

Based on the results of **Chapter 3**, we found that the fat network only showed limited effects on hardness, and hardness was more affected by overrun. Fat can therefore play an indirect role in texture through its effect on overrun (Chang & Hartel, 2002; Goff, 1997; Méndez-Velasco & Goff, 2012; VanWees & Hartel, 2018). However, in **Chapters 2 and 3**, we found that both fat content and degree of fat destabilization had limited effect on the overrun values, which is in contradiction with the current literature. Instead, overrun was mainly influenced by the freezing process. As freezing proceeded, the air cells were progressively more destabilized and the overrun decreased. This occurred in both the batch freezer and liquid nitrogen freezing process. The air cells were mainly stabilized by the formation of fat network or ice crystal-structure at the end of the freezing process. These stabilized air cells play an important role in the textural properties. The dominant effect of overrun on hardness was verified in **Chapters 4 and 5**, in which a negative correlation was observed between them. This relationship has been reported by many researchers (Freire, et al., 2020; Sofjan, et al., 2004; Warren, et al., 2018; Wildmoser, Scheiwiller, & Windhab, 2004a; Wu, et al., 2019).

Apart from overrun, we also clarified the individual contribution of ice-related properties, including ice crystal size and ice fraction, to the hardness. In all cases, overrun and fat content were kept similar to isolate the effect of the studied variables. In the case of ice crystal size, conflicting results were found in previous studies (Sakurai, 1996; Sofjan, et al., 2004). In some studies, larger ice crystals have been shown to increase hardness, while in others they decreased it. This can probably be attributed to differences in secondary effects (overrun, fat aggregation degree, etc.), as these features were often not kept constant. When other elements were kept constant, hardness was found to be only slightly affected by the ice crystal size (**Chapter 3**), and ice fraction itself played a much larger role (**Chapter 4**).

Also mix viscosity has been discussed to affect the hardness of ice cream (Amador, et al., 2017; Freire, et al., 2020). However, we propose that this relation is not very relevant, as the hardness of frozen ice cream is not related to the viscosity of the initial

mix, but to that of the unfrozen serum phase in the frozen ice cream. This point has never been addressed in current literature, as the viscosity of the serum phase is difficult to measure, due to the presence of ice crystals. We developed a new approach to measure such viscosity, by simulating the composition of the serum phase from estimations of its volume fraction. Based on the results in **Chapter 4,** it was clear that serum phase viscosity was more related to hardness than mix viscosity, and therefore indeed more relevant. The development of the viscosity during ice cream production has therefore to be taken into account when relating structure to specific textural properties.

7.3.4 New indicators of ice cream texture

In literature, hardness is often measured with a penetration test (Muse, et al., 2004; Roland, et al., 1999a, 1999b; Sakurai, 1996). However, the relevance of this measurement is likely limited, as hardness is often experienced when scooping ice cream with a spoon. Therefore, we also aimed to measure ice cream "scoopability", for which a new method was developed in **Chapter 4.** The results showed that the measurement of hardness and scoopability provide slightly different results. Although hardness was affected only by ice fraction, overrun and serum phase viscosity, the scoopability test was also able to measure the influence of the structure formation by different polysaccharides in the serum phase. For example, when a gel network was formed by rigid polysaccharides in the serum phase, a denser structure was formed, which resulted in more energy required during scooping. In addition, the process of scooping involves friction between the scoop and the sample, and the scoopability is thus a complex structural parameter. The scoopability test is therefore a promising test to extract more specific information on the structural organization of ice cream.

Besides hardness and scoopability, the structural features of our experimental samples were also investigated by measuring the viscoelastic changes with increasing temperature by oscillatory measurements (Freire, et al., 2020; Granger, Langendorff, Renouf, Barey, & Cansell, 2004; Velásquez-Cock, et al., 2019; Wildmoser, et al., 2004a). In the temperature range from -20 to -3 °C (zone I), the value of storage modulus (G') was closely correlated with the hardness, indicating that both measurements give similar results when ice cream is in the frozen state. However, oscillatory measurements can provide additional information, as they are also able to measure changes in "hardness" during melting, as the temperature can be slowly increased. From -3 to 5 °C (zone II), both viscoelastic moduli decrease, indicating the collapse of the structure, as already discussed before. Effects of different structural

features could easily be identified, and therefore changes in G' are a good indicator of the melting behavior. Based on this technique, we were able to measure the onset of melting, related to the decrease in both G' and G''. Also from these results, the effect of fat on melting became apparent, as a late and slow decrease in both moduli was seen for the sample with fat network formation. This result is in agreement with the insights given by shape retention obtained from the gravimetric melting test. Although oscillatory rheology has been used in ice cream research, the studies in question mainly focused on the effect of different components or formulations (Amador, et al., 2017; Granger, et al., 2004; Velásquez-Cock, et al., 2019). Limited studies have discussed how the specific melting profile is related to the structural organization of the ice cream. Our results showed that oscillatory measurements can provide valuable information on the structural organization of ice cream, in which the changes of moduli in different regimes showed close correlations with different textural properties. A combination of different techniques may thus be useful to gain more insights into the complex structure of ice cream, both in the frozen state and during melting.

7.3.5 Key determinants of ice cream sensory perception

In this thesis, the exact role of fat in the sensory perception of ice cream was also clarified. Full-fat ice cream has been shown to have a significantly higher score of overall liking than low-fat or fat-free samples, indicating the importance of fat content for consumer preference (Guinard, et al., 1997; Güzeler, Kaçar, & Say, 2011; Javidi & Razavi, 2018; Mostafavi, Tehrani, & Mohebbi, 2017; Nagarawatta, 2000; Roland, et al., 1999b). The higher overall liking of full-fat ice cream is also reported in **Chapters 4 and 5**. Compared with low-fat or fat-free ice creams, the full-fat sample also showed higher scores in sensory attributes, such as creaminess, smoothness, thickness and mouth coating. Therefore, these sensory attributes are normally considered the drivers of liking. In comparison, the sensory attributes coldness, grittiness and meltdown, which scored lower in full-fat ice cream, are considered the drivers of disliking. This relation can be explained by the contributions of fat particles to ice cream structure. In **Chapters 2 and 3**, we already found that fat mainly affects the melting behavior and viscosity by forming a network in the serum phase, and thus, leading to the improvement of sensory perception. Therefore, manipulating the structure formation in the serum phase is believed to be a promising strategy to improve the ice cream sensory perception. In **Chapter 4** this was achieved by using different types of polysaccharides. More specifically, we found that the sensory attributes of samples with a network formed by rigid polysaccharides were closer to

the low-fat ice cream, while those containing flexible polysaccharides were closer to full-fat ice cream. This could be due to the fact that charged rigid polysaccharides form an irreversible gel network with divalent calcium ions via salt bridges and provides a more solid-like structure after melting. This was confirmed by comparing the viscosity of molten ice cream to that of the ice cream mix. Another possibility could be the effect on overrun on perception. In the frozen state, such network may still be beneficial, but the remainder of such a gel network during melting leads to undesired properties. The polysaccharide structure also showed a significant effect on the overrun values: polysaccharides with a flexible structure provided a higher overrun and thus a softer texture, corresponding with higher creaminess-related properties and overall liking. In contrast, the samples with rigid polysaccharides had lower overrun, were hard to scoop, and scored higher for coldness. It is therefore not completely clear whether the improved perception was related to the structure of the polysaccharide itself or to the secondary effect it had on the overrun. In **Chapter 5**, the effect of overrun itself was further verified. The fact that the sample with the highest overrun did not show the best sensory results indicated that other structural features may also be important for sensory appreciation. A higher score for liking was found in samples with a protein network in the serum phase, although the overrun was relatively lower. This protein network is formed due to the freeze concentration, which is reversible during the ice cream melting process. These results suggest that the serum phase and possibly reversible structure formation of ingredients in the serum phase are more important.

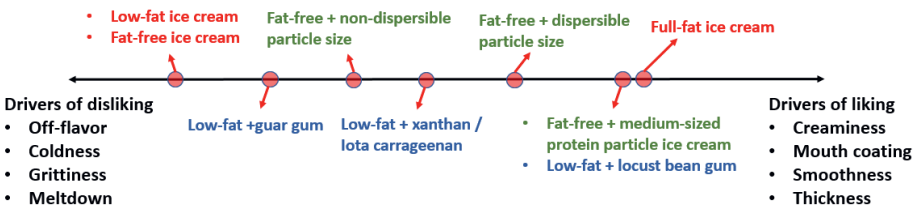

Fig. 7.3. Overview of the sensory evaluation after adding different fat replacers.

An overview of the effect of the addition of different fat replacers to low-fat and fat-free ice creams on sensory is provided in Fig. 7.3. Although the dominant factor affecting the creaminess-related attributes remains unclear, it seems that the higher overrun (around 55%) achieved with the use of flexible polysaccharides (low-fat + locust bean gum) contribute to higher creaminess-related properties. At the similar overrun level, the network formation obtained with large protein aggregates (fat-free + medium-sized protein particles) also corresponded to higher creaminess-related

properties. Therefore, to achieve a better sensory perception of low-fat or fat-free samples, creaminess-related attributes should be improved by a combination of different strategies: (1) increasing overrun and (2) promoting the formation of a reversible network in the serum phase upon melting, such as flexible polysaccharides or protein aggregates. As coldness and grittiness are related to low appreciation, the overall liking can also be improved by decreasing these attributes. Also in this case, a higher serum phase viscosity is beneficial, as in **Chapters 4 and 5** these attributes were found to be negatively correlated with serum phase viscosity. Moreover, according to the results of these two chapters, overall liking can be negatively affected by off-flavors, which should be an important factor when selecting fat replacers. Therefore, polysaccharides or plant proteins with less off-flavor would be better choices.

7.3.6 Key determinants of ice cream tribology

Apart from the ability to form a network in the serum phase, fat can also act as an effective lubricant, leading to a significantly lower friction coefficient, thereby improving the lubrication behavior (Chojnicka-Paszun, De Jongh, & De Kruif, 2012; Dresselhuis, et al., 2007). There seems to be an agreement that lubrication properties can reflect surface-related sensorial attributes, such as creaminess, mouthcoating and smoothness (Rudge, Scholten, & Dijksman, 2019; Selway & Stokes, 2013; Shewan, Pradal, & Stokes, 2020). In our case, the lubrication behavior of the molten ice cream containing fat also showed significantly better lubrication than low-fat or fat-free samples (**Chapters 4 and 5**). Next to fat content, we did not see an effect of polysaccharide type on lubrication behavior (**Chapter 4**). This is in contrast with results found in literature on the lubrication properties of polysaccharides (Agnieszka Chojnicka-Paszun & de Jongh, 2014; Garrec & Norton, 2012; Ji, Orthmann, et al., 2022; Stokes, Macakova, Chojnicka-Paszun, de Kruif, & de Jongh, 2011). In these studies, it has been shown that the structure of polysaccharides plays an important effect. This suggests that in more complex mixtures, such as ice cream, lubrication properties are not dominated by the individual ingredients, but more by the overall structure of the system, as shown by Ji et al. (2022) for other multi-component systems. The limited effect of the individual ingredients on lubrication was also seen in **Chapter 5**, where protein particle size seemed to have a limited effect on the lubrication properties of fat-free samples. In a complex system such as ice cream, lubrication properties can be affected by different ingredients, and may also be determined by the structure complexity. In addition, for sensory perception, the relevance of the lubrication of molten ice cream may be limited, and the changes in

lubrication during melting may be more important. Using a tribometer with adjustable probe height, we were able to clarify that the lubrication properties of ice cream during melting are mainly affected by factors that can influence the lubrication layer on the interacting surfaces, such as ice fraction, fat content and overrun. Overall, the new method shows that measuring friction coefficients during melting is possible, but we need to verify the significance of the obtained data. It also needs to be confirmed how these data could be related to sensory perception.

7.3.7 Suitability of fat replacers

The formation of a fat network in the serum phase provides a 3D structure that prevents the ice cream from completely collapsing and slows down melting. The structure formed by fat aggregates significantly improves the stability of incorporated air cells. In addition, solid fat particles can also adsorb onto the air-water interface, contributing to the overrun, although this effect was shown to be less relevant. As we discussed above, fat contributes to lubrication. Suitable fat replacers need thus to provide three functions: (1) they should have a positive effect on air inclusion, (2) they should create reversible structures within the serum phase upon melting, and (3) they should be able to decrease friction.

It is common for manufacturers to use polysaccharides in ice cream. A wide range of polysaccharides with various physicochemical properties have been investigated as fat replacers in this product, and the main function of the tested polymers was attributed to the modification of the viscosity and the thixotropy of ice cream mixes due to water binding and network formation (Javidi & Razavi, 2018; Kurt & Atalar, 2018; Mansour, et al., 2021; Velásquez-Cock, et al., 2019; Yu, Zeng, Wang, & Regenstein, 2021). No studies have explored the role of the specific structure of polysaccharides. From our previous discussion, it is clear that also the structure of the polysaccharide plays a role in its functionality in ice cream. Especially flexible polysaccharides seem to be more suitable, because of its positive effect on overrun and ability to form of a reversible network in the serum phase. However, the studied polysaccharides were not able to provide lubrication for complex ice cream systems. It may be beneficial to select polysaccharides that are still able to improve lubrication in complex systems.

Besides polysaccharides, proteins are also promising fat replacers due to their well-known foaming and network-forming abilities. Previous studies have reported that protein-based replacers have the potential to improve the sensory perception of low-

fat products (López-Martínez, Moreno-Fernández, & Miguel, 2021; Mostafavi, Tehrani, & Mohebbi, 2017; Polishchuk, et al., 2020). However, no studies have explored the impact of protein dispersibility on the structural and sensory properties of fat-free ice cream. We found that both dispersible and non-dispersible fractions are necessary to provide good sensory properties. Protein aggregates of different size provide different functionalities, and both dispersible and non-dispersible particles are required; (1) small dispersible protein particles for air incorporation, and (2) large non-dispersible protein particles for network formation in the serum phase to block the lamellae between the air cells. However, the non-dispersible particles should not be too large, as they will provide more grittiness and roughness to the ice cream. In our research, a mean size of 4 µm was most beneficial for sensory perception. In the case of protein particles, they did not contribute to lubrication either, mainly due to structure complexity. It is still necessary to verify whether it is a beneficial to use the protein particles that can improve the lubrication.

To investigate the potential of particles with different sizes as fat replacers, we also tried to use starch particles with different swelling degrees. The particle size of different starches was varied by heating, and mean size values ranging between 15 and 37 µm could be achieved. The results showed that starch granules with higher amylose content had a lower swelling degree after heating, but a higher ability to keep their specific morphology after freezing. Higher amylose starch (75% amylose) provided lower overrun compared with the normal (25% amylose) and waxy starch (< 1% amylose), and the corresponding hardness increased with decreasing overrun. However, limited differences could be found in melting properties. This may be due to the fact that the morphology and the size of the swelling starch granules in normal and waxy starches were destroyed during the freezing process, which did not occur in the case of high amylose starch. Additionally, we did not find significant differences in the sensory properties of starch-containing samples during a preliminary sensory test, and the taste of these samples was worse than that of the full-fat sample. Due to the large effect of the freezing process on granules integrity, it seems that starch is not directly suitable as a fat replacer, although it may be able to increase viscosity.

7.4 Future perspective

The future perspective of ice cream research holds exciting potential for development in both texture and taste considerations. In this thesis, we aimed to get a better understanding on the role of fat and explored ways to create healthier alternatives

with reduced fat. The focus on the selection and evaluation of fat replacers suitable for ice cream can be expected to continue in the future. Although we have found that apart from viscosity, the properties of the fat replacers themselves also play important roles, such as polysaccharide structure and protein dispersibility, there are still some other properties of fat replacers that may affect the results, such as polysaccharide molecular weight. Moreover, based on the sensory evaluation, some attributes did not seem to be directly related to the properties of fat replacers themselves, but to other characteristics. For example, sensory attributes such as creaminess, thickness and mouthcoating showed strong correlations with lubrication behavior. Further clarification is needed on the key determinants of various sensory attributes. To achieve this aim, the effect of different properties of a specific fat replacer on the structural elements and textural properties of ice cream should be explored individually, and then relationship between texture and sensory properties should be established.

Although a new method has been developed to measure the lubrication of ice cream during the melting process and at the molten states, the relations between the obtained data and sensory perception remain unclear. We found that friction coefficients during melting can be measured, but it is still not clear that we really measure lubrication effects or just the hardness upon melting. In addition, we assume that friction is related to specific attributes, but we did not verify the relation with sensory perception. Therefore, a sensory study for the samples in **Chapter 6** should be done, and correlations should be established to gain insights into the relationships between measured parameters and sensory attributes. In addition, the lubrication behavior of molten ice cream was very similar in all studied samples, so the structural elements (composition, overrun, viscosity) of the samples should be more different to test whether the new method is able to measure differences of molten samples.

Among all the structural features considered in the present work, the effect of ice-related properties remains unclear. For instance, a sample with a larger ice crystal size would be grittier, and a higher ice fraction would lead to a higher coldness. However, we mainly focused on the exact role of fat, which has a limited effect on ice-related properties. Instead, sugar content, sugar type and anti-freezing agents (salts or protein hydrolysates) play important roles in affecting ice crystal size and ice content. The relative importance of these ice-related properties and other structural elements (overrun, fat content, degree of fat aggregation, etc.) on the textural, melting, viscoelastic and sensory properties of ice cream is unclear. However, this information is crucial for gaining a better understanding of ice cream texture and sensory

perception, and can be used for the development of ice cream with both low-fat and low-sugar. Additionally, the incorporation of some functional ingredients, such as probiotics or antioxidants, may be interesting in enhancing the nutritional profile of ice cream recipes. This will benefit the rational design of ice cream formulations and improve the satisfaction of low-fat or fat-free ice cream products.

References

Amador, J., Hartel, R., & Rankin, S. (2017). The effects of fat structures and ice cream mix viscosity on physical and sensory properties of ice cream. *Journal of food science, 82*(8), 1851-1860.

Chang, Y., & Hartel, R. W. (2002). Stability of air cells in ice cream during hardening and storage. *Journal of Food Engineering, 55*(1), 59-70.

Cheng, J., Dudu, O. E., Li, X., & Yan, T. (2020). Effect of emulsifier-fat interactions and interfacial competitive adsorption of emulsifiers with proteins on fat crystallization and stability of whipped-frozen emulsions. *Food hydrocolloids, 101*, 105491.

Chojnicka-Paszun, A., & de Jongh, H. H. J. (2014). Friction properties of oral surface analogs and their interaction with polysaccharide/MCC particle dispersions. *Food Research International, 62*, 1020-1028.

Chojnicka-Paszun, A., De Jongh, H. H. J., & De Kruif, C. G. (2012). Sensory perception and lubrication properties of milk: Influence of fat content. *International Dairy Journal, 26*(1), 15-22.

Dresselhuis, D. M., Klok, H. J., Stuart, M. A. C., de Vries, R. J., van Aken, G. A., & de Hoog, E. H. A. (2007). Tribology of o/w emulsions under mouth-like conditions: determinants of friction. *Food Biophysics, 2*, 158-171.

Eisner, M. D., Wildmoser, H., & Windhab, E. J. (2005). Air cell microstructuring in a high viscous ice cream matrix. *Colloids and Surfaces A: Physicochemical and Engineering Aspects, 263*(1-3), 390-399.

Freire, D. O., Wu, B., & Hartel, R. W. (2020). Effects of structural attributes on the rheological properties of ice cream and melted ice cream. *Journal of food science, 85*(11), 3885-3898.

Garrec, D. A., & Norton, I. T. (2012). The influence of hydrocolloid hydrodynamics on lubrication. *Food hydrocolloids, 26*(2), 389-397.

Goff, H. D. (1997). Colloidal aspects of ice cream—a review. *International Dairy Journal, 7*(6-7), 363-373.

Goff, H. D., Hartel, R. W., Goff, H. D., & Hartel, R. W. (2013). Ice cream structure. *Ice cream*, 313-352.

Granger, C., Langendorff, V., Renouf, N., Barey, P., & Cansell, M. (2004). Short Communication: Impact of Formulation on Ice Cream Microstructures: an Oscillation Thermo-Rheometry Study. *Journal of dairy science, 87*(4), 810-812.

Guinard, J. X., Zoumas-Morse, C., Mori, L., Uatoni, B., Panyam, D., & Kilara, A. (1997). Sugar and Fat Effects on Sensory Properties of Ice Cream. *Journal*

of food science, 62(5), 1087-1094.

Guinard, J. X., Zoumas-Morse, C., Mori, L., Uatoni, B., Panyam, D., & Kilara, A. (2006). Sugar and Fat Effects on Sensory Properties of Ice Cream. *Journal of food science, 62*, 1087-1094.

Güzeler, N., Kaçar, A., & Say, D. (2011). Effect of Milk Powder, Maltodextrin and Polydextrose Use on Physical and Sensory Properties of Low Calorie Ice Cream during Storage. *Academic Food Journal/Akademik GIDA*.

Javidi, F., & Razavi, S. (2018). Rheological, physical and sensory characteristics of light ice cream as affected by selected fat replacers. *Journal of Food Measurement and Characterization, 12*, 1-13.

Javidi, F., & Razavi, S. M. A. (2018). Rheological, physical and sensory characteristics of light ice cream as affected by selected fat replacers. *Journal of Food Measurement and Characterization, 12*, 1872-1884.

Ji, L., Cornacchia, L., Sala, G., & Scholten, E. (2022). Lubrication properties of model dairy beverages: Effect of the characteristics of protein dispersions and emulsions. *Food Research International, 157*, 111209.

Ji, L., Orthmann, A., Cornacchia, L., Peng, J., Sala, G., & Scholten, E. (2022). Effect of different molecular characteristics on the lubrication behavior of polysaccharide solutions. *Carbohydrate Polymers, 297*, 120000.

Kurt, A., & Atalar, I. (2018). Effects of quince seed on the rheological, structural and sensory characteristics of ice cream. *Food hydrocolloids, 82*, 186-195.

López-Martínez, M. I., Moreno-Fernández, S., & Miguel, M. (2021). Development of functional ice cream with egg white hydrolysates. *International Journal of Gastronomy and Food Science, 25*, 100334.

Mahdian, E., & Karazhian, R. (2013). Effects of fat replacers and stabilizers on rheological, physicochemical and sensory properties of reduced-fat ice cream. *Journal of Agricultural Science and Technology, 15*(6), 1163-1174.

Mansour, A. I. A., Ahmed, M. A., Elfaruk, M. S., Alsaleem, K. A., Hammam, A. R. A., & El-Derwy, Y. M. A. (2021). A novel process to improve the characteristics of low-fat ice cream using date fiber powder. *Food Science & Nutrition, 9*(6), 2836-2842.

Méndez-Velasco, C., & Goff, H. D. (2012). Fat structure in ice cream: A study on the types of fat interactions. *Food hydrocolloids, 29*(1), 152-159.

Mostafavi, F. S., Tehrani, M. M., & Mohebbi, M. (2017). Rheological and sensory properties of fat reduced vanilla ice creams containing milk protein concentrate (MPC). *Journal of Food Measurement and Characterization, 11*, 567-575.

Mostafavi, F. S., Tehrani, M. M., & Mohebbi, M. (2017). Rheological and sensory

properties of fat reduced vanilla ice creams containing milk protein concentrate (MPC). *Journal of Food Measurement and Characterization, 11*(2), 567-575.

Muse, M. R., & Hartel, R. W. (2004). Ice cream structural elements that affect melting rate and hardness. *Journal of dairy science, 87*(1), 1-10.

Nagarawatta, G. U. (2000). Effect of fat and sucrose replacers on physical, chemical, and sensory properties of reduce calorie ice cream.

Ohmes, R. L., Marshall, R. T., & Heymann, H. (1998). Sensory and Physical Properties of Ice Creams Containing Milk Fat or Fat Replacers1. *Journal of dairy science, 81*(5), 1222-1228.

Polishchuk, G., Breus, N. M., Shevchenko, I., Gnitsevych, V., Yudina, T., Nozhechkina-Yeroshenko, G., & Semko, T. (2020). Determining the effect of casein on the quality indicators of ice cream with different fat content. *Eastern-European Journal of Enterprise Technologies, 4*, 24-30.

Rios, R. V., Pessanha, M. D. F., Almeida, P. F. d., Viana, C. L., & Lannes, S. C. d. S. (2014). Application of fats in some food products. *Food Science and Technology, 34*, 3-15.

Roland, A. M., Phillips, L. G., & Boor, K. J. (1999a). Effects of fat content on the sensory properties, melting, color, and hardness of ice cream. *Journal of dairy science, 82*(1), 32-38.

Roland, A. M., Phillips, L. G., & Boor, K. J. (1999b). Effects of fat replacers on the sensory properties, color, melting, and hardness of ice cream. *Journal of dairy science, 82*(10), 2094-2100.

Rudge, R. E. D., Scholten, E., & Dijksman, J. A. (2019). Advances and challenges in soft tribology with applications to foods. *Current Opinion in Food Science, 27*, 90-97.

Sakurai, K. (1996). Effect of production conditions on ice cream melting resistance and hardness. *Milchwissenschaft, 51*, 451-454.

Selway, N., & Stokes, J. R. (2013). Insights into the dynamics of oral lubrication and mouthfeel using soft tribology: Differentiating semi-fluid foods with similar rheology. *Food Research International, 54*(1), 423-431.

Shewan, H. M., Pradal, C., & Stokes, J. R. (2020). Tribology and its growing use toward the study of food oral processing and sensory perception. *Journal of Texture Studies, 51*(1), 7-22.

Sofjan, R. P., & Hartel, R. W. (2004). Effects of overrun on structural and physical characteristics of ice cream. *International Dairy Journal, 14*(3), 255-262.

Stokes, J. R., Macakova, L., Chojnicka-Paszun, A., de Kruif, C. G., & de Jongh, H. H. J. (2011). Lubrication, Adsorption, and Rheology of Aqueous

Polysaccharide Solutions. *Langmuir, 27*(7), 3474-3484.

VanWees, S. R., & Hartel, R. W. (2018). Microstructure of ice cream and frozen dairy desserts. *Microstructure of dairy products*, 237-260.

Velásquez-Cock, J., Serpa, A., Vélez, L., Gañán, P., Gómez Hoyos, C., Castro, C., Duizer, L., Goff, H. D., & Zuluaga, R. (2019). Influence of cellulose nanofibrils on the structural elements of ice cream. *Food hydrocolloids, 87*, 204-213.

Warren, M. M., & Hartel, R. W. (2018). Effects of emulsifier, overrun and dasher speed on ice cream microstructure and melting properties. *Journal of food science, 83*(3), 639-647.

Wildmoser, H., Scheiwiller, J., & Windhab, E. J. (2004a). Impact of disperse microstructure on rheology and quality aspects of ice cream. *LWT - Food Science and Technology, 37*(8), 881-891.

Wildmoser, H., Scheiwiller, J., & Windhab, E. J. (2004b). Impact of disperse microstructure on rheology and quality aspects of ice cream. *LWT-Food Science and Technology, 37*(8), 881-891.

Wu, B., Freire, D. O., & Hartel, R. W. (2019). The effect of overrun, fat destabilization, and ice cream mix viscosity on entire meltdown behavior. *Journal of food science, 84*(9), 2562-2571.

Yu, B., Zeng, X., Wang, L., & Regenstein, J. M. (2021). Preparation of nanofibrillated cellulose from grapefruit peel and its application as fat substitute in ice cream. *Carbohydrate Polymers, 254*, 117415.

Zembyla, M., Liamas, E., Andablo-Reyes, E., Gu, K., Krop, E. M., Kew, B., & Sarkar, A. (2021). Surface adsorption and lubrication properties of plant and dairy proteins: A comparative study. *Food hydrocolloids, 111*, 106364.

Summary

Although consumers are becoming increasingly aware of the negative health effects of certain food ingredients, the consumption of non-healthy foods continues to rise. An example is ice cream, which is often high in fat and not in line with a healthy lifestyle. Research efforts have therefore been made to lower fat content in ice cream and increase the flexibility in the ingredient choice. For ice cream, this is a major technological challenge, as fat plays a key role in determining the texture of the final product. In this thesis, we aimed to clarify the exact role of fat on the textural and sensory properties of ice cream and develop some potential fat replacing strategies based on the obtained knowledge.

The exact role of fat on the melting properties of ice cream was first clarified. In **Chapter 2**, we investigated the effect of fat aggregate size and percentage on the formation of a fat network, and, ultimately, on the melting properties of ice cream. We found that the fat destabilization degree and fat network formation have a significant effect on the melting behavior of ice cream. By investigating the effect of different fat particle characteristics, such as size and percentage, on the microstructure and melting behavior, we showed that the degree of fat destabilization is more important than fat content in determining the melting properties of ice cream with low overrun. The fat particle characteristics were found to be related to different melting properties: the fat aggregate size was found to be the dominant factor influencing the lag time, whereas the percentage of fat aggregates influenced more the melting rate and melted percentage. The results also showed that the stability of the fat network was mainly determined by the percentage of fat aggregates, and that a certain critical aggregate size was needed to form a network, which is most likely related to the lamellae thickness between air cells.

Next to fat destabilization degree, also the effect of overrun and ice crystal size on the textural, melting and viscoelastic properties of ice cream was explored in **Chapter 3**. To distinguish the individual contributions, we changed only one parameter at a time. Depending on the composition of the ice cream, we identified two main types of structures: one dominated by the ice crystals and one dominated by a fat network. The results showed that an ice crystal-dominated structure contributed particularly to viscoelastic behavior and hardness, whereas the fat network had a larger effect on melting. Only a limited effect of ice crystal size on the properties of the ice cream was seen, independently of the type of dominant structure. In both types of ice cream, increasing overrun induced a loss of connectivity between ice crystals and thus led to

lower viscoelastic moduli and hardness. Only in ice crystal-dominated samples the overrun also affected melting. The lower connectivity between ice crystals caused earlier melting of the ice crystal-dominated ice cream in the initial melting stage. At later stages of melting, higher overrun was able to slow down the melting process, leading to a two-step melting process. In fat network-dominated ice cream, higher values of overrun showed faster melting, as a higher overrun disrupted the fat network. This result revealed that the effect of fat network on the melting behavior was more prominent than the effect of overrun.

Based on the results obtained from **Chapters 2 and 3**, two different fat replacing strategies were proposed. In **Chapter 4**, we identified the role of polysaccharide structure in determining the structural, rheological, tribological and sensory properties of ice cream, by separating the effect of molecular structure from the effect of viscosity. The polysaccharides taken into consideration varied from flexible (locust bean gum and guar gum) to rigid (xanthan gum and iota carrageenan). Mixes with flexible polysaccharides showed a higher ability to incorporate air cells, while rigid polysaccharides provided a more solid-like behavior and tended to form an irreversible network in the serum phase, related to less air incorporation. The higher overrun of samples containing flexible polysaccharides led to lower hardness, while ice cream with rigid polysaccharides were harder to scoop. Melting rate was not related to the type of polysaccharide, but to serum phase viscosity. Results of a sensory study showed that the properties of ice cream with flexible polysaccharides were closer to those of full-fat ice cream, while those of samples with rigid polysaccharides were closer to those of low-fat ice cream. Therefore, polysaccharides with a flexible structure are a better choice for improving the textural and sensory properties of low-fat ice cream.

The second strategy involved the use of soy protein, based on the ability of protein to increase viscosity and foaming (**Chapter 5**). We investigated the individual effect of soy protein particle size, dispersibility and mix viscosity on the textural and sensory properties of fat-free ice cream. Protein particle size appeared to play an important role in determining different properties of ice cream. Dispersible protein particles (0.25 μm) led to higher air incorporation and thus lower hardness and higher scoopability. In comparison, large non-dispersible particles (3.8-145 μm) enhanced the melting resistance by forming a network in the serum phase. When both the dispersible and non-dispersible particles were present, serum phase viscosity appeared to be the dominant factor in affecting the melting rate, while particle size had a larger effect on melting lag time. Ice creams with a relatively denser structure

and lower melting rate provided higher creaminess and mouth coating, and lower coldness and grittiness. Overall, samples with a protein particle size of approximately 4 µm showed a positive effect on the properties of fat-free ice cream, resulting in overall liking similar to that of full-fat ice cream. Medium-sized protein particles thus have a higher potential to act as a suitable fat replacer for improving the textural and sensory properties of fat-free ice cream. In addition, positive sensory attributes were also related to lower friction coefficients of molten ice cream, although we were not able to link this to a specific structural feature. This work clearly demonstrates that the quality of fat-free ice cream can be improved by manipulating plant protein characteristics.

In both **Chapters 4 and 5**, sensory perception was related to the lubrication properties of molten ice cream. As lubrication properties upon melting may be more relevant for sensory perception, in **Chapter 6,** we aimed to develop a new method to measure the lubrication properties of ice cream during melting, and we investigated how different structural elements would affect the lubrication parameters. We saw that the ice fraction mainly contributed to the lubrication at the initial stage of melting, while the fat content dominated lubrication at the later stage and in molten ice cream. Fat aggregation, serum phase viscosity and overrun did not appear to have a significant effect on the lubrication properties during melting. Together with the friction coefficient, we also measured the distance that the probe entered the ice cream samples during melting, which was found to be mainly related to the ice fraction and hardness. The distance may thus be used as an indication of the melting behavior or hardness, which may provide more realistic results for melting in the mouth than currently used melting tests. Overall, our new method shows that measuring lubrication properties during melting is possible. However, the exact significance of the obtained data to describe changes in lubrication upon melting and how these data would be related to sensory perception need to be confirmed. In **Chapter 7**, we provided a discussion on the main structural determinants of melting behavior, hardness, scoopability and sensory perception. Additionally, the suitability and the required functions of different fat replacers was also discussed.

In conclusion, the thesis contributes to the understanding of the exact role of fat in ice cream and, finally, to the development of potential fat replacing strategies. The knowledge obtained from this thesis can be applied to the reformulation and production of low-fat or fat-free ice cream, but also provides basic insight for the relationship between texture and quality characteristics, which benefits the development of low-fat products as well as other frozen desserts.

Acknowledgement

I look back on my PhD journey with immense gratitude and affection. These four years have marked a period of incredible growth, both academically and personally. I would like to express my deepest gratitude to all those who supported me throughout this wonderful journey of pursuing my PhD.

Firstly, I would like to thank my promotor and daily supervisor, Dr. **Elke Scholten**, for giving me the opportunity to pursue this PhD. **Elke**, thank you very much for always being available to resolve my questions, provide quick feedback on my manuscripts and improve my scientific abilities. I appreciate the freedom and opportunities that you provided me throughout the entire PhD. I also appreciate your efforts in organizing different social activities (Christmas dinner, 'Elke dag', trips to Efteling, etc.). These moments are deeply imprinted in my mind, providing me with fun memories and a sense of 'family' in a foreign land. Secondly, I would like to thank my co-promotor, **Dr. Guido Sala**, for the support during my whole PhD. **Guido**, thank you as well. You always have unique perspectives about scientific questions, which inspired me a lot to rethink them in different directions. I enjoyed our insightful discussions and benefited from the new ideas that emerged. I also enjoyed several times of running in the forest and participating in the Veluweloop three times. Your healthy lifestyle has greatly encouraged me to find a balance between work and life.

I would like to thank **Prof. Dr. Kasper Hettinga, Dr. Ir. Frank Boerboom, Dr. Sergio Martinez-Monteagudo**, and **Dr. Marcel Meinders** for agreeing to serve as members of my thesis committee. Thank you for taking the time to read and evaluate my thesis.

Next, I would like to express my gratitude to the FPH employees. I am so lucky that I could work in the FPH, which is really like a big family with an amazing academic atmosphere and colorful activities. **Els and Maruschka**, thank you very much for your support with administrative matters and for preparing warm-hearted greeting cards. **Harry, Floris and David**, thank you all for supporting my lab work and making countless introductions. I also want to thank other staff at FPH: **Erik, Leonard, Mehdi, Jasper, Jack, Paul, Maria, Arjen, Karlijn, Mark and Roel,** for their support and assistance throughout various activities during my PhD.

Finally, I would like to thank all my PhD fellows and friends who shared this journey with me. I thank all my students for their great efforts and contributions to this project: **Daniel, Jingxuan, Haoyu, Alison, Rania, Wanrong, Robert, Marton and Xiaobing**. I am happy to be your daily supervisor for your thesis, and I wish you all

the best in your working/ studying life. To my officemates: **Xilong, Zhihong, Gerard, Annika, Senna, Ashoka, Chaya, Chonchanok and Nana**. You are the ideal officemates, always friendly and supportive, bringing joy and encouragement to my daily life. To my foreign colleagues: **Aref, Naomi, Melika, Robert, Thiemo, Nirzar, Remco, Philipp, Belinda, Anteun, Dieke, Diana, Ployfon, Roy, Ahmed, Claudine, Parisa, Naoya and Shuzo**. I am grateful for the opportunity to work alongside such talented and dedicated colleagues. I appreciate the collaborative spirit and enthusiasm that you bring to the FPH. To my Chinese colleagues and friends: **Lei, Qi, Ferry, Weiwei, Gu Yu, Wenjie, Qiuhui, Jiaqi, Hongyu, Cheng Zhe, Caicai, Zhihong, Xilong, Mengyue, Xingfa, Nana, Ting, Xudong, Huizi, Ziyang, Bo, Penghui, Cai Yang, Xiaoning, Yifan, Qimeng, Wanting, and Xiaofei**. Meeting with all of you in a foreign land has been a true pleasure. Your presence has added so much value to this trip. To my basketball homies: **文杰，磊哥，喻琦，嘉宇，老韩，康康，刘玉，智尧，胡博, 一丁等**。Playing with all of you is both a joy and an honor. Thank you for the support, encouragement, and incredible memories. Special thanks to my paranympths: Qi and Weiwei. Thank you for your support during my PhD journey and for preparing everything. I wish you all the best for the rest of your PhD.

最后还要把感谢送给我的亲朋好友们。感谢**磊哥**和**涛哥**，作为我刚到瓦村的领路人，对我科研和生活中的帮助。感谢我的亲友团成员们：**丁军，赵凯，唯健，泽文，张衡，鸡蛋，小白，孟捷，姐夫，小健，苏醒，张璐，远哥等**。感谢你们的付出和帮助，很庆幸时间没有冲淡我们的友情，希望我们友谊长存。还要把感谢送给：**小雨**和**龙宇**。一定是特别的缘分使我们相遇，感谢你们的出现以及所有的一切。最美好的祝福送给你们，希望你们可以早日修成正果。感谢我的**父母**，你们永远是我最坚实的后盾，感谢你们对我的教导以及无条件的支持，希望我也能成为你们的骄傲。还要感谢我的各位**亲戚长辈**，谢谢你们的谆谆教诲以及深切的爱，让我心中常怀感恩。最后的最后，想把感谢送给我的**妻子**：十年感情我们终于走进婚姻殿堂，你一直是我的精神支柱，在生活和科研中给予我无数的鼓励和帮助，是你的优秀一直激励我，鞭策我向前，四年前做出来荷兰决定的那个晚上依然历历在目，很庆幸，蓦然回首，你依然还在灯火阑珊处。

Xiangyu Liu/刘翔宇 22/10/2023
The Netherlands, Wageningen

About the author

Xiangyu Liu was born on March 16, 1992 in Qinhuangdao City, Hebei province, China. His hometown is a beautiful coastal city located in the northeastern part of China.

He studied Food Science and Engineering at Nanchang University (NCU) for four years as a BSc student from 2012 to 2016.

After he obtained his BSc degree, he continued his MSc study in the same year at Ocean University of China (OUC). He chose the topic entitled "Study on cold gelation process and oil emulsion gel of Alaska Pollock surimi" and completed it in 2019, earning the honor of "Outstanding Master Thesis of Shandong Province".

During the MSc study, he discovered a deep interest in scientific research and decided to pursue a PhD career. In the same year, he went to the Netherlands and started his project in the group of Physics and Physical Chemistry of Foods (FPH) at Wageningen University. He successfully completed his PhD project in 2024 under the supervision of Dr Elke Scholten and Dr Guido Sala.

Email: Xiangyu.liu0316@outlook.com

List of publications

Liu, X., Sala, G., & Scholten, E. (2022). Effect of fat aggregate size and percentage on the melting properties of ice cream. Food Research International, 160, 111709.

Liu, X., Sala, G., & Scholten, E. (2023). Structural and functional differences between ice crystal-dominated and fat network-dominated ice cream. Food Hydrocolloids, 138, 108466.

Liu, X., Sala, G., & Scholten, E. (2023). Role of polysaccharide structure in the rheological, physical and sensory properties of low-fat ice cream. Current Research in Food Science, 100531.

Liu, X., Sala, G., & Scholten, E. (2023). Impact of soy protein dispersibility on the structural and sensory properties of fat-free ice cream. Food Hydrocolloids, 109340.

Liu, X.*, Ji L.*, Sala, G., & Scholten, E. Ice cream tribology: effect of different structural elements. (To be submitted)

*shared first authorship

Overview of Completed Training Activities

Discipline specific activities

Reaction kinetics in food science	VLAG, the Netherlands	2021
Healthy and sustainable diets	VLAG, the Netherlands	2021
Healthy food design	VLAG, the Netherlands	2021
Sensory perception & food preference	VLAG, the Netherlands	2021
Dairy protein biochemistry	VLAG, the Netherlands	2022
Mini Symposium December 13th	Wageningen, the Netherlands	2022
Benelux Lipid Network Fats & Oils course/ Hive	Wageningen, the Netherlands	2023

Conferences

35th EFFoST International conference[1]	Lausanne, Switzerland	2021
2nd Edible Soft Matter Workshop & Conference[1]	Wageningen, the Netherlands	2022
32nd Dutch Soft Matter Meeting[2]	Wageningen, the Netherlands	2022
International Symposium on Food Rheology and Structure[2]	Wageningen, the Netherlands	2023

[1] Poster presentation
[2] Oral presentation

General courses

VLAG PhD week	VLAG, the Netherlands	2019
Scientific Integrity	WGS, the Netherlands	2021
Scientific Writing	WGS, the Netherlands	2021
Scientific Publishing	WGS, the Netherlands	2022
The Essentials of Scientific Writing and Presenting	WGS, the Netherlands	2022
Research Data Management	WGS, the Netherlands	2022

Other activities

Preparation of research proposal	Wageningen, the Netherlands	2019
Weekly science meeting	Wageningen, the Netherlands	2019-2023
Ice cream regular update meeting	Wageningen, the Netherlands	2019-2023
Organization of FPH PhD trip	Sweden and Denmark	2023

Teaching and supervision

Advanced Molecular Gastronomy (Practical)	FPH	2021-2022
Supervision of 4 BSc students	FPH	2019-2023
Supervision of 5 MSc students	FPH	2019-2023

Approved by graduated school VLAG

Colophon

The research described in this thesis was financially supported by the China Scholarship Council (CSC, No. 201906330088), and was co-financed by Chicecream (Shanghai, China).

Financial support from Wageningen University for printing this thesis is gratefully acknowledged.

Cover design: Xiangyu Liu and Lu Zhang

Printed by Proefschriftmaken.nl